D-MEM
PhD-UNIMI

Doctorate program
Milan
EXPERIMENTAL
MEDICINE


# Università degli Studi di Milano

**PhD Course in Experimental Medicine**

**CYCLE XXXVIII**

---

**PhD thesis**

# PHARMACOGENOMICS OF OPIOID RESPONSE IN EUROPEAN ADVANCED CANCER PATIENTS

---

Candidate: **Dr. Francesca Minnai**

Matr. ID: R13697

Orcid ID: 0000-0003-3646-3800

Tutor: **Prof. Cristina Battaglia**

Supervisor: **Dr. Francesca Colombo**

Director: **Prof. Nicoletta Landsberger**

**Academic Year 2024-2025**

# Table of contents

# 1. Abstract

**Background:** Strong opioids, which are drugs in the third step of the World Health Organization's analgesic ladder, are the standard of care for treating pain in advanced cancer patients. Unfortunately, a significant minority of them do not benefit from analgesic therapy, or experience several side effects, such as nausea and vomiting. Genetics might play a role in predisposing patients to a good or poor response to opioids. To investigate this issue, two different genome-wide association studies (GWAS) were conducted to identify genetic variants modulating opioid efficacy and toxicity.

**Methods:** We genotyped over two thousand European patients with advanced cancer, treated with morphine, buprenorphine, fentanyl, and oxycodone. Data about toxicity (nausea-vomiting score, NVS) and efficacy (pain intensity, PI) and other relevant clinical information were collected. We carried out two whole genome regression models (using REGENIE software) to test the association between genotypes and the two opioid response phenotypes, both defined as numerical scores, one measuring patient pain intensity and the other nausea/vomiting intensity. To understand the functional role of the variants significantly associated with opioid response, several "*in silico"* post-GWAS analyses were conducted. Colocalization between pain intensity phenotype and gene expression was explored, as well as the tissue-type enrichment for our significant variants, using stratified linkage disequilibrium score regression (sLDSC). Finally, Mendelian randomization, using our pain intensity GWAS datasets, was performed to investigate causal relationships between putative pain risk factors, such as inflammation, sleep alteration, and psychiatric conditions, and cancer pain intensity.

**Results:** For the opioid-induced toxicity phenotype, 65 variants associated with NVS (at *P*-value < $1.0 \times 10^{-5}$) were found. Among these, 14 variants on chromosome 2 mapped in intronic regions of *NPAS2* gene, which encodes a circadian transcription factor. This gene is reported to influence the sleep-awake cycles; several studies suggested a reciprocal link between the circadian and pain systems, and the modulation of opioid drugs. Also, some of these variants were previously identified as splicing quantitative trait loci of the *NPAS2* (HGNC:7895) gene.

The second GWAS for opioid efficacy identified five variants (rs6062363, rs6062365, rs13043326, rs6089804, and rs1806952) whose minor alleles negatively correlated with pain intensity, at genome-wide statistically significance level (*P*-value < $5.0 \times 10^{-8}$). This negative correlation indicates that subjects homozygous, for the minor alleles or

heterozygous, experienced lower pain intensity than patients homozygous for the major allele. These variants mapped to a non-coding region of chromosome 20 downstream *PCMTD2* (HGNC:15882) gene, and less than 200kbp far from *OPRL1* gene. While information on the role of *PCMTD2* is scarce, *OPRL1* encodes the opioid related nociceptin receptor 1, belonging to the opioid receptor family. The identified polymorphisms were reported to be modulators of the expression of both *PCMTD2* and *OPRL1* genes, in eQTLGen database. Also, variants in the same chromosomal region were recently reported to be significantly associated with pain intensity in a GWAS conducted in subjects with different chronic pain conditions. The colocalization analyses showed that there was low evidence for shared variants regulating both pain intensity and *PCMTD2* gene expression. sLDSC indicated that variants associated with pain intensity were enriched in liver and central nervous system. Finally, the Mendelian Randomization did not support causal relationships for the analyzed traits.

**Conclusions:** The results obtained support the hypothesis of a genetic role in modulating the opioid response of advanced cancer patients. However, in *vivo* functional analyses are needed to understand the biological mechanism underlying the observed association. Also, validation in an independent but homogeneous patient series would be advisable. Those herein reported are the first two GWAS for opioid response, both in terms of efficacy and toxicity, so far performed in cancer patients. They represent the starting point for further pharmacogenomics studies of opioid therapy in larger sample sizes, which might be more representative of the whole population. This study provides new insights into the genetic factors influencing pain intensity suggesting new potential markers of opioid response, which could lead to personalized cancer pain management. The development of individualized pain treatment plans, ultimately, will pave the way to an improvement of advanced cancer patients' quality of life.

## 2. Disclosure for research integrity

All the study activities were conducted in accordance to the European General Data Protection Regulation and the ALLEA European Code of conduct for Research Integrity.

The protocol of this pharmacogenomic study was approved by the Committee for Ethics of the Fondazione IRCCS Istituto Nazionale dei Tumori, Milan, Italy (INT 20/20). Protocols for patients' recruitment in the MOLO, EPOS, and CERP studies were approved by the Committees for Ethics of each recruiting hospital. The study was performed in accordance with the Declaration of Helsinki. Also, to contribute to the awareness of the patients and respect the principle of transparency, written informed consent was provided by each enrolled patient before biological sample and data collection, to allow researchers to use them for opioid pharmacogenomic research purposes. Clinicians, patient representatives and research partners were engaged during the study design and result interpretation to lead to correct clinical answers to biological interpretation. To ensure reproducibility, genetic analyses and Mendelian randomization were conducted following standard guidelines (STREGA, STROBE-MR) and bioinformatic code used to perform the analyses is available on DATAVERSE at the link https://doi.org/10.13130/RD_UNIMI/ZQMSCY.

The text in this thesis is my own (unless otherwise specified) and generative AI has only been used for grammar editing. I have reviewed and edited the content as needed and I take full responsibility for the content of the thesis. The results obtained from the genetic analyses are publicly available in GWAS Catalog. Also, to share the results with other peers and academics, Open Access publication in two international peer-reviewed journals had been made. Fondazione AIRC per la ricerca sul cancro [MFAG 2019 - ID. 22950 - P.I. Colombo Francesca] supported this three-year project; the funding organization had no role in the design and performing of the study; collection, management, analysis, and interpretation of the data; preparation, review. I declare, like the other researchers collaborating on this project, no conflicts of interest.

# 3. Introduction

## 3.1 General physiology and clinical classification of pain

Pain is currently defined, by the International Association for the Study of Pain, as an "unpleasant sensory and emotional experience associated with actual or potential tissue damage".[1] It is a complex and protective mechanism that alerts the organism in case of damage. The first sensory modality in which the pain stimuli are detected peripherally and transmitted centrally to the central nervous system is nociception (**Figure 1),** and it is characterized by four different stages: 1) transduction, 2) transmission, 3) modulation, 4) perception.[2]

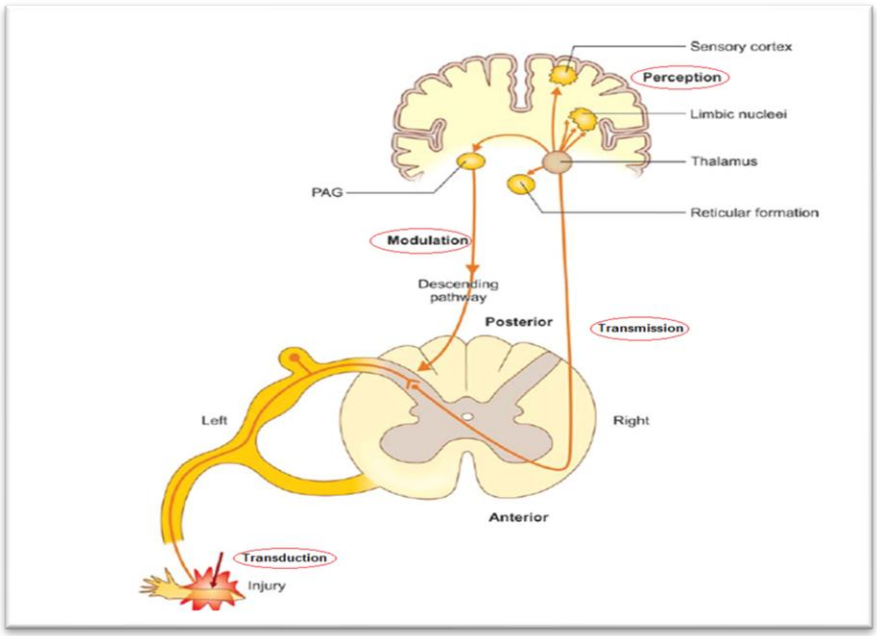


**Figure 1.** Pain pathway; readapted from "Basics from Chronic Pain management" (10.25259/VJIM_16_2022)

Nociceptors are the main protagonists in this complex pathway: they are the primary afferent neurons for pain, presenting specialized nerve endings able to respond to different types of chemical thermal or mechanical stimuli.[2]

**Transduction** occurs when a painful stimulus is converted into an electrical signal by peripheral nociceptors, expressing receptors and ion channels such as the transient receptors potential (TRP) channels.[3]

When those channels are activated, due to a sufficient strength of the stimulus, there is a transient drop in the resting membrane potential that generates an action potential. It enables the **transmission** of signals from the peripheral nervous system (PNS) to the dorsal

horn of the spinal cord. Here, interneurons release excitatory neurotransmitters, such as glutamate, or inhibitors, such as endogenous relay toward supraspinal centers.[4]

The **modulation** of the pain signal occurs at the spinal and supraspinal levels; this process involves an interplay of descending inhibitory circuits in different brainstem structures[5,6] such as periaqueductal gray (PAG), the rostroventular medulla (RVM) which regulate facilitation and inhibition at the spinal level, the locus coeruleus and the dorsolateral funiculus that regulate the emotional aspects of pain.[6]

Finally, the **perception** of pain happens when the nociceptive signal is processed in brain regions, and the signal is transformed from a simple sensory input to a conscious emotional experience. Among these, the anterior cingulate cortex (ACC), part of the limbic system, is centrally involved in the emotional-affective dimension of pain. The activation starts with the unpleasantness or distress associated with pain and, also, chronic pain conditions are often associated with increased baseline activity in the ACC.[7,8] Then, the prefrontal cortex, especially the medial and dorsolateral subregions, is involved in cognitive evaluation, decision-making, and modulation of the pain experience a critical role in pain processing.[9] Also, the thalamus is the major station for nociceptive input ascending from the spinal cord. It projects both sensory and limbic structures and coordinates input from different nociceptive pathways (spinothalamic, spinoreticular, etc.), allowing the mediation of pain stimuli localization and discrimination.[2] The mediodorsal, ventroposterolateral (VPL), and ventroposteromedial nuclei (VPM) are particularly involved in pain processing, and a reciprocal link between them demonstrates that the PAG and the sensory thalamus interact reciprocally at short latency, which may be related to pain modulation. Finally, the amygdala, another limbic structure, assigns emotional salience to painful stimuli. It receives nociceptive input directly from the parabrachial nucleus and is involved in pain-related fear and memory formation.[10]

Clinical description of pain is based on physiology or pathology, its anatomical location, the duration or qualitative descriptors; based on this, there are three different types of pain: *acute, phasic* and *chronic pain*. Acute pain occurs immediately as a protective response from illness or inflammation, with a clear onset and a well-defined cause that lasts until the complete healing of the illness; examples of acute pain can be traumas, burns, or acute infections.[11] The pathophysiology of acute pain involves the primary activation of nociceptors that, through ion channels such as TRPs, send signals to Ad or C fibers for slow and persistent pain, respectively, to the dorsal horn of the spinal cord. Here, glutamate and P-substance allow the transmission of the signal to synapsis. Then, pain signals arrive at

higher brain centers, such as the VPL and VPM cortexes of the thalamus. They are then sent to the somatosensory cortex, where the quality, location and type of pain are discriminated, and to the limbic system where they can be emotionally processed through different types of symptoms, such as an increased heart rate or nausea.[11] The response to the pain perception is then done through descendant pain modulation pathways, in charge of the RVM and the dorsal horn of the spinal cord. Here, the pain signal can be amplified, modulated, or suppressed using endogenous opioids, norepinephrine, or serotonin.[12]

Phasic pain is a brief, transient noxious sensation, caused by a short-duration stimulus, that stops when the stimulus is removed.[2] In healthy individuals, phasic pain is used to study pain thresholds, response latency, and pain modulation mechanisms such as conditioned pain modulation or temporal summation.[13] It is used to assess the integrity of nociceptive pathways in clinical and research settings, activating Ad fibers in the central nervous system (CNS) and leading to a well-localized pain. It is also used to experimentally investigate quantitative sensory testing and psychophysical evaluation of pain sensitivity.[14]

Unlike acute and phasic pain, chronic pain (Human Phenotype Ontology code: HP:0012532) is a persistent multifaceted condition that can exist in the absence of active tissue injury. It can last more than 3 to 6 months [15], and be considered a disease rather than a symptom. First, chronic pain causes peripheral sensitization through cytokines or prostaglandins which lower pain activation threshold of nociceptors. This is followed by central sensitization, which is characterized by an increased glutamatergic transmission through N-methyl-D-aspartate receptor (NMDA) receptors, disinhibition due to a loss of GABAergic (gamma-aminobutyric acid) and glycinergic (glycine) control, and finally activation of microglia and astrocytes that release further pro-nociceptive molecules. This leads to activation of neurons in the dorsal horn of the spinal cord.[16,17] Also, in chronic pain there is a malfunctioning of the common neurological processes in cortical regions such as the anterior cingulate cortex or the insula, that can altern pain perception. Furthermore, there are changes in the descending pain modulation system in structures such as the rostroventular medulla, leading to an alteration of the pain modulation.[16,17]

Chronic pain has different subtypes, for instance *neuropathic, breakthrough, or cancer-related (chronic) pain*. Neuropathic pain affects 10% of the general population and can be caused by dysfunctional or damaged nerves or induced by infections (e.g. HIV) or chemotherapy, that generate aberrant pain signals in the absence of an external noxious stimulus.[18] Neuropathic pain (HP:6000040) results from the invasion of neural structures such as the brachial plexus, peripheral nerves or spinal cords, and it is described by patients

as burning.[19] Breakthrough pain (HP:0032149) is instead characterized by an intense but short pain episode that occurs contemporary to a stable and well managed baseline pain.[20] It is usually common in patients with cancer. Breakthrough pain can be idiopathic, triggered by a specific movement or activity, or can be felt immediately after the end of the analgesic dose effect. Both neuropathic and breakthrough pain assessments are difficult due to the multifaceted type of pain and the underlying unknown cause.

Another important subtype of chronic pain is cancer pain, which is caused by disease progression and metastatization, leading to severe and persistent pain. For example, in breast, lung and prostate cancer, bone metastases are the more common cause of pain: bone involvement led to osteolysis with consequent structural instability and periosteal nociceptive nerves stimulation.[21] Indeed, in the tumor microenvironment, the release of cytokines or growth factors (e.g., tumor necrosis factor-α or the interleukin-1β), leading to inflammation, and the sensitization of peripheral nociceptors, as well as their interaction with immune cells can amplify the pain signal.[22] Cancer pain is not only caused by tumor growth.[23] In fact, different types of anticancer therapies can lead to pain. For example, chemotherapy-induced peripheral neuropathy can cause persistent burning or tingling in the extremities, due to the different chemotherapy agents such as taxanes or platinum compounds.[24] Also, radiation therapy can lead to pain due to nerve injuries or tissue fibrosis, and surgical intervention can lead to after-resection pain syndrome due to nerve damage.

All these factors can contribute to an increased severity of pain and more difficult pain relief treatment.[25]

## 3.2 Pharmacological treatment of pain

Opioids drugs are the primary analgesics capable of effectively managing moderate to severe cancer-related pain [26] The World Health Organization (WHO) defined an analgesic ladder [27] for the treatment of pain based on its severity. In case of mild pain, treatment with non-opioid drugs such as non-steroid anti-inflammatory drugs (NSAIDs) is recommended. Thus, NSAIDs are defined as the Step 1 of the WHO analgesic lagger. When patients experience moderate pain, treatment with weak opioids (e.g., codeine and tramadol) is recommended (Step 2 of the WHO analgesic ladder. Severe and persistent pain, instead, needs to be treated with strong opioids, such as morphine, fentanyl, oxycodone, and buprenorphine (Step 3).

Opioid drugs can interact with the endogenous opioid system, targeting opioid receptors,

which are G-protein coupled receptors (GPCRs) distributed in different organs such as CNS, PNS, or the digestive trait.[28] We can distinguish three primary different opioid receptor types:

1. μ-opioid receptor (MOR), encoded by the *OPRM1* (ENSG00000112038) gene, involved in the primary analgesia response and responsible for different adverse effects such as drug dependence;[29,30]
2. δ-opioid receptor (DOR), encoded by the *OPRD1* (ENSG00000116329) gene, primarily modulator of emotional response to pain, involved in the reduction of hyperalgesia in chronic pain, as well as in antidepressant and anxiolytic behaviors;[30]
3. κ-opioid receptors (KOR), encoded by the *OPRK1* (ENSG00000082556) gene, involved in spinal analgesia and implicated in other physiological processes, highly expressed in the CNS but also distributed in heart, lung and small intestine.[31]

A cascade of intracellular events is triggered by the binding of ligands to the opioid receptors: the initial change in conformation activates G-protein subunit Gα and Gβγ. This leads to the inhibition of adenylate cyclase activity and the concurrent opening of potassium channel.[32] The transmission of signals from the periphery to the brain is interrupted in their ascending pathway; at the same time, opioid can activate a descending pathway that reduces the pain transmission.[33]

Ligands of opioid receptors are mostly endogenous opioids such as endorphins, enkephalins, or dynorphins. These are peptides produced in response to positive or negative stimuli, such as stress, pain, or happiness. They specifically bind to different opioid receptors:

1. Endorphins bind MORs, inducing euphoria and stress relief;[34]
2. Enkephalins mainly bind DORs and are mostly involved in mood modulation;[35]
3. Dynorphins bind KORs and contribute to stress-related dysphoria and pain chronification.[36]

Another endogenous peptide, nociceptine, binds to a different receptor of the opioid receptor family. This receptor is encoded by the *OPRL1* (opioid related nociceptine receptor 1, or ORL-1) gene, also called the nociceptine/orphanin FQ peptide receptor (NOP) [37]. Although it is structurally similar and is part of the same opioid receptors' family, NOP has totally different physiological and pharmacological characteristics. In fact, nociceptine binding to NOP can modulate pain but also contribute to mood and stress/anxiety regulation.[38] Regarding pain modulation, it has different effects based on where the NOP gene is expressed. In the spinal cord, it has an analgesic effect inhibiting the pain transmission; if the nociceptine is mostly expressed in supraspinal region, we can observe hyperalgesia and

anti-opioid action.[39]

Focusing on clinical practice and palliative care settings, exogenous strong opioids are used to mimic the effect of endogenous ones, and they are used to relieve moderate to severe acute or chronic pain. They primarily bind to the MORs that, with their cascade pathway, inhibit the nociceptive transmission and relief of pain. The most used are morphine, buprenorphine, fentanyl, oxycodone, and others from the third step of the WHO analgesic ladder.

Morphine (Drugbank code DB00295) is the gold standard for analgesic treatment with opioids, but it can lead to several adverse effects such as respiratory depression, tolerance, or addiction. Therefore, morphine, as well as codeine, have undergone different molecular conformational studies over the years to improve efficacy without those important side effects.[40] Buprenorphine (DB00921) is a partial MOR ligand, with an agonist action of KOR, widely used for the treatment of acute postoperative pain, particularly when administered via sublingual or via transdermal routes. This drug is highly safe due to the reduced addiction effect and the less predisposition to respiratory depression, as well as the absence of immunosuppressive effects.[41,42] Fentanyl (DB00813) is, instead, a synthetic strong opioid used to treat chronic pain, with an analgesic effect 100-fold stronger than morphine. With a rapid onset and short duration. Unfortunately, fentanyl use can rapidly become abuse and create strong addiction, particularly in opioid-naive patients.[43] Then, oxycodone (DB00921) is a semisynthetic opioid with a higher bioavailability than morphine, widely used in outpatients to treat severe chronic pain, but also severe cancer pain. It has been observed that advanced cancer patients treated with a combination of oxycodone/naloxone have a reduced opioid-induced bowel disfunction and constipation and less abuse risk.[44]

Although the effectiveness of these treatments, they reported several adverse effects that can affect patients' quality of life. Among them, we can include addiction, constipation, due to a reduced gastrointestinal motility, respiratory depression, that can be fatal if not monitored (particularly in case of dependence), nausea and vomiting, opioid-induced hyperalgesia, where the prolonged use of these drugs can lead to an increased pain sensitivity. Understanding the precise molecular and cellular mechanisms of opioid analgesia is essential for optimizing pain management strategies and minimizing risks associated with opioid therapy.

Different strategies could be applied to improve efficacy and reduce the adverse effects. For example, opioid rotation can reduce tolerance and addiction by switching opioids after a certain amount of time.[45] Another strategy is to use different combination therapies, such as

oxycodone/naloxone.[46]

Another important consideration is that there is a significant variability among patients in the efficacy and side effects of opioid therapy. Genetics, and other factors such as stress, trauma history, mental health comorbidities, and opioid-induced hyperalgesia could be responsible for this variability. These factors can affect individual opioid response. For this reason, it is important that the clinical setting was efficient and well defined: the screening of patients at each visit and comprehensive pain management should be held by a multidisciplinary team, due to the different patho-physiologic conditions in which pain can occur. It is important that the pain intensity is quantified and qualified at each follow-up visit accounting for the high subjectivity due to the pain perception. Analgesic treatment should be administered considering multiple symptoms and the complex combinations of pharmacologic therapies that are generally prescribed.[47] It is also important to take into account the different types of treatment and dosage in patients that take opioids for the first time (called “opioid-naive”) and in “opioid-tolerant” patients who have already taken opioid for cancer pain.[48,49]

For all these reasons, a personalized therapeutic approach integrating pharmacogenomics and behavioral interventions for pain treatment could improve clinical practice and patient quality of life.[50]

## 3.3. The role of genetics in the management of pain in cancer patients

The wide human genetic variability involves also genes encoding drug receptors, metabolizers, and transporters. Pharmacogenomics is the field of medicine that studies how genetic variants modified the action of drug. It investigates the effect of genetic variations on pharmacokinetics (how drugs are absorbed, metabolized and excreted from the body) and pharmacodynamics, that is how drugs act (physiologically and biochemically) at the body’s organs or sub-cellular levels. Pain sensitivity and management are influenced by genetics. Genetic studies in twins estimated the effect of heritability for several pain phenotypes, showing that there is a heritable component up to 60% in different types of pain.[51] The same heritable component is demonstrated also for opioid response in pain treatment: in fact, other studies in monozygotic and dizygotic twins have shown that genetics may explain from 12% to 60% of variance in alfentanil-induced analgesia.[52]

Also, a heritability up to 56% has been observed for opioid-induced adverse effects,

particularly those due to nausea and vomiting.[53]

### *3.3.1 Candidate-SNP and gene studies*

*So* far, researchers investigating the genetic underpinnings of individual diversity in opioid responsiveness have done it through candidate genes studies.

Candidate-gene studies are characterized by an approach that consists in the selection of one, or a few, genes for a narrow examination of statistical association with a given trait or disease. The selection of these genes depends usually on previous knowledge about a possible involvement in relevant biological pathways related to the trait of interest. Particularly, in these studies, candidate-gene single nucleotide polymorphisms (SNPs) are evaluated, usually comparing allele or genotype frequencies between case and control groups, or correlating variants with quantitative traits.

Focusing the attention of opioid response, so far researchers centered their interest in those genes involved in pharmacokinetics, such as *CYP2D6, CYP3A4, CYP3A5, UGT2B7, ABCB1 (MDR1*), *COMT,* or in pharmacodynamics (e.g., *OPRM1, OPRD1, OPRK1*). In addition, most of these studies were not carried out in cancer patients and analyzed the genetics of drug response in patients suffering from different types of pain. Early pharmacogenetic studies of polymorphisms in genes involved in opioid pharmacokinetics suggested that genetic variations in the *CYP2D6* gene had a role in codeine metabolism and response. *CYP2D6* (ENSG00000100197) encodes an isoform of the cytochrome p450 enzyme, that metabolizes a quarter of all prescribed drugs, including the conversion of codeine into morphine.[54] Individuals with two inactive copies of *CYP2D6* can be classified as poor metabolizers, and are unable to efficiently synthetize morphine, resulting in insufficient pain relief. Conversely, ultrarapid metabolizers have more than two functioning copies of the *CYP2D6* gene and can therefore metabolize codeine into morphine more rapidly. Even with therapeutic doses of codeine, ultrarapid metabolizers can experience symptoms of morphine overdose, including extreme sleepiness, confusion, and shallow breathing, which in some instances can be fatal.[55] Conversely, ultrarapid metabolizers have more than two functioning copies of the *CYP2D6* gene and can therefore metabolize codeine into morphine more rapidly. Even with therapeutic doses of codeine, ultrarapid metabolizers can experience symptoms of morphine overdose, including extreme sleepiness, confusion, and shallow breathing, which in some instances can be fatal.[55] Additionally, a more recent review of pharmacogenetic studies on *CYP2D6* variants in

patients treated with oxycodone revealed the importance of this gene in converting oxycodone to oxymorphone, thus leading to better bioavailability and enhanced drug response.[56]

Another candidate-gene study of 60 Japanese cancer patients identified associations between *CYP3A5* and *ABCB1* gene polymorphisms (such as CYP3A5*3 or *ABCB1* C1236T) and fentanyl clinical response or incidence of side effects. Like *CYP2D6*, the *CYP3A5* gene (ENSG00000106258) encodes a member of the superfamily of cytochrome p450 enzymes, involved in drug metabolism. [57]

The *ABCB1* variant C3435T (rs1045642) was reported to be associated with morphine pain relief, playing a role in morphine pharmacokinetics [58]. *ABCB1* gene (ENSG00000085563), which codes for the isoform MDR-1 of the multi-drug resistance protein, is responsible for the transport of drug through the blood-brain barrier, but it is also involved in hepatic, liver or gut drug level regulation and transportation. This glycoprotein is functional in opioid transportation outside of the CNS, regulating their bioavailability.

Another candidate gene for opioid pharmacogenetic studies is *COMT* (ENSG00000093010). It encodes the enzyme catechol-O methyltransferase, metabolizes catecholamine such as dopamine, noradrenaline, and has a role in the opioid signaling pathways in the CNS. In an independent study, the polymorphism rs4680 of *COMT* gene (and its minor allele, A) was reported as a marker of opioid sensitivity.[59]

Focusing instead on the variants in genes involved in opioid pharmacodynamics (i.e., opioid receptors), a coding polymorphism (rs1799971) in the opioid receptor mu 1 (*OPRM1*) gene, encoding the primary target of opioids, has been extensively investigated for its impact on opioid response variability. This variant not only affects the binding affinity between opioids and OPRM1, but also a different opioid ability in relieving pain, (as reviewed in [60]). For instance, cancer patients homozygous for GG allele (*OPRM1* rs1799971 variant) receive higher morphine than heterozygous AG or homozygous AA carriers.[61]

An exploratory analysis was performed to evaluate the role of *OPRK1* polymorphisms in opioid response. The study investigated 353 patients treated with fentanyl, morphine, oxycodone, and/or hydromorphone. Only rs12948783 (in *RHBDF2* gene, ENSG00000129667) and rs7016778 (in *OPRK1* gene) were significantly associated with drug response in univariable, but not multivariable model. [62]

Then, a pharmacogenomic study on 69 patients with colorectal cancer patients treated with different types of opioids for cancer pain, reported the associations of the G allele of rs1799971 polymorphism in *OPRM1* with pain presence, and of *OPRD1* rs2236861 variant

and adverse drug reaction risk. [63]

A recent systematic review reported the results of a meta-analysis of four pharmacogenetic studies on 118A>G variant of *OPRM1*, indicating that patients with this variant had a higher pain score than those with wild-type genotype. [64] However, this result was not validated in an independent cohort of 620 patients.[65]

Although the above presented results (summarized in **Table 1**) support a possible role for genetics in modulating the interindividual variability in opioids response, they were often uncoherent between each other, also when evaluating the role of the same polymorphisms in different cohorts. A lack of validation could be due to several reasons, such as the small sample size or the difference in allele frequencies due to a different genetic ancestry between individuals.[63] Indeed, a study on animal models receiving morphine to treat pain provided clear evidence of the genetic complexity of opioid response, considered as a quantitative polygenic trait.[66] This emphasizes the need to address the study of the opioid response phenotype, both in terms of efficacy and toxicity, not only with a candidate-gene approach, but with a genome-wide strategy.[67]

### *3.3.2 Genome-wide Association Studies (GWAS)*

Genome-Wide Association Study (GWAS) is an approach used in population genetics to investigate the statistical association between genetic variations (usually millions of single nucleotide polymorphisms, or SNPs) across the genome, and a specific phenotype or trait of interest, such as disease presence, quantitative traits (e.g., blood pressure or height), or drug treatment response. To test this association, usually statistical methods such as linear or logistic regression are applied, adjusted for relevant covariates that could act as a confounding factor such as, for instance, a clinical variable that can be associated both with the risk factor and the disease, distorting the strength of the genetic association (e.g., age, sex, but also genotyping batch, or population substructures).

The association test between each germline variant and a specific trait in a GWAS can be performed using three different models:

1. Additive Model: genotypes are coded as 0 for homozygous for the major allele, 1 for the heterozygous, 2 for homozygous for the minor allele; this is the default model in GWAS and it assumes a linearity between the different genotypes and the effect provided by the minor allele. Mathematically, genotypes are treated as continuous variables.
2. Dominant Model: genotypes are coded as 0 for homozygous for the major allele, 1 for

heterozygous and homozygous for the minor allele; in this case, the basic assumption is that only one copy of the minor allele is required to produce a phenotypic effect. Mathematically, genotypes are treated as binary variables.

3. Recessive Model: in this model, only the homozygous for the minor allele is coded as 1, while homozygous for the major allele and heterozygous are coded as 0. Similarly, for the dominant model, genotypes are mathematically treated as binary variables but, in this case, the effect on the phenotype is shown only when two copies of the minor allele are present.

The choice of the model mostly depends on the biological question: usually, the additive model is recommended because it is more powerful to detect a statistical signal. When the true effect is dominant or recessive, the additive model can visualize the signal with a reduced statistical power, but this is not ensured when using a dominant or recessive model, in which the statistical power is highly reduced.[68]

To account for the very large number of statistical tests performed across the genome, a stringent significance threshold is commonly set (P-value < 5 x $10^{-8}$) to control false positives. While the candidate gene approach looks for a significant association between genetic variants in pre-specified genes of interest, determined by an a priori knowledge of the genetic effect on the specific trait, a genome-wide association studies (GWAS), could be defined more as a “discovery” approach that tests the association between a specific trait and a genome-wide set of genetic variants in different individuals. The loci identified can highlight candidate genes or biological pathways and regulatory mechanisms of complex traits.

So far, several genome-wide association studies have evaluated opioid genetics, but mainly in relation to opioid use disorder. For instance, a large GWAS meta-analysis on European samples identified two variants, rs1799971 and rs79704991, mapping in OPRM1 gene and rs11372849, in FURIN gene (ENSG00000140564), associated with opioid use disorder [69], at a genome-wide significance level. A large multi-ancestry GWAS meta-analysis of opioid use disorder in Million Veteran Program confirmed the previously identified loci and identified 12 new ones.[70] Another GWAS in the same cohort, investigating the genetics of buprenorphine drug response in opioid use disorder, identified one genome-wide significant locus (rs149319538) mapping in SLC39A10 (ENSG00000196950).[69]

Conversely, GWAS of opioid therapy response in advanced cancer patients are scarce. The first one was published in 2011 [71] and used a DNA-pooling approach and a discovery-validation study design to investigate genetic variants associated with pain relief in 1,008 Europeans cancer patients treated with opioids for cancer pain. This study identified eight

genetic variations associated with response to opioids, both in discovery and validation series, in genes involved in processes of neurological system. Another GWAS performed on 426 Japanese cancer patients showed a significant association (P-value < $5.0 \times 10^{-8}$) between opioid analgesic requirements per day and two intronic single nucleotide polymorphisms (SNPs), rs1283671 and rs1283720, of ANGPT1 gene (ENSG00000154188), with a P-value < $5.0 \times 10^{-8}$ .[72] Finally, a GWAS looking for genetic variants associated with opioid toxicity (i.e., nausea-vomiting adverse effect) was performed on a European cohort of more than 1,000 patients using a DNA-pooling approach and a discovery-validation study design.[73] Only one SNP, rs12305038 in PDE3A gene (ENSG00000172572), was confirmed in both series, although with opposite effects of the minor allele on the investigated phenotype. Although these results are promising (summarized in **Table 2**), these GWAS have limitations, in fact they used a DNA-pooled approach, not individually genotyping the SNPs and they were not yet validated in other independent series.

Another aspect to consider is that both candidate gene studies and GWAS methods present limitations in the understanding of causality mechanisms. Since they only provide a statistical association between a trait of interest and a genetic variant, they do not address the question about the causal relationship behind this association, without distinguishing whether these genetic signals play a causative role in drug response or pain perception. Indeed, functional validation of GWAS findings is advisable for transitioning from statistical association to understanding the underlying biological mechanisms. In silico functional validation is commonly used to prioritize candidate variants and genes. Fine-mapping[74], identification of expression quantitative trait loci (eQTLs)[75], colocalization and genetic correlation analyses[76] are just some of the most used approaches to functionally investigate, for example, whether the same variant can influence the phenotype of interest and gene expression or other correlated traits. These types of analyses are collectively referred to as post-GWAS analyses.

The Mendelian Randomization (MR)[77] method is another post-GWAS analysis which has become a complementary approach to infer causal relationship between different traits, using genetic variants as instrumental variables (IVs), under specific assumptions.[77,78] MR is based on the principle that, if a genetic variant is robustly associated with an exposure (e.g., inflammatory cytokines or opioid metabolism), and if this exposure influences an outcome (e.g., pain severity or opioid toxicity), then a causal relationship exists between them. Also, MR relies on three core assumptions to produce interpretable results.[78]

1. Relevance: the genetic variant used as IVs need to be robustly associated (at genome-wide statistical significance level) with the exposure of interest, to avoid biases and loss of MR statistical power.
2. Independence: the genetic variant must be independent of any confounding factors that might influence both the exposure and the outcome. Population stratification or cryptic relatedness can violate this assumption.
3. Exclusion restriction or no horizontal pleiotropy: the genetic variant must affect the outcome only through its effect on the exposure. This assumption can be violated by horizontal pleiotropy, where a variant influences multiple traits, including the outcome, thus becoming a confounding factor.

To the best of my knowledge, MR studies in the field of pain have thus far focused on chronic, noncancerous pain conditions, whereas the topics of cancer pain and opioid treatment response remain unexplored. For example, a causal relationship between elevated levels of circulating inflammatory proteins and an increased risk of multisite chronic pain was reported.[79]. Other studies have explored the bidirectional relationships between chronic pain and psychiatric comorbidities, such as major depressive disorders, using UK Biobank data, suggesting a causal relationship among them. Other putative risk factors for pain could be sleep disorders: indeed, an association between insomnia and pain was reported[80] and, thus, novel MR studies might reveal interesting insights also in this field. Specifically, new MR studies would be helpful in elucidating the causality of cancer pain and the mechanisms of opioid analgesia.

**Table 1.** Summary of results from candidate gene studies on drug response in pain treatment.

| rsID | Gene | Trait of interest | Treatment | OR/F | P | N | Ethnicity | PMID |
|---|---|---|---|---|---|---|---|---|
| | *CYP2D6* | | oxycodone | | | | | 34575542 |
| *CYP3A5*3/*3* | *CYP3A5* | Drug response | fentanyl | 3.49 | 0.029 | 60 | Asiatic | 22277678 |
| 1236TT | *ABCB1* | Side effect incidence | fentanyl | 0.17 | 0.036 | 60 | Asiatic | |
| C3435T | *ABCB1* | Pain relief | morphine | 19.8 | <0.00001 | 137 | European | 17898703 |
| rs4680 | *COMT* | Drug response | morphine | 0.71 | 0.005 | 197 | European | 19094200 |
| rs1799971 | *OPRM1* | Pain score | | 1.61 | 0.0002 | | | 38700261 |
| rs1799971 | *OPRM1* | Drug response | morphine | - | 0.006 | 207 | European | 15504181 |
| rs7016778 | *OPRK1* | Drug response | oxycodone | 0.30 | 0.05 | 353 | European | 27472837 |
| rs12948783 | *RHBDF2* | Drug response | | | | 353 | European | |
| rs1799971 | *OPRM1* | Pain treatment efficacy | Step III opioids | - | 0.007955 | 69 | American | 40006034 |
| | *OPRD1* | ADR | Step III opioids | | 0.042 | 69 | American | |

OR, odds ratio; F, F-value Fisher's statistics; P, *P*-value; N, sample size; ADR, adverse drug reaction;

**Table 2.** Summary of results from three different genome-wide association studies for opioid response in opioid use disorders or pain treatment

| rsID | Gene | Trait of interest | Treatment | OR/F/HR | P | N | Ethnicity | PMID |
|---|---|---|---|---|---|---|---|---|
| rs13421094 | - | Pain relief | opioids | 0.09789 | $8.0 \times 10^{-5}$ | 1,008 | European | 21622719 |
| rs12211463 | - | Pain relief | opioids | 0.07732 | $6.6 \times 10^{-4}$ | 1,008 | European | |
| rs7757130 | - | Pain relief | opioids | −0.1157 | $5.4 \times 10^{-4}$ | 1,008 | European | |
| rs2473967 | - | Pain relief | opioids | −0.1434 | $6.2 \times 10^{-5}$ | 1,008 | European | |
| rs2884129 | - | Pain relief | opioids | −0.09343 | $7.5 \times 10^{-5}$ | 1,008 | European | |
| rs7104613 | *SPON1* | Pain relief | opioids | −0.1172 | $7.3 \times 10^{-4}$ | 1,008 | European | |
| rs12948783 | *RHBDF2* | Pain relief | opioids | −0.1415 | $1.1 \times 10^{-8}$ | 1,008 | European | |
| rs10413396 | *ZNF235* | Pain relief | opioids | −0.1447 | $4.1 \times 10^{-4}$ | 1,008 | European | |
| rs1283671 | *ANGPT1* | Cancer pain relief | Morphine; oxycodone | - | $3.876 \times 10^{-11}$ | 428 | Asiatic | 36230616 |
| rs1283720 | *ANGPT1* | Cancer pain relief | Morphine; oxycodone | - | $4.007 \times 10^{-1}$ | 428 | Asiatic | |

| | | | | | | | | |
|---|---|---|---|---|---|---|---|---|
| rs12305038 | *PDE3A* | AED in cancer pain treatment | Step III opioids | −3.325 | 0.002 | 1494 | European | 31953506 |
| rs12305038 | *PDE3A* | AED in cancer pain treatment | Step III opioids | 3.982 | 0.029 | 264 | European | |

OR, odds ratio; F, F-value Fisher's statistics; HR, hazard ratio; P, *P*-value; N, sample size; *F-value Fisher's statistics was used; **hazard ratio was used.

# 4. Aim

The aim of this study is to investigate the genetic basis of inter-individual variability in opioid response, in terms of efficacy and toxicity, in advanced cancer patients, treated with four different strong opioids for cancer pain. In fact, despite the use of these drugs as gold standards for cancer pain management, about 20-30% of patients have a low pain relief, do not benefit at all from the therapy, or experience different adverse effects, such as nausea and vomiting. Previous literature suggests a heritable component in opioid response, and previously published candidate-gene or DNA-pooled pharmacogenomic studies have already tried to identify this genetic basis. Unfortunately, due to the limited sample size and differences in methodologies that led to incongruent results, this answer remains incomplete. To fill this gap, two GWAS on more than 2,000 European adult cancer patients were carried out to identify polymorphisms significantly associated with opioid response, in particular with pain intensity and with nausea–vomiting side effect.

In addition, several post-GWAS analyses, such as colocalization with gene expression, tissue type enrichment, and causal relationship between opioid response and other potential related traits such as inflammation, immune response, sleep traits and psychiatric conditions, were performed to explore, at least in *silico,* the function of the identified variants, and provide insights about the biological mechanism underlying opioid response genetic variability.

The final purpose of this study is to contribute to the field of pain pharmacogenomics, setting the basis for tailored opioid therapy, to improve the quality of life of cancer patients by achieving good pain relief. Moreover, the discovery of genetic markers associated with opioid toxicity will be helpful in inferring patients' risk of developing nausea vomiting side effects and thus, in personalizing therapy for minimizing this adverse event.

# 5. Materials and Methods

The study workflow, that briefly summarizes the entire method section, can be visualized in **Figure 2.** It started with patient enrollment and clinical data collection, where the clinician checked if the patients met the inclusion criteria and collected clinical information about the patient's history using standardized questionnaires, and blood samples. Then, genomic DNA extraction, quantification, and genotyping, followed by variant calling, allowed for obtaining genetic data to be used in the Genome-Wide Association Study pipeline and subsequent post-GWAS analyses.

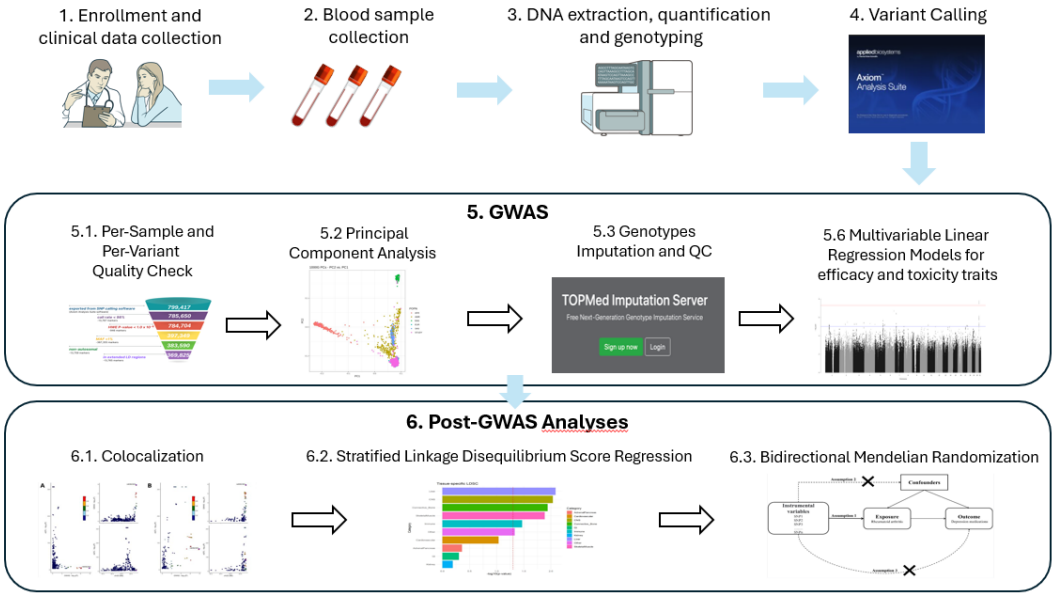


**Figure 2**. General workflow of the methodology used for this research project.

## 5.1 Patients series, samples and data collection

This study included 2,193 European adult patients with locally advanced or metastatic tumors. Opioids from the third step of the WHO analgesic (i.e., buprenorphine, fentanyl, morphine and oxycodone) were administered to the patients for the treatment of cancer pain. The patients were previously enrolled as participants to three clinical studies: CERP[81], an Italian multicenter, randomized, and longitudinal phase IV clinical trial; EPOS[82], a European multicentric and cross-sectional study; and MOLO[83], an Italian, longitudinal study. The recruitment was conducted under ethical approval, as already stated in section 2. The inclusion criteria for the three studies are listed in **Table 3**.

**Table 3.** Patient inclusion criteria for the three clinical studies.

| Study | Inclusion criteria | Reference |
|---|---|---|
| CERP | Adults with histological or cytological evidence of advanced solid tumor, with a level of pain intensity greater than 4 (on a 0-10 numerical rating scale) requiring, for the first time, an analgesic treatment with step III WHO opioids (opioid-naïve patients); life expectancy >1 month; no contraindications to fentanyl, oxycodone, buprenorphine or morphine | Corli et al, 2016 [81] |
| EPOS | Adults with malignant disease, who were using an opioid for moderate to severe pain (step III on the WHO treatment ladder for cancer pain). | Kurita et al, 2011 [82] |
| MOLO | Adult patients with solid or metastatic tumor, with a level of pain intensity greater than 4 (on a 0-10 numerical rating scale) and a life expectancy >1 month. | Shkodra et al, 2022 [83] |

For each patient, the following clinical and personal information was collected: age, sex, country of origin, cancer diagnosis, chemotherapy treatment at the time of recruitment, opioid drug and dose in morphine milligram equivalents (MME), calculated as in Caraceni et al, 2012[84]. Also, information about the quality of life, response to opioids (i.e., the experienced pain intensity), and intensity of side effects experienced during the therapy, was collected. In detail, in MOLO and CERP studies, the two longitudinal ones, data were collected at the enrolment and in five following visits (72 hours, 7, 14, 21 and 28 days after recruitment, during opioid antalgic therapy); in EPOS, since it was a cross-sectional prevalence study, data were collected at a single time point during opioid treatment.

## 5.2 Definition of opioid efficacy and toxicity phenotypes

For the opioid efficacy phenotype, clinical data regarding patients' pain experiences were collected using the brief pain inventory (BPI) questionnaire.[85] This instrument was developed by the pain research group of the WHO collaborating center for symptom evaluation in cancer care. It includes questions about several pain-related information, such as the

intensity of pain, location(s) of pain, and various aspects related to analgesic treatment. The overall response to opioid treatment was evaluated through the average pain intensity (PI) score measured in the last 24 hours preceding the clinician visit. Particularly, pain intensity was measured using an 11-point numerical rating scale ranging from 0 (no pain) to 10 (worst imaginable pain). Within this scale, higher scores indicated increased or worsening pain, whereas lower scores were interpreted as greater analgesic effectiveness, reflecting a positive response to opioid therapy. For the CERP and MOLO longitudinal series, the pain intensity was calculated as the average across all time points. For EPOS, due to its cross-sectional nature, a single value was used per patient. For opioid-induced toxicity, I focused on one of the most common and distressing side effects: nausea and vomiting. This phenotype was defined using a composite nausea vomiting score (NVS), which was derived from patient responses to the European Organization for Research and Treatment of Cancer Core Quality of Life Questionnaire (EORTC QLQ-C30)[86], in particular, questions n. 14 ("Have you felt nauseated?") and n. 15 ("Have you vomited?"). This questionnaire is a standardized tool that assesses the quality of life of cancer patients, including the impact of treatment-related symptoms. Patients could answer to these two questions by using a 4-point rating scale as follows: 1, "not at all", 2, "a little"), 3 ("quite a bit"), 4 ("very much") The NVS was calculated based on a composite formula aligned with the EORTC scoring guidelines [l]: a raw score was calculated performing the mean of the different component items. For nausea and vomiting, the raw score was calculated for each patient as follows:

$$eq.1\ Raw\ Score = RS = (Q_{14} + Q_{15})/2$$

Then, the composite NVS was calculated using the formula in eq.2.

$$eq.2\ \ NVS = \{(RS-1)/2\}x100$$

The resulting NVS ranged from 0 to 100, with 0 indicating no symptoms of nausea or vomiting, and 100 reflecting the most severe symptoms. As above, for the CERP and MOLO longitudinal series, the NVS was calculated as the average across all time points, ensuring a comprehensive view of each patient's symptom burden over time, whereas for EPOS patients a single NVS value was used. This rigorous and standardized approach to phenotype definition aimed to ensure consistency across cohorts and to maximize the

[l] EORTC QLQ-C30 Scoring Manual: Quality of Life Assessment

reliability of subsequent GWAS analyses investigating the genetic determinants of opioid response and toxicity.

## 5.3 DNA extraction, quantification and genotyping

For all EPOS and CERP patients (enrolled in the years from 2000 and 2015) and for the first 200 patients enrolled in the MOLO study before 2020, genomic DNA was already available in the biobanks of collaborating hospitals. An additional 100 patients were prospectively recruited in the MOLO study during the first year of this scientific project, and 5 ml of peripheral blood samples were collected in EDTA-containing tubes. Genomic DNA was then extracted from whole blood, using the DNeasy Blood & Tissue kit (Qiagen); DNA quantification was fluorometrically assessed using the Quant-iT PicoGreen dsDNA Assay (Thermo Fisher Scientific).

## 5.4 Multivariable linear regression model with clinical data

### *5.4.1 Opioid Toxicity*

To understand which of the collected clinical variable were significantly associated with the opioid toxicity phenotype, a multivariable linear regression was performed using the generalized linear model implemented in the `glm()` function in R v.4.2.[87] NVS was used as dependent and quantitative variable, while all the collected available clinical variables (sex, age, genotyping batch, the study and country in which each patient were recruited, the administered opioid, the morphine-equivalent dose, tumor diagnosis and chemotherapy treatment) were used as independent ones. The model used was designed as followed:

*eq.3 NVS ~ sex + age + study + batch + country + opioid + dosage + cancer diagnosis + chemotherapy*

To reduce the risk of overfitting, a stepwise model selection based on the Akaike information criterion (AIC) was performed. The model with the lowest AIC balances goodness of fitness and complexity best, allowing for the identification of the factors that are significantly and independently associated with the toxicity phenotype. The variables selected from the AIC-based stepwise selection model were then retained and used as covariates in the subsequent GWAS.

### *5.4.2. Opioid efficacy*

Similarly to the toxicity phenotype, the following multivariable linear regression model was tested for pain intensity using all the available collected clinical variables:

*eq.4 pain intensity ~ sex + age + study + batch + country + opioid + cancer diagnosis + chemotherapy*

This linear model allowed to estimate the contribution of each clinical factor in the interindividual variability in pain response (defined as a quantitative trait). Once fitted, the model residuals were assessed for normality, applying the Shapiro–Wilk test, with the `shapiro.test` function in `stats` package in R (v.4.2) environment.[88] If the residuals were significantly non-normal (*P*-value < 0.05), further transformation was necessary to normalize them. Model residuals were transformed using the inverse-normal transformation (INT) using the following formula:

*eq.5 qnorm((rank(r, na.last = "keep") - 0.5) / sum(!is.na(r)))*

where *r* are the model residuals.[89] This rank-based INT maps the residuals to a standard normal distribution (mean = 0, SD = 1), while maintaining the ordinal relationships among the data points. The approach has been widely adopted in GWAS to control non-normality and reduce the influence of outliers. The resulting normalized residuals were then used as the quantitative phenotype in GWAS to identify genetic variants associated with variability in opioid-related pain intensity, while adjusting for potential clinical confounders.

## 5.5 Genotype calling and quality check, relatedness and genetic ancestry detection, and genotype imputation

### *5.5.1. Genotype calling and quality check*

Genome-wide genotyping was carried out using Axiom Precision Medicine Research Arrays (Thermo Fisher Scientific). These arrays comprise over 900,000 SNPs, including 5,000 pharmacogenomic variants, from PharmGKB, and more than 800,000 GWAS markers. Genotype variant calling was performed using the Axiom Analysis Suite v.5.01.38 software,

with the “Best Practice Workflow” and default quality check (QC) settings, except for the average call rate for passing samples which was set to ≥ 97%. After removing samples that failed Axiom QC, as shown in *eq.6*, patient’s genotypes were extracted and converted into binary PLINK format, including only biallelic SNPs (options *--snps-only just-acgt* and *–biallelic-only* flag of PLINK software v.1.9.[90]

*eq.6 plink --file MyInputFile --snps-only just-acgt --biallelic-only --make-bed --out MyOutputFile*

Quality checks were performed at the per-sample and per-marker level. In detail, discrepancies between the sex reported in the clinical records and that imputed from each patients’ genotypes were detected using the flag *--check-sex* and samples with sex discrepancies were removed. Samples with low call rates, i.e., with a missing genotype rate > 5% with respect to the number of typed SNPs, were filtered out using the flag *--mind 0.05*. All SNPs with a missing call rate exceeding 2% were removed using the flag *--geno 0.02.* Then, the Hardy-Weinberg (HW) exact test was performed to remove variants in high HW disequilibrium (*--hwe* 1e-6). Finally, rare SNPs (with a minor allele frequency, MAF < 1%) were excluded, with the *--maf* 0.01 option, as follows:

*eq.7 plink --bfile MyOutputFile --geno 0.02 --mind 0.05 --remove SexProblems.txt -- hwe* 1e-6 *--maf 0.01 --out MyOutputFile_1*

### *5.5.2 Relatedness and genetic ancestry detection*

Individuals who are first- or second-degree relatives share a higher number of genetic loci and chromosomal regions than unrelated individuals. This introduces an important bias into population genetic analyses, as it can reduce the observed genetic variability. Therefore, related individuals must be excluded from the sample sets analyzed. Individual relatedness i.e., the degree of recent shared ancestry for a pair of individuals (identity by descent, IBD), is usually estimated through the calculation of the genome-wide identity by state (IBS)[91], by examining the number of segments shared by individuals that were inherited from a common ancestor. The higher the number, the higher the probability that these individuals are related to each other. The IBS statistics need to be performed on independent SNPs, i.e. SNPs that

are not in linkage disequilibrium (LD). LD is defined as the non-random association, at different and close loci on the same chromosome, of alleles in each population. To avoid biases in IBS calculation, it is necessary to identify and exclude the subset of SNPs in LD with each other from the dataset, performing the so called “pruning” of the genetic dataset. *Pruning* can be achieved by using the *--indep-pairwise* option of PLINK, which is based on the measure of pairwise genotypic correlation. It is necessary to specify three different parameters: the windows size (i.e., the SNPs to be analyzed each time), the step size (i.e., the SNPs number to shift the windows at each step) and $r^2$ threshold, a measure of LD. The option *--indep-pairwise 20 2 0.2* was applied to identified SNPs with an $r^2 > 0.2$, with a 20-SNPs sliding window and a step of 2 SNPs which were then removed with the *--exclude* option, as described in *eq.8* and *eq.9.*

*eq.8 plink --bfile MyOutputFile_1 --indep-pairwise 20 2 0.2 --out MyOutputFile_1_prune*

*eq.9 plink --bfile MyOutputFile_1 --exclude MyOutputFile_1_prune.prune.out --make-bed --out MyOutputFile_1_pruned*

The IBS/IBD test was performed with PLINK using the *--genome* option and individuals showing a PI_HAT value > 0.185, which means a genetic relatedness halfway between the expected IBD for third- and second-degree relatives (IBD = 0.125 and 0.25, respectively), were removed using the *--remove* PLINK option, as described in *eq.10* and *eq.11.*

*eq.10 plink --bfile MyOutputFile_1_pruned –genome --min 0.185 --out MyOutputFile_1_pruned_IBD*

*eq.11 plink --bfile MyOutputFile_1 --remove MyRelatedIDs.txt --make-bed --out MyOutputFile_1_IBD*

Then, principal component analysis (PCA) was used to quantify and identify population structure and stratification due to different genetic ancestry, PCA is widely used in population genetic studies.[92–94] It is a dimensionality reduction method used to reduce the complexity of large datasets without losing important information. It transforms correlated variables into

new variables, called principal components (PCs), which are uncorrelated and ordered by decreasing variability. Principal components are represented in the orthogonal axes of a new bidimensional (or tridimensional) graph. The first two principal components describe the greatest possible variance present in the original dataset (PC1 has higher variance than PC2 and so on for all the considered PCs). The same pruned SNPs set (n = 176,597 variants) used for IBD analysis, was then used to perform PCA using *--pca* in PLINK, as follows:

*eq.12 plink --bfile MyOutputFile_1_pruned --pca --out MyOutputFile_1_pca*

To better understand the genetic ancestry of our patient series, we projected the PCs of our patients along those of individuals from five populations of different ancestries, selected from 1000Genome Projects [95]. Particularly, we selected 1,563 individuals from Africa (AFR), America (AMR), South-East Asia (SAS), East Asia (EAS), and Europe (EUR). The scatterplot of the PC1 vs. PC2 and PC3 vs. PC4 was then plotted by grouping and coloring dots at continental level. Patients that did not cluster with Europeans were removed from the dataset, as shown in *eq.13*. To perform the PCs projection, the same workflow described at this link (https://github.com/long-covid-hg/pca_projection) was followed.

*eq.13 plink --bfile MyOutputFile_1_IBD --remove NonEuropean.txt --make-bed --out MyOutputFile_2_DEF*

### *5.5.3 Genotype imputation*

The genotype imputation has the aim of inferring genotypes at untyped loci, enhancing genome coverage, increasing the ability to detect genetic associations, and improving interpretation of the results of the association studies.[96] Genotype imputation methods rely on the reconstruction of haplotype segments, shared by the study's individuals and a reference panel of sequenced genomes, to assign missing genotyping data. For this study, we split our dataset by chromosome and then imputed the genotype of 2,130 individuals using the TopMED imputation server.[97] The following parameters were set using Build: hg38; Reference Panel: TopMED; Population: All; Phasing: Eagle; Mode: Imputation. The imputed genotypes were then filtered to exclude rare variants (MAF < 2%) and those with a low-quality imputation ($R^2$ info score ≤ 0.3).[98]

## 5.6. Genome-wide association studies

GWAS was performed using REGENIE software, with the default settings[II]. REGENIE is a C++ program based on a machine learning algorithm, developed at the Regeneron Genetics Center.[99] It is used for whole-genome regression modelling in large genome-wide association studies. It efficiently processes quantitative, binary, and categorical traits. The REGENIE pipeline is split into two steps:

- ***Step 1****:* a whole-genome regression model is fitted to a subset of the available genetic markers (defined ***a priori*** in N blocks using the option *--bsize*). The ridge regression is performed considering the LD to calculate a set of ridge regression predictors in each block of genetic variants. The aim is to "capture the unknown number and size of truly associated genetic markers within each window". Then, a K-fold cross validation is performed to assess the predictive performance of the whole-genome model and control overfitting induced by using the first level of ridge regression to derive the predictors. Finally, the genetic predictors are calculated for all chromosomes except for one, one at the time, using a leave one chromosome out (LOCO, using the *--loocv* flag) approach.

A `.loco` prediction file is generated, containing the calculated genetic predictors. The Regenie Step 1 is performed as follows, specifying the names of the trait to be used as phenotype and the names of the covariates to be included in the model. Also, additional options are included to reduce computational time and the output file dimension.

```
eq.14 ./regenie_v3.2.5.gz_x86_64_Centos7_mkl --bed MyOutputFile_2
--step 1 --phenoFile MyPhenotypeFile.txt --phenoCol av_NVS, PI_resINT
--covarFile MyCovariatesFile.txt --covarColList age,OMED
--catCovarList sex01,study_bisNUM_2,study_bisNUM_1,country_simply01
--qt --lowmem --threads 12 --bsize 1000 --gz --loocv
--out MyRegenieSte1.Output
```

[II] https://rgcgithub.github.io/regenie/options/

- ***Step 2***: the second step is performed using the imputed genotypes. Here, a single-variant association test is performed on a larger set of markers, using the `.loco` file generated in step 1 as genetic predictors. To ensure the highest statistical power and to catch every signal of association between genetic data and our trait of interest, the additive model was used.

Whole-genome regression for the toxicity phenotype (NVS) was performed, with those clinical variables that resulted significantly associated with NVS, as covariates (i.e., age, sex, the opioid morphine-equivalent dose, and the study in which each patient was recruited, coded as a dummy variable). For the pain intensity analysis, the INT residuals of the model with clinical variables were used as dependent variable in the whole genome regression with genotypes (n= 7,669,761).

```
eq.15 ./regenie_v3.2.5.gz_x86_64_Centos7_mkl --gen MyImputedFile
--step 2 –pred MyGeneticPredictors.pred.list
--phenoFile MyPhenotypeFile.txt --phenoCol av_NVS,PI_resINT
--covarFile MyCovariatesFile.txt --covarColList age,OMED
--catCovarList sex01,study_bisNUM_2,study_bisNUM_1,country_simply01
--qt --lowmem --threads 12 --bsize 1000 --gz
--out MyRegenieStep2.output
```

The genome-wide significance threshold was set at a *P*-value < $5.0 \times 10^{-8}$ and a suggestive threshold was set at *P*-value < $1.0 \times 10^{-5}$. The results of the two association analyses were reported in Manhattan plots, drawn using the `Manhattan()` function of the `qqman` package in R environment.[100] Also-significant variants were drawn using the function *`locus.zoom()`* in R environment.[101] The LD square matrix was calculated with PLINK v.2 software.[102]

## 5.7 Heritability estimation

SNPs-based heritability is the proportion of the phenotypic variance explained by all the SNPs along the genome, used in GWAS. SNP-based heritability was estimated from GWAS summary statistics using linkage disequilibrium score regression (LDSC) [103]. Using GWAS summary statistics to calculate heritability, it relied on the fact that SNPs in high LD with many neighboring variants are more likely to tag causal variants and will have higher test statistics in a GWAS. LDSC usually performs a regression between the chi-squared values from the GWAS and the LD score from a reference population: the slope of this regression provides evidence of the SNP-based heritability. Here, our pain intensity GWAS summary statistics were standardized, and alleles were aligned and merged with a reference SNP list from HapMap3. The Python script *munge_sumstats.py* provided by LDSC was used, and specifying the flag *–h2*, our summary statistics were merged with pre-computed LD scores from 500 European samples from 1000 Genome project, to calculate the heritability of pain intensity phenotype.

## 5.8 In *silico* functional analyses and post-GWAS analyses for opioid efficacy

### *5.8.1 Functional annotation*

The identified germline polymorphisms associated with phenotypic traits at the suggestive threshold (*P*-value < $1.0 \times 10^{-5}$) were annotated using the SNPnexus tool.[104] In addition, candidate cis-regulatory regions (cCREs), according to ENCODE data[105] (Registry of cCREs V3, accessed on 08/05/2024), that matched the positions of the identified variants were searched. The identified polymorphisms were also mapped to transcription factor binding sites, using the SNP2TFBS tool[106] (accessed on 09/05/2024), which relies on the JASPAR database of transcription factor binding sites.[107] Functional annotation with RegulomeDB 2.2[108] was also performed (accessed on 21/05/2024). Then, the same polymorphisms were investigated for their possible regulatory role by searching for them in three public eQTL databases: GTEx (Analysis V8 release, GTEx_Analysis_v8_eQTL_EUR.tar), eQTLGen [109] (accessed on 17 April 2024) and MetaBrain [110] (accessed on 17 April 2024). GTEx search for candidate variants associated with NVS was also done (accessed on 08/24/2023). Finally, the top-significant variants were searched in the Open Target Genetics portal [111,112] to retrieve phenome-wide association study (PheWAS) information across UK Biobank phenotypes. Only traits associated with the searched variants with *P*-values $<1.0 \times 10^{-5}$ were reported.

### *5.8.2 Colocalization analysis*

Colocalization analyses were carried out using the `coloc` R package [113] applying default prior settings. These analyses integrated our GWAS summary statistics with data from the eQTLGen dataset. The colocalization analysis evaluates five hypotheses: no association with either trait (H0); association with only pain intensity (H1) or only gene expression (H2); association with both traits but due to independent causal variants (H3); and a shared causal variant regulating both traits (colocalization, H4). Following standard assumptions, a posterior probability ≥0.8 for H4 was considered strong evidence of colocalization, while values between 0.5 and 0.8 were interpreted as moderate evidence. Colocalization plots were also generated using the same `coloc` package.

### *5.8.3. Linkage Disequilibrium score regression analysis*

In order to observe the tissue-specific contribution of germline variants to the genetic architecture of pain intensity in advanced cancer patients, stratified Linkage Disequilibrium Score Regression (sLDSC) analysis was applied. Generally, this method allows to extend the traditional LDSC, incorporating functional genomic annotation, and partitioning a SNP-based heritability across biologically meaningful categories related to tissue-specific regulatory activity. In general, LDSC estimates SNP heritability using a regression of the association test statistics from a GWAS on the corresponding linkage disequilibrium (LD) scores, which represent the degree of correlation a given variant has with surrounding variants. The underlying assumption is that SNPs in higher LD with other variants tend to capture more heritability if polygenicity is present. The stratified version, sLDSC, expands this model, evaluating whether specific functional categories of SNPs contribute disproportionately to heritability. A category is considered enriched when SNPs with high LD to that category show systematically elevated $\chi^2$ statistics compared with SNPs with low LD to that category[114]. To achieve this, sLDSC incorporates a set of binary or continuous annotation terms representing functional categories (e.g., tissue-specific chromatin marks, eQTL regions, or regulatory domains).[115] Particularly, sLDSC analysis was carried out using the LDSC software [III]: the enrichment for central nervous system (CNS), kidney, pancreas, skeletal muscle, gastrointestinal tissue (GI), cardiovascular, and liver was estimated using eQTL reference datasets, based on GTEx or other relevant eQTLs[116], to ensure a robust annotation coverage. These annotation datasets allowed the mapping of

[III] https://github.com/bulik/ldsc

SNPs in those genomic regions with a high tissue-specific transcriptional activity and potential regulatory function in that tissue.

The summary statistics from our genome-wide association study of pain intensity in advanced cancer patients was used as input file and the heritability for it was calculated (using the flag `--h2`) for the sLDSC analysis. Then, we used default LDSC parameters, setting a reference panel for each different tissue and a baseline control (calculated on 1000 Genomes Project samples) to minimize confounding factors (using the flag `--ref-ld-chr`). Also, to perform the sLDSC the allele frequencies for the same population whose LD score regression was available (using `--freqfile-chr /1000G.mac5eur`) and the regression weights for each chromosome, to correct for heteroskedasticity in the regression model (using `--w-ld-chr /weights`) were needed. Statistical significance was determined by enrichment scores and *P*-values < 0.05. The results were then visualized using v.3.4.0 R's `ggplot2()` package, generating a barplot to compare expression patterns across tissues and observe the contribution of each tissue type to the genetic architecture of pain intensity.

### *5.8.4. Bidirectional Mendelian Randomization*

To infer the causal relationship between some possible pain risk factors, such as inflammatory, immune, sleep disorders and psychiatric conditions, and cancer-related pain intensity, a forward Mendelian Randomization analyses were performed.

The Mendelian Randomization looks for causal relationship between a specific disease (called "outcome") and a risk factor (called "exposure") using GWAS significant genetic variants as instrumental variables, since the exposure could influence the outcome only through the IVs. Here, the results from our GWAS summary statistics for pain intensity in advanced cancer patients, performed to test the association between genetics and cancer pain, were used as MR outcome. The significant variants from 23 different GWAS for inflammation, immune system, sleep disorders, and psychiatric conditions were instead used as exposures. They were filtered on the basis of the publication data and sample size (from 2020 up to now, and with a minimum sample size of 3,000) and then downloaded from IEU Open GWAS project [117], using the `TwoSampleMR` R package [118,119], including data about inflammatory biomarkers (e.g. C-reactive protein), psychiatric traits (e.g. depression), sleep traits (e.g. insomnia), opioid related use and abuse.

To explore also the reverse causality between sleep traits, psychiatric conditions, and cancer pain intensity, a reverse Mendelian Randomization was performed. Particularly, the significant top variant from our cancer pain GWAS was used as exposure, while the results

from different GWAS about different mental health conditions (i.e. depression, sleep duration, opioid use) were used as outcome (**Table 4**).

As a preliminary quality control step, the top genome-wide significant (*P*-value < $5 \times 10^{-8}$) variants for the chronic pain intensity were retained and then clumped with PLINK v.2.0, using a windows size of 10000 kb, a LD threshold of $r^2 = 0.005$ and a *P*-value = 0.99, to ensure independence of the selected IVs.

For each exposure-outcome pair, significant matching SNPs were retained, effect alleles were harmonized through the specific function `harmonize()` of the `TwoSampleMR` package, to ensure the same directionality between exposure and outcome datasets. To deal with the robustness of the IVs, F-statistics test was calculated using the following formula:

*eq.16* `(beta.exposure)^2 / (se.exposure)^2`

and IVs with a F statistic < 10 were excluded by the analyses. Also, the function `steiger_filtering()` was performed to deal with the presence of overlapping samples. Non overlapping samples, together with IVs robustness, are necessary in MR to detect valid causal inference between exposures and outcomes.

MR analyses were conducted using different methods to account for potential violations of standard MR assumptions: Inverse Variance Weighted (IVW),assuming no horizontal pleiotropy; Sample and Weighted modes, that group SNPs with similar causal effect estimates, assuming that the larger cluster is the true causal effect; Weighted median, which provides consistent estimates if at least 50% of the weight comes from valid instruments; MR Egger, that detect unbalanced horizontal pleiotropy.

Also, a sensitivity test, to detect heterogeneity, using the corresponding `mr_heterogeneity()` R function of the `TwoSampleMR` package, was carried out to check the variability in causal estimates across SNPs. Results of the analyses were then compared and then *P*-values, causal estimates and confidence intervals for each exposure, using the IVW method were then plotted using `grid.extra` R package, while dotplots for each single exposure-outcome pair were drawn using the `mr_scatter_plot()` function of the corresponding `TwoSampleMR` package. The STROBE-MR guidelines[IV] were followed in this study, to ensure transparent reporting of MR results.

[IV] https://www.strobe-mr.org/

**Table 4**. List of GWAS summary statistics downloaded from IEU Open GWAS project website for Mendelian Randomization analysis with corresponding PMID and sample size

| Phenotype ID | Phenotype Definition | Sample Size | PMID |
|---|---|---|---|
| *ebi-a-GCST004433* | Macrophage inflammatory protein 1b levels | 8,243 | 27989323 |
| *finn-b-K11_OTHINFLIV* | Other inflammatory liver diseases | 214,517 | - |
| *prot-c-2849_49_1* | AIF1 | 3,788 | 28240269 |
| *prot-a-62* | Allograft inflammatory factor 1 | 3,301 | 29875488 |
| *ebi-a-GCST90029070* | C-reactive protein levels | 575,531 | 35459240 |
| *ukb-d-30710_irnt* | C-reactive protein levels | 469,528 | - |
| *ebi-a-GCST90025985* | white blood cell counts | 444,734 | 34226706 |
| *ebi-a-GCST90025977* | neutrophil counts | 443,782 | 34226706 |
| *ebi-a-GCST90002379* | Basophil count | 408,112 | 32888494 |
| *ebi-a-GCST90002381* | Eosinophil count | 408,112 | 32888494 |
| *ebi-a-GCST90002316* | lymphocite count | 524,923 | 32888493 |
| *prot-a-341* | procalcitonin | 3,301 | 29875488 |
| *ebi-a-GCST005902* | depression (broad)* | 322,580 | 29662059 |
| *ukb-d-F5_DEPRESSIO* | Depression* | 361,194 | - |
| *finn-b-F5_SLEEP* | sleep disorders* | 216,454 | - |
| *ukb-b-4424* | sleep duration* | 460,099 | - |
| *finn-b-F5_INSOMNIA* | Insomnia* | 217,855 | - |
| *ieu-b-4861* | chronotype | 244,207 | - |
| *ebi-a-GCST90018994* | medication use (opioids)* | 78,808 | 34594039 |
| *finn-b-F5_OPIOIDS* | mental and behavioural disorders due to opioids* | 215,650 | - |
| *prot-c-3634_5_4* | OBCAM* | 3,788 | 28240269 |
| *prot-a-2149* | Opioid-binding protein/cell adhesion molecule | 3,301 | 29875488 |
| *ebi-a-GCST90018924* | substance dependence* | 483,856 | 34594039 |

AIF1, allograft inflammatory factor 1; OBCAM, opioid-binding protein/cell adhesion molecule-like; *Bidirectional Mendelian Randomization was performed;

# 6. Results

The results presented from section 6.1 to 6.4 have been published in the *Journal of Pain and Symptoms Management* under the title "*Genomic Study in Opioid-Treated Cancer Patients Identifies Variants Associated With Nausea-Vomiting*".[120] The same quality-control pipeline for clinical and genetic data, together with the results described from section 6.5 to section 6.6 and in 6.8 were reported in the *European Journal of Pain*, with the title "A *genome-wide association study of European advanced cancer patients treated with opioids identifies regulatory variants on chromosome 20 associated with pain intensity.*" [121]
Finally, the results described in sections 6.7 and 6.9 are original to this thesis and have not been previously published.

## 6.1 More than two thousand cancer patients treated with strong opioids are genotyped and analyzed

The whole patient series comprised 2,193 advanced cancer patients treated with opioids for cancer pain whose genomic DNA was genome-wide genotyped. The first quality check excluded 30 samples which failed genotyping quality controls of Axiom pipeline. In the subsequent per-sample quality check steps, 23 samples were removed due to sex inconsistencies, six individuals were discarded due to a low call rate, two duplicated and two related patients were removed **(Supplementary Figure 1)**. PCA detected 30 individuals with non-European ancestry that were excluded from the subsequent analyses. (**Supplementary Figure 2**). Then, 48 and 43 patients without complete NVS and pain intensity data, respectively, were excluded: The analyses were then performed on 2,052 and 2,057 patients, respectively, whose personal and clinical characteristics are summarized in **Table 5**, separately for toxicity and efficacy patient series. In detail, patients were equally distributed by sex and had a median age of 64. They received four different opioids of the III step of WHO analgesic ladder: buprenorphine (5%), fentanyl (35%), morphine (35%), and oxycodone (25%). The median morphine milligrams equivalent dose was 110 MME. The most common types of cancer were gastro-enteric (~ 18%), lung (~ 18%) or breast (~ 14%) cancer. More than two thirds of patients did not receive chemotherapy. Regarding the study of enrollment, 67% of patients were from the EPOS study, while 12% and 21% of subjects belonged to CERP and MOLO, respectively. Additionally, patients were mostly Italian (46%), Norwegian (19%), British (10%) and German (6%). Of note, all non-Italian patients were in the EPOS study. Then, about the

opioid toxicity phenotype, the median value for the NVS was 11.11 with an interquartile range of 33.33 and the mean value was 18.8 (standard deviation, SD = 24.9). The EORTC QLQ-C30 reference values for NVS in recurrent/metastatic cancer patients were lower than ours (median = 0, range: 0 – 16.7; mean = 13.1, SD = 22.5).

About the efficacy phenotype, instead, the average pain intensity measured through the Brief Pain Inventory Questionary was 3.67 with an IQR of 3.

**Table 5.** Clinical characteristics of patients.

| **Patient characteristic** | **NVS GWAS (n = 2052)** | **PI GWAS (n = 2057)** |
|---|---|---|
| Age, years, median (range) | 64 (18–91) | 64 (18–91) |
| Sex, n (%) | | |
| *Female* | 1043 (50.8) | 1044 (50.8) |
| *Male* | 1009 (49.2) | 1013 (49.2) |
| *Opioid, n (%)* | | |
| *Buprenorphine* | 103 (5.0) | 109 (5.3) |
| *Fentanyl* | 698 (34.0) | 694 (33.7) |
| *Morphine* | 711 (34.6) | 707 (34.4) |
| *Oxycodone* | 540 (26.3) | 547 (26.6) |
| Opioid dose, MME, median (IQR) | 110 (180) | |
| Tumor diagnosis, n (%) | | |
| *Lung* | 356 (17.3) | 362 (17.6) |
| *Breast* | 296 (14.4) | 299 (14.5) |
| *Gastro-enteric* | 369 (18.0) | 366 (17.8) |
| *Pancreas* | 85 (4.1) | 90 (4.4) |
| *Prostate* | 209 (10.2) | 207 (10.1) |
| *Urinary traits* | 142 (6.9) | 142 (6.9) |
| *Head and neck* | 96 (4.7) | 98 (4.8) |
| *Gynecological* | 172 (8.4) | 169 (8.2) |
| *Other or unknown* | 327 (15.9) | 324 (15.8) |
| Chemotherapy, n (%) | | |
| *Yes* | 646 (31.5) | 656 (31.9) |
| *No* | 1406 (68.5) | 1401 (68.1) |
| Study | | |
| *EPOS* | 1390 (67.7) | 1372 (66.7) |
| *CERP* | 214 (10.4) | 247 (12.0) |

| | | |
|---|---|---|
| *MOLO* | 448 (21.8) | 438 (21.9) |
| Country of enrollment (%) | | |
| *Switzerland* | 83 (4.0) | 83 (4.0) |
| *Germany* | 131 (6.4) | 127 (6.2) |
| *Denmark* | 12 (0.6) | 12 (0.6) |
| *Finland* | 28 (1.4) | 28 (1.4) |
| *Great Britain* | 207 (10.0) | 204 (10.0) |
| *Greece* | 4 (0.2) | - |
| *Island* | 122 (5.9) | 122 (5.9) |
| *Italy* | 940 (45.8) | 963 (46.8) |
| *Lithuania* | 48 (2.3) | 46 (2.2 |
| *Norway* | 382 (18.6) | 377 (18.3) |
| *Sweden* | 95 (4.6) | 95 (4.6) |
| Average NVS, median (IQR) | 11.11 (33.33) | - |
| Average PI, median (IQR) | - | 3.67 (2–5) |

## 6.2 Multivariable linear regression model identifies clinical variables associated with opioid efficacy and toxicity

To observe which clinical variables were significantly associated with the NVS and PI phenotypes, two different multivariable linear regression models were performed. About the toxicity phenotype, we observed that females have a higher NVS than males. Also, elderly people experience less nausea and vomiting than young patients and patients belonging to the EPOS group experience more nausea and vomiting side effects compared to MOLO and CERP. Regarding the administered drug, morphine-treated patients experienced more NVS than those receiving buprenorphine. Concerning the other clinical variables, there is no significant association between them and NVS. The results of this multivariable analysis are shown in **Table 6**.

**Table 6.** Multivariable linear regression model performed for opioid toxicity phenotype

| **Characteristic** | | **Beta** | ***P*-Value** |
|---|---|---|---|
| **Sex** (Male as reference) | Female | 5.5 | **$3.9\times10^{-5}$** |
| **Age** | | -0.12 | **0.0090** |
| **Study** (EPOS as reference) | CERP | -10.9 | **$4.7\times10^{-5}$** |
| | MOLO | -15.6 | **$8.6\times10^{-14}$** |
| **Opioid** (Morphine as reference) | Buprenorphine | -6.2 | **0.026** |
| | Fentanyl | -1.9 | 0.27 |
| | Oxycodone | -0.44 | 0.79 |
| **Opioid dose (MME)** | | 0.0027 | 0.12 |
| **Tumor site** (Lung as reference) | Gastro-enteric | 0.54 | 0.76 |
| | Breast | -0.40 | 0.85 |
| | Prostate | 2.1 | 0.34 |
| | Pancreas | -0.45 | 0.88 |
| | Urinary tracts | 0.96 | 0.69 |
| | Head and neck | 3.5 | 0.21 |
| | Gynecologic | 3.5 | 0.15 |
| | Other | -2.1 | 0.26 |
| **Genotyping batch** (I as reference) | II | 2.9 | 0.13 |
| | III | 1.9 | 0.28 |
| | IV | 2.0 | 0.21 |
| **Chemotherapy** (No as reference) | yes | 1.4 | 0.29 |

About the efficacy phenotype, instead, we observed that females experience more pain intensity compared to male patients, and patients belonging to the MOLO series experience more pain intensity compared to CERP and EPOS. Also, regarding the administered opioids, morphine-receiving patients experienced lower pain intensity than patients treated, instead, with fentanyl and oxycodone. Regarding the other tested clinical variables, no association had been found with the pain intensity for age, chemotherapy, tumor type, country of enrollment or genotyping batch, as shown in **Table 7.**

**Table 7.** Multivariable linear regression model performed for opioid efficacy phenotype

| Characteristic | | Beta | *P*-Value |
|---|---|---|---|
| **Sex** (Male as reference) | Female | 0.24 | **0.021** |
| **Age** | | 0.0026 | 0.47 |
| **Study** (CERP as reference) | EPOS | 0.10 | 0.66 |
| | MOLO | 0.79 | **$3.5\times10^{-6}$** |
| **Opioid** (Morphine as reference) | Buprenorphine | 0.20 | 0.35 |
| | Fentanyl | 0.38 | **0.0031** |
| | Oxycodone | 0.29 | **0.031** |
| **Tumor site** (Lung as reference) | Gastro-enteric | -0.25 | 0.071 |
| | Breast | −0.18 | 0.28 |
| | Prostate | -0.34 | 0.050 |
| | Pancreas | -0.42 | 0.065 |
| | Urinary tracts | 0.037 | 0.85 |
| | Head and neck | 0.26 | 0.24 |
| | Gynecologic | -0.0073 | 0.97 |
| | Other | -0.021 | 0.89 |
| **Genotyping batch** (I as reference) | II | 0.14 | 0.36 |
| | III | 0.26 | 0.067 |
| | IV | 0.15 | 0.24 |

For both the two phenotypes, a stepwise model selection (based on AIC), was performed to select the covariates to be used in the GWAS: age, sex, study, and dose (although the latter was not statistically significant) for the NVS phenotype, while for the PI phenotype a different approach was applied. In particular, the residuals from the above-described multivariable linear regression were extracted and inverse-normal transformed. In this case, since the residuals already contained the correction for the statically significant clinical variable, there was no need to correct for other covariates in the GWAS.

### 6.3 Genotypes quality check excludes those variants affecting the statistical power of the analyses

Genotyping data of 888,799 variants were initially obtained for each patient, and 799,417 of them passed the quality controls of the Axiom pipeline, which evaluated different metrics such as genotypes clusters, plates quality controls and genotyping call rates. To ensure reliability of the results that will be obtained from association analyses, per-marker quality controls were done. Variants with missing genotyping data > 2% were removed (n = 13,767).

The Hardy Weinberg-equilibrium test was applied, since deviation from HWE can be due to population stratification or genotyping errors and 946 variants were filtered out. Also, since rare variants could lead to false-positive associations because they are underpowered in GWAS, a filtering for low allele frequency (MAF < 1%) was applied (n = 387,355 variants). Then, 13,759 non-autosomal variants and 13,765 variants in extended LD were excluded. This final dataset comprising 369,825 variants was used in REGENIE step 1. After imputation and filtering by MAF < 2% and imputation score $R^2$ < 0.3, the dataset for the step 2 of REGENIE included 7,588,110 polymorphisms.

## 6.4 GWAS on toxicity phenotype identifies variants related to sleep and circadian rhythms

The association between the genotypes of over seven million variants, in 2,052 advanced cancer patients treated with opioids for cancer pain, and the opioid-induced nausea and vomiting, was tested. NVS was used as trait of interest in a linear regression model with the genotypes, while age, sex, study, and opioid dose were used as covariates to account for potential confounding factors. The results of this GWAS are shown in the Manhattan plot reported in **Figure 3**.

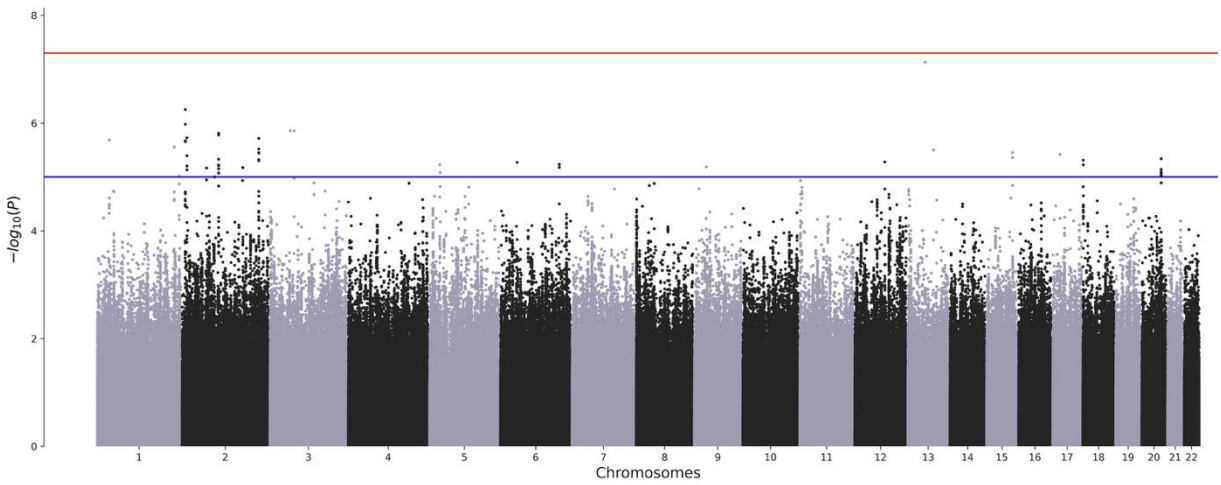


**Figure 3.** Manhattan plot of the results of the GWAS on NVS with sex, age, study, and opioid morphine-equivalent dose as covariates. Each dot represents tested polymorphisms whose coordinates are determined according to their genomic position (GChr38, hg38 release) on the x axis, and *P*-values (-log10(*P*)) of their association with NVS on the y-axis. The horizontal red line represents the genome-wide level threshold of significance (*P*-value < $5.0 \times 10^{-8}$), while the blue line is a suggestive threshold at *P*-value < $1.0 \times 10^{-5}$.

In this GWAS, no associations reached the genome-wide statistical significance threshold (*P*-value < $5.0 \times 10^{-8}$). Nevertheless, 65 variants were associated with NVS with a nominal *P*-value < $1.0 \times 10^{-5}$, the common suggestive threshold used in GWAS. Details about the results can be found in **Supplementary Table S1**.

The most significant association was observed for the intronic variant rs6562126, whose minor allele was negatively associated with NVS (*P*-value = $7.4 \times 10^{-8}$; beta = -4.34). This SNP mapped in the long noncoding gene *LINC00378* (ENSG00000225249*),* on chromosome 13, also, this variant is approximately located 118 kb downstream of the *TDRD3* (ENSG00000083544) gene, previously implicated in transcriptional regulation and RNA processing. The negative beta coefficient of this variant means that patients carrying the minor allele experienced lower nausea and vomiting intensity than carriers of major alleles.

Among the other suggestive significant signals, more than half of them mapped to six different loci. In detail, four of them mapped on chromosome 2 (with a set of four variants at six Mb, four at 10 Mb, 14 at 100 Mb, and another set of six at position 219 Mb), one additional locus was identified on chromosome 20, with a set of 12 variants and another one on chromosome 13, with four variants (19 Mb downstream the top-significant polymorphism).

Considering the two most numerous loci, the 14 variants on chromosome 2 mapped to the *NPAS2* gene (ENSG00000170485), a core circadian transcription factor. Those variants were all negatively correlated with NVS, meaning that patients carrying the minor alleles for these polymorphisms experienced less nausea and vomiting than patients carrying the major alleles. Conversely, the 12 variants on chromosome 20 mapped in an intergenic region, approximately 80 kb from the *ZNF217* (ENSG00000171940) gene, a zinc finger protein involved in transcriptional regulation. In this locus, all these polymorphisms had positive beta coefficients, indicating that the minor alleles were associated with higher nausea and vomiting incidence.

To observe the role of these variants, functional annotation has been performed, particularly with a focus on variants mapping in the *NPAS2* gene. Using GTEx database, six variants were reported as splicing quantitative trait loci (sQTLs) for *NPAS2* gene, in the esophagus mucosa. Here, an increasing number of minor alleles of these SNPs was reported to be associated with a high level of transcript splicing alteration, supporting the hypothesis that genetic variation in this locus may influence post-transcriptional regulation and, ultimately, protein function. The results from GTEx can be found in **Table 8.**

Then, carefully studying the REGENIE output, we specifically searched for variants

previously reported in the literature in relation to nausea and vomiting in opioid-treated cancer patients [67,73]. The summary statistics from the opioid toxicity phenotypes, as well as the results from the two published association studies, are shown in **Table 9.** Among them, the rs12305038 variant, originally described by Colombo *et al.*[73], was also nominally significant in our dataset (*P*-value < 0.05) and showed concordant beta coefficients across studies. None of the significant variants originally reported by *Laugsand et al.* [67] were found to be significantly associated with nausea and vomiting in our GWAS.

**Table 8.** Variants Associated with NVS and Mapping in the *NPAS2* Gene Were Previously Reported as *NPAS2* sQTLs, in GTEx.

| Variant ID | Phenotype ID * | *P*-Value | NES | Tissue |
|---|---|---|---|---|
| rs7558747 | chr2:100977799:100979559:clu_45742: ENSG00000170485.16 | $2.0 \times 10^{-8}$ | -0.64 | Esophagus - Mucosa |
| rs2289950 | chr2:100977799:100979559:clu_45742: ENSG00000170485.16 | $1.9 \times 10^{-6}$ | -0.52 | Esophagus - Mucosa |
| rs4851393 | chr2:100977799:100979559:clu_45742: ENSG00000170485.16 | $2.3 \times 10^{-6}$ | -0.51 | Esophagus - Mucosa |
| rs75107839 | chr2:100977799:100979559:clu_45742: ENSG00000170485.16 | $2.3 \times 10^{-6}$ | -0.51 | Esophagus - Mucosa |
| rs3768985 | chr2:100977799:100979559:clu_45742: ENSG00000170485.16 | $2.4 \times 10^{-6}$ | -0.52 | Esophagus - Mucosa |
| rs17025086 | chr2:100977799:100979559:clu_45742: ENSG00000170485.16 | $2.7 \times 10^{-6}$ | -0.51 | Esophagus - Mucosa |

Abbreviations: NES = normalized effect size.

∗As reported in GTEx and defined as the intron (chr:start:end) and cluster of connected components (clu_) to which the intron belongs.

**Table 9.** Comparison between the summary statistics of the genetic variants, previously reported (by Colombo *et al*. [73], Laugsand *et al*. [67]) as being associated with nausea and vomiting in opioid-treated cancer patients, and our results.

| | | previous studies | | present study | |
|---|---|---|---|---|---|
| | **variant ID** | ***P*-value** | **Beta** | ***P*-value** | **Beta** |
| **Colombo *et al*.** | rs36024412 | 0.04 | -2.2 | 0.15 | -1.1 |
| | rs168107 | 0.001 | -3.5 | 0.11 | -1.3 |
| | rs41269255 | 0.03 | 3.3 | 0.11 | 2.7 |
| | rs9393888 | 0.01 | -3.1 | 0.33 | -1.2 |
| | rs12305038 | 0.002 | -3.3 | **0.015** | -1.9 |
| | rs11882256 | 0.02 | 2.8 | 0.21 | 1.1 |
| | rs10405238 | 0.02* | 5.5* | 0.67 | 0.42 |
| **Laugsand *et al*.** | rs685550 | 0.006 | -6.7 | 0.67 | 0.35 |
| | rs1176744 | 0.005 | 4.1 | 0.33 | -0.76 |
| | rs1672717 | 0.004 | 5.8 | 0.48 | -0.53 |
| | rs165722 | 0.001 | 5.0 | 0.53 | -0.46 |
| | rs4680 | 0.002 | 4.4 | 0.51 | -0.48 |
| | rs4633 | 0.008 | 8.9 | 0.5 | -0.44 |

* summary statistics from the validation study

## 6.5 GWAS on PI phenotypes identifies five non-coding variants associated with pain intensity

A second GWAS was performed using the imputed genotypes and inverse-normal transformed (INT) residues of the model described above. The overall results for all the tested variants of this GWAS can be observed in the Manhattan plot in **Figure 4**.

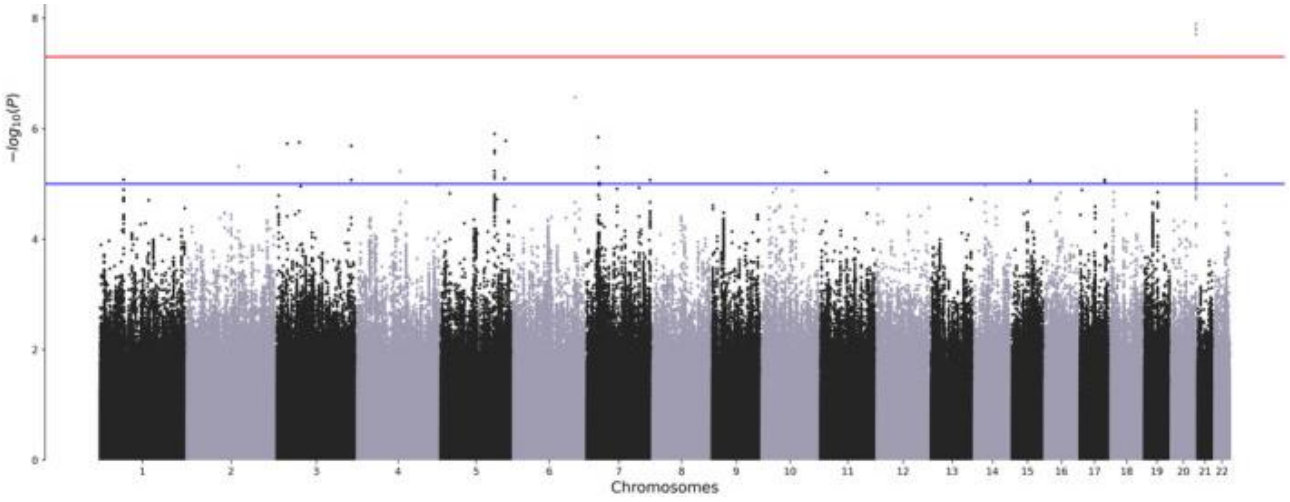


**Figure 4.** Manhattan plot of the results from the GWAS with the inverse-normal transformed residuals of the linear regression model for pain intensity phenotype, with sex, age, opioid type, cancer diagnosis, chemotherapy treatment, country of origin, study of enrolment and genotyping batch, as covariates. Each dot represents a polymorphism whose coordinates are determined according to the genomic position (GChr38, hg38 release) on the x-axis and p-values (−log10(*P*-value)) of the association with the phenotype on the y-axis. The horizontal red line represents the threshold of significance (*P*-value $<5.0 \times 10^{-8}$), while the blue line is a suggestive threshold at *P* -value $<1.0 \times 10^{-5}$.

Five germline variants (rs6062363, rs6062365, rs13043326, rs6089804 and rs1806952) associated with the pain intensity phenotype at the genome-wide significance level (*P*-value $< 5.0 \times 10^{-8}$). In detail, these variants span a non-coding region of chromosome 20, downstream *PCMTD2* gene coding isoforms. PCMTD2 is a gene encoding protein-L-isoaspartate (D-aspartate) O-methyltransferase domain-containing isoforms, implied in modulation pathways and protein repair (**Table 10**).

Considering instead the GWAS suggestive threshold of *p*-value $<1.0 \times 10^{-5}$, 66 different variants were identified and details about these variants can be found in **(Supplementary Table S2)** Notably, 31 out of 66 mapped to the chromosome 20 locus, from position 64,257,449 to 64,285,790. The complete summary statistics are publicly available in the GWAS catalog under the GCST90435150 accession code.

**Table 10.** Summary statistics of the GWAS for pain intensity (*P*-value < $5.0 \times 10^{-8}$); variants are sorted according to their *P*-value

| variant ID* | rsID | Allele 0 | Allele 1^ | Allele 1 frequency | BETA | SE | P -value | FDR |
|---|---|---|---|---|---|---|---|---|
| **chr20:64281110:G:A** | rs6062363[a] | G | A | 0.39 | -0.17 | 0.03 | $1.27 \times 10^{-8}$ | 0.03 |
| **chr20:64281343:G:A** | rs6062365[a] | G | A | 0.39 | -0.17 | 0.03 | $1.55 \times 10^{-8}$ | 0.03 |
| **chr20:64285790:T:C** | rs6089804[a] | T | C | 0.61 | -0.17 | 0.03 | $1.60 \times 10^{-8}$ | 0.03 |
| **chr20:64282739:C:A** | rs13043326[a] | C | A | 0.39 | -0.17 | 0.03 | $1.60 \times 10^{-8}$ | 0.03 |
| **chr20:64283546:A:T** | rs1806952[a] | A | T | 0.61 | -0.17 | 0.03 | $1.95 \times 10^{-8}$ | 0.03 |

* genomic position According to GRCh38 human genome reference assembly

^ Effect allele

[a] predicted function: intergenic

The negative beta coefficients of the association of the five genome-wide significant variants indicate that the minor alleles of these polymorphisms were inversely correlated with pain intensity values. Particularly, patients carrying at least one copy of the minor allele experienced a lower pain intensity than patients homozygous for the major allele. This is shown in the boxplot in **Figure 5**, where the median pain intensity values in the three patient genotyping groups, according to the top-significant variant, rs6062363 (G/A), are plotted as an example. Although the differences were quite small, patients carrying the AA genotype had the lowest median PI score (3.17), while the GA and GG carriers had increasing median PI values (3.33 and 4.00, respectively; Kruskal–Wallis *P*-value = $3.11 \times 10^{-5}$).

The leading variant was in strong LD with the other 31 suggestively significant variants on chromosome 20 (*P*-value <$1.0 \times 10^{-5}$). Particularly, an $r^2 > 0.97$ had been observed for the other four polymorphisms above the genome-wide significance threshold; all the others, except for rs58586141, rs41279358 and rs41279358, had $r^2 > 0.60$. The zoom plot in **Figure 6** reported the LD between rs6062363 and the variants in a ~200 kb region.

Finally, the estimation of heritability has been performed using the INT residuals of PI and the pre-computed LD scores for 1,146,582 SNPs. This analysis revealed that the heritability of pain intensity in cancer patients treated with opioids was quite low ($h^2 = 0.0746$; SE = 0.2062; lambda = 1.0046; mean $\chi^2 = 1.006$). This means that 7% of the pleiotropic variance

can be explained by common genetic variants. Nonetheless, this finding is consistent with the $h^2$ estimate calculated on a larger GWAS on pain intensity in individuals with different types of chronic pain [122].

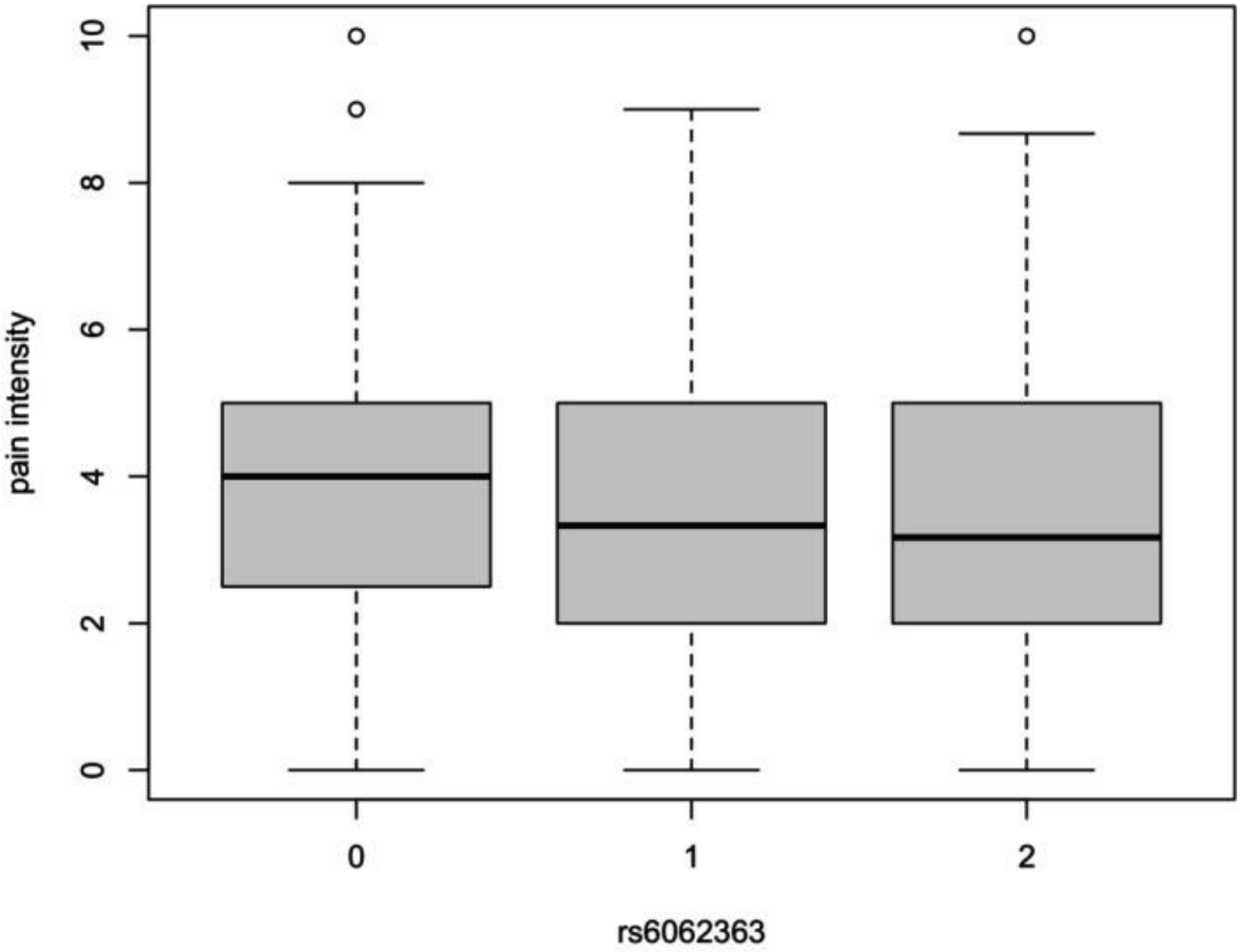


**Figure 5.** Pain intensity values in the three genotyping groups of patients, according to the top-significant variant, rs6062363 (0, GG; 1, GA; 2, AA). The line within each box represents the median pain intensity values; the upper and lower edges of each box are the 75th and 25th percentiles, respectively; the upper and lower bars indicate the highest and lowest values, respectively; outliers are indicated as circles. Differences between the differences of the pain intensity values were tested using a Kruskal Wallis, showing a significant difference between the homozygous for the major and minor alleles of $3.11 \times 10^{-5}$.

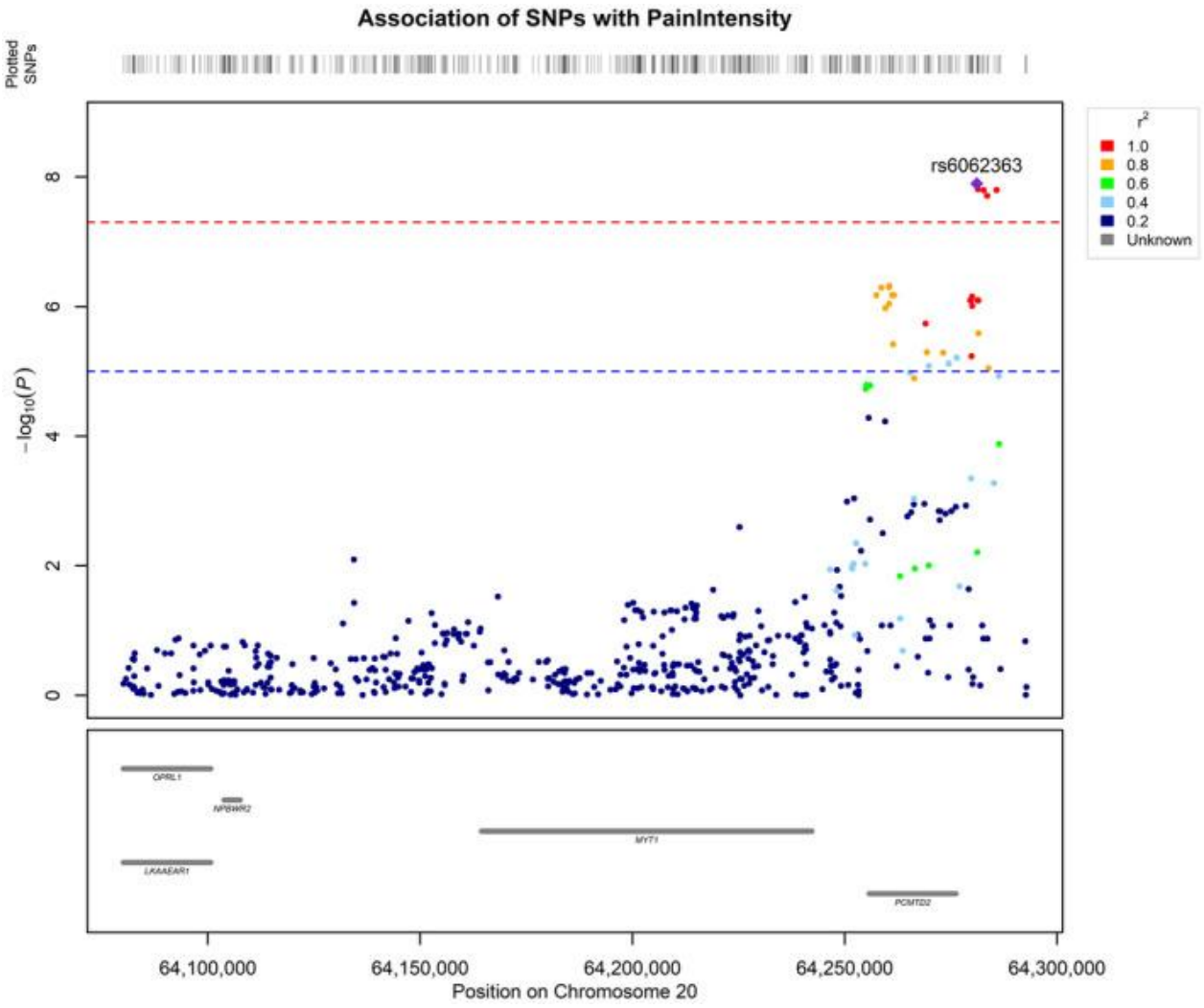


**Figure 6.** Zoom plot of the locus on chromosome 20 identified in the GWAS. The plots span the region from 64,292,800 to 64,080,100 bp. Polymorphisms are plotted according to their position on chromosome 20, along the *x*-axis, and to *p*-values ($-\log_{10} P$) for their association with pain intensity, on the y-axis. Genome-wide (*p*-value $<5.0 \times 10^{-8}$) and suggestive (*p*-value $<1.0 \times 10^{-5}$) thresholds of significance are represented as red and blue dashed lines, respectively. Dot color indicates linkage disequilibrium ($r^2$) between each polymorphism and the lead variant (rs6062363, purple diamond).

## 6.6 PCMTD2 gene expression is regulated by our top five pain-intensity associated variants

Considering that the most significant variants on chromosome 20 mapped in non-coding regions of the genome, such as introns or 3'-UTR, the hypothesis of a regulatory role of these variants on the nearest genes had been postulated. This hypothesis was supported by their functional annotation. Indeed, it has been observed that some of them mapped in candidate cis-regulatory elements (cCREs): rs1806952 is in a CTCF-binding site (EH38E3450000), while rs6512309, rs6062357, and rs7270745 localize to a distal enhancer-like region (EH38E2130198). This suggests potential effects on chromatin looping and gene insulation and is consistent with a role in transcriptional regulation. Also, using SNP2TFBS online tool, a transcription factor binding site analysis has been performed and it predicted that nine variants (rs6062681, rs6512309, rs11474881, rs6062359, rs58586141, rs1570520, rs6089801, and rs6089804) can alter transcription factor (TF) binding through a disruption of existing motifs or creating novel ones, where the minor allele is present. These results are shown in **Supplementary Table S3.**

Another functional annotation had been performed using RegulomeDB, and the results prioritized several variants as likely regulatory using a descending ranking score from 1a to 7 based on the evidence (likelihood) to be a functional variant. Particularly, two of them had a high functional probability score and the most stringent ranking classification (rs6062357, rs6089801 with PS > 0.9 and a ranking = 1b), supported by TF binding, chromatine accessibility, DNAse footprint and eQTL evidence. Conversely, rs76240558 had probability score > 0.9 but it had not been ranked in the 1b category, and the opposite was observed for rs1570520. Also, rs6512309 and rs11474881 reported strong evidence of functionality, being ranked in 1d and 2b categories meaning that the evidence for their prioritization as regulatory variants is supported by eQTL evidence, DNAse footprint, TF binding, chromatine accessibility peak, and TF binding, DNAse footprint, chromatin accessibility peak respectively. For the remaining SNPs there was only minimal supporting data for a possible regulatory function. Details from this functional annotation are shown in **Supplementary Table S4.**

A query using large-scale eQTL datasets was performed to investigate if our GWAS variants were linked to gene expression changes. Using GTEx, 29 out of 31 variants were reported as acting as eQTLs across 18 different tissues for *PCMTD2* gene, with a high involvement of central nervous system with *P*-value < $1 \times 10^{-5}$; results of this search can be found in **Supplementary Table S5**. The same variants were also queried into eQTLGen database:

here, 29 out of 31 variants were defined as eQTLs not only for *PCMTD2* gene but also for *OPRL1* and *PPDPF* in blood tissue (**Supplementary Table S6**).

Specifically focusing on brain-specific expression, a third query had been performed using MetaBrain dataset: 24 of these polymorphisms were reported as eQTLs for *PCMTD2* in the cerebellum and cortex tissues with a *P*-value < $1 \times 10^{-5}$ **(Supplementary Table S7a** and **S7b**). An inverse correlation between these variants and gene expression was observed across all datasets: in fact, the presence of minor alleles correlated with reduced *PCMTD2* expression, and in blood, with decreased expression of *OPRL1* and *PPDPF*.

To determine if our GWAS variants drove both pain intensity association signal and gene expression, a colocalization analysis had been performed using *coloc* packages, combining and comparing GWAS summary statistics with summary results from eQTLGen database (focusing on blood tissue), for *PCMTD2*, *OPRL1* and *PPTDF* genes. As graphically visualized in **Figure 7**, only mild evidence of colocalization can be found for *PCMTD2* gene, with a posterior probability of 43%, while a low posterior probability for *OPRL1* and *PPTDF* genes (0.006% and 0.23%, respectively) indicated no evidence of colocalization (**Table 11**). These results rejected the hypothesis that gene expression and pain intensity phenotypes are driven by a common causal variant.

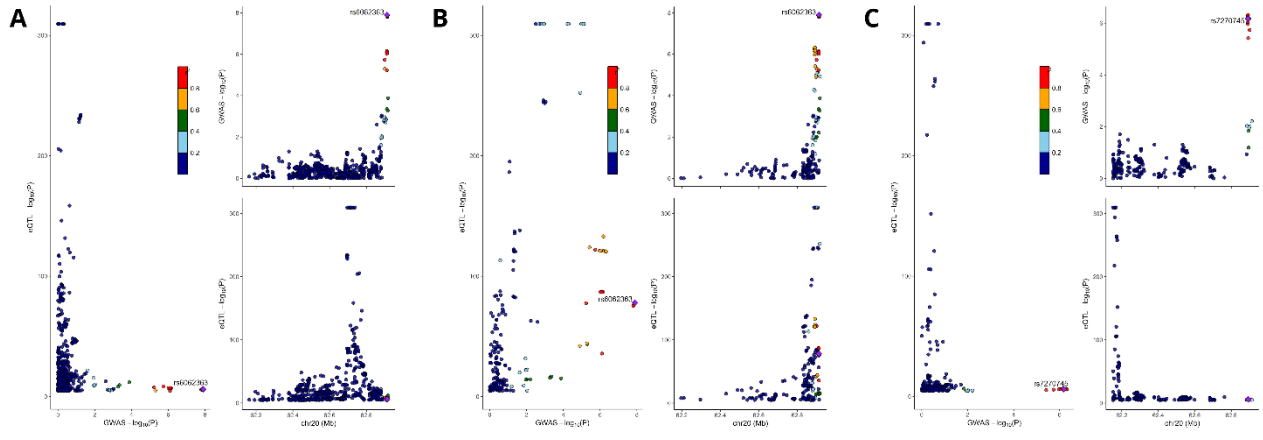


**Figure 7.** Colocalization plots for the *OPRL1* (a), *PCMTD2* (b) and *PPDPF* (c) genes using the whole-blood tissue expression data from the eQTLGen database (numbers of SNPs included in the analyses were 755, 224, and 293, respectively). Dots are colored based on linkage disequilibrium ($r^2$) with the lead variants, rs6062363 (a, b) and rs7270745 (c; *PPDPF* expression was not associated with the 5 top-significant variants associated with pain intensity).

**Table 11.** Colocalization analyses did not support the hypothesis of a shared variant regulating both pain intensity and gene expression.

| gene | N variants | P0 | P1 | P2 | P3 | P4 |
|---|---|---|---|---|---|---|
| OPRL1 | 755 | 0 | 0.00321 | 0 | 0.997 | 0.0000659 |
| PCMTD2 | 224 | 0 | 0.00166 | 0 | 0.559 | 0.439 |
| PPDPF | 293 | 0 | 0.0380 | 0 | 0.960 | 0.00237 |

P0 = probability of H0, no association with either trait

P1 = probability of H1, association with pain intensity only

P2 = probability of H2, association with expression only

P3 = probability of H3, association with both traits, but with independent causal variants

P4 = probability of H4, a shared causal variant associated with both traits

Finally, to assess broader phenotypic association, PheWAS data associated with our GWAS variants had been examined. Particularly, two lifestyle traits – tea and coffee intake – from UK Biobank had been reported as associated with the top variants identified in this GWAS, with a *P*-value < $1 \times 10^{-5}$. Particularly, tea intake was associated with all five GWAS variants for pain intensity in advanced cancer patients. Details of the PheWAS are reported in **Table S7.**

## 6.7 Stratified Linkage Disequilibrium Score Regression identifies an enrichment in brain, liver, connective bone and skeletal muscles

To reveal tissue-specific enrichment patterns for our GWAS germline variants associated with pain intensity in advanced cancer patients, stratified linkage disequilibrium score regression was performed. Details of these results can be observed in **Figure 8.**

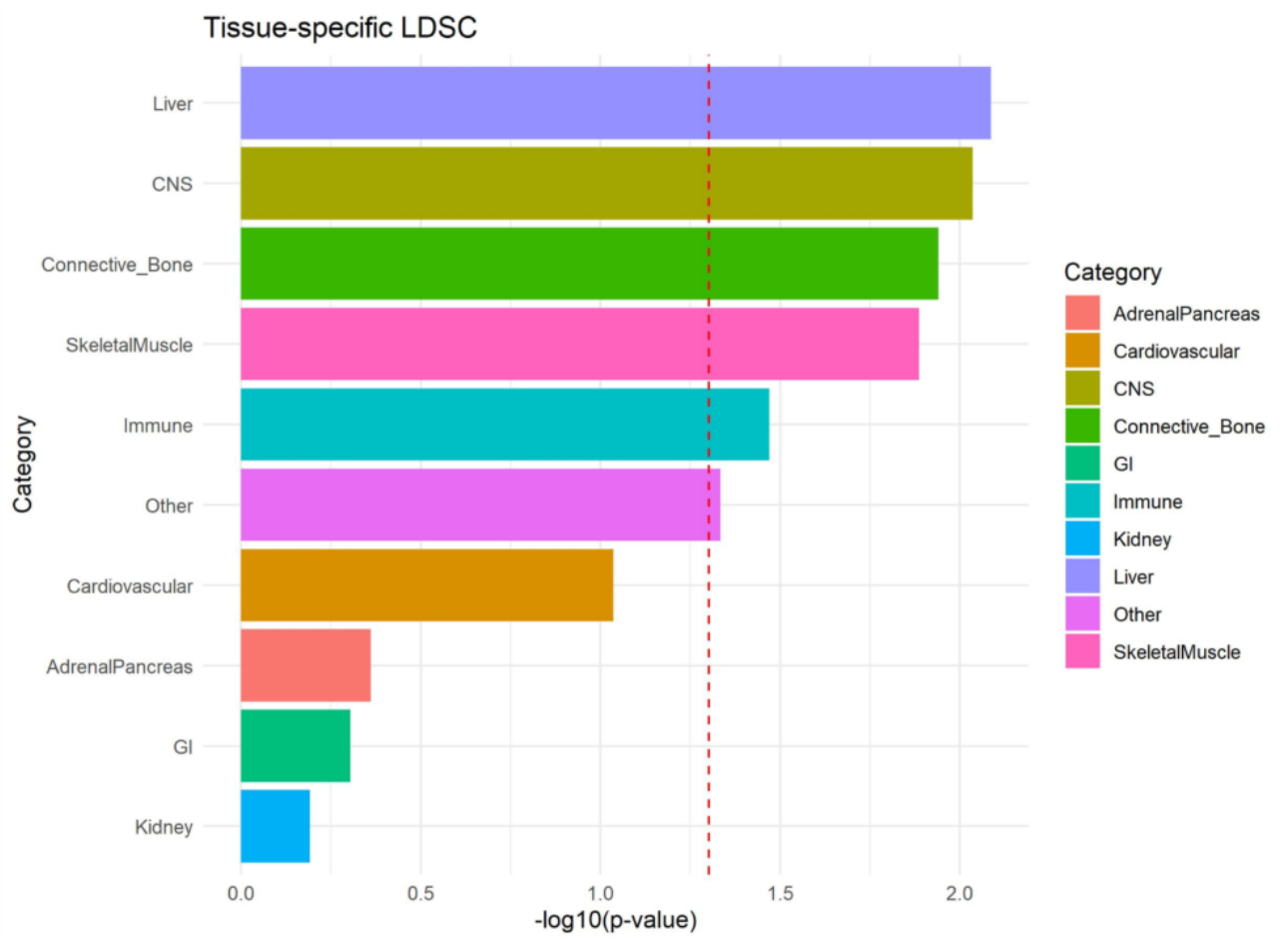


**Figure 8.** Results of the tissue specific analysis performed with sLDSC software. Tissue types were plotted on the -$\log_{10}$(*P*-value) of their enrichment. The red dashed line represents the statistically significant threshold set at *P*-value 0.05. CNS, central nervous system; GI, gastro-intestinal tissues.

Testing the enrichment patterns across nine different tissues, the strongest enrichment signals were observed in the liver (enrichment coefficient, EC = 29.25, *P*-value = $8.2 \times 10^{-3}$), and central nervous system (CNS, EC = 17.96, *P*-value = $9.2 \times 10^{-3}$). Also, connective bone and skeletal muscle were enriched (EC = 23.82, *P*-value = 0.011; EC = 22.81 and a *P*-value = 0.013, respectively). A moderate tissue-specific enrichment was observed for immune-

related tissues (EC = 13.42, *P*-value = 0.034) and other unspecified tissues (EC = 14.99, *P*-value = 0.046). These findings suggest that the heritability of pain intensity in advanced cancer patients is highly concentrated in the liver and CNS. All the calculated ECs and *P*-values for each tissue can be found in **Table 12.**

**Table 12.** Results from the stratified linkage disequilibrium score regression for nine different tissues using pain intensity phenotype

| Tissue | Enrichment coefficient | *P*-value (-log10(*P*-value)) |
|---|---|---|
| Liver | 29.250 | 0.008 (2.086) |
| CNS | 17.959 | 0.009 (2.035) |
| Connective bone | 23.818 | 0.011 (1.940) |
| Skeletal muscle | 22.806 | 0.013 (1.885) |
| Immune | 13.420 | 0.033 (1.469) |
| Other | 14.988 | 0.046 (1.333) |
| Cardiovascular | 18.984 | 0.092 (1.035) |
| Adrenal-Pancreas | 9.595 | 0.435 (0.361) |
| GI | 6.283 | 0.495 (0.304) |
| Kidney | 9.561 | 0.644 (0.191) |

CNS, central nervous system; GI, gastro-intestinal tissues.

## 6.8 The identified locus on chromosome 20 is already involved in pain related traits

Using the Human Pain Genetic DataBase (HPGDB), a comparison between the previously reported associations for pain and our findings had been performed to test whether our study independently verified any previous results. Of the 1,264 genetic variants reported, 1,170 were present in our GWAS summary statistics, and 69 of them showed a nominal association for pain intensity in our advanced cancer patients' cohorts, treated with opioids for cancer pain (*P*-value < 0,05, **Table S8**). These variants included six polymorphisms previously linked to analgesia, including one located upstream *OPRM1*. Also, four of them were previously linked to cancer pain. Unfortunately, none of these associations survived

multiple testing correction (FDR > 0.05), indicating they may represent weak or context-dependent signals.

Then, a comparison of our results with those of four previously published GWAS has been made. The earlier GWAS performed in cancer patients treated with opioids for cancer pain[71] reported eight variants associated with pain relief, although none of them had been reported as significant in our expanded dataset (**Table S9**). Then, three variants reported by Nishizawa *et al*. [72] were not replicated in our study. Comparing our results with those of another GWAS, in the UK Biobank cohort, evaluating seventeen different pain traits [123], only five reached a nominal association with a *P*-value < 0.05, as shown in **Table S10.** Finally, we compared our results with the largest GWAS performed for different types of chronic pain in veterans [122]: out of 124 significant variants reported, only 109 were tested in our opioid-treated cancer patients, finding nominal significance (*P*-value < 0.05) for nine of them, as reported in **Table S11.** However, it has been observed that our lead SNP on chromosome 20, rs6062363, lies <500 kb from the Toikumo *et al*.[122] lead SNP rs4809370. Similarly, other suggestive loci in our study (on chromosomes 1, 5, 6, 7, and 11) mapped within <500 kb—or in one case <1 Mb—of pain loci identified in Mocci *et al.* [123] and Toikumo *et al.* [122]. These results support the idea of shared regional signals between chronic and cancer pain.

### 6.9 Mendelian Randomization suggests causality for neutrophil count in our GWAS

To assess potential causal relationships between putative risk factors (exposures), such as inflammation, sleep disturbance, opioid abuse, and the intensity of cancer-related pain, a Mendelian randomization analysis was performed. [124–127] For inflammatory traits, I evaluated the causality of inflammation on cancer pain, while for the other conditions a bidirectional MR was carried out. For the first analysis, 12 inflammatory traits were available, but four of them did not share significant variants to be used as IVs.

No statistically significant causal effect on pain intensity was observed, except for the neutrophil count (*P*-value = 0.0364, beta coefficient = -0.18), using the Inverse Variance Weighted method. Other MR methods such as MR Egger, Weighted median, Simple, and Weighted mode were tested. However, no statistically significant findings were obtained, even for neutrophil count exposure. This suggests the presence of possible heterogeneity and pleiotropy.

The results, using the Inverse Variance Weighted method, can be found in **Figure 9** and **Table 13**.

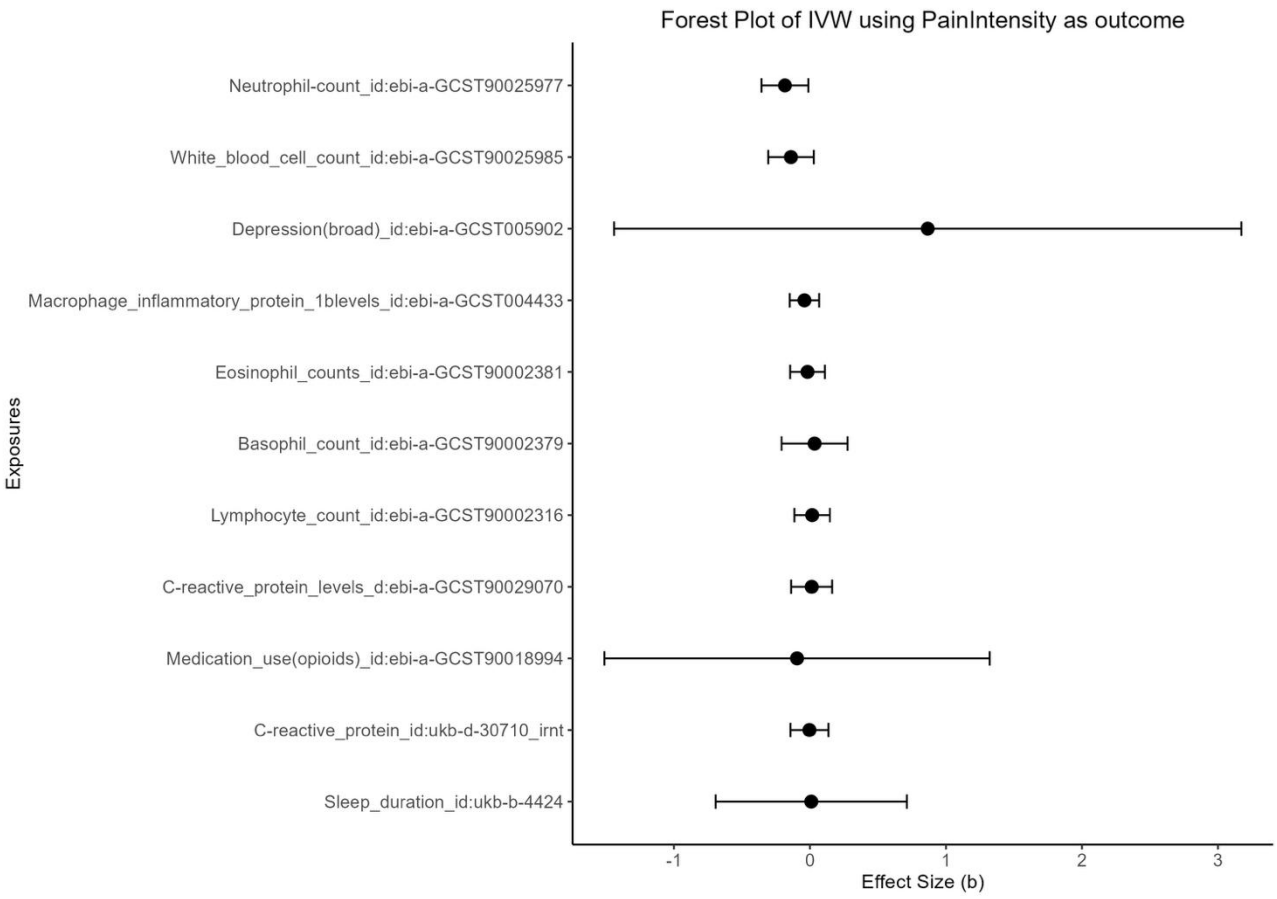


**Figure 9.** Forest plot with the results of the IVW MR performed using 11 exposures and the cancer pain intensity, as outcome. The effect size and the confidential intervals are plotted on the x-axis; exposures are plotted on y-axis, in a descendant order according to their *P*-values.

**Table 13.** Results from the Mendelian Randomization analysis (Inverse Variance Weighted method) for eleven different exposures, using cancer pain intensity as outcome

| Exposures ID | Exposure | n SNPs | SE | BETA | P | Lower CI | Upper CI |
|---|---|---|---|---|---|---|---|
| ebi-a-GCST90025977 | neutrophil counts | 308 | 0.087 | -0.183 | 0.036 | -0.356 | -0.11 |
| ebi-a-GCST90025985 | white blood cell counts | 364 | 0.085 | -0.139 | 0.103 | -0.306 | 0.028 |
| ebi-a-GCST005902 | depression (broad) | 13 | 1.176 | 0.865 | 0.461 | -1.439 | 3.171 |
| ebi-a-GCST004433 | Macrophage inflammatory protein 1b levels | 4 | 0.055 | -0.040 | 0.462 | -0.148 | 0.067 |
| ebi-a-GCST90002381 | Eosinophil count | 368 | 0.064 | -0.017 | 0.783 | -0.145 | 0.109 |
| ebi-a-GCST90002379 | Basophil count | 148 | 0.123 | 0.033 | 0.784 | -0.208 | 0.276 |
| ebi-a-GCST90002316 | lymphocyte count | 463 | 0.066 | 0.016 | 0.805 | -0.113 | 0.146 |
| ebi-a-GCST90029070 | C-reactive protein levels | 206 | 0.077 | 0.013 | 0.865 | -0.137 | 0.163 |
| ebi-a-GCST90018994 | medication use (opioids) | 2 | 0.722 | -0.094 | 0.895 | -1.510 | 1.321 |
| ukb-d-30710_irnt | C-reactive protein levels | 165 | 0.070 | -0.003 | 0.956 | -0.142 | 0.135 |
| ukb-b-4424 | sleep duration | 65 | 0.358 | 0.009 | 0.978 | -0.693 | 0.712 |

SE, standard error; CI, 95% confidential interval.

Sensitivity analyses were performed to detect horizontal pleiotropy and heterogeneity. Evidence of heterogeneity was found for basophil count (MR-Egger Q_pval = 0.029, IVW Q_pval = 0.033), neutrophil count (MR-Egger Q_pval = 0.033, IVW Q_pval = 0.036), white blood cell count (MR-Egger Q_pval = 0.011, IVW Q_pval = 0.012), suggesting potential violations of MR assumptions for these traits. Pleiotropy assessment using the MR-Egger intercept indicated limited directional pleiotropy for most exposures (*P*-value > 0.05), except for chronotype (intercept *P*-value = 0.031) and C-reactive protein from UK Biobank (*P*-value = 0.040), where evidence of horizontal pleiotropy was observed. Details of these results are shown in **Table 14**.

**Table 14.** Pleiotropy and heterogeneity tests performed for the forward Mendelian Randomization for eleven different exposures, using cancer pain intensity as outcome.

| Exposures ID | Exposure | n SNPs | IVW Q | IVW Q_Pval | MR_Egger Q | MR Egger Q_Pval | P* |
|---|---|---|---|---|---|---|---|
| ebi-a-GCST90025977 | neutrophil counts | 308 | 352.893 | 0.036 | 352.871 | 0.033 | 0.890 |
| ebi-a-GCST90025985 | white blood cell counts | 364 | 426.644 | 0.011 | 426.604 | 0.010 | 0.853 |
| ebi-a-GCST005902 | depression (broad) | 13 | 10.078 | 0.609 | 8.446 | 0.672 | 0.227 |
| ebi-a-GCST004433 | Macrophage inflammatory protein 1b levels | 4 | 2.535 | 0.468 | 2.431 | ; 0.269 | 0.797 |
| ebi-a-GCST90002381 | Eosinophil count | 368 | 361.085 | 0.577 | 360.640 | 0.569 | 0.505 |

| | | | | | | | |
|---|---|---|---|---|---|---|---|
| ebi-a-GCST90002379 | Basophil count | 148 | 180.084 | 0.032 | 179.999 | 0.029 | 0.818 |
| ebi-a-GCST90002316 | lymphocite count | 463 | 469.121 | 0.399 | 466.966 | 0.413 | 0.148 |
| ebi-a-GCST90029070 | C-reactive protein levels | 206 | 216.296 | 0.280 | 214.545 | 0.292 | 0.198 |
| ebi-a-GCST90018994 | medication use (opioids) | 2 | 4.394 | 0.036 | - | - | - |
| ukb-d-30710_irnt | C-reactive protein levels | 165 | 166.676 | 0.514 | 162.369 | 0.586 | 0.039 |
| ukb-b-4424 | sleep duration | 65 | 67.975 | 0.343 | 65.752 | 0.381 | 0.149 |

Q, Cochran's Q statistic; **P*-value for pleiotropy test.

Then, for mental health conditions (including psychiatric and sleep traits), 11 summary statistics were available, and only 3 and 10, respectively, shared significant variants to be used as IVs, for the forward and reverse MR. In the forward MR, where sleep and psychiatric traits were used as exposure, no significant results were obtained. Conversely, when using these traits as outcomes, it was observed to have a significant causality between cancer pain and sleep duration (*P*-value = 0.009, beta coefficient = -0.02). No other significant results were obtained. These results can be observed in **Figure 10** and **Table 15**. However, the power of this analysis is quite low, since only one significant variant from our cancer pain GWAS was used as IV and, therefore, the only applicable method was the Wald Ratio. Also, with only one SNPs, sensitivity analysis cannot be performed.

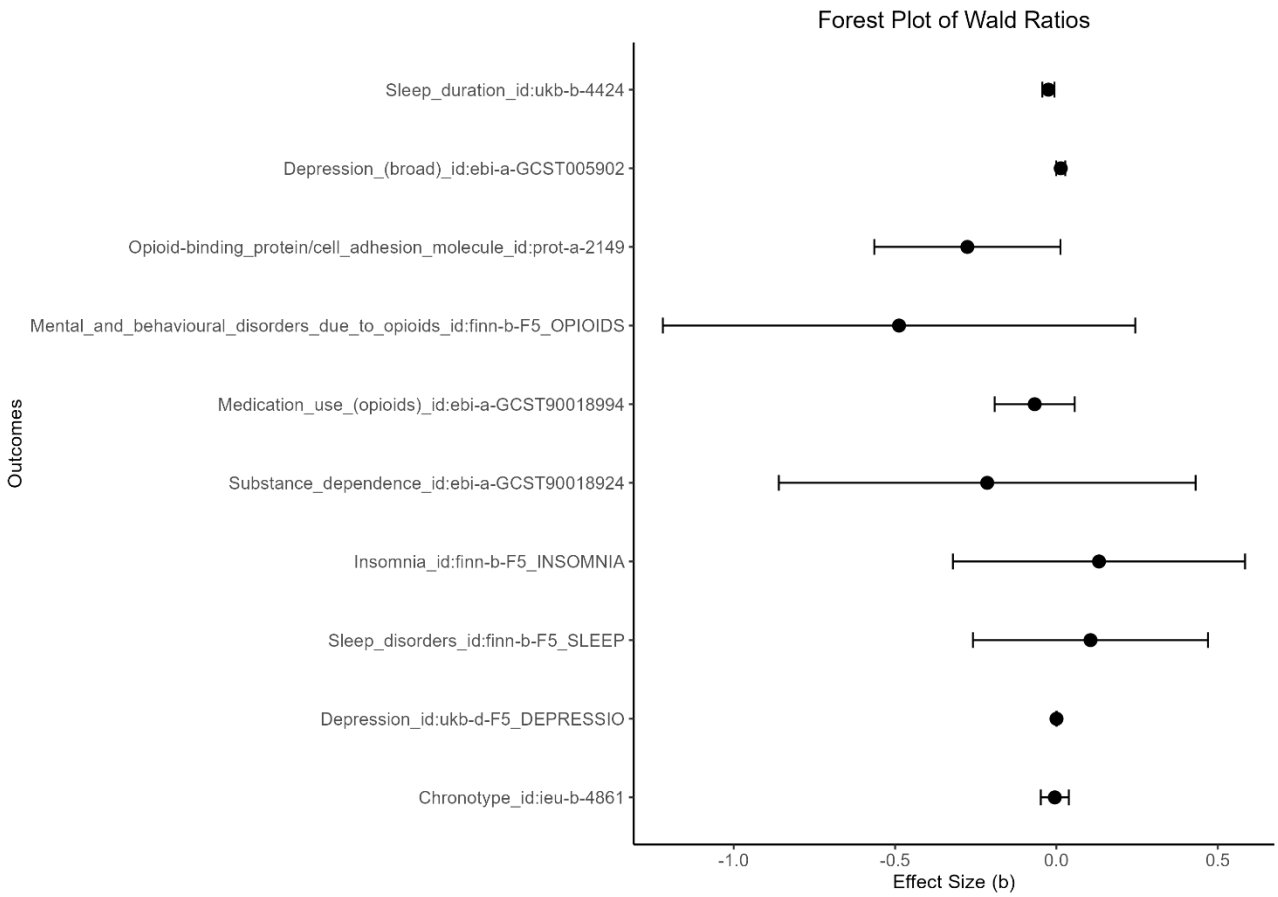


**Figure 10.** Forest plot with the results of the Wald Ratio MR performed using cancer pain as exposure and ten different outcomes. The effect size and the confidential intervals are plotted on the x-axis; outcomes are plotted on y-axis, in a descendant order according to their *P*-values.

**Table 15.** Results from the Mendelian Randomization analysis (Wald Ratio method) for cancer pain as exposure, using eleven different exposures

| Exposures ID | Exposure | n SNPs | SE | BETA | P | Lower CI | Upper CI |
|---|---|---|---|---|---|---|---|
| ukb-b-4424 | sleep duration | 1 | 0.009 | -0.024 | 0.009 | -0.043 | -0.006 |
| ebi-a-GCST005902 | depression (broad) | 1 | 0.007 | 0.013 | 0.057 | -0.0004 | 0.027 |
| prot-a-2149 | OBCAM | 1 | 0.147 | -0.276 | 0.060 | -0.564 | 0.012 |
| finn-b-F5_OPIOIDS | Mental and behavioural disorders due to opioids | 1 | 0.373 | -0.487 | 0.191 | -1.219 | 0.244 |
| ebi-a-GCST90018994 | medication use (opioids) | 1 | 0.063 | -0.067 | 0.286 | -0.191 | 0.056 |
| ebi-a-GCST90018994 | Substance dependence | 1 | 0.329 | -0.214 | 0.514 | -0.860 | 0.431 |
| finn-b-F5_INSOMNIA | Insomnia | 1 | 0.230 | 0.131 | 0.567 | -0.320 | 0.584 |
| finn-b-F5_SLEEP | Sleep disorders | 1 | 0.185 | 0.105 | 0.570 | -0.258 | 0.469 |
| ukb-d-F5_DEPRESSIO | Depression | 1 | 0.0007 | 0.0001 | 0.816 | -0.001 | 0.001 |
| ieu-b-4861 | Chronotype | 1 | 0.022 | -0.005 | 0.817 | -0.048 | 0.038 |

SE, standard error; CI, 95% confidential interval.

# 7. Discussion and conclusions

## 7.1 GWAS on toxicity phenotype identifies variants related to sleep and circadian rhythms

In this pharmacogenomic study, performed on more than 2,000 advanced cancer patients treated with step III WHO analgesic ladder opioids to relieve pain (i.e. morphine, buprenorphine, fentanyl, oxycodone), we looked for polymorphisms associated with opioid response, both in term of toxicity (nausea and vomiting intensity, calculated through a nausea vomiting score, NVS) and efficacy, in term of pain intensity experienced by the patients.

Looking at the results from the GWAS performed on opioid toxicity, 65 different variants were associated with NVS at a nominal *P*-value < $1.0 \times 10^{-5}$. Although none reached the conventional genome-wide significance threshold of $5.0 \times 10^{-8}$, variants surpassing the commonly used suggestive threshold ($1.0 \times 10^{-5}$) are typically examined further to identify potentially relevant loci. Here, an intronic polymorphism mapping in a long noncoding gene, LINC00378, rs6562126, had been found as lead variant, near the *TDRD3* gene (Tudor domain containing 3) gene. To the best of our knowledge, there is no previously published literature implicating these two genes in nausea and vomiting. No information is available on LINC00378 functional role, whereas it is known that the protein coded by *TDRD3* is responsible for the regulation of transcription, acting as a co-activator of arginine-methylated histones.[128] Also, this protein interacts with factors such as FMRP and TOP3β, linking chromatin regulation to mRNA processing and stability, whose alteration can lead to neurodevelopmental disorders.[129] To the best of my knowledge, there is no evidence for its involvement in opioid response or drug toxicity. Of note, 14 of the identified 65 variants mapped to the *NPAS2* (Neuronal PAS Domain Protein 2) gene, encoding a transcription factor regulating circadian rhythm genes, whose role had been largely studied in sleep conditions [130]. In GTEx database, six of these variants are reported to act as splicing quantitative trait loci (sQTLs) of the NPAS2 gene in the esophageal mucosa, influencing the splicing of pre-mRNA into different isoforms. However, there is no further explanation in understanding the possible role of these SNPs and how they influence the *NPAS2* isoform function, as well as the role of this circadian gene in affecting opioid-induced nausea-vomiting. Instead, the role of circadian rhythm on gastrointestinal toxicity due to other cancer therapies (e.g., chemotherapy) is under investigation (as reviewed in [131]). Nonetheless, it has been reported that NPAS2 might affect another common opioid side effect, i.e., the

alteration of the sleep-wake cycle. Indeed, in mice, it was observed that NPAS2 absence exacerbated the harmful effect of fentanyl on sleep.[132] Also, a sex-specific role of *NPAS2* was reported in mediating reward behaviors, for instance, fentanyl seeking and craving, in mice.[133] This sex-specific role was also observed in the treatment of chronic pain, particularly, in the regulation of fentanyl-induced tolerance, hyperalgesia and dependence.[134] In general, this association between germline variants mapping to a circadian gene and nausea-vomiting in cancer patients treated with opioids for cancer pain needs to be extensively studied, considering the complex relationship existing between circadian rhythm, pain, and opioids (as reviewed in [135]. The circadian rhythm can be modified by endogenous and exogenous opioids, and a disrupted sleep-wake cycle can affect the efficacy of opioid treatment, altering pain sensitivity. Additional investigations are required to better understand the role of this reciprocal link and the role of *NPAS2* gene in opioid-induced nausea and vomiting.

## 7.2 Results about GWAS on toxicity phenotype present several limitations, compared to previous opioid response and GWA studies

I compared our results with the already reported associations between germline variants and nausea-vomiting in opioid-treated cancer patients. Unfortunately, none of the SNPs reported by Laugsand *et al.* [67] was validated, although more than 80% of the EPOS patients analyzed in that study were included in our dataset. One reason might be the different genetic model used: Laugsand *et al.*[67] used three different methods (codominant, dominant and recessive) to test the association between the genotypes and nausea and vomiting, evaluating multiple inheritance models in a targeted gene analysis. In contrast, our genome-wide study used only the additive model, which is the standard approach in GWAS: the additive framework maximizes statistical power across allele frequencies, avoids the instability associated with dominant and recessive coding for rare genotypes, and mitigates the multiple-testing burden inherent to genome-wide analyses. Another reason could be the difference in the covariates used: in fact, Laugsand *et al*. [67] stratified each regression model by country, adding a binary covariate, i.e., the use of antiemetic drugs in the last 24 hours, and correcting for Karnofsky Performance Status (KPS), that is a numerical score ranging from 100 to 0 measuring the ability of each patients of conduct everyday life activity. The lack of this clinical information in our dataset reduced the possibility of an investigation of

this aspect in our GWAS. The only SNPs reported as associated with nausea and vomiting, in both the two studies, was rs1672717, passing the Benjamini-Hochberg threshold set by Laugsand *et al.* [67] at 10% in a dominant model testing only the association with nausea.

Another comparison was made between the results reported by Colombo F. *et al.*[73] and ours. They performed a first discovery exome-wide study in the EPOS series (93% overlapping with EPOS patients in this study), and then, significant associations were tested in the CERP series (82% overlapping with CERP patients in this study) for validation, confirming the association of rs12305038 SNP and nausea and vomiting in both the discovery and validation sets but with opposite beta coefficients. In our GWAS, instead, this SNP was reported as associated with NVS at *P*-value = 0.015, with a concordant beta coefficient with that of the discovery study. The DNA pooling strategy and exome sequencing, *versus* the individual genome-wide genotyping using SNP-array, as well as the choice to not adjust for confounding factors in the exome data analysis, probably reduced the rate of result validation considering the differences in the approach used.

To understand if shared genetic factors might control other nausea and vomiting phenotypes, these results were compared with those of other studies that evaluated the association between genotypes and nausea and vomiting with different etiologies such as chemotherapy [136] or postoperative nausea [137]. In the first reported systematic review, 29 different pharmacogenomics studies were evaluated in the context of chemotherapy-induced nausea and vomiting, highlighting the contribution of variants in genes involved in drug metabolism and transportation, DNA repair, neurotransmitter pathways, and cell cycle and death processes. Similarly, in the context of postoperative nausea and vomiting, 14 different genetic studies have revealed associations with polymorphisms in genes related to serotonergic and dopaminergic signaling, as well as drug metabolism and opioid receptors. Although the etiologies of nausea and vomiting in these settings are different from the one herein investigated, the potential overlap in genetic architecture with opioid-induced toxicity could provide important insights into shared pathways of susceptibility, pointing to a broader, genetically determined predisposition to nausea and vomiting across clinical contexts. Unfortunately, none of these variants match the significant ones in our GWAS.

Our nausea and vomiting GWAS presents some limitations: firstly, the lack of the clinical information, for most of the patients, regarding the use of other concomitant drugs, such as antiemetics or antidepressant. Similarly, other concurrent disease conditions that patients could have experienced, such as anxiety or intestine bowel disease, that could possibly have affected the presence of nausea and vomiting, were not evaluated, since such data

were not available. On the other hand, adding these further covariates to the GWAS would have reduced the power of the study. Another limitation is the relatively small sample size, that led to finding significant loci associated with nausea and vomiting only at the suggestive and not genome-wide significance threshold. Also, nausea and vomiting are complex phenotypes: to reduce potential bias, their definitions were standardized using questionnaires and recognized methods to calculate the NVS, but they are highly subjective feelings, influenced by external factors in addition to genetics, that plays a very small effect. Although these limitations, this GWAS on NVS in individually genotyped, opioid-treated cancer patients, is the largest performed so far. A great collaborative effort had been required from the different recruiting centers to collect such a wide patient series and related homogeneously recorded data. To validate these results, there is the need to recruit, or to use, existing broader and independent series, that could strengthen the results obtained and better dissect the genetic complexity of opioid toxicity. Also, to ensure the generalizability of the findings, further studies involving patients of different ancestries are advisable. Also, it could be worth investigating the hypothesis of a possible involvement of the circadian genes. Particularly, to understand how the identified variants affect the splicing of *NPAS2*, and how the NPAS2 splicing isoforms act in the circadian rhythm, new experimental tests are required, before exploring the mechanisms linking circadian rhythm and nausea-vomiting. In conclusion, these results regarding the genetic control of nausea and vomiting encourage the scientific community focused on opioid therapy to improve their recruitment efforts, to increase the statistical power and clinical applicability of pharmacogenomic studies for opioid therapy.

## 7.3 GWAS on efficacy phenotype identifies variants associated with pain intensity at a genome-wide level threshold, mapping near the *OPRL1* gene

In the second GWAS performed instead on the opioid efficacy phenotype, a locus on chromosome 20, significantly associated with pain intensity, has been identified at a genome-wide level threshold. To be precise, the minor alleles of five variants were markers of good response to opioid analgesic therapy: patients heterozygous or homozygous for the minor allele had lower pain intensity than patients homozygous for the major alleles. Also, these five variants were in strong linkage disequilibrium with each other and were also linked to 26 other SNPs less associated with pain intensity. These variants are in a 30 kbp region, where the protein-L-isoaspartate (D-aspartate) O-methyltransferase domain containing 2

(*PCMTD2*) gene is located. Additionally, less than 200 kbp apart mapped other protein-coding genes including the *MYT1* (myelin transcription factor 1), *NPBWR2* (neuropeptides B and W receptor 2) and *OPRL1* (opioid-related nociceptin receptor 1) genes: these are mostly expressed in the brain, and the latter two genes encoded for two different proteins involved in pain modulation (as reviewed in [138,139]). The gene *OPRL1* does not have high affinity for standard opiate ligands but it encodes for a G protein-coupled receptor of the opioid receptor family, binding nociceptine, an endogenous neuropeptide with an opioid modulatory activity and affecting analgesia [39]. Regarding the function of *PCMTD2*, literature reported that it interacts with the CUL5 protein, leading to the ubiquitination of IL2RB and negatively regulating IL2 signalling in CD8+ T cells.[140] However, its role in pain modulation is still unknown. In a study on subjects with neuropathy after traumatic nerve injuries, it has been reported that ILR2B plasma levels have been associated with neuropathic pain (but not after correction for multiple testing).[141]

The top five variants on chromosome 20 identified in our GWAS were previously reported to act as eQTLs in GTEx and eQTLGen (where the association was tested only in the blood) databases, both for *PCMTD2* and *OPRL1* genes. In fact, these genetic variants can negatively modulate the expression levels of these genes and, specifically, carriers of one or two copies of minor alleles expressed lower levels of these genes in blood, as well as in other central nervous system tissues. The *OPRL1* gene, encoding the nociceptin/orphanin FQ receptor, is of particular interest in the context of opioid pharmacogenomics as it specifically binds nociceptine, a neuropeptide that plays a role in inducing hyper- or hypoalgesia based on the modulation of this expression. *PCMTD2*, a member of methyltransferase-like proteins family, a protein group involved in protein repair or modification processes, may influence neuronal signaling stability. The fact that it is also expressed in different brain regions such as cerebellum, spinal cord and cortex, could suggest the possibility of a role of this gene to central and peripheral pathways that regulate also opioid response, but this still needs to be investigated through new functional analyses. Unfortunately, the colocalization analyses that tested if the same variants affecting gene expression are also responsible for the modulation of pain intensity does not support this hypothesis, although different tools predict these polymorphisms to be functional, potentially affecting transcription factor binding sites or other regulatory elements. Of course, further studies are needed to better understand the regulatory role of these variants and the mechanism underlying their association with pain intensity. It would be worth investigating how these variants affect OPRL1 levels in the brain or in other nervous system tissues

involved in pain signaling. Also, the impact of the lead variants on *OPRL1* expression should be evaluated in other publicly available eQTL datasets: these resources differ in tissue coverage and statistical power. For example, MetaBrain, that focuses on brain tissues, was already used, but it has lower power to detect *OPRL1* eQTLs than eQTLgen, for instance, which include data from a very large number of individuals. The lack of large datasets from relevant peripheral or central nervous system tissues (e.g., dorsal root ganglia, spinal cord, or specific cortical nuclei involved in nociception) limits the mechanistic interpretation.
Also, this study lacks functional validation performed with molecular assays that directly test the effect of the identified variants (or the true causal ones) on *OPRL1* transcription.

## 7.4 Post-GWAS analyses on efficacy phenotype identifies the central nervous system as the most enriched tissue

The results of the sLDSC suggested that the heritability of pain intensity is enriched in the liver and central nervous system, followed by connective bone and skeletal muscle tissues. This pattern aligns with known biological processes. While the liver is critically involved in drug metabolism, including the biotransformation of opioids, such as oxycodone[142,143], the CNS plays a central role in pain perception and modulation.[144,145] Also, the enrichment of connective bones and skeletal muscles was interesting, as it is known that these tissues are highly implicated in tumor invasion, metastasis and inflammation, that cause pain intensity in advanced cancer patients.[146,147] Interestingly, our results are quite consistent with the findings from the sLDSC performed for chronic non-cancer pain by Toikumo *et al.*[122] particularly for the CNS-specific enrichment as the major contributor for pain-related genetic variants and liver. Toikumo *et al.*[122] also evaluated the cell-type-specific regulation, noticing that the major contribution was, for CNS tissues, in the brain, limbic system, hippocampus, cortex, and cerebellum. Unfortunately, at the time of our GWAS analysis, the cell-type specific dataset was no longer publicly available. Thus, we could not download the information about the partitioned SNPs at a cell-type level and perform this additional analysis. However, it could be worthwhile investigating it in the future, considering a possible limitation of this approach which assumes that LD patterns and gene regulatory architectures are consistent across populations. Indeed, this may not be true for admixed populations, where LD patterns can differ from those observed in the reference panels typically used for fine-mapping or annotation: methods that explicitly account for individual ancestry could improve the resolution of variant-level effects.[148] Approaches that incorporate

a kinship matrix can better model relatedness and reduce confounding from population structure[149,150;] also, tools inferring local or global admixture proportions could quantify the contribution of each ancestral component, allowing to understand whether certain variants have an effect in specific ancestral backgrounds.[151] Such strategies could ultimately support a more precise interpretation of genetic associations and, in the longer term, contribute to more personalized therapeutic approaches. For this reason, extending these analyses to cohorts with different ancestries would help determine whether the observed associations are consistent across populations or driven by population-specific genetic structure.
Overall, our findings from sLDSC analysis provide novel insights for tissue enrichment in the heritability of cancer pain that needs further investigation.

## 7.5 Contextualization of the results from the efficacy phenotype GWAS

To contextualize our findings within the existing literature on pain genetics, I first observed if the variants reported in the Human Pain Genetic Database[152] were nominally significantly associated with pain intensity in our GWAS. These results came mostly from candidate-gene studies and one pharmacogenomics studies. Particularly, a lot of them tried to evaluate the associations between cancer pain or analgesia and genetics using a relatively small sample size. Except for the pharmacogenomics study[67], that was performed on a partial cohort of 1567 advanced cancer patients from the EPOS study here investigated, the candidate-gene study focused their attention of cohort < 400 patients. Also, the cancer pain phenotype evaluated was more specific than the one here investigated, focusing their attention on gastric, breast or lung cancer, while we evaluated the pain intensity of a different range of tumor diagnosis. Moreover, the studies evaluated were not coherent in term of genetic ancestry: some candidate gene studies, performed to evaluate the effect of the analgesia in genetics, were performed on South African advanced cancer patients or cancer patients from East Asia. This explains why the order of magnitude of significance is different from the statistical association obtained here.
Moreover, our results did not replicate the findings of the previous pain GWAS such as Galvan *et al.*[71] or Nishizawa *et al*.[72] . This lack of validation is probably due to a smaller sample size of and to the different study designs in Galvan *et al.*[71], where genetic data were obtained from pooled DNA and not individually genotyped. Also, the phenotype was based on a measure of pain relief and not intensity, which are quite different.
In Nishizawa *et al*.[72], the small sample size, the different phenotypes used (opioid

requirement) and the different genetic ancestry probably contributed to the lack of validation of the results from the Asiatic study in our GWAS.

In the multi-ancestry GWAS for chronic pain[122], a locus on chromosome 20 (20q13.33) was reported as associated with pain intensity. This is the same genomic region as our locus. Their top-significant variant, mapping 400 kbp far from ours, was not significantly associated with pain intensity in our GWAS for cancer pain, but we cannot exclude that the identified locus could be the same. In addition, other five loci, less significantly associated with pain intensity in our opioid-treated cancer patients GWAS, mapped near the lead variants of the loci identified in the other previous GWAS [122,123] . Therefore, we can affirm that our results independently validate previous findings under different pain conditions, indicating that genetics may have a role in influencing different types of pain.

Then, associations of our variants in chromosome 20 with tea and coffee intake phenotypes were revealed through the PheWAS performed with UK Biobank traits; these associations were also confirmed in a recent study in a US cohort (23andMe, Inc. research participants), suggesting a possible shared genetic control of pain intensity and caffeine (and other related natural xanthines) consumption [153]. Caffeine has an antagonistic effect on adenosine receptors, and it can induce pain relief (as reviewed in [154]) in animal models. It has been observed that interaction between caffeine, theophylline and morphine can enhance the morphine analgesic effect [155]. These findings suggest that a more in-depth study of the shared genetic mechanisms modulating both coffee/tea intake, pain intensity and opioid response are warranted. Broader studies evaluating the role of genetics on opioid-treated cancer patients for pain relief are needed to confirm our findings and, possibly, discover additional genetic loci modulating this specific type of pain. Also, our results might not be generalized to patients of ancestry different from the European one, since the variants affecting opioid response could be different in other populations. The analyzed phenotype could be considered as another limitation of our study, since pain intensity in each individual is highly subjective; however, we tried to overcome this bias with the use of standardized questionnaires to report this patient outcome. Additionally, pain intensity might be influenced by other external factors (e.g. co-existent mood disorders or other comorbidities) that we could not consider in our regression model, because we did not have this kind of information. Also, the different types of studies where our patients came from (EPOS, MOLO and CERP) probably contributed to increase the heterogeneity of this phenotype.

## 7.6 Bidirectional Mendelian Randomization results present some limitations due to the relatively small sample size

Different studies have suggested a relationship between inflammation and cancer pain, or a link between the latter and mental health.[156,157] Herein, taking advantage of our results from the GWAS on cancer pain intensity, the possible causal relationship between putative pain risk factors (e.g., inflammatory traits, psychiatric and sleep-related conditions), as well as the causality of cancer pain on mental health conditions, were investigated through bidirectional Mendelian randomization analyses, applying different methods, when possible, to ensure robustness. Unfortunately, some of the available summary statistics of the investigated traits did not include the significant germline variants identified in our GWAS, thus reducing the number of analyzable traits, since shared instrumental variables are mandatory. This may be due to the low number of statistically significant variants in our GWAS (due to its relatively limited sample size), that increase the risk of weak instrument bias, leading to a imprecise estimates and inflated Type I errors.[158] Overall, no significant results were obtained for any exposure trait, except for neutrophil count, which, however, was not confirmed using different MR methods. This may again be due to the limited statistical power of the analysis. This limitation should also be considered when discussing the interesting result of a possible causal relationship between cancer pain and sleep disturbance, since it did not allow us to test other MR methods to confirm the Wald ratio test. Another limitation of these MR analyses might be the heterogeneity and horizontal pleiotropy (violating the third assumption of MR), resulting from the sensitivity analyses performed. Larger GWAS on cancer pain would be helpful in better investigating the causal relationships preliminarily explored herein.

Several MR studies investigated the causal relationship between psychiatric, inflammation factors and sleep-related traits in different population ancestries, with chronic pain. For instance, Toikumo *et al.* [122] investigated the role of 18 different psychiatric risk factors such as drug dependences, depressive disorders, cognitive performance, finding a causal relationship between chronic pain intensity and use of opioids, depression, smoking initiation and neuroticism. Farrell *et al.* identified a causal relationship between higher C-reactive protein levels and different pain types, such as chronic pain of back, neck, shoulder and widespread pain.[159] Liang *et al.* reported also a causal relationship, in European populations, of interleukin-18 levels in neuropathic pain, to be precise in postherpetic neuralgia risk.[160] Another MR study evaluating the role of circulating inflammatory proteins

in multisite chronic pain (MCP) and site-specific chronic pain (SSCP), reported that there is a causality between them, identifying 14 different proteins such as colony-stimulating factor 1, human glial cell line-derived neurotrophic factor, IL-17C or TNF as risk factors for MCP and SSCP.[161] These results indicated that chronic pain is modulated by several inflammation factors.

Different MR studies, instead, tried to identify the causality between different sleep and psychiatric traits, and chronic pain conditions. In a bidirectional MR that evaluated the causality between mental health disorders and chronic pain, it has been observed that insomnia, depression and anxiety are causally related to the genetic susceptibility of multisite pain, including headache, back, shoulder, stomach, and abdominal pain. Reversely, some types of pain were causally related to insomnia and depression.[162] This bidirectional relationship between mental health conditions and different types of pain (e.g., widespread, chronic, short-term, and neuropathic pain) was investigated by several authors[163–166], who reported interesting findings regarding, for instance, neuroticism major depressive disorder, insomnia, and sleep duration. Generally, these findings evidence the heterogeneity of the chronic pain phenotype that is influenced by different and multiple biological and environmental factors. A limitation of these analyses can be also the use of summary statistics form large biobank resources (i.e. UK Biobank) that can suffer from selection bias due to the healthier and more socioeconomically advantaged profile of participants, that not represent correctly the general population.[167]

To the best of my knowledge, no MR studies have been performed specifically on cancer-related pain (as no specific GWAS data were available, thus far), leading to a major gap in the field, that needs to be filled. Here I proposed the first Mendelian Randomization performed for cancer pain, but a larger GWAS sample size is needed to increase the probability to detect a causality between pain intensity in cancer patients and other different risk factors. Future MR analyses would benefit from larger, multi-ancestry GWAS of cancer pain, harmonized exposure datasets, and the possibility to employ alternative sensitivity methods such as weighted median, MR-PRESSO, or multivariable MR, which are currently underpowered due to the scarcity of strong instruments. These improvements would increase robustness against pleiotropy and allow for a more comprehensive assessment of causal mechanisms.

## 7.7 Conclusions and future perspectives

To conclude and summarize, this is the largest pharmacogenomic study performed in more than 2,000 European advanced cancer patients treated with opioids of the III step of the WHO analgesic ladder for cancer pain. It allowed the identification of genetic variants modulating opioid response, both in terms of efficacy and tolerability.

This study expands the knowledge of the genetic architecture of opioid response in cancer pain, highlighting the role of genetics in opioid response and suggesting new hypotheses about the biological mechanisms contributing to this inter-individual variability. The findings obtained also underscore the importance of further replication and functional validation analyses to address the limitations encountered, such as the complexity of the opioid response phenotype as well as the limited sample size of our cancer-pain cohort.

Setting the basis for future large-scale, multi-ancestry and multi-omics studies in this field will be helpful to bring these pharmacological findings into clinical practice, personalizing the opioid therapies, improving the efficacy and minimizing the incidence of adverse effects in advanced cancer patients undergoing opioid treatment for cancer pain relief.

The next step will be the validation of the observed association in independent cohorts. So far, to the best of our knowledge, other datasets related to advanced cancer patients (treated with morphine, buprenorphine, oxycodone and fentanyl for cancer pain), evaluating nausea/vomiting intensity and pain intensity in the same way that we did, are not available. This highlights the need to improve the patient's recruitment strategies to obtain a valid replication cohort for validation. One suggestion might be using the clinical and genetic data available in existing biobanks such as UK Biobank or FinnGen. However, it is important to consider that biobanks lack accurate information about opioid use in the specific context of patients with cancer pain. For example, dosage information may be missing, or different questionnaires may have been used to collect pain information, resulting in different phenotypic data types or inconsistent clinical annotation. These issues may be even worse in the case of data on opioid adverse events. All these limitations should be considered when using biobank data to replicate the obtained findings, at least until drug-response-focused biobanks are available.

Another future perspective of my job thesis is to address the analysis of additional pain-related phenotypes (e.g. pain relief, neuropathic pain, breakthrough pain), and opioid-induced adverse effects, such as constipation, hallucinations, insomnia or respiratory depression, for some of which we already have data. These analyses will be performed not

only using the additive model, as done in the present work, but also dominant and recessive models, allowing to obtain a more precise and extended view of the genetic architecture behind the response to opioid treatment.

Also the analysis of opioid efficacy and toxicity through the use of longitudinal data (available for CERP and MOLO patients), using method such as trajGWAS[168], that take into account the changes in phenotypes across different time-point, could be useful to better explore the genetics of the dynamic changes in drug efficacy and tolerance over time, as well as the change of pain perception at each follow-up point. This would be helpful to reveal also potential biomarkers and trajectories of response that are not captured, instead, in a cross-sectional design.

Moving into the understanding of the biological role of the identified variants, functional analyses are highly necessary. These analyses can include in *vitro* or in *vivo* experiments with the aim of understanding the mechanism by which the statistically associated variants modulate opioid response, nausea/vomiting, and pain intensity. Since the identified variants are reported to act as regulatory polymorphisms, this might be tested and validated *in vitro*. For instance, a method to directly demonstrate that a SNP acts as a *cis* regulatory variant on a target gene consists in the measurement of allelic differential expression [169,170], using public transcriptomic data. In addition, although quite challenging, as most of the variants associated with the phenotype of interest map to non-coding regions of the genome, the high-throughput pooled CRISPR base editing screen[171] could be used to investigate whether specific variants influence *OPRL1* or *PCMTD2* expression, providing evidence for the mechanism underlying the observed association with pain intensity.

Then, given the fact that the genetic heritability detected explains only a small proportion of the variability in pain sensitivity and analgesic response, it could be also useful to integrate genomics with other multi-omics approaches to identify additional biomarkers of opioid response. For example, transcriptomics, epigenomics, proteomics and metabolomics can give a complementary perspective, to understand insights behind complex gene and environment interactions and their role in the treatment efficacy. Finally, artificial intelligence algorithms, as those reviewed by Acharya D. *et al.* [172], can be also used to integrate omics data and identify biomarkers predictive of opioid response.

These future directions will not only enhance the scientific rigor of pain genetics research but also pave the way for more personalized and effective approaches to pain management, to ensure better care and quality of life for advanced cancer patients.

# 8. Acknowledgements (grant)

The research leading to these results was made possible thanks to the funding received from AIRC under MFAG 2019 (ID. 22950—Principal Investigator: Francesca Colombo. The funding organization had no role in the design or execution of the study; collection, management, analysis, or interpretation of the data; or preparation, review, or approval of the manuscript.

I would like to express my deepest gratitude to my supervisor, Dr. Francesca Colombo, for her constant guidance, encouragement, and support throughout these three years of doctoral research. Her expertise, constructive feedback, and trust in doing different activities and abroad experiences have been invaluable for both my scientific and personal growth. Thanks.

I am really grateful also to my university tutor, Prof. Cristina Battaglia, whose precious advice and support during the academic activities of the PhD have greatly enriched my training and experience; a thank you also goes to my external reviewers, who, thanks to their valuable advice, allowed me to improve the drafting of this thesis, making it even more detailed and accurate.

I am also warmly thankful to my external advisor, Dr. Hanna Ollila, who generously hosted me at FIMM. This experience was fundamental in allowing me to broaden my scientific skills, work in an international environment, and develop a stronger sense of autonomy as a researcher.

Special thanks also go to my colleagues at the CNR, Tania, Martina E. e Martina S., Camilla, Eleonora, Clarissa, Roberta, Gianluca, Ugo, Elisa, Eva, Ingrid, Marco, who have always been willing to listen, share ideas, and offer constructive discussions that helped me refine my work. I am sincerely thankful to my fellow PhD colleagues as well, for their companionship, collaboration, and for creating a stimulating and supportive environment during these years of shared challenges and achievements. Finally, I wish to thank my family and friends, whose patience, encouragement, and understanding have been a constant source of strength throughout this journey.

# 9. References


1. Raja, S. N. *et al.* The revised International Association for the Study of Pain definition of pain: concepts, challenges, and compromises. *Pain* **161**, 1976–1982 (2020).

2. Lin, T. Physiology of pain. in *Fundamentals of Anaesthesia* 431–453 (Cambridge University Press, 2016). doi:10.1017/9781139626798.023.

3. Rosenbaum, T., Morales-Lázaro, S. L. & Islas, L. D. TRP channels: a journey towards a molecular understanding of pain. *Nat Rev Neurosci* **23**, 596–610 (2022).

4. Cordero-Erausquin, M., Inquimbert, P., Schlichter, R. & Hugel, S. Neuronal networks and nociceptive processing in the dorsal horn of the spinal cord. *Neuroscience* **338**, 230–247 (2016).

5. Basbaum, A. I. & Fields, H. L. Endogenous Pain Control Systems: Brainstem Spinal Pathways and Endorphin Circuitry. *Annu Rev Neurosci* **7**, 309–338 (1984).

6. Llorca-Torralba, M., Borges, G., Neto, F., Mico, J. A. & Berrocoso, E. Noradrenergic Locus Coeruleus pathways in pain modulation. *Neuroscience* **338**, 93–113 (2016).

7. Afridi, B., Khan, H., Akkol, E. K. & Aschner, M. Pain Perception and Management: Where do We Stand? *Curr Mol Pharmacol* **14**, 678–688 (2021).

8. Bliss, T. V. P., Collingridge, G. L., Kaang, B.-K. & Zhuo, M. Synaptic plasticity in the anterior cingulate cortex in acute and chronic pain. *Nat Rev Neurosci* **17**, 485–496 (2016).

9. Ong, W.-Y., Stohler, C. S. & Herr, D. R. Role of the Prefrontal Cortex in Pain Processing. *Mol Neurobiol* **56**, 1137–1166 (2019).

10. McCarberg, B. & Peppin, J. Pain Pathways and Nervous System Plasticity: Learning and Memory in Pain. *Pain Medicine* **20**, 2421–2437 (2019).

11. Mears, L. & Mears, J. The pathophysiology, assessment, and management of acute pain. *British Journal of Nursing* **32**, 58–65 (2023).

12. Ossipov, M. H., Dussor, G. O. & Porreca, F. Central modulation of pain. *Journal of Clinical Investigation* **120**, 3779–3787 (2010).

13. Granot, M., Sprecher, E. & Yarnitsky, D. Psychophysics of phasic and tonic heat pain stimuli by quantitative sensory testing in healthy subjects. *European Journal of Pain* **7**, 139–143 (2003).

14. Arendt-Nielsen, L. & Yarnitsky, D. Experimental and Clinical Applications of Quantitative Sensory Testing Applied to Skin, Muscles and Viscera. *J Pain* **10**, 556–572 (2009).

15. Russo, M. M. & Sundaramurthi, T. An Overview of Cancer Pain: Epidemiology and Pathophysiology. *Semin Oncol Nurs* **35**, 223–228 (2019).

16. Ji, R.-R., Nackley, A., Huh, Y., Terrando, N. & Maixner, W. Neuroinflammation and Central Sensitization in Chronic and Widespread Pain. *Anesthesiology* **129**, 343–366 (2018).

17. Latremoliere, A. & Woolf, C. J. Central Sensitization: A Generator of Pain Hypersensitivity by Central Neural Plasticity. *J Pain* **10**, 895–926 (2009).

18. Finnerup, N. B., Kuner, R. & Jensen, T. S. Neuropathic Pain: From Mechanisms to Treatment. *Physiol Rev* **101**, 259–301 (2021).

19. Fallon, M. T. Neuropathic pain in cancer. *Br J Anaesth* **111**, 105–111 (2013).

20. Portenoy, R. K. & Hagen, N. A. Breakthrough pain: definition, prevalence and characteristics. *Pain* **41**, 273–281 (1990).

21. Macedo, F. *et al.* Bone metastases: an overview. *Oncol Rev* https://doi.org/10.4081/oncol.2017.321 (2017) doi:10.4081/oncol.2017.321.

22. Wang, K. *et al.* Nociceptor neurons promote PDAC progression and cancer pain by interaction with cancer-associated fibroblasts and suppression of natural killer cells. *Cell Res* **35**, 362–380 (2025).

23. Wang, W.-L., Hao, Y.-H., Pang, X. & Tang, Y.-L. Cancer pain: molecular mechanisms and management. *Molecular Biomedicine* **6**, 45 (2025).

24. Loprinzi, C. L. *et al.* Prevention and Management of Chemotherapy-Induced Peripheral Neuropathy in Survivors of Adult Cancers: ASCO Guideline Update. *Journal of Clinical Oncology* **38**, 3325–3348 (2020).

25. Greco, M. T. *et al.* Quality of Cancer Pain Management: An Update of a Systematic Review of Undertreatment of Patients With Cancer. *Journal of Clinical Oncology* **32**, 4149–4154 (2014).

26. Caraceni, A. *et al.* Use of opioid analgesics in the treatment of cancer pain: evidence-based recommendations from the EAPC. *Lancet Oncol* **13**, (2012).

27. Anekar, A. A., Hendrix, J. M. & Cascella, M. *WHO Analgesic Ladder*. (2025).

28. Pasternak, G. W. & Pan, Y.-X. Mu Opioids and Their Receptors: Evolution of a Concept. *Pharmacol Rev* **65**, 1257–1317 (2013).

29. Swingler, M., Donadoni, M., Unterwald, E. M., Maggirwar, S. B. & Sariyer, I. K. Molecular and cellular basis of mu-opioid receptor signaling: mechanisms underlying tolerance and dependence development. *Front Neurosci* **19**, (2025).

30. El Daibani, A., Burgess, G., Rysztak, L., Jutkiewicz, E. & Pradhan, A. A. Delta opioid receptors: Overlooked outlier or the next big thing. *Curr Opin Pharmacol* **83**, 102528 (2025).

31. Zhang, L. *et al.* Supraspinal kappa-opioid receptors: new therapeutic strategies for pain, pruritus, and negative emotions. *Exp Brain Res* **243**, 116 (2025).

32. Yaksh T, W. M. Opioids, Analgesia, and Pain Management. in *The Pharmacological Basis of Therapeutics* (ed. Laurence L. Brunton) (2017).

33. Lau, B. K., Winters, B. L. & Vaughan, C. W. Opioid presynaptic disinhibition of the midbrain periaqueductal grey descending analgesic pathway. *Br J Pharmacol* **177**, 2320–2332 (2020).

34. Terenius, L. Endorphins and Pain. in *Hormones and the Brain* 231–240 (Springer Netherlands, Dordrecht, 1980). doi:10.1007/978-94-009-8709-8_19.

35. García-Domínguez, M. Enkephalins and Pain Modulation: Mechanisms of Action and Therapeutic Perspectives. *Biomolecules* **14**, 926 (2024).

36. Podvin, S., Yaksh, T. & Hook, V. The Emerging Role of Spinal Dynorphin in Chronic Pain: A Therapeutic Perspective. *Annu Rev Pharmacol Toxicol* **56**, 511–533 (2016).

37. El Daibani, A. & Che, T. Spotlight on Nociceptin/Orphanin FQ Receptor in the Treatment of Pain. *Molecules* **27**, 595 (2022).

38. Gavioli, E. C., Holanda, V. A. D., Calo, G. & Ruzza, C. Nociceptin/orphanin FQ receptor system blockade as an innovative strategy for increasing resilience to stress. *Peptides (N.Y.)* **141**, 170548 (2021).

39. Toll, L., Bruchas, M. R., Calo', G., Cox, B. M. & Zaveri, N. T. Nociceptin/Orphanin FQ Receptor Structure, Signaling, Ligands, Functions, and Interactions with Opioid Systems. *Pharmacol Rev* **68**, 419–457 (2016).

40. Zarin, M. K. Z., Dehaen, W., Salehi, P. & Asl, A. A. B. Synthesis and Modification of Morphine and Codeine, Leading to Diverse Libraries with Improved Pain Relief Properties. *Pharmaceutics* **15**, 1779 (2023).

41. Szczupak, M. *et al.* Strategy for effective analgesia with intravenous buprenorphine in patients with acute postoperative pain. *BMC Anesthesiol* **25**, 216 (2025).

42. Albaqami, M. S. *et al.* Buprenorphine for acute post-surgical pain. *Saudi J Anaesth* **17**, 65–71 (2023).

43. Barletta, C. *et al.* The Rise of Fentanyl: Molecular Aspects and Forensic Investigations. *Int J Mol Sci* **26**, 444 (2025).

44. Formenti, P. *et al.* Managing Severe Cancer Pain with Oxycodone/Naloxone Treatment: A Literature Review Update. *J Pers Med* **14**, 483 (2024).

45. Swegle, J. M. & Logemann, C. Management of common opioid-induced adverse effects. *Am Fam Physician* **74**, 1347–54 (2006).

46. Huynh, P., Villaluz, J., Bhandal, H., Alem, N. & Dayal, R. Long-Term Opioid Therapy: The Burden of Adverse Effects. *Pain Medicine* **22**, 2128–2130 (2021).

47. Swarm, R. A. *et al.* Adult Cancer Pain. *Journal of the National Comprehensive Cancer Network* **11**, 992–1022 (2013).

48. Portenoy, R. K. & Lesage, P. Management of cancer pain. *The Lancet* **353**, 1695–1700 (1999).

49. Mercadante, S., Arcuri, E., Ferrera, P., Villari, P. & Mangione, S. Alternative Treatments of Breakthrough Pain in Patients Receiving Spinal Analgesics for Cancer Pain. *J Pain Symptom Manage* **30**, 485–491 (2005).

50. Teunissen, S. C. C. M. *et al.* Symptom prevalence in patients with incurable cancer: a systematic review. *J Pain Symptom Manage* **34**, 94–104 (2007).

51. Nielsen, C., Knudsen, G. & Steingrímsdóttir, Ó. Twin studies of pain. *Clin Genet* **82**, 331–340 (2012).

52. Angst, M. S. *et al.* Pain sensitivity and opioid analgesia: A pharmacogenomic twin study. *Pain* **153**, 1397–1409 (2012).

53. Raad, M., López, W. O. C., Sharafshah, A., Assefi, M. & Lewandrowski, K.-U. Personalized Medicine in Cancer Pain Management. *J Pers Med* **13**, 1201 (2023).

54. Caraco, Y., Sheller, J. & Wood, A. J. Pharmacogenetic determination of the effects of codeine and prediction of drug interactions. *J Pharmacol Exp Ther* **278**, 1165–74 (1996).

55. Dean, L. & Kane, M. *Codeine Therapy and CYP2D6 Genotype*. (2012).

56. Deodhar, M., Turgeon, J. & Michaud, V. Contribution of CYP2D6 Functional Activity to Oxycodone Efficacy in Pain Management: Genetic Polymorphisms, Phenoconversion, and Tissue-Selective Metabolism. *Pharmaceutics* **13**, 1466 (2021).

57. Takashina, Y. *et al.* Impact of CYP3A5 and ABCB1 gene polymorphisms on fentanyl pharmacokinetics and clinical responses in cancer patients undergoing conversion to a transdermal system. *Drug Metab Pharmacokinet* **27**, 414–21 (2012).

58. Campa, D., Gioia, A., Tomei, A., Poli, P. & Barale, R. Association of ABCB1/MDR1 and OPRM1 Gene Polymorphisms With Morphine Pain Relief. *Clin Pharmacol Ther* **83**, 559–566 (2008).

59. Rakvåg, T. T. *et al.* Genetic Variation in the *Catechol-O-Methyltransferase (COMT)* Gene and Morphine Requirements in Cancer Patients with Pain. *Mol Pain* **4**, (2008).

60. Mura, E. *et al.* Consequences of the 118A>G polymorphism in the OPRM1 gene: translation from bench to bedside? *J Pain Res* **6**, 331–53 (2013).

61. Klepstad, P. *et al.* The 118 A > G polymorphism in the human μ-opioid receptor gene may increase morphine requirements in patients with pain caused by malignant disease. *Acta Anaesthesiol Scand* **48**, 1232–1239 (2004).

62. Oosten, A. W. *et al.* Opioid Treatment Failure in Cancer Patients: The Role of Clinical and Genetic Factors. *Pharmacogenomics* **17**, 1391–1403 (2016).

63. Haupt, L. M. *et al.* The effects of OPRM1 118A>G on methadone response in pain management in advanced cancer at end of life. *Sci Rep* **14**, 3411 (2024).

64. Lingaratnam, S. *et al.* A systematic review and meta-analysis of the impacts of germline pharmacogenomics on severe toxicity and symptom burden in adult patients with cancer. *Clin Transl Sci* **17**, (2024).

65. Fladvad, T., Fayers, P., Skorpen, F., Kaasa, S. & Klepstad, P. Lack of association between genetic variability and multiple pain-related outcomes in a large cohort of patients with advanced cancer: the European Pharmacogenetic Opioid Study (EPOS). *BMJ Support Palliat Care* **2**, 351–355 (2012).

66. Bergeson, S. E. *et al.* Quantitative trait loci influencing morphine antinociception in four mapping populations. *Mammalian Genome* **12**, 546–553 (2001).

67. Laugsand, E. A. *et al.* Clinical and genetic factors associated with nausea and vomiting in cancer patients receiving opioids. *Eur J Cancer* **47**, 1682–1691 (2011).

68. Sham, P. C. & Purcell, S. M. Statistical power and significance testing in large-scale genetic studies. *Nat Rev Genet* **15**, 335–346 (2014).

69. Kember, R. L. *et al.* Cross-ancestry meta-analysis of opioid use disorder uncovers novel loci with predominant effects in brain regions associated with addiction. *Nat Neurosci* **25**, 1279–1287 (2022).

70. Davis, C. N. *et al.* Multi-ancestry genome-wide association meta-analysis of buprenorphine treatment response. *Neuropsychopharmacology* **50**, 1346–1353 (2025).

71. Galvan, A. *et al.* Multiple Loci Modulate Opioid Therapy Response for Cancer Pain. *Clinical Cancer Research* **17**, 4581–4587 (2011).

72. Nishizawa, D. *et al.* Genome-Wide Association Study Identifies Candidate Loci Associated with Opioid Analgesic Requirements in the Treatment of Cancer Pain. *Cancers (Basel)* **14**, 4692 (2022).

73. Colombo, F. *et al.* Identification of genetic polymorphisms modulating nausea and vomiting in two series of opioid-treated cancer patients. *Sci Rep* **10**, 542 (2020).

74. Zou, Y., Carbonetto, P., Wang, G. & Stephens, M. Fine-mapping from summary data with the “Sum of Single Effects” model. *PLoS Genet* **18**, e1010299 (2022).

75. Võsa, U. *et al.* Large-scale cis- and trans-eQTL analyses identify thousands of genetic loci and polygenic scores that regulate blood gene expression. *Nat Genet* **53**, 1300–1310 (2021).

76. Bulik-Sullivan, B. *et al.* An atlas of genetic correlations across human diseases and traits. *Nat Genet* **47**, 1236–41 (2015).

77. Davey Smith, G. & Ebrahim, S. ‘Mendelian randomization’: can genetic epidemiology contribute to understanding environmental determinants of disease?*. *Int J Epidemiol* **32**, 1–22 (2003).

78. Burgess, S. & Thompson, S. G. Avoiding bias from weak instruments in Mendelian randomization studies. *Int J Epidemiol* **40**, 755–764 (2011).

79. Wang, Y. *et al.* Exploring the bidirectional causal associations between pain and circulating inflammatory proteins: A Mendelian randomization study. *Clin Exp Pharmacol Physiol* **51**, (2024).

80. Johnston, K. J. A. *et al.* Genome-wide association study of multisite chronic pain in UK Biobank. *PLoS Genet* **15**, e1008164 (2019).

81. Corli, O. *et al.* Are strong opioids equally effective and safe in the treatment of chronic cancer pain? A multicenter randomized phase IV ‘real life’ trial on the variability of response to opioids. *Annals of Oncology* **27**, 1107–1115 (2016).

82. Kurita, G. P. *et al.* Prevalence and Predictors of Cognitive Dysfunction in Opioid-Treated Patients With Cancer: A Multinational Study. *Journal of Clinical Oncology* **29**, 1297–1303 (2011).

83. Shkodra, M. *et al.* Cancer pain: Results of a prospective study on prognostic indicators of pain intensity including pain syndromes assessment. *Palliat Med* **36**, 1396–1407 (2022).

84. Caraceni, A. *et al.* Use of opioid analgesics in the treatment of cancer pain: evidence-based recommendations from the EAPC. *Lancet Oncol* **13**, e58–e68 (2012).

85. Poquet, N. & Lin, C. The Brief Pain Inventory (BPI). *J Physiother* **62**, 52 (2016).

86. Aaronson, N. K. *et al.* The European Organization for Research and Treatment of Cancer QLQ-C30: A Quality-of-Life Instrument for Use in International Clinical Trials in Oncology. *JNCI Journal of the National Cancer Institute* **85**, 365–376 (1993).

87. R Core Team (2023). _R: A Language and Environment for Statistical Computing_. R Foundation for Statistical Computing, Vienna, Austria. <https://www.R-project.org/>.

88. STAT: Interactive Document for Working with Basic Statistical Analysis. *CRAN: Contributed Packages* Preprint at https://doi.org/10.32614/CRAN.package.STAT (2019).

89. Yang, J. *et al.* FTO genotype is associated with phenotypic variability of body mass index. *Nature* **490**, 267–272 (2012).

90. Purcell, S. *et al.* PLINK: A Tool Set for Whole-Genome Association and Population-Based Linkage Analyses. *The American Journal of Human Genetics* **81**, 559–575 (2007).

91. Anderson, C. A. *et al.* Data quality control in genetic case-control association studies. *Nat Protoc* **5**, 1564–1573 (2010).

92. Pearson, K. LIII. *On lines and planes of closest fit to systems of points in space*. *The London, Edinburgh, and Dublin Philosophical Magazine and Journal of Science* **2**, 559–572 (1901).

93. Price, A. L. *et al.* Principal components analysis corrects for stratification in genome-wide association studies. *Nat Genet* **38**, 904–909 (2006).

94. Novembre, J. & Stephens, M. Interpreting principal component analyses of spatial population genetic variation. *Nat Genet* **40**, 646–649 (2008).

95. Delaneau, O. *et al.* Integrating sequence and array data to create an improved 1000 Genomes Project haplotype reference panel. *Nat Commun* **5**, 3934 (2014).

96. Das, S. *et al.* Next-generation genotype imputation service and methods. *Nat Genet* **48**, 1284–1287 (2016).

97. Taliun, D. *et al.* Sequencing of 53,831 diverse genomes from the NHLBI TOPMed Program. *Nature* **590**, 290–299 (2021).

98. Verlouw, J. A. M. *et al.* A comparison of genotyping arrays. *European Journal of Human Genetics* **29**, 1611–1624 (2021).

99. Mbatchou, J. *et al.* Computationally efficient whole-genome regression for quantitative and binary traits. *Nat Genet* **53**, 1097–1103 (2021).

100. D. Turner, S. qqman: an R package for visualizing GWAS results using Q-Q and manhattan plots. *J Open Source Softw* **3**, 731 (2018).

101. Pruim, R. J. *et al.* LocusZoom: regional visualization of genome-wide association scan results. *Bioinformatics* **26**, 2336–2337 (2010).

102. Chang, C. C. *et al.* Second-generation PLINK: rising to the challenge of larger and richer datasets. *Gigascience* **4**, (2015).

103. Bulik-Sullivan, B. K. *et al.* LD Score regression distinguishes confounding from polygenicity in genome-wide association studies. *Nat Genet* **47**, 291–5 (2015).

104. Oscanoa, J. *et al.* SNPnexus: a web server for functional annotation of human genome sequence variation (2020 update). *Nucleic Acids Res* **48**, W185–W192 (2020).

105. An integrated encyclopedia of DNA elements in the human genome. *Nature* **489**, 57–74 (2012).

106. Kumar, S., Ambrosini, G. & Bucher, P. SNP2TFBS – a database of regulatory SNPs affecting predicted transcription factor binding site affinity. *Nucleic Acids Res* **45**, D139–D144 (2017).

107. Mathelier, A. *et al.* JASPAR 2014: an extensively expanded and updated open-access database of transcription factor binding profiles. *Nucleic Acids Res* **42**, D142–D147 (2014).

108. Boyle, A. P. *et al.* Annotation of functional variation in personal genomes using RegulomeDB. *Genome Res* **22**, 1790–7 (2012).

109. Võsa, U. *et al.* Large-scale cis- and trans-eQTL analyses identify thousands of genetic loci and polygenic scores that regulate blood gene expression. *Nat Genet* **53**, 1300–1310 (2021).

110. de Klein, N. *et al.* Brain expression quantitative trait locus and network analyses reveal downstream effects and putative drivers for brain-related diseases. *Nat Genet* **55**, 377–388 (2023).

111. Ghoussaini, M. *et al.* Open Targets Genetics: systematic identification of trait-associated genes using large-scale genetics and functional genomics. *Nucleic Acids Res* **49**, D1311–D1320 (2021).

112. Mountjoy, E. *et al.* An open approach to systematically prioritize causal variants and genes at all published human GWAS trait-associated loci. *Nat Genet* **53**, 1527–1533 (2021).

113. Wallace, C. & Giambartolomei, C. coloc: Colocalisation Tests of Two Genetic Traits. *CRAN: Contributed Packages* Preprint at https://doi.org/10.32614/CRAN.package.coloc (2012).

114. Finucane, H. K. *et al.* Partitioning heritability by functional annotation using genome-wide association summary statistics. *Nat Genet* **47**, 1228–35 (2015).

115. Bulik-Sullivan, B. K. *et al.* LD Score regression distinguishes confounding from polygenicity in genome-wide association studies. *Nat Genet* **47**, 291–295 (2015).

116. Pers, T. H. *et al.* Biological interpretation of genome-wide association studies using predicted gene functions. *Nat Commun* **6**, 5890 (2015).

117. Elsworth, B. *et al.* The MRC IEU OpenGWAS data infrastructure. Preprint at https://doi.org/10.1101/2020.08.10.244293 (2020).

118. Hemani, G. *et al.* The MR-Base platform supports systematic causal inference across the human phenome. *Elife* **7**, (2018).

119. Hemani, G., Tilling, K. & Davey Smith, G. Orienting the causal relationship between imprecisely measured traits using GWAS summary data. *PLoS Genet* **13**, e1007081 (2017).

120. Minnai, F. *et al.* Genomic Study in Opioid-Treated Cancer Patients Identifies Variants Associated With Nausea-Vomiting. *J Pain Symptom Manage* **69**, 175-182.e5 (2025).

121. Minnai, F. *et al.* A genome-wide association study of European advanced cancer patients treated with opioids identifies regulatory variants on chromosome 20 associated with pain intensity. *European Journal of Pain* **29**, (2025).

122. Toikumo, S. *et al.* A multi-ancestry genetic study of pain intensity in 598,339 veterans. *Nat Med* **30**, 1075–1084 (2024).

123. Mocci, E. *et al.* Genome wide association joint analysis reveals 99 risk loci for pain susceptibility and pleiotropic relationships with psychiatric, metabolic, and immunological traits. *PLoS Genet* **19**, e1010977 (2023).

124. Jain, S. V., Panjeton, G. D. & Martins, Y. C. Relationship Between Sleep Disturbances and Chronic Pain: A Narrative Review. *Clin Pract* **14**, 2650–2660 (2024).

125. Herrero Babiloni, A. *et al.* The Impact of Sleep Disturbances on Endogenous Pain Modulation: A Systematic Review and Meta-Analysis. *J Pain* **25**, 875–901 (2024).

126. Ghitani, N. *et al.* A distributed coding logic for thermosensation and inflammatory pain. *Nature* **642**, 1016–1023 (2025).

127. Ji, J., Yuan, M. & Ji, R.-R. Inflammation and Pain. in *Neuroimmune Interactions in Pain* 17–41 (Springer International Publishing, Cham, 2023). doi:10.1007/978-3-031-29231-6_2.

128. Yang, Y. *et al.* TDRD3 is an effector molecule for arginine-methylated histone marks. *Mol Cell* **40**, 1016–23 (2010).

129. Stoll, G. *et al.* Deletion of TOP3β, a component of FMRP-containing mRNPs, contributes to neurodevelopmental disorders. *Nat Neurosci* **16**, 1228–1237 (2013).

130. Peng, L. u, Bai, G. & Pang, Y. Roles of NPAS2 in circadian rhythm and disease. *Acta Biochim Biophys Sin (Shanghai)* **53**, 1257–1265 (2021).

131. Hofmeister, E. N., Fisher, S., Palesh, O. & Innominato, P. F. Does circadian rhythm influence gastrointestinal toxicity? *Curr Opin Support Palliat Care* **14**, 120–126 (2020).

132. Gamble, M. C. *et al.* A role for the circadian transcription factor NPAS2 in the progressive loss of non-rapid eye movement sleep and increased arousal during fentanyl withdrawal in male mice. *Psychopharmacology (Berl)* **239**, 3185–3200 (2022).

133. Barko, K. *et al.* Sex-specific Regulation of Fentanyl Reward by the Circadian Transcription Factor NPAS2. *bioRxiv* https://doi.org/10.1101/2024.11.12.623242 (2024) doi:10.1101/2024.11.12.623242.

134. Puig, S., Shelton, M. A., Barko, K., Seney, M. L. & Logan, R. W. Sex-specific role of the circadian transcription factor NPAS2 in opioid tolerance, withdrawal and analgesia. *Genes Brain Behav* **21**, e12829 (2022).

135. Bumgarner, J. R., McCray, E. W. & Nelson, R. J. The disruptive relationship among circadian rhythms, pain, and opioids. *Front Neurosci* **17**, 1109480 (2023).

136. Jin, Y. *et al.* An Update in Our Understanding of the Relationships Between Gene Polymorphisms and Chemotherapy-Induced Nausea and Vomiting. *Int J Gen Med* **14**, 5879–5892 (2021).

137. Klenke, S. & Frey, U. H. Genetic variability in postoperative nausea and vomiting: A systematic review. *Eur J Anaesthesiol* **37**, 959–968 (2020).

138. Chottova Dvorakova, M. Distribution and Function of Neuropeptides W/B Signaling System. *Front Physiol* **9**, 981 (2018).

139. El Daibani, A. & Che, T. Spotlight on Nociceptin/Orphanin FQ Receptor in the Treatment of Pain. *Molecules* **27**, (2022).

140. Liao, X. *et al.* The CUL5 E3 ligase complex negatively regulates central signaling pathways in CD8+ T cells. *Nat Commun* **15**, 603 (2024).

141. Miclescu, A. A., Granlund, P., Butler, S. & Gordh, T. Association between systemic inflammation and experimental pain sensitivity in subjects with pain and painless neuropathy after traumatic nerve injuries. *Scand J Pain* **23**, 184–199 (2023).

142. Shum, S. & Isoherranen, N. Human Fetal Liver Metabolism of Oxycodone Is Mediated by CYP3A7. *AAPS J* **23**, 24 (2021).

143. Rascón-Martínez, D. M. *et al.* Role of Opioid-Sparing Techniques in Pain Management for General Surgery Patients With Hepatic Dysfunction: An Observational Cohort Study. *Cureus* **17**, e77117 (2025).

144. Ferrini, F., Goldstein, P. A. & Labrakakis, C. Editorial: CNS pain circuits in health and disease. *Front Neural Circuits* **16**, 977404 (2022).

145. Murray, G. M. & Sessle, B. J. Pain-sensorimotor interactions: New perspectives and a new model. *Neurobiol Pain* **15**, 100150 (2024).

146. Mantyh, P. W. Bone cancer pain: from mechanism to therapy. *Curr Opin Support Palliat Care* **8**, 83–90 (2014).

147. Waning, D. L. & Guise, T. A. Cancer-associated muscle weakness: What's bone got to do with it? *Bonekey Rep* **4**, 691 (2015).

148. Lee, H., Lee, M. H., Hou, K., Pasaniuc, B. & Han, B. Admixed and single-continental genome segments of the same ancestry have distinct linkage disequilibrium patterns. *Genome Biol* **26**, 201 (2025).

149. Hou, Z. & Ochoa, A. Genetic association models are robust to common population kinship estimation biases. *Genetics* **224**, (2023).

150. Ochoa, A. & Storey, J. D. Estimating FST and kinship for arbitrary population structures. *PLoS Genet* **17**, e1009241 (2021).

151. Uren, C., Hoal, E. G. & Möller, M. Putting RFMix and ADMIXTURE to the test in a complex admixed population. *BMC Genet* **21**, 40 (2020).

152. Meloto, C. B. *et al.* Human pain genetics database: a resource dedicated to human pain genetics research. *Pain* **159**, 749–763 (2018).

153. Thorpe, H. H. A. *et al.* Genome-wide association studies of coffee intake in UK/US participants of European ancestry uncover cohort-specific genetic associations. *Neuropsychopharmacology* **49**, 1609–1618 (2024).

154. Faudone, G., Arifi, S. & Merk, D. The Medicinal Chemistry of Caffeine. *J Med Chem* **64**, 7156–7178 (2021).

155. Malec, D. & Michalska, E. The effect of methylxanthines on morphine analgesia in mice and rats. *Pol J Pharmacol Pharm* **40**, 223–32 (1988).

156. Beniwal, S. S. *et al.* Inflammation in cardio-oncology and psychological disorders: mechanisms, biomarkers, pain management, and therapeutic strategies. *Ann Med Surg (Lond)* **87**, 4229–4236 (2025).

157. Szczepaniak, A., Machelak, W., Fichna, J. & Zielińska, M. The role of kappa opioid receptors in immune system - An overview. *Eur J Pharmacol* **933**, 175214 (2022).

158. Davies, N. M. *et al.* The many weak instruments problem and Mendelian randomization. *Stat Med* **34**, 454–468 (2015).

159. Farrell, S. F. *et al.* Genetic impact of blood C-reactive protein levels on chronic spinal & widespread pain. *European Spine Journal* **32**, 2078–2085 (2023).

160. Liang, X. & Fan, Y. Bidirectional two-sample Mendelian randomization analysis reveals a causal effect of interleukin-18 levels on postherpetic neuralgia risk. *Front Immunol* **14**, 1183378 (2023).

161. Wang, Y. *et al.* Exploring the bidirectional causal associations between pain and circulating inflammatory proteins: A Mendelian randomization study. *Clin Exp Pharmacol Physiol* **51**, e13905 (2024).

162. Yao, C. *et al.* Exploring the bidirectional relationship between pain and mental disorders: a comprehensive Mendelian randomization study. *J Headache Pain* **24**, 82 (2023).

163. Zhu, Y., Bi, Y. & Zhu, T. Mendelian randomization highlights sleep disturbances mediated the effect of depression on chronic pain. *Brain Behav* **14**, e3596 (2024).

164. Williams, J. C., Hum, R. M., Alam, U. & Zhao, S. S. Insomnia and short sleep duration, but not chronotype, is associated with chronic widespread pain: Mendelian randomization study. *Rheumatol Int* **44**, 2961–2966 (2024).

165. Broberg, M., Karjalainen, J., FinnGen & Ollila, H. M. Mendelian randomization highlights insomnia as a risk factor for pain diagnoses. *Sleep* **44**, (2021).

166. Chen, M., Li, S., Zhu, Z., Dai, C. & Hao, X. Investigating the shared genetic architecture and causal relationship between pain and neuropsychiatric disorders. *Hum Genet* **142**, 431–443 (2023).

167. Fry, A. *et al.* Comparison of Sociodemographic and Health-Related Characteristics of UK Biobank Participants With Those of the General Population. *Am J Epidemiol* **186**, 1026–1034 (2017).

168. Ko, S. *et al.* GWAS of longitudinal trajectories at biobank scale. *Am J Hum Genet* **109**, 433–445 (2022).

169. Xavier, J. M. *et al.* Identification of candidate causal variants and target genes at 41 breast cancer risk loci through differential allelic expression analysis. *Sci Rep* **14**, 22526 (2024).

170. Ge, B. *et al.* Global patterns of cis variation in human cells revealed by high-density allelic expression analysis. *Nat Genet* **41**, 1216–1222 (2009).

171. Hanna, R. E. *et al.* Massively parallel assessment of human variants with base editor screens. *Cell* **184**, 1064-1080.e20 (2021).

172. Acharya, D. & Mukhopadhyay, A. A comprehensive review of machine learning techniques for multi-omics data integration: challenges and applications in precision oncology. *Brief Funct Genomics* **23**, 549–560 (2024).

# 10. Data availability

The genotyping data are not publicly available due to privacy or ethical restrictions. The GWAS summary statistics for pain intensity are publicly available in the GWAS Catalog (GCST90435150), while the GWAS summary statistics for nausea and vomiting will be soon available in GWAS catalog[V]. The bioinformatic code used to perform all the analyses mentioned in this thesis are available on Dataverse at https://doi.org/10.13130/RD_UNIMI/ZQMSCY.

# 11. Dissemination of results

The results of this project were disseminated through different and complementary ways, to reach both the academic and non-academic public.

The major achievement during this PhD was the publication of the results in two different peer-reviewed journals. Particularly, I contributed as first author to the manuscript entitled

[V] https://www.ebi.ac.uk/gwas/

*Genomic Study in Opioid-Treated Cancer Patients Identifies Variants Associated With Nausea-Vomiting*, published in the *Journal of Pain and Symptom Management* (2025, 69(2):175-182.e5; doi: 10.1016/j.jpainsymman.2024.10.033), and to the article *A genome-wide association study of European advanced cancer patients treated with opioids identifies regulatory variants on chromosome 20 associated with pain intensity*, published in the *European Journal of Pain* (2025, 29:e4764; doi: 10.1002/ejp.4764). In both, I was first line involved in the conceptualization and design of the project, as well as the analyses and the interpretation of the results. Through these two published articles, these results were disseminated to the international scientific community, contributing to the advancement of pharmacogenomics field of the opioid-treated advanced cancer patients.

Also, the results were presented through different oral and poster presentations at international and national conferences and workshops. In the last year, I was invited to present my results, in a speech entitled *Pharmacogenomics of opioid therapy in advanced cancer patients* at the PhD Meeting, held by the Istituto di Ricerche Farmacologiche Mario Negri (Milan, 9–11 June 2025), and at SIGU 2025, the annual conference held by the Italian Society of Human Genetics, (Rimini, 23-25 September 2025).

In the past years I had the opportunity to present these results through four different poster presentations at the European Society of Human Genetics Conference 2022, 2023 and 2024, and at the Nordic-EMBL conference held in Glasgow (Scotland), Vienna (Austria), Berlin (Germany), and Trondheim (Norway), respectively. During these events other researchers gave me inputs and insights on how to proceed with my research. They also gave me the opportunity of exchanging knowledge, feedback and contacts with other researchers. Also, it allowed to disseminate the obtained findings to experts in palliative care, pharmacology, personalized medicine and genomics.

Beyond the dissemination to an academic public, my findings were share to a non-academic audience. Particularly, I actively participated in a third mission dissemination event organized within the PhD retreat. There, I delivered a lecture on the potential and challenges of precision medicine, presenting complex biomedical concepts in a simple terminology to an audience composed by young students and adult employees.

Overall, this experience and the more academic ones, contributed to strengthen my science communication skills, as well as to manage the stress related to the public speaking. It is important to disseminate the scientific progress both within the international research community and the general public, ensuring connection and dialogue between them, to reinforce the impact of this work beyond the academic field.

# 12. List of Figures and Tables

***Figures***

dashed lines, respectively. Dot colour indicates linkage disequilibrium ($r^2$) between each polymorphism and the lead variant (rs6062363, purple diamond).

**Figure 7.** Colocalization plots for the *OPRL1* (a), *PCMTD2* (b) and *PPDPF* (c) genes using the whole-blood tissue expression data from the eQTLGen database (numbers of SNPs included in the analyses were 755, 224 and 293, respectively). Dots are colored based on linkage disequilibrium ($r^2$) with the lead variants, rs6062363 (a, b) and rs7270745 (c; *PPDPF* expression was not associated with the 5 top-significant variants associated with pain intensity).

**Figure 8.** Results of the tissue specific analysis performed with sLDSC software. Tissue types were plotted on the −log10(*P*-value) of their enrichment. Red dashed line represent the statistically significant threshold set at *P*-value 0.05. CNS, central nervous system; GI, gastro-intestinal tissues.

**Figure 9.** Forest plot with the results of the IVW MR performed using 11 exposures and the cancer pain intensity as outcome. The effect size and the confidential intervals are plotted on the x-axis; exposures are plotted on y-axis, in a descendant order according to their *P*-value.

**Figure 10.** Forest plot with the results of the Wald Ratio MR performed using the cancer pain as exposure and ten different outcomes. The effect size and the confidential intervals are plotted on the x-axis; outcomes are plotted on y-axis, in a descendant order according to their *P*-values.

***Tables***

**Table 1.** Summary of results from candidate gene studies on drug response in pain treatment.

**Table 2.** Summary of results from genome-wide association studies for opioid response in opioid use disorders or pain treatment.

**Table 3.** Patient inclusion criteria of the three clinical studies.

**Table 4.** List of GWAS summary statistics downloaded from IEU Open GWAS project

website for Mendelian Randomization analyses with corresponding PMID and sample size.

**Table 5.** Clinical characteristics of the patients.

**Table 6.** Multivariable linear regression model performed for opioid toxicity phenotype.

**Table 7.** Multivariable linear regression model performed for opioid efficacy phenotype.

**Table 8.** Variants associated with NVS and mapping in the *NPAS2* gene were previously reported as *NPAS2* sQTLs, in GTEx.

**Table 9.** Comparison between the summary statistics of the genetic variants, previously reported (by Colombo *et al*. and Laugsand *et al*.) as being associated with nausea and vomiting in opioid-treated cancer patients, and our results.

**Table 10.** Summary statistics of the GWAS for pain intensity (*P*-value < $5.0 \times 10^{-8}$); variants are sorted according to their *P*-value.

**Table 11.** Colocalization analyses did not support the hypothesis of a shared variant regulating both pain intensity and gene expression.

**Table 12.** Results from the stratified linkage disequilibrium score regression for nine different tissues using pain intensity phenotype.

**Table 13.** Results from the Mendelian Randomization analysis (Inverse Variance Weighted method) for eleven different exposures, using cancer pain intensity as outcome.

**Table 14.** Pleiotropy and heterogeneity tests performed for the forward Mendelian Randomization for eleven different exposures, using cancer pain intensity as outcome.

**Table 15.** Results from the Mendelian Randomization analysis (Wald Ratio method) for cancer pain as exposure, using eleven different exposures.

# 13. Appendix

**Supplementary Figure 1.** Details about per-sample and per-variant QCs

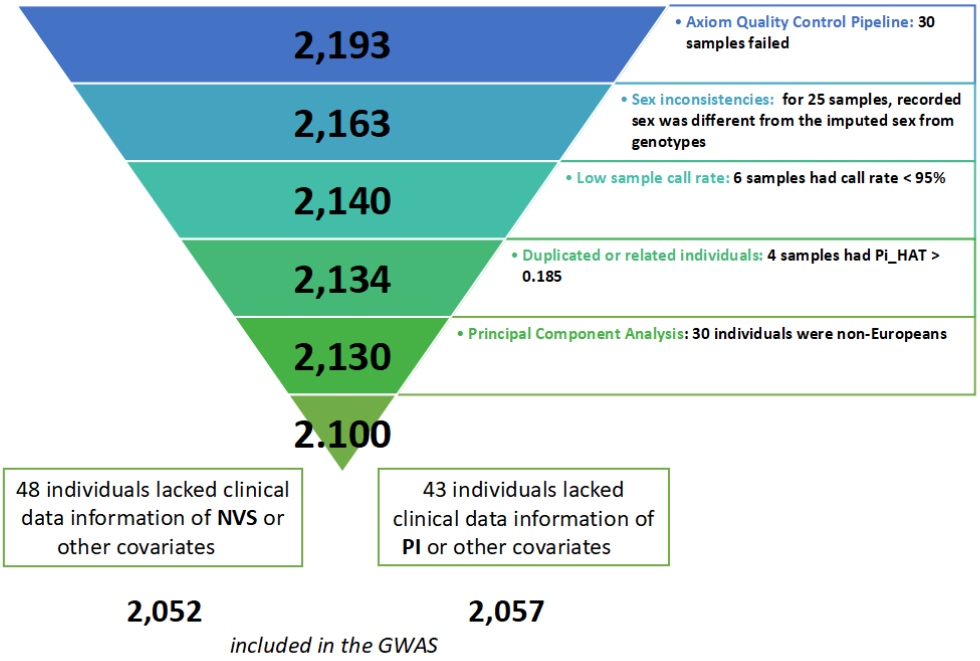


**Supplementary Figure 2.** First four principal components (PCs) projections of our samples (STUDY) together with those of the 1000 Genome reference populations; AFR = Africans; AMR = Americans; EAS = East Asians; EUR = Europeans; SAS = South-East Asians.

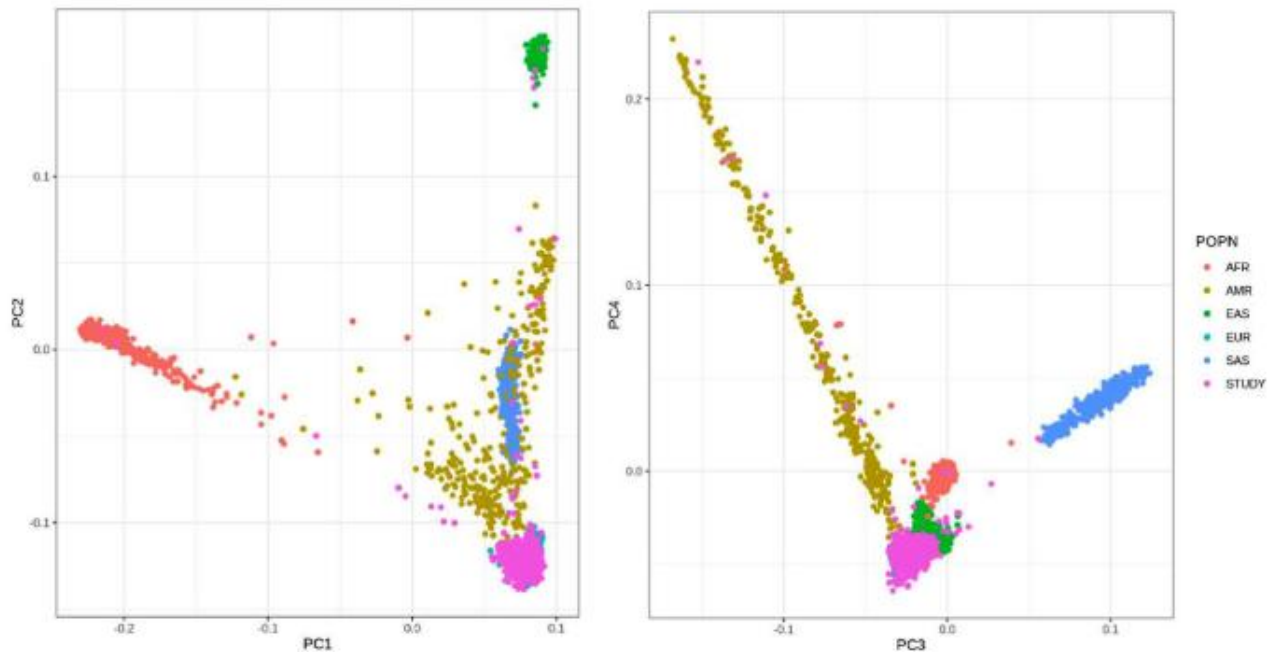

**List of Supplementary Tables**

**Supplementary Table S1.** Top loci (*P*-value < $1.0 \times 10^{-5}$) of the GWAS performed on opioid toxicity phenotype; variants are sorted according to their *P*-values.

**Supplementary Table S2.** Summary statistics of the GWAS for pain intensity (*P*-value < $1.0 \times 10^{-5}$); variants are sorted according to their *P* -value.

**Supplementary Table S3.** Results of SNP2TFBS prediction for the 31 polymorphisms on chromosome 20.

**Supplementary Table S4.** Results from functional annotation of the 31 variants on chromosome 20, in RegulomeDB.

**Supplementary Table S5.** eQTLs reported in GTEx, for the 31 variants on chromosome 20 (*P*-value < $1.0 \times 10^{-5}$).

**Supplementary Table S6.** eQTLs reported in eQTLGen, for the 31 variants on chromosome 20 (*P*-value < $1.0 \times 10^{-5}$).

**Supplementary Table S7a.** eQTLs reported in MetaBrain (cerebellum), for for the 31 variants on chromosome 20 (*P*-value < $1.0 \times 10^{-5}$).

**Supplementary Table S7b.** eQTLs reported in MetaBrain (cortex), for for the 31 variants on chromosome 20 (P-value < 1.0 x 10-5).

**Supplementary Table S8.** PheWAS results for the 31 variants on chromosome 20, across all UK Biobank phenotypes (*P*-value < $1.0 \times 10^{-5}$). Data are sorted according to variant position.

**Supplementary Table S9.** Summary statistics from our GWAS of variants reported in the Human Pain Gene Database, sorted on the basis of their *P*-value of association with pain intensity in our study.

**Supplementary Table S10.** Summary statistics from our GWAS of variants reported by *Galvan A. et al.* and by *Nishizawa D. et al.* as significantly associated with pain relief and opioid requirements, respectively.

**Supplementary Table S11.** Summary statistics from our GWAS of variants reported by *Mocci e. et al.,* sorted on the basis of their *P*-value of association with pain intensity in our study.

**Supplementary Table S12.** Summary statistics from our GWAS of variants reported by *Zorina-Lichtenwalter et al.,* sorted on the basis of their *P*-value of association with pain intensity in our study.

**Supplementary Table S13.** Summary statistics from our GWAS of variants reported by *Toikumo S. et al.,* sorted based on their *P*-value of association with pain intensity in our study.

**Supplementary Table S1**. Top loci (P-value < $1.0 \times 10^{-5}$) of the GWAS performed on opioid toxicity phenotype; variants are sorted according to their *P*-values.

| Variant ID | rsID ^ | Chr | Position (bp) * | Minor allele | MAF | *P*-value | Beta | Variant category | Gene symbol § | Gene start - end |
|---|---|---|---|---|---|---|---|---|---|---|
| chr13:60691995:C:A | rs6562126 | 13 | 60.691.995 | A | 0,72 | 7,42E-08 | -4,3 | ncRNA_intronic | TDRD3 (118,117 bp) | 60,396,457-60,573,878 |
| chr2:6214860:A:G | rs2044651 | 2 | 6.214.860 | G | 0,19 | 5,59E-07 | 4,7 | intergenic | SOX11 (513,475 bp) | 5,692,384-5,701,385 |
| chr2:6210802:G:A | rs1562619 | 2 | 6.210.802 | A | 0,19 | 1,05E-06 | 4,6 | intergenic | SOX11 (509,417 bp) | 5,692,384-5,701,385 |
| chr3:46866766:T:C | rs144291461 | 3 | 46.866.766 | C | 0,02 | 1,38E-06 | 12,0 | intronic | MYL3 | 46,835,110-46,882,178 |
| chr3:60120266:G:T | rs11715819 | 3 | 60.120.266 | T | 0,02 | 1,39E-06 | 11,9 | intronic | FHIT | 59,747,277-61,251,459 |
| chr2:100967367:C:CA | rs899688453 | 2 | 100.967.367 | CA | 0,08 | 1,54E-06 | -6,5 | intronic | NPAS2 | 100,820,139-100,996,829 |
| chr2:100979570:A:G | rs7558747 | 2 | 100.979.570 | G | 0,08 | 1,65E-06 | -6,6 | intronic | NPAS2 | 100,820,139-100,996,829 |
| chr2:10455408:T:C | rs6721235 | 2 | 10.455.408 | C | 0,36 | 1,87E-06 | 3,5 | ncRNA_intronic | ODC1 (7,081 bp) | 10,439,968-10,448,327 |
| chr2:219493864:G:A | rs16859981 | 2 | 219.493.864 | A | 0,27 | 1,92E-06 | 3,9 | ncRNA_intronic | SPEG (235 bp) | 219,434,843-219,493,629 |
| chr1:30859255:C:T | rs41269495 | 1 | 30.859.255 | T | 0,12 | 2,07E-06 | 5,2 | ncRNA_exonic | SDC3 (49,503 bp) | 30,869,466-30,908,758 |
| chr2:6212925:A:T | rs74474922 | 2 | 6.212.925 | T | 0,19 | 2,11E-06 | 4,5 | intergenic | SOX11 (511,540 bp) | 5,692,384-5,701,385 |
| chr2:6213775:T:C | rs77772208 | 2 | 6.213.775 | C | 0,19 | 2,21E-06 | 4,5 | intergenic | SOX11 (512,390 bp) | 5,692,384-5,701,385 |
| chr1:235354265:G:A | rs12120237 | 1 | 235.354.265 | A | 0,14 | 2,78E-06 | 4,8 | intronic | GGPS1-TBCE | 235,342,252-235,448,929 |
| chr2:219491798:G:T | rs12473286 | 2 | 219.491.798 | T | 0,27 | 3,01E-06 | 3,8 | exonic | SPEG | 219,434,843-219,493,629 |
| chr13:79720492:T:C | rs113196013 | 13 | 79.720.492 | C | 0,03 | 3,15E-06 | 10,9 | intergenic | NDFIP2 (239,337 bp) | 79,481,155-79,556,076 |
| chr13:79727627:C:T | rs138202697 | 13 | 79.727.627 | T | 0,03 | 3,15E-06 | 10,9 | intergenic | NDFIP2 (246,472 bp) | 79,481,155-79,556,077 |
| chr13:79757834:G:A | rs113650764 | 13 | 79.757.834 | A | 0,03 | 3,15E-06 | 10,9 | intergenic | NDFIP2 (276,679 bp) | 79,481,155-79,556,077 |
| chr13:79774110:C:T | rs112441841 | 13 | 79.774.110 | T | 0,03 | 3,15E-06 | 10,9 | intergenic | NDFIP2 (292,955 bp) | 79,481,155-79,556,077 |
| chr15:92363732:T:A | rs75516006 | 15 | 92.363.732 | A | 0,03 | 3,52E-06 | 9,4 | intergenic | ST8SIA2 (30,149 bp) | 92,393,881-92,468,728 |
| chr2:219491357:G:A | rs4674405 | 2 | 219.491.357 | A | 0,27 | 3,52E-06 | 3,8 | ncRNA_intronic | SPEG (2,272 bp) | 219,434,843-219,493,629 |
| chr2:219489643:C:T | rs56132883 | 2 | 219.489.643 | T | 0,27 | 3,60E-06 | 3,8 | exonic | SPEG | 219,434,843-219,493,629 |
| chr17:15590028:G:A | rs3859258 | 17 | 15.590.028 | A | 0,03 | 3,78E-06 | 9,6 | intronic | FBXW10B | 15,565,483-15,619,704 |
| chr2:10452054:C:T | rs2357551 | 2 | 10.452.054 | T | 0,33 | 4,05E-06 | 3,4 | intergenic | ODC1 (3,727 bp) | 10,439,968-10,448,327 |
| chr15:92360112:A:T | rs76838139 | 15 | 92.360.112 | T | 0,03 | 4,34E-06 | 9,3 | intergenic | ST8SIA2 (33,769 bp) | 92,393,881-92,468,728 |
| chr20:53689497:C:A | rs6022667 | 20 | 53.689.497 | A | 0,13 | 4,59E-06 | 4,9 | intergenic | ZNF217 (79,590 bp) | 53,567,071-53,609,907 |
| chr2:100969022:T:C | rs4851393 | 2 | 100.969.022 | C | 0,09 | 4,70E-06 | -6,1 | intronic | NPAS2 | 100,820,139-100,996,829 |
| chr2:219488291:G:A | rs875098 | 2 | 219.488.291 | A | 0,269737 | 4,77E-06 | 3,7 | exonic | SPEG | 219,434,843-219,493,629 |
| chr18:565760:A:C | rs486633 | 18 | 565.760 | C | 0,79 | 4,89E-06 | -4,1 | intergenic | CETN1 (14,620 bp) | 580,380-582,114 |
| chr2:219486657:C:T | rs6726806 | 2 | 219.486.657 | T | 0,269493 | 4,98E-06 | 3,7 | intronic | SPEG | 219,434,843-219,493,629 |
| chr12:78344470:G:A | rs688403 | 12 | 78.344.470 | A | 0,220273 | 5,27E-06 | -4,0 | ncRNA_intronic | NAV3 (131,460 bp) | 77,324,641-78,213,010 |
| chr6:35827923:ACT:A | | 6 | 35.827.923 | A | 0,02 | 5,36E-06 | 11,3 | intronic | LHFPL5 | 35,797,206-35,845,397 |
| chr6:146586022:G:A | rs62436209 | 6 | 146.586.022 | A | 0,11306 | 5,82E-06 | 5,2 | intergenic | ADGB (12,945 bp) | 146,598,967-146,815,462 |

| | | | | | | | | | | |
|---|---|---|---|---|---|---|---|---|---|---|
| chr5:23357704:T:A | rs76437223 | 5 | 23.357.704 | A | 0,02 | 5,93E-06 | 11,2 | intergenic | PRDM9 (85,882 bp) | 23,443,586-23,528,093 |
| chr18:576287:C:G | rs507731 | 18 | 576.287 | G | 0,179581 | 5,94E-06 | 4,3 | intergenic | CETN1 (4,093 bp) | 580,380-582,114 |
| chr2:100965046:A:G | rs17025086 | 2 | 100.965.046 | G | 0,08 | 6,02E-06 | -6,1 | intronic | NPAS2 | 100,820,139-100,996,829 |
| chr2:100965272:T:C | rs3768985 | 2 | 100.965.272 | C | 0,08 | 6,02E-06 | -6,1 | intronic | NPAS2 | 100,820,139-100,996,829 |
| chr2:100965783:AGCCCAGGCATGGGG:A | rs774019923 | 2 | 100.965.783 | A | 0,08 | 6,02E-06 | -6,1 | intronic | NPAS2 | 100,820,139-100,996,829 |
| chr2:100966205:C:T | rs1867862 | 2 | 100.966.205 | T | 0,08 | 6,02E-06 | -6,1 | intronic | NPAS2 | 100,820,139-100,996,829 |
| chr2:100968433:C:T | rs2289950 | 2 | 100.968.433 | T | 0,08 | 6,02E-06 | -6,1 | intronic | NPAS2 | 100,820,139-100,996,829 |
| chr2:100965484:C:T | rs3768986 | 2 | 100.965.484 | T | 0,08 | 6,19E-06 | -6,1 | intronic | NPAS2 | 100,820,139-100,996,829 |
| chr2:10456151:C:T | rs62127117 | 2 | 10.456.151 | T | 0,35575 | 6,24E-06 | 3,4 | intergenic | ODC1 (7,824 bp) | 10,439,968-10,448,327 |
| chr9:22853832:A:G | rs117959313 | 9 | 22.853.832 | G | 0,03 | 6,50E-06 | 9,2 | ncRNA_intronic | DMRTA1 (398,092 bp) | 22,446,824-22,455,740 |
| chr6:146609106:A:G | rs1115208 | 6 | 146.609.106 | G | 0,130117 | 6,61E-06 | 4,8 | intronic | ADGB | 146,598,967-146,815,462 |
| chr2:167772826:A:G | rs77352129 | 2 | 167.772.826 | G | 0,03 | 6,67E-06 | 9,1 | intronic | B3GALT1 | 167,293,001-167,874,045 |
| chr2:56224617:T:C | rs114727015 | 2 | 56.224.617 | C | 0,029971 | 6,80E-06 | 9,7 | intronic | CCDC85A | 56,183,990-56,386,172 |
| chr2:100971180:A:T | rs75107839 | 2 | 100.971.180 | T | 0,09 | 7,07E-06 | -5,9 | intronic | NPAS2 | 100,820,139-100,996,829 |
| chr20:53692448:T:A | rs141742171 | 20 | 53.692.448 | A | 0,13 | 7,22E-06 | 4,7 | intergenic | ZNF217 (82,541 bp) | 53,567,071-53,609,907 |
| chr20:53692564:G:A | rs73134247 | 20 | 53.692.564 | A | 0,13 | 7,22E-06 | 4,7 | intergenic | ZNF217 (82,657 bp) | 53,567,071-53,609,907 |
| chr2:10456888:C:T | rs11685132 | 2 | 10.456.888 | T | 0,353801 | 7,33E-06 | 3,4 | intergenic | ODC1 (8,561 bp) | 10,439,968-10,448,327 |
| chr20:53694463:C:T | rs6022675 | 20 | 53.694.463 | T | 0,13 | 8,14E-06 | 4,7 | intergenic | ZNF217 (84,556 bp) | 53,567,071-53,609,907 |
| chr20:53695294:G:A | rs6022677 | 20 | 53.695.294 | A | 0,13 | 8,14E-06 | 4,7 | intergenic | ZNF217 (85,387 bp) | 53,567,071-53,609,907 |
| chr20:53695395:T:C | rs7264081 | 20 | 53.695.395 | C | 0,13 | 8,14E-06 | 4,7 | intergenic | ZNF217 (85,488 bp) | 53,567,071-53,609,907 |
| chr20:53695568:G:A | rs6022679 | 20 | 53.695.568 | A | 0,13 | 8,14E-06 | 4,7 | intergenic | ZNF217 (85,661 bp) | 53,567,071-53,609,907 |
| chr20:53696291:A:G | rs16998327 | 20 | 53.696.291 | G | 0,13 | 8,14E-06 | 4,7 | intergenic | ZNF217 (86,384 bp) | 53,567,071-53,609,907 |
| chr5:23958489:C:A | rs138045800 | 5 | 23.958.489 | A | 0,02 | 8,27E-06 | 11,0 | ncRNA_intronic | PRDM9 (514,903 bp) | 23,443,586-23,528,093 |
| chr2:100967073:C:CTCAA | rs1573743506 | 2 | 100.967.073 | CTCAA | 0,08 | 8,45E-06 | -6,0 | intronic | NPAS2 | 100,820,139-100,996,829 |
| chr2:100967124:A:T | rs7340468 | 2 | 100.967.124 | T | 0,08 | 8,45E-06 | -6,0 | intronic | NPAS2 | 100,820,139-100,996,829 |
| chr2:100967496:G:C | rs59951797 | 2 | 100.967.496 | C | 0,08 | 8,45E-06 | -6,0 | intronic | NPAS2 | 100,820,139-100,996,829 |
| chr2:100968489:A:G | rs35503589 | 2 | 100.968.489 | G | 0,08 | 8,45E-06 | -6,0 | intronic | NPAS2 | 100,820,139-100,996,829 |
| chr20:53696033:C:T | rs66951711 | 20 | 53.696.033 | T | 0,13 | 8,64E-06 | 4,7 | intergenic | ZNF217 (86,126 bp) | 53,567,071-53,609,907 |
| chr20:53698485:A:G | rs73283718 | 20 | 53.698.485 | G | 0,13 | 9,34E-06 | 4,7 | intergenic | ZNF217 (88,558 bp) | 53,567,071-53,609,907 |
| chr20:53697154:G:A | rs7348874 | 20 | 53.697.154 | A | 0,13 | 9,44E-06 | 4,7 | intergenic | ZNF217 (87,247 bp) | 53,567,071-53,609,907 |
| chr1:245880428:C:T | rs12041538 | 1 | 245.880.428 | T | 0,11 | 9,65E-06 | 5,3 | intronic | SMYD3 | 245,749,342-246,507,312 |
| chr20:53697273:G:A | rs7348908 | 20 | 53.697.273 | A | 0,13 | 9,78E-06 | 4,7 | intergenic | ZNF217 (87,366 bp) | 53,567,071-53,609,907 |
| chr2:77359143:C:T | rs17014022 | 2 | 77.359.143 | T | 0,03192 | 9,97E-06 | 9,2 | intronic | LRRTM4 | 76,747,685-77,593,319 |

^ rsID, variant ID from dbSNP; * According to GRCh38 human genome reference assembly; § Coding gene where the variants map or nearest coding gene (distance is indicated in brackets).
Chr, chromosome; MAF, minor allele frequency.

**Supplementary Table S2**. Summary statistics of the GWAS for pain intensity (*P* -value < $1.0 \times 10^{-5}$); variants are sorted according to their *P* -value.

| Chromosome | Position (bp) * | variant ID | rsID | Allele 0 | Allele 1 ^ | Allele 1 frequency | BETA | SE | *P* -value | FDR | Predicted Function | RefSeq Gene |
|---|---|---|---|---|---|---|---|---|---|---|---|---|
| 20 | 64281110 | chr20:64281110:G:A | rs6062363 | G | A | 0,39 | -0,17 | 0,03 | 1,27E-08 | 0,030 | intergenic | |
| 20 | 64281343 | chr20:64281343:G:A | rs6062365 | G | A | 0,39 | -0,17 | 0,03 | 1,55E-08 | 0,030 | intergenic | |
| 20 | 64285790 | chr20:64285790:T:C | rs6089804 | T | C | 0,61 | 0,17 | 0,03 | 1,60E-08 | 0,030 | intergenic | |
| 20 | 64282739 | chr20:64282739:C:A | rs13043326 | C | A | 0,39 | -0,17 | 0,03 | 1,60E-08 | 0,030 | intergenic | |
| 20 | 64283546 | chr20:64283546:A:T | rs1806952 | A | T | 0,61 | 0,17 | 0,03 | 1,95E-08 | 0,030 | intergenic | |
| 6 | 150123675 | chr6:150123675:C:T | rs9479734 | C | T | 0,19 | 0,19 | 0,04 | 2,69E-07 | 0,32 | intergenic | |
| 20 | 64260534 | chr20:64260534:G:A | rs6062683 | G | A | 0,47 | -0,15 | 0,03 | 4,81E-07 | 0,32 | intronic | PCMTD2 |
| 20 | 64260450 | chr20:64260450:A:G | rs6062681 | A | G | 0,47 | -0,15 | 0,03 | 5,03E-07 | 0,32 | intronic | PCMTD2 |
| 20 | 64258638 | chr20:64258638:T:C | rs6062679 | T | C | 0,47 | -0,15 | 0,03 | 5,13E-07 | 0,32 | intronic | PCMTD2 |
| 20 | 64257449 | chr20:64257449:G:T | rs6062678 | G | T | 0,47 | -0,15 | 0,03 | 6,69E-07 | 0,32 | intronic | PCMTD2 |
| 20 | 64261231 | chr20:64261231:A:G | rs6512309 | A | G | 0,47 | -0,15 | 0,03 | 6,69E-07 | 0,32 | intronic | PCMTD2 |
| 20 | 64261403 | chr20:64261403:C:G | rs7270745 | C | G | 0,47 | -0,15 | 0,03 | 6,69E-07 | 0,32 | intronic | PCMTD2 |
| 20 | 64261602 | chr20:64261602:GT:G | rs11474881 | GT | G | 0,47 | -0,15 | 0,03 | 6,69E-07 | 0,32 | intronic | PCMTD2 |
| 20 | 64279990 | chr20:64279990:C:A | rs6090105 | C | A | 0,43 | -0,15 | 0,03 | 7,02E-07 | 0,32 | intergenic | |
| 20 | 64279601 | chr20:64279601:A:G | rs1570520 | A | G | 0,44 | -0,15 | 0,03 | 8,06E-07 | 0,32 | intergenic | |
| 20 | 64279666 | chr20:64279666:G:T | rs1570521 | G | T | 0,44 | -0,15 | 0,03 | 8,06E-07 | 0,32 | intergenic | |
| 20 | 64281260 | chr20:64281260:T:C | rs6062688 | T | C | 0,44 | -0,15 | 0,03 | 8,06E-07 | 0,32 | intergenic | |
| 20 | 64281378 | chr20:64281378:C:T | rs6090107 | C | T | 0,44 | -0,15 | 0,03 | 8,06E-07 | 0,32 | intergenic | |
| 20 | 64281456 | chr20:64281456:G:A | rs6089803 | G | A | 0,44 | -0,15 | 0,03 | 8,06E-07 | 0,32 | intergenic | |
| 20 | 64260467 | chr20:64260467:C:T | rs6062682 | C | T | 0,47 | -0,15 | 0,03 | 9,06E-07 | 0,34 | intronic | PCMTD2 |
| 20 | 64280038 | chr20:64280038:T:G | rs6089801 | T | G | 0,44 | -0,15 | 0,03 | 9,74E-07 | 0,35 | intergenic | |
| 20 | 64259579 | chr20:64259579:G:A | rs1808056 | G | A | 0,47 | -0,14 | 0,03 | 1,06E-06 | 0,37 | intronic | PCMTD2 |
| 5 | 138125415 | chr5:138125415:A:C | rs58312963 | A | C | 0,05 | -0,32 | 0,07 | 1,24E-06 | 0,41 | intronic | NME5 |
| 7 | 20198076 | chr7:20198076:A:T | rs28469242 | A | T | 0,46 | -0,14 | 0,03 | 1,42E-06 | 0,45 | intronic | STEAP1B |
| 5 | 167004270 | chr5:167004270:T:C | rs35961649 | T | C | 0,02 | -0,48 | 0,10 | 1,65E-06 | 0,50 | intergenic | |
| 3 | 54542522 | chr3:54542522:C:A | rs9868245 | C | A | 0,05 | -0,33 | 0,07 | 1,77E-06 | 0,50 | intronic | LPP |
| 20 | 64269027 | chr20:64269027:T:G | rs6062359 | T | G | 0,44 | -0,14 | 0,03 | 1,84E-06 | 0,50 | intronic | PCMTD2 |
| 3 | 21528263 | chr3:21528263:G:GA | rs34651874 | G | GA | 0,04 | -0,36 | 0,08 | 1,86E-06 | 0,50 | intronic | LPP |
| 3 | 188518203 | chr3:188518203:TA:T | rs562876208 | TA | T | 0,17 | 0,19 | 0,04 | 2,04E-06 | 0,53 | intronic | ZNF385D |
| 5 | 138339617 | chr5:138339617:C:T | rs17171802 | C | T | 0,04 | -0,33 | 0,07 | 2,48E-06 | 0,63 | intronic, 5' upstream | CDC25C, FAM53C |
| 20 | 64281506 | chr20:64281506:C:T | rs4809259 | C | T | 0,52 | 0,14 | 0,03 | 2,58E-06 | 0,63 | intergenic | |
| 5 | 138300258 | chr5:138300258:C:T | rs75792163 | C | T | 0,11 | -0,21 | 0,05 | 2,78E-06 | 0,66 | intronic | CDC25C |
| 20 | 64261386 | chr20:64261386:C:T | rs6062357 | C | T | 0,47 | -0,14 | 0,03 | 3,81E-06 | 0,88 | intronic | PCMTD2 |
| 2 | 139244964 | chr2:139244964:T:C | rs7567555 | T | C | 0,48 | -0,13 | 0,03 | 4,83E-06 | 0,93 | intergenic | |
| 7 | 20196513 | chr7:20196513:A:G | rs5026218 | A | G | 0,34 | -0,14 | 0,03 | 5,02E-06 | 0,93 | intronic | MACC1 |
| 20 | 64269364 | chr20:64269364:C:T | rs2427638 | C | T | 0,49 | -0,13 | 0,03 | 5,09E-06 | 0,93 | intronic | PCMTD2 |
| 20 | 64273189 | chr20:64273189:A:G | rs6062361 | A | G | 0,49 | -0,13 | 0,03 | 5,16E-06 | 0,93 | intronic | PCMTD2 |
| 5 | 138335720 | chr5:138335720:G:A | rs113885171 | G | A | 0,11 | -0,21 | 0,05 | 5,83E-06 | 0,93 | intronic, 5' upstream, non-coding intronic | CDC25C, FAM53C, LOC100128966 |
| 20 | 64279876 | chr20:64279876:A:G | rs6062362 | A | G | 0,44 | -0,13 | 0,03 | 5,86E-06 | 0,93 | intergenic | |
| 4 | 99500654 | chr4:99500654:C:A | rs6848752 | C | A | 0,02 | 0,42 | 0,09 | 5,94E-06 | 0,93 | intergenic | |
| 11 | 10570705 | chr11:10570705:A:G | rs6484374 | A | G | 0,93 | -0,27 | 0,06 | 6,10E-06 | 0,93 | 5' upstream, non-coding intronic | LYVE1, MRVI1-AS1 |
| 20 | 64276336 | chr20:64276336:ATAT:A | rs76240558 | ATAT | A | 0,14 | -0,19 | 0,04 | 6,16E-06 | 0,93 | 3' downstream | PCMTD2 |
| 22 | 44670653 | chr22:44670653:C:T | rs78122049 | C | T | 0,03 | -0,38 | 0,09 | 6,82E-06 | 0,93 | intronic | PRR5 |
| 5 | 138459388 | chr5:138459388:C:A | rs740075 | C | A | 0,12 | -0,20 | 0,04 | 6,90E-06 | 0,93 | intergenic | |
| 20 | 64274498 | chr20:64274498:C:A | rs41279358 | C | A | 0,14 | -0,19 | 0,04 | 7,59E-06 | 0,93 | 3'-utr | PCMTD2 |
| 5 | 138093459 | chr5:138093459:C:T | rs146145625 | C | T | 0,04 | -0,32 | 0,07 | 7,88E-06 | 0,93 | 3' downstream | WNT8A |

| | | | | | | | | | | | | |
|---|---|---|---|---|---|---|---|---|---|---|---|---|
| 5 | 163737489 | chr5:163737489:C:T | rs148238732 | C | T | 0,11 | -0,20 | 0,05 | 8,00E-06 | 0,93 | intergenic | |
| 5 | 163740680 | chr5:163740680:C:T | rs17538629 | C | T | 0,11 | -0,20 | 0,05 | 8,00E-06 | 0,93 | intergenic | |
| 20 | 64269826 | chr20:64269826:G:A | rs58586141 | G | A | 0,14 | -0,19 | 0,04 | 8,26E-06 | 0,93 | intronic | PCMTD2 |
| 1 | 66447783 | chr1:66447783:C:T | rs79108599 | C | T | 0,05 | -0,31 | 0,07 | 8,37E-06 | 0,93 | intergenic | |
| 1 | 66450826 | chr1:66450826:G:GA | rs145469499 | G | GA | 0,05 | -0,31 | 0,07 | 8,37E-06 | 0,93 | intergenic | |
| 1 | 66453395 | chr1:66453395:A:G | rs75901315 | A | G | 0,05 | -0,31 | 0,07 | 8,37E-06 | 0,93 | intergenic | |
| 1 | 66458248 | chr1:66458248:A:G | rs111664353 | A | G | 0,05 | -0,31 | 0,07 | 8,37E-06 | 0,93 | intergenic | |
| 1 | 66458730 | chr1:66458730:CTTGT:C | rs139409774 | CTTGT | C | 0,05 | -0,31 | 0,07 | 8,37E-06 | 0,93 | intergenic | |
| 1 | 66459442 | chr1:66459442:T:C | rs111703121 | T | C | 0,05 | -0,31 | 0,07 | 8,37E-06 | 0,93 | intergenic | |
| 1 | 66460374 | chr1:66460374:T:A | rs79090084 | T | A | 0,05 | -0,31 | 0,07 | 8,37E-06 | 0,93 | intergenic | |
| 1 | 66461113 | chr1:66461113:G:A | rs75846596 | G | A | 0,05 | -0,31 | 0,07 | 8,37E-06 | 0,93 | intergenic | |
| 1 | 66464467 | chr1:66464467:C:A | rs75042283 | C | A | 0,05 | -0,31 | 0,07 | 8,37E-06 | 0,93 | intergenic | |
| 1 | 66472487 | chr1:66472487:T:G | rs111798660 | T | G | 0,05 | -0,31 | 0,07 | 8,37E-06 | 0,93 | intergenic | |
| 17 | 74031845 | chr17:74031845:T:C | rs74339503 | T | C | 0,04 | 0,32 | 0,07 | 8,41E-06 | 0,93 | intergenic | |
| 3 | 188518650 | chr3:188518650:C:A | rs6805030 | C | A | 0,16 | 0,18 | 0,04 | 8,45E-06 | 0,93 | intronic | CACNA2D3 |
| 7 | 157576872 | chr7:157576872:C:G | rs3095212 | C | G | 0,81 | -0,16 | 0,04 | 8,51E-06 | 0,93 | intronic | MACC1 |
| 15 | 69839420 | chr15:69839420:T:C | rs16953814 | T | C | 0,03 | -0,38 | 0,09 | 8,79E-06 | 0,93 | non-coding intronic | LINC00593 |
| 17 | 74031826 | chr17:74031826:C:T | rs80347687 | C | T | 0,04 | 0,33 | 0,07 | 8,98E-06 | 0,93 | intergenic | |
| 20 | 64283878 | chr20:64283878:G:A | rs4809418 | G | A | 0,51 | 0,13 | 0,03 | 9,02E-06 | 0,93 | intergenic | |
| 7 | 22482241 | chr7:22482241:G:A | rs7811696 | G | A | 0,29 | -0,14 | 0,03 | 9,54E-06 | 0,93 | intronic | STEAP1B |

* According to genomic release GRCh38; ^ Effect allele

rsID, variant ID in dbSNP; SE, standard error; FDR, false discovery rate

**Supplementary Table S3**. Results of SNP2TFBS prediction for the 31 polymorphisms on chromosome 20.

| rsID | TF name | score difference * |
|---|---|---|
| rs6062679 | SREBF1,SREBF2 | 0 |
| rs6062681 | Arnt_Ahr | 0 |
| rs6512309 | NFATC2 | 0 |
| rs11474881 | FOXP1 | -111 |
| rs6062359 | Hoxc9,Hoxa9 | -86,-18 |
| rs58586141 | Arnt | 0 |
| rs1570520 | ESR1 | -39 |
| rs6089801 | MZF1_1-4 | 0 |
| **rs6089804** | CTCF | 107 |

rsID, variant ID in dbSNP; TF, transcription factor.

* Difference in positional weight matrix (PWM) scores between alternate and reference allele. For more details about the scores, see frequently asked question page (https://epd.expasy.org/snp2tfbs/FAQ_SNP2TFBS.php)

In bold, one of the top-significant variants.

**Supplementary Table S4.** Results from functional annotation of the 31 variants on chromosome 20, in RegulomeDB.

| rsID | probability | ranking | tissue specific scores | ChIP | Chromatin accessibility | Footprint | Footprint matched | PWM | PWM matched | QTL |
|---|---|---|---|---|---|---|---|---|---|---|
| rs6062357 | 0,95833 | 1b | {'adipose tissue': '0.56791', 'adrenal gland': '0.29363', 'arterial blood vessel': '0.56791', 'blood': '0.40729', 'blood vessel': '0.56791', 'bone element': '0.50255', 'bone marrow': '0.50255', 'brain': '0.40729', 'breast': '0.59043', 'colon': '0.59225', 'connective tissue': '0.56791', 'ear': '0.28328', 'embryo': '0.50255', 'eni | True | True | True | False | True | False | True |
| rs1570520 | 0,65401 | 1b | {'adipose tissue': '0.19333', 'adrenal gland': '0.19333', 'arterial blood vessel': '0.19333', 'blood': '0.36729', 'blood vessel': '0.19333', 'bone element': '0.19758', 'bone marrow': '0.19758', 'brain': '0.19333', 'breast': '0.19333', 'colon': '0.33721', 'connective tissue': '0.21013', 'ear': '0.19333', 'embryo': '0.19333', 'eni | True | True | True | False | True | False | True |
| rs6089801 | 0,94984 | 1b | {'adipose tissue': '0.28077', 'adrenal gland': '0.28077', 'arterial blood vessel': '0.48974', 'blood': '0.53343', 'blood vessel': '0.48974', 'bone element': '0.53343', 'bone marrow': '0.53343', 'brain': '0.28077', 'breast': '0.28077', 'colon': '0.48974', 'connective tissue': '0.48974', 'ear': '0.28077', 'embryo': '0.28077', 'eni | True | True | True | False | True | False | True |
| rs6512309 | 0,3525 | 1d | {'adipose tissue': '0.20515', 'adrenal gland': '0.16416', 'arterial blood vessel': '0.20515', 'blood': '0.15376', 'blood vessel': '0.20515', 'bone element': '0.11566', 'bone marrow': '0.11566', 'brain': '0.15376', 'breast': '0.21545', 'colon': '0.16416', 'connective tissue': '0.20515', 'ear': '0.1042', 'embryo': '0.11566', 'endo | True | True | False | False | True | False | True |
| rs6062678 | 0,55436 | 1f | {'adipose tissue': '0.29464', 'adrenal gland': '0.24896', 'arterial blood vessel': '0.29464', 'blood': '0.29464', 'blood vessel': '0.29464', 'bone element': '0.24896', 'bone marrow': '0.24896', 'brain': '0.32264', 'breast': '0.29464', 'colon': '0.24896', 'connective tissue': '0.29464', 'ear': '0.16387', 'embryo': '0.29464', 'eni | True | True | False | False | False | False | True |
| rs6062679 | 0,55436 | 1f | {'adipose tissue': '0.24896', 'adrenal gland': '0.24896', 'arterial blood vessel': '0.24896', 'blood': '0.24896', 'blood vessel': '0.24896', 'bone element': '0.24896', 'bone marrow': '0.24896', 'brain': '0.32264', 'breast': '0.16387', 'colon': '0.16387', 'connective tissue': '0.24896', 'ear': '0.16387', 'embryo': '0.29464', 'eni | True | True | False | False | False | False | True |
| rs1808056 | 0,22271 | 1f | {'adipose tissue': '0.06583', 'adrenal gland': '0.10002', 'arterial blood vessel': '0.06583', 'blood': '0.10002', 'blood vessel': '0.06583', 'bone element': '0.05893', 'bone marrow': '0.05893', 'brain': '0.10002', 'breast': '0.06583', 'colon': '0.06583', 'connective tissue': '0.06583', 'ear': '0.06583', 'embryo': '0.10002', 'eni | False | True | False | False | False | False | True |
| rs6062681 | 0,22271 | 1f | {'adipose tissue': '0.07307', 'adrenal gland': '0.07307', 'arterial blood vessel': '0.10002', 'blood': '0.05893', 'blood vessel': '0.10002', 'bone element': '0.05893', 'bone marrow': '0.05893', 'brain': '0.07307', 'breast': '0.11229', 'colon': '0.07307', 'connective tissue': '0.07307', 'ear': '0.06583', 'embryo': '0.07307', 'eni | False | True | False | False | False | False | True |
| rs6062682 | 0,22271 | 1f | {'adipose tissue': '0.07307', 'adrenal gland': '0.07307', 'arterial blood vessel': '0.10002', 'blood': '0.05893', 'blood vessel': '0.10002', 'bone element': '0.07307', 'bone marrow': '0.07307', 'brain': '0.07307', 'breast': '0.11229', 'colon': '0.07307', 'connective tissue': '0.07307', 'ear': '0.06583', 'embryo': '0.07307', 'eni | False | True | False | False | False | False | True |
| rs6062683 | 0,15481 | 1f | {'adipose tissue': '0.0721', 'adrenal gland': '0.08118', 'arterial blood vessel': '0.06953', 'blood': '0.04096', 'blood vessel': '0.08694', 'bone element': '0.05079', 'bone marrow': '0.05079', 'brain': '0.08118', 'breast': '0.07806', 'colon': '0.09567', 'connective tissue': '0.05079', 'ear': '0.04576', 'embryo': '0.08118', 'endo | False | True | True | False | True | False | True |
| rs7270745 | 0,55436 | 1f | {'adipose tissue': '0.32264', 'adrenal gland': '0.27951', 'arterial blood vessel': '0.32264', 'blood': '0.24181', 'blood vessel': '0.32264', 'bone element': '0.18189', 'bone marrow': '0.18189', 'brain': '0.24181', 'breast': '0.33882', 'colon': '0.25817', 'connective tissue': '0.32264', 'ear': '0.16387', 'embryo': '0.18189', 'eni | True | True | False | False | False | False | True |
| rs6062359 | 0,05 | 1f | {'adipose tissue': '0.01321', 'adrenal gland': '0.01321', 'arterial blood vessel': '0.01321', 'blood': '0.01321', 'blood vessel': '0.01321', 'bone element': '0.01321', 'bone marrow': '0.01321', 'brain': '0.01805', 'breast': '0.01478', 'colon': '0.01321', 'connective tissue': '0.01321', 'ear': '0.01478', 'embryo': '0.01321', 'eni | False | True | True | False | True | False | True |
| rs2427638 | 0,22271 | 1f | {'adipose tissue': '0.05884', 'adrenal gland': '0.06583', 'arterial blood vessel': '0.05884', 'blood': '0.05884', 'blood vessel': '0.05884', 'bone element': '0.05884', 'bone marrow': '0.05884', 'brain': '0.05884', 'breast': '0.06583', 'colon': '0.05884', 'connective tissue': '0.05884', 'ear': '0.06583', 'embryo': '0.05884', 'eni | False | True | False | False | False | False | True |
| rs58586141 | 0,55436 | 1f | {'adipose tissue': '0.14646', 'adrenal gland': '0.14646', 'arterial blood vessel': '0.16387', 'blood': '0.14668', 'blood vessel': '0.16387', 'bone element': '0.14646', 'bone marrow': '0.14646', 'brain': '0.20007', 'breast': '0.16387', 'colon': '0.26853', 'connective tissue': '0.17124', 'ear': '0.16387', 'embryo': '0.13975', 'eni | True | True | False | False | False | False | True |
| rs6062361 | 0,22271 | 1f | {'adipose tissue': '0.05884', 'adrenal gland': '0.05884', 'arterial blood vessel': '0.05884', 'blood': '0.05884', 'blood vessel': '0.05884', 'bone element': '0.05884', 'bone marrow': '0.05884', 'brain': '0.07307', 'breast': '0.05884', 'colon': '0.05884', 'connective tissue': '0.05884', 'ear': '0.06583', 'embryo': '0.05884', 'eni | False | True | False | False | False | False | True |
| rs76240558 | 0,905 | 1f | {'adipose tissue': '0.26752', 'adrenal gland': '0.26752', 'arterial blood vessel': '0.26752', 'blood': '0.26752', 'blood vessel': '0.26752', 'bone element': '0.2391', 'bone marrow': '0.2391', 'brain': '0.4563', 'breast': '0.26752', 'colon': '0.26752', 'connective tissue': '0.26752', 'ear': '0.26752', 'embryo': '0.2391', 'endocrii | False | True | False | False | True | False | True |
| rs1570521 | 0,55436 | 1f | {'adipose tissue': '0.16387', 'adrenal gland': '0.16387', 'arterial blood vessel': '0.16387', 'blood': '0.24896', 'blood vessel': '0.16387', 'bone element': '0.15228', 'bone marrow': '0.15228', 'brain': '0.16387', 'breast': '0.16387', 'colon': '0.16387', 'connective tissue': '0.17812', 'ear': '0.16387', 'embryo': '0.16387', 'eni | True | True | False | False | False | False | True |
| rs6090105 | 0,55436 | 1f | {'adipose tissue': '0.16387', 'adrenal gland': '0.16387', 'arterial blood vessel': '0.16387', 'blood': '0.24896', 'blood vessel': '0.16387', 'bone element': '0.24896', 'bone marrow': '0.24896', 'brain': '0.16387', 'breast': '0.16387', 'colon': '0.16387', 'connective tissue': '0.16387', 'ear': '0.16387', 'embryo': '0.16387', 'eni | True | True | False | False | False | False | True |
| **rs6062363** | 0,55436 | 1f | {'adipose tissue': '0.16387', 'adrenal gland': '0.16387', 'arterial blood vessel': '0.16387', 'blood': '0.24896', 'blood vessel': '0.16387', 'bone element': '0.16387', 'bone marrow': '0.16387', 'brain': '0.27951', 'breast': '0.16387', 'colon': '0.16387', 'connective tissue': '0.17812', 'ear': '0.16387', 'embryo': '0.16387', 'eni | True | True | False | False | False | False | True |
| rs6062688 | 0,55324 | 1f | {'adipose tissue': '0.16354', 'adrenal gland': '0.16354', 'arterial blood vessel': '0.16354', 'blood': '0.24846', 'blood vessel': '0.16354', 'bone element': '0.16354', 'bone marrow': '0.16354', 'brain': '0.27894', 'breast': '0.16354', 'colon': '0.16354', 'connective tissue': '0.17776', 'ear': '0.16354', 'embryo': '0.16354', 'eni | True | False | False | False | False | False | True |
| rs6090107 | 0,22271 | 1f | {'adipose tissue': '0.06583', 'adrenal gland': '0.06583', 'arterial blood vessel': '0.06583', 'blood': '0.10002', 'blood vessel': '0.06583', 'bone element': '0.06583', 'bone marrow': '0.06583', 'brain': '0.11229', 'breast': '0.06583', 'colon': '0.06583', 'connective tissue': '0.07156', 'ear': '0.06583', 'embryo': '0.06583', 'eni | False | True | False | False | False | False | True |
| rs6089803 | 0,22271 | 1f | {'adipose tissue': '0.06583', 'adrenal gland': '0.06583', 'arterial blood vessel': '0.06583', 'blood': '0.10002', 'blood vessel': '0.06583', 'bone element': '0.06583', 'bone marrow': '0.06583', 'brain': '0.11229', 'breast': '0.06583', 'colon': '0.06583', 'connective tissue': '0.07156', 'ear': '0.06583', 'embryo': '0.06583', 'eni | False | True | False | False | False | False | True |
| rs4809259 | 0,22271 | 1f | {'adipose tissue': '0.06583', 'adrenal gland': '0.06583', 'arterial blood vessel': '0.06583', 'blood': '0.10002', 'blood vessel': '0.06583', 'bone element': '0.06583', 'bone marrow': '0.06583', 'brain': '0.11229', 'breast': '0.06583', 'colon': '0.06583', 'connective tissue': '0.06583', 'ear': '0.06583', 'embryo': '0.06583', 'eni | False | True | False | False | False | False | True |
| **rs13043326** | 0,22271 | 1f | {'adipose tissue': '0.06583', 'adrenal gland': '0.06583', 'arterial blood vessel': '0.06583', 'blood': '0.10002', 'blood vessel': '0.06583', 'bone element': '0.07156', 'bone marrow': '0.06583', 'brain': '0.05136', 'breast': '0.06583', 'colon': '0.06583', 'connective tissue': '0.07156', 'ear': '0.06583', 'embryo': '0.06583', 'eni | False | True | False | False | False | False | True |
| **rs1806952** | 0,22271 | 1f | {'adipose tissue': '0.06583', 'adrenal gland': '0.06583', 'arterial blood vessel': '0.06583', 'blood': '0.10002', 'blood vessel': '0.06583', 'bone element': '0.06583', 'bone marrow': '0.06583', 'brain': '0.10002', 'breast': '0.06583', 'colon': '0.06583', 'connective tissue': '0.07156', 'ear': '0.06583', 'embryo': '0.06583', 'eni | False | True | False | False | False | False | True |
| **rs6089804** | 0,55436 | 1f | {'adipose tissue': '0.16387', 'adrenal gland': '0.16387', 'arterial blood vessel': '0.16387', 'blood': '0.16387', 'blood vessel': '0.16387', 'bone element': '0.13975', 'bone marrow': '0.13975', 'brain': '0.27951', 'breast': '0.16387', 'colon': '0.16387', 'connective tissue': '0.16387', 'ear': '0.16387', 'embryo': '0.17812', 'eni | True | True | False | False | False | False | True |
| rs6089804 | 0,55436 | 1f | {'adipose tissue': '0.16387', 'adrenal gland': '0.16387', 'arterial blood vessel': '0.16387', 'blood': '0.16387', 'blood vessel': '0.16387', 'bone element': '0.13975', 'bone marrow': '0.13975', 'brain': '0.27951', 'breast': '0.16387', 'colon': '0.16387', 'connective tissue': '0.16387', 'ear': '0.16387', 'embryo': '0.17812', 'eni | True | True | False | False | False | False | True |
| rs11474881 | 0,48203 | 2b | {'adipose tissue': '0.28565', 'adrenal gland': '0.29789', 'arterial blood vessel': '0.28054', 'blood': '0.1489', 'blood vessel': '0.28054', 'bone element': '0.27071', 'bone marrow': '0.21648', 'brain': '0.21026', 'breast': '0.24853', 'colon': '0.29789', 'connective tissue': '0.28565', 'ear': '0.14249', 'embryo': '0.22448', 'endo | True | True | True | False | True | False | False |
| rs6062362 | 0,60906 | 4 | {'adipose tissue': '0.18004', 'adrenal gland': '0.18004', 'arterial blood vessel': '0.18004', 'blood': '0.27353', 'blood vessel': '0.18004', 'bone element': '0.27353', 'bone marrow': '0.27353', 'brain': '0.18004', 'breast': '0.18004', 'colon': '0.18004', 'connective tissue': '0.18004', 'ear': '0.18004', 'embryo': '0.18004', 'eni | True | True | False | False | False | False | False |
| **rs6062365** | 0,1625 | 6 | {'adipose tissue': '0.04803', 'adrenal gland': '0.04803', 'arterial blood vessel': '0.04803', 'blood': '0.07298', 'blood vessel': '0.04803', 'bone element': '0.04803', 'bone marrow': '0.04803', 'brain': '0.08193', 'breast': '0.04803', 'colon': '0.04803', 'connective tissue': '0.05221', 'ear': '0.04803', 'embryo': '0.04803', 'eni | False | False | False | False | True | False | True |
| rs41279358 | 0,51392 | 7 | {'adipose tissue': '0.13578', 'adrenal gland': '0.15191', 'arterial blood vessel': '0.15191', 'blood': '0.13578', 'blood vessel': '0.15191', 'bone element': '0.13578', 'bone marrow': '0.13578', 'brain': '0.18547', 'breast': '0.15191', 'colon': '0.13578', 'connective tissue': '0.13578', 'ear': '0.15191', 'embryo': '0.13578', 'eni | False | False | False | False | False | False | True |

rsID, variant ID in dbSNP; PWM, position weight matrix; QTL, quantitative trait locus.

In bold, the top-significant variants in our GWAS.

**Supplementary Table S5**. eQTLs reported in GTEx, for the 31 variants on chromosome 20 (*P* -value < 1.0 x $10^{-5}$).

| Variant ID | rsID | gene ID | TSS distance | MAF | MA samples | MA count | *P* -value | slope | slope SE | tissue |
|---|---|---|---|---|---|---|---|---|---|---|
| chr20_64257449_G_T_b38 | rs6062678 | ENSG00000203880.11 | 1754 | 0,496364 | 205 | 273 | 8,31E-21 | -0,305059 | 0,0293835 | Esophagus_Gastroesophageal_Junction |
| chr20_64257449_G_T_b38 | rs6062678 | ENSG00000203880.11 | 1754 | 0,479123 | 356 | 459 | 2,85E-17 | -0,205605 | 0,0232554 | Adipose_Subcutaneous |
| chr20_64257449_G_T_b38 | rs6062678 | ENSG00000203880.11 | 1754 | 0,491597 | 363 | 468 | 1,77E-15 | -0,208714 | 0,0251988 | Artery_Tibial |
| chr20_64257449_G_T_b38 | rs6062678 | ENSG00000203880.11 | 1754 | 0,5 | 255 | 329 | 6,27E-14 | -0,263862 | 0,0333475 | Artery_Aorta |
| chr20_64257449_G_T_b38 | rs6062678 | ENSG00000203880.11 | 1754 | 0,473236 | 303 | 389 | 2,99E-10 | -0,230665 | 0,0355313 | Esophagus_Mucosa |
| chr20_64257449_G_T_b38 | rs6062678 | ENSG00000203880.11 | 1754 | 0,486395 | 220 | 286 | 2,75E-09 | -0,186083 | 0,0301138 | Colon_Transverse |
| chr20_64257449_G_T_b38 | rs6062678 | ENSG00000203880.11 | 1754 | 0,479323 | 193 | 255 | 3,14E-08 | -0,205701 | 0,0357899 | Colon_Sigmoid |
| chr20_64257449_G_T_b38 | rs6062678 | ENSG00000203880.11 | 1754 | 0,490881 | 247 | 323 | 4,87E-07 | -0,169925 | 0,0329648 | Breast_Mammary |
| chr20_64257449_G_T_b38 | rs6062678 | ENSG00000203880.11 | 1754 | 0,483461 | 291 | 380 | 3,32E-06 | -0,0943795 | 0,019943 | Adipose_Visceral_Omentum |
| chr20_64258638_T_C_b38 | rs6062679 | ENSG00000203880.11 | 2943 | 0,496364 | 205 | 273 | 8,31E-21 | -0,305059 | 0,0293835 | Esophagus_Gastroesophageal_Junction |
| chr20_64258638_T_C_b38 | rs6062679 | ENSG00000203880.11 | 2943 | 0,479123 | 356 | 459 | 2,85E-17 | -0,205605 | 0,0232554 | Adipose_Subcutaneous |
| chr20_64258638_T_C_b38 | rs6062679 | ENSG00000203880.11 | 2943 | 0,491597 | 363 | 468 | 1,77E-15 | -0,208714 | 0,0251988 | Artery_Tibial |
| chr20_64258638_T_C_b38 | rs6062679 | ENSG00000203880.11 | 2943 | 0,5 | 255 | 329 | 6,27E-14 | -0,263862 | 0,0333475 | Artery_Aorta |
| chr20_64258638_T_C_b38 | rs6062679 | ENSG00000203880.11 | 2943 | 0,473236 | 303 | 389 | 2,99E-10 | -0,230665 | 0,0355313 | Esophagus_Mucosa |
| chr20_64258638_T_C_b38 | rs6062679 | ENSG00000203880.11 | 2943 | 0,486395 | 220 | 286 | 2,75E-09 | -0,186083 | 0,0301138 | Colon_Transverse |
| chr20_64258638_T_C_b38 | rs6062679 | ENSG00000203880.11 | 2943 | 0,479323 | 193 | 255 | 3,14E-08 | -0,205701 | 0,0357899 | Colon_Sigmoid |
| chr20_64258638_T_C_b38 | rs6062679 | ENSG00000203880.11 | 2943 | 0,490881 | 247 | 323 | 4,87E-07 | -0,169925 | 0,0329648 | Breast_Mammary |
| chr20_64258638_T_C_b38 | rs6062679 | ENSG00000203880.11 | 2943 | 0,483461 | 291 | 380 | 3,32E-06 | -0,0943795 | 0,019943 | Adipose_Visceral_Omentum |
| chr20_64259579_G_A_b38 | rs1808056 | ENSG00000203880.11 | 3884 | 0,498182 | 205 | 274 | 1,00E-20 | -0,30245 | 0,0292076 | Esophagus_Gastroesophageal_Junction |
| chr20_64259579_G_A_b38 | rs1808056 | ENSG00000203880.11 | 3884 | 0,478079 | 355 | 458 | 2,93E-17 | -0,204798 | 0,0231734 | Adipose_Subcutaneous |
| chr20_64259579_G_A_b38 | rs1808056 | ENSG00000203880.11 | 3884 | 0,490546 | 362 | 467 | 1,25E-15 | -0,209041 | 0,0250936 | Artery_Tibial |
| chr20_64259579_G_A_b38 | rs1808056 | ENSG00000203880.11 | 3884 | 0,49848 | 254 | 328 | 6,65E-14 | -0,262661 | 0,033234 | Artery_Aorta |
| chr20_64259579_G_A_b38 | rs1808056 | ENSG00000203880.11 | 3884 | 0,472019 | 302 | 388 | 1,16E-10 | -0,235107 | 0,0353486 | Esophagus_Mucosa |
| chr20_64259579_G_A_b38 | rs1808056 | ENSG00000203880.11 | 3884 | 0,484694 | 219 | 285 | 2,43E-09 | -0,185975 | 0,0299852 | Colon_Transverse |
| chr20_64259579_G_A_b38 | rs1808056 | ENSG00000203880.11 | 3884 | 0,477444 | 192 | 254 | 4,52E-08 | -0,202422 | 0,0356623 | Colon_Sigmoid |
| chr20_64259579_G_A_b38 | rs1808056 | ENSG00000203880.11 | 3884 | 0,489362 | 246 | 322 | 6,07E-07 | -0,168333 | 0,0329459 | Breast_Mammary |
| chr20_64259579_G_A_b38 | rs1808056 | ENSG00000203880.11 | 3884 | 0,482188 | 290 | 379 | 2,18E-06 | -0,0958431 | 0,0198699 | Adipose_Visceral_Omentum |
| chr20_64260450_A_G_b38 | rs6062681 | ENSG00000203880.11 | 4755 | 0,496364 | 205 | 273 | 8,31E-21 | -0,305059 | 0,0293835 | Esophagus_Gastroesophageal_Junction |
| chr20_64260450_A_G_b38 | rs6062681 | ENSG00000203880.11 | 4755 | 0,479123 | 356 | 459 | 2,85E-17 | -0,205605 | 0,0232554 | Adipose_Subcutaneous |
| chr20_64260450_A_G_b38 | rs6062681 | ENSG00000203880.11 | 4755 | 0,491597 | 363 | 468 | 1,77E-15 | -0,208714 | 0,0251988 | Artery_Tibial |
| chr20_64260450_A_G_b38 | rs6062681 | ENSG00000203880.11 | 4755 | 0,5 | 255 | 329 | 6,27E-14 | -0,263862 | 0,0333475 | Artery_Aorta |
| chr20_64260450_A_G_b38 | rs6062681 | ENSG00000203880.11 | 4755 | 0,473236 | 303 | 389 | 2,99E-10 | -0,230665 | 0,0355313 | Esophagus_Mucosa |
| chr20_64260450_A_G_b38 | rs6062681 | ENSG00000203880.11 | 4755 | 0,486395 | 220 | 286 | 2,75E-09 | -0,186083 | 0,0301138 | Colon_Transverse |
| chr20_64260450_A_G_b38 | rs6062681 | ENSG00000203880.11 | 4755 | 0,479323 | 193 | 255 | 3,14E-08 | -0,205701 | 0,0357899 | Colon_Sigmoid |
| chr20_64260450_A_G_b38 | rs6062681 | ENSG00000203880.11 | 4755 | 0,490881 | 247 | 323 | 4,87E-07 | -0,169925 | 0,0329648 | Breast_Mammary |
| chr20_64260450_A_G_b38 | rs6062681 | ENSG00000203880.11 | 4755 | 0,483461 | 291 | 380 | 3,32E-06 | -0,0943795 | 0,019943 | Adipose_Visceral_Omentum |
| chr20_64260467_C_T_b38 | rs6062682 | ENSG00000203880.11 | 4772 | 0,498182 | 205 | 274 | 1,00E-20 | -0,30245 | 0,0292076 | Esophagus_Gastroesophageal_Junction |

| | | | | | | | | | | |
|---|---|---|---|---|---|---|---|---|---|---|
| chr20_64260467_C_T_b38 | rs6062682 | ENSG00000203880.11 | 4772 | 0,478079 | 355 | 458 | 2,93E-17 | -0,204798 | 0,0231734 | Adipose_Subcutaneous |
| chr20_64260467_C_T_b38 | rs6062682 | ENSG00000203880.11 | 4772 | 0,490546 | 362 | 467 | 1,25E-15 | -0,209041 | 0,0250936 | Artery_Tibial |
| chr20_64260467_C_T_b38 | rs6062682 | ENSG00000203880.11 | 4772 | 0,49848 | 254 | 328 | 6,65E-14 | -0,262661 | 0,033234 | Artery_Aorta |
| chr20_64260467_C_T_b38 | rs6062682 | ENSG00000203880.11 | 4772 | 0,472019 | 302 | 388 | 1,16E-10 | -0,235107 | 0,0353486 | Esophagus_Mucosa |
| chr20_64260467_C_T_b38 | rs6062682 | ENSG00000203880.11 | 4772 | 0,484694 | 219 | 285 | 2,43E-09 | -0,185975 | 0,0299852 | Colon_Transverse |
| chr20_64260467_C_T_b38 | rs6062682 | ENSG00000203880.11 | 4772 | 0,477444 | 192 | 254 | 4,52E-08 | -0,202422 | 0,0356623 | Colon_Sigmoid |
| chr20_64260467_C_T_b38 | rs6062682 | ENSG00000203880.11 | 4772 | 0,489362 | 246 | 322 | 6,07E-07 | -0,168333 | 0,0329459 | Breast_Mammary |
| chr20_64260467_C_T_b38 | rs6062682 | ENSG00000203880.11 | 4772 | 0,482188 | 290 | 379 | 2,18E-06 | -0,0958431 | 0,0198699 | Adipose_Visceral_Omentum |
| chr20_64260534_G_A_b38 | rs6062683 | ENSG00000203880.11 | 4839 | 0,496364 | 205 | 273 | 8,31E-21 | -0,305059 | 0,0293835 | Esophagus_Gastroesophageal_Junction |
| chr20_64260534_G_A_b38 | rs6062683 | ENSG00000203880.11 | 4839 | 0,479123 | 356 | 459 | 2,85E-17 | -0,205605 | 0,0232554 | Adipose_Subcutaneous |
| chr20_64260534_G_A_b38 | rs6062683 | ENSG00000203880.11 | 4839 | 0,491597 | 363 | 468 | 1,77E-15 | -0,208714 | 0,0251988 | Artery_Tibial |
| chr20_64260534_G_A_b38 | rs6062683 | ENSG00000203880.11 | 4839 | 0,5 | 255 | 329 | 6,27E-14 | -0,263862 | 0,0333475 | Artery_Aorta |
| chr20_64260534_G_A_b38 | rs6062683 | ENSG00000203880.11 | 4839 | 0,473236 | 303 | 389 | 2,99E-10 | -0,230665 | 0,0355313 | Esophagus_Mucosa |
| chr20_64260534_G_A_b38 | rs6062683 | ENSG00000203880.11 | 4839 | 0,486395 | 220 | 286 | 2,75E-09 | -0,186083 | 0,0301138 | Colon_Transverse |
| chr20_64260534_G_A_b38 | rs6062683 | ENSG00000203880.11 | 4839 | 0,479323 | 193 | 255 | 3,14E-08 | -0,205701 | 0,0357899 | Colon_Sigmoid |
| chr20_64260534_G_A_b38 | rs6062683 | ENSG00000203880.11 | 4839 | 0,490881 | 247 | 323 | 4,87E-07 | -0,169925 | 0,0329648 | Breast_Mammary |
| chr20_64260534_G_A_b38 | rs6062683 | ENSG00000203880.11 | 4839 | 0,483461 | 291 | 380 | 3,32E-06 | -0,0943795 | 0,019943 | Adipose_Visceral_Omentum |
| chr20_64261231_A_G_b38 | rs6512309 | ENSG00000203880.11 | 5536 | 0,496364 | 205 | 273 | 8,31E-21 | -0,305059 | 0,0293835 | Esophagus_Gastroesophageal_Junction |
| chr20_64261231_A_G_b38 | rs6512309 | ENSG00000203880.11 | 5536 | 0,479123 | 356 | 459 | 2,85E-17 | -0,205605 | 0,0232554 | Adipose_Subcutaneous |
| chr20_64261231_A_G_b38 | rs6512309 | ENSG00000203880.11 | 5536 | 0,491597 | 363 | 468 | 1,77E-15 | -0,208714 | 0,0251988 | Artery_Tibial |
| chr20_64261231_A_G_b38 | rs6512309 | ENSG00000203880.11 | 5536 | 0,5 | 255 | 329 | 6,27E-14 | -0,263862 | 0,0333475 | Artery_Aorta |
| chr20_64261231_A_G_b38 | rs6512309 | ENSG00000203880.11 | 5536 | 0,473236 | 303 | 389 | 2,99E-10 | -0,230665 | 0,0355313 | Esophagus_Mucosa |
| chr20_64261231_A_G_b38 | rs6512309 | ENSG00000203880.11 | 5536 | 0,486395 | 220 | 286 | 2,75E-09 | -0,186083 | 0,0301138 | Colon_Transverse |
| chr20_64261231_A_G_b38 | rs6512309 | ENSG00000203880.11 | 5536 | 0,479323 | 193 | 255 | 3,14E-08 | -0,205701 | 0,0357899 | Colon_Sigmoid |
| chr20_64261231_A_G_b38 | rs6512309 | ENSG00000203880.11 | 5536 | 0,490881 | 247 | 323 | 4,87E-07 | -0,169925 | 0,0329648 | Breast_Mammary |
| chr20_64261231_A_G_b38 | rs6512309 | ENSG00000203880.11 | 5536 | 0,483461 | 291 | 380 | 3,32E-06 | -0,0943795 | 0,019943 | Adipose_Visceral_Omentum |
| chr20_64261386_C_T_b38 | rs6062357 | ENSG00000203880.11 | 5691 | 0,492727 | 204 | 271 | 2,50E-20 | -0,301976 | 0,0295328 | Esophagus_Gastroesophageal_Junction |
| chr20_64261386_C_T_b38 | rs6062357 | ENSG00000203880.11 | 5691 | 0,483299 | 358 | 463 | 6,36E-16 | -0,197467 | 0,023448 | Adipose_Subcutaneous |
| chr20_64261386_C_T_b38 | rs6062357 | ENSG00000203880.11 | 5691 | 0,495798 | 365 | 472 | 2,13E-14 | -0,200737 | 0,0253096 | Artery_Tibial |
| chr20_64261386_C_T_b38 | rs6062357 | ENSG00000203880.11 | 5691 | 0,495441 | 253 | 326 | 1,33E-12 | -0,249459 | 0,0335467 | Artery_Aorta |
| chr20_64261386_C_T_b38 | rs6062357 | ENSG00000203880.11 | 5691 | 0,475669 | 303 | 391 | 1,68E-09 | -0,219639 | 0,0354532 | Esophagus_Mucosa |
| chr20_64261386_C_T_b38 | rs6062357 | ENSG00000203880.11 | 5691 | 0,491497 | 222 | 289 | 9,32E-09 | -0,180137 | 0,0302594 | Colon_Transverse |
| chr20_64261386_C_T_b38 | rs6062357 | ENSG00000203880.11 | 5691 | 0,483083 | 194 | 257 | 1,01E-07 | -0,197984 | 0,0358936 | Colon_Sigmoid |
| chr20_64261386_C_T_b38 | rs6062357 | ENSG00000203880.11 | 5691 | 0,495441 | 248 | 326 | 1,32E-06 | -0,163064 | 0,0329636 | Breast_Mammary |
| chr20_64261386_C_T_b38 | rs6062357 | ENSG00000203880.11 | 5691 | 0,487277 | 292 | 383 | 9,82E-06 | -0,0894637 | 0,0199145 | Adipose_Visceral_Omentum |
| chr20_64261403_C_G_b38 | rs7270745 | ENSG00000203880.11 | 5708 | 0,496364 | 205 | 273 | 8,31E-21 | -0,305059 | 0,0293835 | Esophagus_Gastroesophageal_Junction |
| chr20_64261403_C_G_b38 | rs7270745 | ENSG00000203880.11 | 5708 | 0,479123 | 356 | 459 | 2,85E-17 | -0,205605 | 0,0232554 | Adipose_Subcutaneous |
| chr20_64261403_C_G_b38 | rs7270745 | ENSG00000203880.11 | 5708 | 0,491597 | 363 | 468 | 1,77E-15 | -0,208714 | 0,0251988 | Artery_Tibial |
| chr20_64261403_C_G_b38 | rs7270745 | ENSG00000203880.11 | 5708 | 0,5 | 255 | 329 | 6,27E-14 | -0,263862 | 0,0333475 | Artery_Aorta |

| | | | | | | | | | | |
|---|---|---|---|---|---|---|---|---|---|---|
| chr20_64261403_C_G_b38 | rs7270745 | ENSG00000203880.11 | 5708 | 0,473236 | 303 | 389 | 2,99E-10 | -0,230665 | 0,0355313 | Esophagus_Mucosa |
| chr20_64261403_C_G_b38 | rs7270745 | ENSG00000203880.11 | 5708 | 0,486395 | 220 | 286 | 2,75E-09 | -0,186083 | 0,0301138 | Colon_Transverse |
| chr20_64261403_C_G_b38 | rs7270745 | ENSG00000203880.11 | 5708 | 0,479323 | 193 | 255 | 3,14E-08 | -0,205701 | 0,0357899 | Colon_Sigmoid |
| chr20_64261403_C_G_b38 | rs7270745 | ENSG00000203880.11 | 5708 | 0,490881 | 247 | 323 | 4,87E-07 | -0,169925 | 0,0329648 | Breast_Mammary |
| chr20_64261403_C_G_b38 | rs7270745 | ENSG00000203880.11 | 5708 | 0,483461 | 291 | 380 | 3,32E-06 | -0,0943795 | 0,019943 | Adipose_Visceral_Omentum |
| chr20_64269027_T_G_b38 | rs6062359 | ENSG00000203880.11 | 13332 | 0,465455 | 193 | 256 | 2,03E-15 | -0,262062 | 0,0306341 | Esophagus_Gastroesophageal_Junction |
| chr20_64269027_T_G_b38 | rs6062359 | ENSG00000203880.11 | 13332 | 0,457203 | 342 | 438 | 2,59E-15 | -0,190616 | 0,0231696 | Adipose_Subcutaneous |
| chr20_64269027_T_G_b38 | rs6062359 | ENSG00000203880.11 | 13332 | 0,475684 | 244 | 313 | 4,43E-12 | -0,243431 | 0,0336057 | Artery_Aorta |
| chr20_64269027_T_G_b38 | rs6062359 | ENSG00000203880.11 | 13332 | 0,459034 | 343 | 437 | 1,19E-11 | -0,17754 | 0,0254272 | Artery_Tibial |
| chr20_64269027_T_G_b38 | rs6062359 | ENSG00000203880.11 | 13332 | 0,442822 | 284 | 364 | 3,97E-08 | -0,195711 | 0,0348238 | Esophagus_Mucosa |
| chr20_64269027_T_G_b38 | rs6062359 | ENSG00000203880.11 | 13332 | 0,454082 | 206 | 267 | 3,48E-07 | -0,159004 | 0,030329 | Colon_Transverse |
| chr20_64269027_T_G_b38 | rs6062359 | ENSG00000203880.11 | 13332 | 0,454887 | 183 | 242 | 1,13E-06 | -0,178527 | 0,0356101 | Colon_Sigmoid |
| chr20_64269027_T_G_b38 | rs6062359 | ENSG00000203880.11 | 13332 | 0,465046 | 235 | 306 | 8,37E-06 | -0,148086 | 0,0326059 | Breast_Mammary |
| chr20_64269364_C_T_b38 | rs2427638 | ENSG00000203880.11 | 13669 | 0,481818 | 199 | 265 | 9,10E-09 | -0,197073 | 0,0329747 | Esophagus_Gastroesophageal_Junction |
| chr20_64269364_C_T_b38 | rs2427638 | ENSG00000203880.11 | 13669 | 0,488518 | 359 | 468 | 2,60E-07 | -0,126969 | 0,0242384 | Adipose_Subcutaneous |
| chr20_64269826_G_A_b38 | rs58586141 | ENSG00000203880.11 | 14131 | 0,165966 | 146 | 158 | 1,09E-23 | -0,325054 | 0,0303897 | Artery_Tibial |
| chr20_64269826_G_A_b38 | rs58586141 | ENSG00000203880.11 | 14131 | 0,160584 | 119 | 132 | 6,17E-20 | -0,410833 | 0,0421844 | Esophagus_Mucosa |
| chr20_64269826_G_A_b38 | rs58586141 | ENSG00000203880.11 | 14131 | 0,18541 | 107 | 122 | 7,40E-18 | -0,353703 | 0,0383038 | Artery_Aorta |
| chr20_64269826_G_A_b38 | rs58586141 | ENSG00000203880.11 | 14131 | 0,170909 | 86 | 94 | 1,15E-14 | -0,356547 | 0,0430339 | Esophagus_Gastroesophageal_Junction |
| chr20_64269826_G_A_b38 | rs58586141 | ENSG00000203880.11 | 14131 | 0,165971 | 146 | 159 | 2,34E-12 | -0,226712 | 0,0313423 | Adipose_Subcutaneous |
| chr20_64269826_G_A_b38 | rs58586141 | ENSG00000203880.11 | 14131 | 0,186047 | 58 | 64 | 2,25E-11 | -0,516838 | 0,0706718 | Brain_Caudate_basal_ganglia |
| chr20_64269826_G_A_b38 | rs58586141 | ENSG00000203880.11 | 14131 | 0,151361 | 82 | 89 | 2,91E-11 | -0,279866 | 0,0401008 | Colon_Transverse |
| chr20_64269826_G_A_b38 | rs58586141 | ENSG00000203880.11 | 14131 | 0,171053 | 83 | 91 | 4,52E-10 | -0,292725 | 0,0447478 | Colon_Sigmoid |
| chr20_64269826_G_A_b38 | rs58586141 | ENSG00000203880.11 | 14131 | 0,171216 | 125 | 138 | 1,32E-09 | -0,123285 | 0,0197521 | Cells_Cultured_fibroblasts |
| chr20_64269826_G_A_b38 | rs58586141 | ENSG00000203880.11 | 14131 | 0,186275 | 51 | 57 | 7,82E-09 | -0,441904 | 0,0708108 | Brain_Putamen_basal_ganglia |
| chr20_64269826_G_A_b38 | rs58586141 | ENSG00000203880.11 | 14131 | 0,176292 | 105 | 116 | 1,78E-08 | -0,250637 | 0,0431819 | Breast_Mammary |
| chr20_64269826_G_A_b38 | rs58586141 | ENSG00000203880.11 | 14131 | 0,152866 | 45 | 48 | 5,56E-08 | -0,433886 | 0,074712 | Brain_Frontal_Cortex |
| chr20_64269826_G_A_b38 | rs58586141 | ENSG00000203880.11 | 14131 | 0,162983 | 55 | 59 | 1,70E-07 | -0,375764 | 0,0682735 | Brain_Nucleus_accumbens_basal_ganglia |
| chr20_64269826_G_A_b38 | rs58586141 | ENSG00000203880.11 | 14131 | 0,173333 | 46 | 52 | 1,84E-07 | -0,365784 | 0,0656972 | Brain_Hippocampus |
| chr20_64269826_G_A_b38 | rs58586141 | ENSG00000203880.11 | 14131 | 0,16285 | 117 | 128 | 2,92E-07 | -0,137029 | 0,0261547 | Adipose_Visceral_Omentum |
| chr20_64269826_G_A_b38 | rs58586141 | ENSG00000203880.11 | 14131 | 0,166667 | 55 | 61 | 1,76E-06 | -0,283844 | 0,0569258 | Brain_Cortex |
| chr20_64269826_G_A_b38 | rs58586141 | ENSG00000203880.11 | 14131 | 0,169872 | 48 | 53 | 2,09E-06 | -0,398948 | 0,0798627 | Brain_Hypothalamus |
| chr20_64273189_A_G_b38 | rs6062361 | ENSG00000203880.11 | 17494 | 0,481818 | 199 | 265 | 9,10E-09 | -0,197073 | 0,0329747 | Esophagus_Gastroesophageal_Junction |
| chr20_64273189_A_G_b38 | rs6062361 | ENSG00000203880.11 | 17494 | 0,489562 | 360 | 469 | 2,16E-07 | -0,128202 | 0,0243047 | Adipose_Subcutaneous |
| chr20_64274498_C_A_b38 | rs41279358 | ENSG00000203880.11 | 18803 | 0,165966 | 146 | 158 | 1,09E-23 | -0,325054 | 0,0303897 | Artery_Tibial |
| chr20_64274498_C_A_b38 | rs41279358 | ENSG00000203880.11 | 18803 | 0,160584 | 119 | 132 | 6,17E-20 | -0,410833 | 0,0421844 | Esophagus_Mucosa |
| chr20_64274498_C_A_b38 | rs41279358 | ENSG00000203880.11 | 18803 | 0,18541 | 107 | 122 | 7,40E-18 | -0,353703 | 0,0383038 | Artery_Aorta |
| chr20_64274498_C_A_b38 | rs41279358 | ENSG00000203880.11 | 18803 | 0,170909 | 86 | 94 | 1,15E-14 | -0,356547 | 0,0430339 | Esophagus_Gastroesophageal_Junction |
| chr20_64274498_C_A_b38 | rs41279358 | ENSG00000203880.11 | 18803 | 0,165971 | 146 | 159 | 2,34E-12 | -0,226712 | 0,0313423 | Adipose_Subcutaneous |

| | | | | | | | | | | |
|---|---|---|---|---|---|---|---|---|---|---|
| chr20_64274498_C_A_b38 | rs41279358 | ENSG00000203880.11 | 18803 | 0,186047 | 58 | 64 | 2,25E-11 | -0,516838 | 0,0706718 | Brain_Caudate_basal_ganglia |
| chr20_64274498_C_A_b38 | rs41279358 | ENSG00000203880.11 | 18803 | 0,151361 | 82 | 89 | 2,91E-11 | -0,279866 | 0,0401008 | Colon_Transverse |
| chr20_64274498_C_A_b38 | rs41279358 | ENSG00000203880.11 | 18803 | 0,171053 | 83 | 91 | 4,52E-10 | -0,292725 | 0,0447478 | Colon_Sigmoid |
| chr20_64274498_C_A_b38 | rs41279358 | ENSG00000203880.11 | 18803 | 0,171216 | 125 | 138 | 1,32E-09 | -0,123285 | 0,0197521 | Cells_Cultured_fibroblasts |
| chr20_64274498_C_A_b38 | rs41279358 | ENSG00000203880.11 | 18803 | 0,186275 | 51 | 57 | 7,82E-09 | -0,441904 | 0,0708108 | Brain_Putamen_basal_ganglia |
| chr20_64274498_C_A_b38 | rs41279358 | ENSG00000203880.11 | 18803 | 0,176292 | 105 | 116 | 1,78E-08 | -0,250637 | 0,0431819 | Breast_Mammary |
| chr20_64274498_C_A_b38 | rs41279358 | ENSG00000203880.11 | 18803 | 0,152866 | 45 | 48 | 5,56E-08 | -0,433886 | 0,074712 | Brain_Frontal_Cortex |
| chr20_64274498_C_A_b38 | rs41279358 | ENSG00000203880.11 | 18803 | 0,162983 | 55 | 59 | 1,70E-07 | -0,375764 | 0,0682735 | Brain_Nucleus_accumbens_basal_ganglia |
| chr20_64274498_C_A_b38 | rs41279358 | ENSG00000203880.11 | 18803 | 0,173333 | 46 | 52 | 1,84E-07 | -0,365784 | 0,0656972 | Brain_Hippocampus |
| chr20_64274498_C_A_b38 | rs41279358 | ENSG00000203880.11 | 18803 | 0,16285 | 117 | 128 | 2,92E-07 | -0,137029 | 0,0261547 | Adipose_Visceral_Omentum |
| chr20_64274498_C_A_b38 | rs41279358 | ENSG00000203880.11 | 18803 | 0,166667 | 55 | 61 | 1,76E-06 | -0,283844 | 0,0569258 | Brain_Cortex |
| chr20_64274498_C_A_b38 | rs41279358 | ENSG00000203880.11 | 18803 | 0,169872 | 48 | 53 | 2,09E-06 | -0,398948 | 0,0798627 | Brain_Hypothalamus |
| chr20_64276336_ATAT_A_b38 | rs76240558 | ENSG00000203880.11 | 20641 | 0,163158 | 144 | 155 | 3,60E-23 | -0,324825 | 0,0307801 | Artery_Tibial |
| chr20_64276336_ATAT_A_b38 | rs76240558 | ENSG00000203880.11 | 20641 | 0,156934 | 117 | 129 | 9,45E-19 | -0,404264 | 0,0430949 | Esophagus_Mucosa |
| chr20_64276336_ATAT_A_b38 | rs76240558 | ENSG00000203880.11 | 20641 | 0,182371 | 106 | 120 | 1,84E-17 | -0,35376 | 0,0388505 | Artery_Aorta |
| chr20_64276336_ATAT_A_b38 | rs76240558 | ENSG00000203880.11 | 20641 | 0,169091 | 85 | 93 | 2,52E-14 | -0,353239 | 0,0432732 | Esophagus_Gastroesophageal_Junction |
| chr20_64276336_ATAT_A_b38 | rs76240558 | ENSG00000203880.11 | 20641 | 0,160377 | 142 | 153 | 2,65E-12 | -0,231447 | 0,0320824 | Adipose_Subcutaneous |
| chr20_64276336_ATAT_A_b38 | rs76240558 | ENSG00000203880.11 | 20641 | 0,185294 | 57 | 63 | 1,37E-11 | -0,527759 | 0,0712528 | Brain_Caudate_basal_ganglia |
| chr20_64276336_ATAT_A_b38 | rs76240558 | ENSG00000203880.11 | 20641 | 0,147959 | 80 | 87 | 1,13E-10 | -0,272678 | 0,0404121 | Colon_Transverse |
| chr20_64276336_ATAT_A_b38 | rs76240558 | ENSG00000203880.11 | 20641 | 0,167293 | 82 | 89 | 6,13E-10 | -0,295829 | 0,0456042 | Colon_Sigmoid |
| chr20_64276336_ATAT_A_b38 | rs76240558 | ENSG00000203880.11 | 20641 | 0,164589 | 121 | 132 | 9,24E-09 | -0,120111 | 0,0203784 | Cells_Cultured_fibroblasts |
| chr20_64276336_ATAT_A_b38 | rs76240558 | ENSG00000203880.11 | 20641 | 0,183007 | 50 | 56 | 1,19E-08 | -0,439754 | 0,0714863 | Brain_Putamen_basal_ganglia |
| chr20_64276336_ATAT_A_b38 | rs76240558 | ENSG00000203880.11 | 20641 | 0,172783 | 103 | 113 | 2,47E-08 | -0,253612 | 0,0441629 | Breast_Mammary |
| chr20_64276336_ATAT_A_b38 | rs76240558 | ENSG00000203880.11 | 20641 | 0,150641 | 44 | 47 | 6,92E-08 | -0,434791 | 0,0754843 | Brain_Frontal_Cortex |
| chr20_64276336_ATAT_A_b38 | rs76240558 | ENSG00000203880.11 | 20641 | 0,161111 | 54 | 58 | 9,14E-08 | -0,390092 | 0,0692137 | Brain_Nucleus_accumbens_basal_ganglia |
| chr20_64276336_ATAT_A_b38 | rs76240558 | ENSG00000203880.11 | 20641 | 0,174497 | 46 | 52 | 1,43E-07 | -0,368746 | 0,0655636 | Brain_Hippocampus |
| chr20_64276336_ATAT_A_b38 | rs76240558 | ENSG00000203880.11 | 20641 | 0,159439 | 115 | 125 | 5,31E-07 | -0,136353 | 0,0266407 | Adipose_Visceral_Omentum |
| chr20_64276336_ATAT_A_b38 | rs76240558 | ENSG00000203880.11 | 20641 | 0,164835 | 54 | 60 | 1,20E-06 | -0,290588 | 0,0572818 | Brain_Cortex |
| chr20_64276336_ATAT_A_b38 | rs76240558 | ENSG00000203880.11 | 20641 | 0,166667 | 47 | 52 | 3,56E-06 | -0,398926 | 0,0819107 | Brain_Hypothalamus |
| chr20_64276336_ATAT_A_b38 | rs76240558 | ENSG00000203880.11 | 20641 | 0,195513 | 56 | 61 | 4,54E-06 | -0,282165 | 0,0586622 | Brain_Cerebellar_Hemisphere |
| chr20_64279601_A_G_b38 | rs1570520 | ENSG00000203880.11 | 23906 | 0,450939 | 339 | 432 | 1,22E-15 | -0,193186 | 0,0231861 | Adipose_Subcutaneous |
| chr20_64279601_A_G_b38 | rs1570520 | ENSG00000203880.11 | 23906 | 0,46 | 192 | 253 | 1,32E-14 | -0,257518 | 0,0311601 | Esophagus_Gastroesophageal_Junction |
| chr20_64279601_A_G_b38 | rs1570520 | ENSG00000203880.11 | 23906 | 0,452731 | 339 | 431 | 1,29E-11 | -0,177078 | 0,025406 | Artery_Tibial |
| chr20_64279601_A_G_b38 | rs1570520 | ENSG00000203880.11 | 23906 | 0,469605 | 241 | 309 | 1,41E-11 | -0,237295 | 0,0336345 | Artery_Aorta |
| chr20_64279601_A_G_b38 | rs1570520 | ENSG00000203880.11 | 23906 | 0,43674 | 281 | 359 | 7,25E-08 | -0,191285 | 0,0347433 | Esophagus_Mucosa |
| chr20_64279601_A_G_b38 | rs1570520 | ENSG00000203880.11 | 23906 | 0,442177 | 201 | 260 | 2,21E-07 | -0,161761 | 0,0303172 | Colon_Transverse |
| chr20_64279601_A_G_b38 | rs1570520 | ENSG00000203880.11 | 23906 | 0,443609 | 180 | 236 | 3,09E-06 | -0,172568 | 0,0359994 | Colon_Sigmoid |
| chr20_64279601_A_G_b38 | rs1570520 | ENSG00000203880.11 | 23906 | 0,460486 | 234 | 303 | 6,24E-06 | -0,15 | 0,032552 | Breast_Mammary |
| chr20_64279601_A_G_b38 | rs1570520 | ENSG00000203880.11 | 23906 | 0,456743 | 277 | 359 | 6,63E-06 | -0,08992 | 0,0196311 | Adipose_Visceral_Omentum |

| | | | | | | | | | | |
|---|---|---|---|---|---|---|---|---|---|---|
| chr20_64279666_G_T_b38 | rs1570521 | ENSG00000203880.11 | 23971 | 0,449896 | 339 | 431 | 2,37E-15 | -0,191644 | 0,02326 | Adipose_Subcutaneous |
| chr20_64279666_G_T_b38 | rs1570521 | ENSG00000203880.11 | 23971 | 0,458182 | 192 | 252 | 9,67E-15 | -0,259144 | 0,0311733 | Esophagus_Gastroesophageal_Junction |
| chr20_64279666_G_T_b38 | rs1570521 | ENSG00000203880.11 | 23971 | 0,468085 | 241 | 308 | 3,06E-11 | -0,234372 | 0,0338342 | Artery_Aorta |
| chr20_64279666_G_T_b38 | rs1570521 | ENSG00000203880.11 | 23971 | 0,451681 | 339 | 430 | 3,27E-11 | -0,174163 | 0,0255299 | Artery_Tibial |
| chr20_64279666_G_T_b38 | rs1570521 | ENSG00000203880.11 | 23971 | 0,435523 | 281 | 358 | 9,98E-08 | -0,19014 | 0,034927 | Esophagus_Mucosa |
| chr20_64279666_G_T_b38 | rs1570521 | ENSG00000203880.11 | 23971 | 0,440476 | 201 | 259 | 4,08E-07 | -0,159089 | 0,0305373 | Colon_Transverse |
| chr20_64279666_G_T_b38 | rs1570521 | ENSG00000203880.11 | 23971 | 0,443609 | 180 | 236 | 3,09E-06 | -0,172568 | 0,0359994 | Colon_Sigmoid |
| chr20_64279666_G_T_b38 | rs1570521 | ENSG00000203880.11 | 23971 | 0,458967 | 234 | 302 | 8,35E-06 | -0,148577 | 0,0327102 | Breast_Mammary |
| chr20_64279990_C_A_b38 | rs6090105 | ENSG00000203880.11 | 24295 | 0,449896 | 339 | 431 | 2,37E-15 | -0,191644 | 0,02326 | Adipose_Subcutaneous |
| chr20_64279990_C_A_b38 | rs6090105 | ENSG00000203880.11 | 24295 | 0,458182 | 192 | 252 | 9,67E-15 | -0,259144 | 0,0311733 | Esophagus_Gastroesophageal_Junction |
| chr20_64279990_C_A_b38 | rs6090105 | ENSG00000203880.11 | 24295 | 0,468085 | 241 | 308 | 3,06E-11 | -0,234372 | 0,0338342 | Artery_Aorta |
| chr20_64279990_C_A_b38 | rs6090105 | ENSG00000203880.11 | 24295 | 0,451681 | 339 | 430 | 3,27E-11 | -0,174163 | 0,0255299 | Artery_Tibial |
| chr20_64279990_C_A_b38 | rs6090105 | ENSG00000203880.11 | 24295 | 0,435523 | 281 | 358 | 9,98E-08 | -0,19014 | 0,034927 | Esophagus_Mucosa |
| chr20_64279990_C_A_b38 | rs6090105 | ENSG00000203880.11 | 24295 | 0,440476 | 201 | 259 | 4,08E-07 | -0,159089 | 0,0305373 | Colon_Transverse |
| chr20_64279990_C_A_b38 | rs6090105 | ENSG00000203880.11 | 24295 | 0,443609 | 180 | 236 | 3,09E-06 | -0,172568 | 0,0359994 | Colon_Sigmoid |
| chr20_64279990_C_A_b38 | rs6090105 | ENSG00000203880.11 | 24295 | 0,458967 | 234 | 302 | 8,35E-06 | -0,148577 | 0,0327102 | Breast_Mammary |
| chr20_64280038_T_G_b38 | rs6089801 | ENSG00000203880.11 | 24343 | 0,450837 | 340 | 431 | 1,82E-15 | -0,192548 | 0,0232658 | Adipose_Subcutaneous |
| chr20_64280038_T_G_b38 | rs6089801 | ENSG00000203880.11 | 24343 | 0,458182 | 192 | 252 | 9,67E-15 | -0,259144 | 0,0311733 | Esophagus_Gastroesophageal_Junction |
| chr20_64280038_T_G_b38 | rs6089801 | ENSG00000203880.11 | 24343 | 0,468085 | 241 | 308 | 3,06E-11 | -0,234372 | 0,0338342 | Artery_Aorta |
| chr20_64280038_T_G_b38 | rs6089801 | ENSG00000203880.11 | 24343 | 0,451681 | 339 | 430 | 3,27E-11 | -0,174163 | 0,0255299 | Artery_Tibial |
| chr20_64280038_T_G_b38 | rs6089801 | ENSG00000203880.11 | 24343 | 0,436585 | 282 | 358 | 1,08E-07 | -0,190115 | 0,0350247 | Esophagus_Mucosa |
| chr20_64280038_T_G_b38 | rs6089801 | ENSG00000203880.11 | 24343 | 0,440476 | 201 | 259 | 4,08E-07 | -0,159089 | 0,0305373 | Colon_Transverse |
| chr20_64280038_T_G_b38 | rs6089801 | ENSG00000203880.11 | 24343 | 0,443609 | 180 | 236 | 3,09E-06 | -0,172568 | 0,0359994 | Colon_Sigmoid |
| chr20_64280038_T_G_b38 | rs6089801 | ENSG00000203880.11 | 24343 | 0,458967 | 234 | 302 | 8,35E-06 | -0,148577 | 0,0327102 | Breast_Mammary |
| chr20_64281110_G_A_b38 | rs6062363 | ENSG00000203880.11 | 25415 | 0,41858 | 323 | 401 | 2,04E-15 | -0,19636 | 0,023772 | Adipose_Subcutaneous |
| chr20_64281110_G_A_b38 | rs6062363 | ENSG00000203880.11 | 25415 | 0,422269 | 324 | 402 | 1,42E-14 | -0,202254 | 0,0253164 | Artery_Tibial |
| chr20_64281110_G_A_b38 | rs6062363 | ENSG00000203880.11 | 25415 | 0,44 | 188 | 242 | 1,13E-13 | -0,251008 | 0,0316748 | Esophagus_Gastroesophageal_Junction |
| chr20_64281110_G_A_b38 | rs6062363 | ENSG00000203880.11 | 25415 | 0,43617 | 230 | 287 | 2,06E-13 | -0,259606 | 0,0335889 | Artery_Aorta |
| chr20_64281110_G_A_b38 | rs6062363 | ENSG00000203880.11 | 25415 | 0,409976 | 271 | 337 | 5,21E-09 | -0,211678 | 0,0353146 | Esophagus_Mucosa |
| chr20_64281110_G_A_b38 | rs6062363 | ENSG00000203880.11 | 25415 | 0,417933 | 218 | 275 | 8,10E-09 | -0,191251 | 0,0321352 | Breast_Mammary |
| chr20_64281110_G_A_b38 | rs6062363 | ENSG00000203880.11 | 25415 | 0,430025 | 266 | 338 | 3,82E-07 | -0,100579 | 0,0193986 | Adipose_Visceral_Omentum |
| chr20_64281110_G_A_b38 | rs6062363 | ENSG00000203880.11 | 25415 | 0,418367 | 197 | 246 | 1,00E-06 | -0,157785 | 0,0314223 | Colon_Transverse |
| chr20_64281110_G_A_b38 | rs6062363 | ENSG00000203880.11 | 25415 | 0,421053 | 175 | 224 | 1,85E-06 | -0,178293 | 0,0363384 | Colon_Sigmoid |
| chr20_64281260_T_C_b38 | rs6062688 | ENSG00000203880.11 | 25565 | 0,449896 | 339 | 431 | 2,37E-15 | -0,191644 | 0,02326 | Adipose_Subcutaneous |
| chr20_64281260_T_C_b38 | rs6062688 | ENSG00000203880.11 | 25565 | 0,458182 | 192 | 252 | 9,67E-15 | -0,259144 | 0,0311733 | Esophagus_Gastroesophageal_Junction |
| chr20_64281260_T_C_b38 | rs6062688 | ENSG00000203880.11 | 25565 | 0,468085 | 241 | 308 | 3,06E-11 | -0,234372 | 0,0338342 | Artery_Aorta |
| chr20_64281260_T_C_b38 | rs6062688 | ENSG00000203880.11 | 25565 | 0,451681 | 339 | 430 | 3,27E-11 | -0,174163 | 0,0255299 | Artery_Tibial |
| chr20_64281260_T_C_b38 | rs6062688 | ENSG00000203880.11 | 25565 | 0,435523 | 281 | 358 | 9,98E-08 | -0,19014 | 0,034927 | Esophagus_Mucosa |
| chr20_64281260_T_C_b38 | rs6062688 | ENSG00000203880.11 | 25565 | 0,440476 | 201 | 259 | 4,08E-07 | -0,159089 | 0,0305373 | Colon_Transverse |

| | | | | | | | | | | |
|---|---|---|---|---|---|---|---|---|---|---|
| chr20_64281260_T_C_b38 | rs6062688 | ENSG00000203880.11 | 25565 | 0,443609 | 180 | 236 | 3,09E-06 | -0,172568 | 0,0359994 | Colon_Sigmoid |
| chr20_64281260_T_C_b38 | rs6062688 | ENSG00000203880.11 | 25565 | 0,458967 | 234 | 302 | 8,35E-06 | -0,148577 | 0,0327102 | Breast_Mammary |
| chr20_64281343_G_A_b38 | rs6062365 | ENSG00000203880.11 | 25648 | 0,413361 | 318 | 396 | 1,17E-15 | -0,195744 | 0,0234768 | Adipose_Subcutaneous |
| chr20_64281343_G_A_b38 | rs6062365 | ENSG00000203880.11 | 25648 | 0,415966 | 319 | 396 | 7,57E-15 | -0,201936 | 0,0249972 | Artery_Tibial |
| chr20_64281343_G_A_b38 | rs6062365 | ENSG00000203880.11 | 25648 | 0,432727 | 184 | 238 | 3,50E-14 | -0,251104 | 0,0309571 | Esophagus_Gastroesophageal_Junction |
| chr20_64281343_G_A_b38 | rs6062365 | ENSG00000203880.11 | 25648 | 0,428571 | 225 | 282 | 2,47E-13 | -0,255757 | 0,0332117 | Artery_Aorta |
| chr20_64281343_G_A_b38 | rs6062365 | ENSG00000203880.11 | 25648 | 0,405109 | 267 | 333 | 6,42E-09 | -0,209236 | 0,0351286 | Esophagus_Mucosa |
| chr20_64281343_G_A_b38 | rs6062365 | ENSG00000203880.11 | 25648 | 0,414894 | 216 | 273 | 1,19E-08 | -0,188209 | 0,0320049 | Breast_Mammary |
| chr20_64281343_G_A_b38 | rs6062365 | ENSG00000203880.11 | 25648 | 0,423664 | 261 | 333 | 1,64E-07 | -0,103029 | 0,0192448 | Adipose_Visceral_Omentum |
| chr20_64281343_G_A_b38 | rs6062365 | ENSG00000203880.11 | 25648 | 0,411565 | 193 | 242 | 1,55E-06 | -0,153722 | 0,031194 | Colon_Transverse |
| chr20_64281343_G_A_b38 | rs6062365 | ENSG00000203880.11 | 25648 | 0,415414 | 172 | 221 | 1,66E-06 | -0,177519 | 0,0360009 | Colon_Sigmoid |
| chr20_64281378_C_T_b38 | rs6090107 | ENSG00000203880.11 | 25683 | 0,449896 | 339 | 431 | 2,37E-15 | -0,191644 | 0,02326 | Adipose_Subcutaneous |
| chr20_64281378_C_T_b38 | rs6090107 | ENSG00000203880.11 | 25683 | 0,458182 | 192 | 252 | 9,67E-15 | -0,259144 | 0,0311733 | Esophagus_Gastroesophageal_Junction |
| chr20_64281378_C_T_b38 | rs6090107 | ENSG00000203880.11 | 25683 | 0,468085 | 241 | 308 | 3,06E-11 | -0,234372 | 0,0338342 | Artery_Aorta |
| chr20_64281378_C_T_b38 | rs6090107 | ENSG00000203880.11 | 25683 | 0,451681 | 339 | 430 | 3,27E-11 | -0,174163 | 0,0255299 | Artery_Tibial |
| chr20_64281378_C_T_b38 | rs6090107 | ENSG00000203880.11 | 25683 | 0,435523 | 281 | 358 | 9,98E-08 | -0,19014 | 0,034927 | Esophagus_Mucosa |
| chr20_64281378_C_T_b38 | rs6090107 | ENSG00000203880.11 | 25683 | 0,440476 | 201 | 259 | 4,08E-07 | -0,159089 | 0,0305373 | Colon_Transverse |
| chr20_64281378_C_T_b38 | rs6090107 | ENSG00000203880.11 | 25683 | 0,443609 | 180 | 236 | 3,09E-06 | -0,172568 | 0,0359994 | Colon_Sigmoid |
| chr20_64281378_C_T_b38 | rs6090107 | ENSG00000203880.11 | 25683 | 0,458967 | 234 | 302 | 8,35E-06 | -0,148577 | 0,0327102 | Breast_Mammary |
| chr20_64281456_G_A_b38 | rs6089803 | ENSG00000203880.11 | 25761 | 0,449896 | 339 | 431 | 2,37E-15 | -0,191644 | 0,02326 | Adipose_Subcutaneous |
| chr20_64281456_G_A_b38 | rs6089803 | ENSG00000203880.11 | 25761 | 0,458182 | 192 | 252 | 9,67E-15 | -0,259144 | 0,0311733 | Esophagus_Gastroesophageal_Junction |
| chr20_64281456_G_A_b38 | rs6089803 | ENSG00000203880.11 | 25761 | 0,468085 | 241 | 308 | 3,06E-11 | -0,234372 | 0,0338342 | Artery_Aorta |
| chr20_64281456_G_A_b38 | rs6089803 | ENSG00000203880.11 | 25761 | 0,451681 | 339 | 430 | 3,27E-11 | -0,174163 | 0,0255299 | Artery_Tibial |
| chr20_64281456_G_A_b38 | rs6089803 | ENSG00000203880.11 | 25761 | 0,435523 | 281 | 358 | 9,98E-08 | -0,19014 | 0,034927 | Esophagus_Mucosa |
| chr20_64281456_G_A_b38 | rs6089803 | ENSG00000203880.11 | 25761 | 0,440476 | 201 | 259 | 4,08E-07 | -0,159089 | 0,0305373 | Colon_Transverse |
| chr20_64281456_G_A_b38 | rs6089803 | ENSG00000203880.11 | 25761 | 0,443609 | 180 | 236 | 3,09E-06 | -0,172568 | 0,0359994 | Colon_Sigmoid |
| chr20_64281456_G_A_b38 | rs6089803 | ENSG00000203880.11 | 25761 | 0,458967 | 234 | 302 | 8,35E-06 | -0,148577 | 0,0327102 | Breast_Mammary |
| chr20_64281506_C_T_b38 | rs4809259 | ENSG00000203880.11 | 25811 | 0,489091 | 202 | 269 | 2,96E-08 | 0,192521 | 0,0334805 | Esophagus_Gastroesophageal_Junction |
| chr20_64281506_C_T_b38 | rs4809259 | ENSG00000203880.11 | 25811 | 0,495825 | 362 | 475 | 3,25E-07 | 0,125491 | 0,024161 | Adipose_Subcutaneous |
| chr20_64282739_C_A_b38 | rs13043326 | ENSG00000203880.11 | 27044 | 0,413361 | 318 | 396 | 1,17E-15 | -0,195744 | 0,0234768 | Adipose_Subcutaneous |
| chr20_64282739_C_A_b38 | rs13043326 | ENSG00000203880.11 | 27044 | 0,415966 | 319 | 396 | 7,57E-15 | -0,201936 | 0,0249972 | Artery_Tibial |
| chr20_64282739_C_A_b38 | rs13043326 | ENSG00000203880.11 | 27044 | 0,432727 | 184 | 238 | 3,50E-14 | -0,251104 | 0,0309571 | Esophagus_Gastroesophageal_Junction |
| chr20_64282739_C_A_b38 | rs13043326 | ENSG00000203880.11 | 27044 | 0,428571 | 225 | 282 | 2,47E-13 | -0,255757 | 0,0332117 | Artery_Aorta |
| chr20_64282739_C_A_b38 | rs13043326 | ENSG00000203880.11 | 27044 | 0,405109 | 267 | 333 | 6,42E-09 | -0,209236 | 0,0351286 | Esophagus_Mucosa |
| chr20_64282739_C_A_b38 | rs13043326 | ENSG00000203880.11 | 27044 | 0,414894 | 216 | 273 | 1,19E-08 | -0,188209 | 0,0320049 | Breast_Mammary |
| chr20_64282739_C_A_b38 | rs13043326 | ENSG00000203880.11 | 27044 | 0,423664 | 261 | 333 | 1,64E-07 | -0,103029 | 0,0192448 | Adipose_Visceral_Omentum |
| chr20_64282739_C_A_b38 | rs13043326 | ENSG00000203880.11 | 27044 | 0,411565 | 193 | 242 | 1,55E-06 | -0,153722 | 0,031194 | Colon_Transverse |
| chr20_64282739_C_A_b38 | rs13043326 | ENSG00000203880.11 | 27044 | 0,415414 | 172 | 221 | 1,66E-06 | -0,177519 | 0,0360009 | Colon_Sigmoid |
| chr20_64283546_A_T_b38 | rs1806952 | ENSG00000203880.11 | 27851 | 0,413361 | 318 | 396 | 1,17E-15 | 0,195744 | 0,0234768 | Adipose_Subcutaneous |

| | | | | | | | | | | |
|---|---|---|---|---|---|---|---|---|---|---|
| chr20_64283546_A_T_b38 | rs1806952 | ENSG00000203880.11 | 27851 | 0,415966 | 319 | 396 | 7,57E-15 | 0,201936 | 0,0249972 | Artery_Tibial |
| chr20_64283546_A_T_b38 | rs1806952 | ENSG00000203880.11 | 27851 | 0,432727 | 184 | 238 | 3,50E-14 | 0,251104 | 0,0309571 | Esophagus_Gastroesophageal_Junction |
| chr20_64283546_A_T_b38 | rs1806952 | ENSG00000203880.11 | 27851 | 0,428571 | 225 | 282 | 2,47E-13 | 0,255757 | 0,0332117 | Artery_Aorta |
| chr20_64283546_A_T_b38 | rs1806952 | ENSG00000203880.11 | 27851 | 0,405109 | 267 | 333 | 6,42E-09 | 0,209236 | 0,0351286 | Esophagus_Mucosa |
| chr20_64283546_A_T_b38 | rs1806952 | ENSG00000203880.11 | 27851 | 0,414894 | 216 | 273 | 1,19E-08 | 0,188209 | 0,0320049 | Breast_Mammary |
| chr20_64283546_A_T_b38 | rs1806952 | ENSG00000203880.11 | 27851 | 0,423664 | 261 | 333 | 1,64E-07 | 0,103029 | 0,0192448 | Adipose_Visceral_Omentum |
| chr20_64283546_A_T_b38 | rs1806952 | ENSG00000203880.11 | 27851 | 0,411565 | 193 | 242 | 1,55E-06 | 0,153722 | 0,031194 | Colon_Transverse |
| chr20_64283546_A_T_b38 | rs1806952 | ENSG00000203880.11 | 27851 | 0,415413 | 172 | 221 | 1,66E-06 | 0,177519 | 0,0360009 | Colon_Sigmoid |
| chr20_64283878_G_A_b38 | rs4809418 | ENSG00000203880.11 | 28183 | 0,490909 | 203 | 270 | 3,14E-08 | 0,192519 | 0,0335491 | Esophagus_Gastroesophageal_Junction |
| chr20_64283878_G_A_b38 | rs4809419 | ENSG00000203880.11 | 28183 | 0,493737 | 362 | 473 | 8,17E-07 | 0,122237 | 0,024405 | Adipose_Subcutaneous |
| chr20_64285790_T_C_b38 | rs6089804 | ENSG00000203880.11 | 30095 | 0,408142 | 315 | 391 | 3,46817E-15 | 0,192113 | 0,0234685 | Adipose_Subcutaneous |
| chr20_64285790_T_C_b38 | rs6089804 | ENSG00000203880.11 | 30095 | 0,429091 | 182 | 236 | 8,10E-15 | 0,255807 | 0,0306705 | Esophagus_Gastroesophageal_Junction |
| chr20_64285790_T_C_b38 | rs6089804 | ENSG00000203880.11 | 30095 | 0,411765 | 317 | 392 | 8,66E-15 | 0,201238 | 0,0249694 | Artery_Tibial |
| chr20_64285790_T_C_b38 | rs6089804 | ENSG00000203880.11 | 30095 | 0,424012 | 222 | 279 | 2,82E-13 | 0,253 | 0,03294 | Artery_Aorta |
| chr20_64285790_T_C_b38 | rs6089804 | ENSG00000203880.11 | 30095 | 0,411854 | 214 | 271 | 8,60E-09 | 0,18883 | 0,0317878 | Breast_Mammary |
| chr20_64285790_T_C_b38 | rs6089804 | ENSG00000203880.11 | 30095 | 0,400243 | 264 | 329 | 1,93E-08 | 0,202433 | 0,0351722 | Esophagus_Mucosa |
| chr20_64285790_T_C_b38 | rs6089804 | ENSG00000203880.11 | 30095 | 0,418575 | 259 | 329 | 1,51E-07 | 0,103502 | 0,0192756 | Adipose_Visceral_Omentum |
| chr20_64285790_T_C_b38 | rs6089804 | ENSG00000203880.11 | 30095 | 0,407895 | 169 | 217 | 7,37E-07 | 0,183659 | 0,0359757 | Colon_Sigmoid |
| chr20_64285790_T_C_b38 | rs6089804 | ENSG00000203880.11 | 30095 | 0,406463 | 190 | 239 | 9,31E-07 | 0,156808 | 0,0311296 | Colon_Transverse |

rsID, variant ID in dbSNP; TSS, transcription start site; MAF, minor allele frequesncy in GTEx; MA samples, number of samples carrying the minor allele; MA count, total number of minor alleles across individuals; SE, standard error.

**Supplementary Table S6**. eQTLs reported in eQTLGen, for the 31 variants on chromosome 20 (*P* -value < $1.0 \times 10^{-5}$).

| rsID | Minor Allele | Major Allele | Z score | *P* -value | Gene ID | GeneSymbol | n cohorts | n samples | FDR |
|---|---|---|---|---|---|---|---|---|---|
| rs17878941 | A | G | -40,298 | 3,27E-296 | ENSG00000203880 | PCMTD2 | 16 | 14263 | 0 |
| rs41279358 | A | C | -40,3424 | 3,27E-296 | ENSG00000203880 | PCMTD2 | 16 | 14263 | 0 |
| rs58586141 | A | G | -40,4442 | 3,27E-296 | ENSG00000203880 | PCMTD2 | 16 | 14263 | 0 |
| rs6512309 | G | A | -24,6192 | 7,87E-134 | ENSG00000203880 | PCMTD2 | 16 | 14261 | 0 |
| rs7270745 | G | C | -24,6144 | 8,81E-134 | ENSG00000203880 | PCMTD2 | 16 | 14261 | 0 |
| rs6062357 | T | C | -23,7404 | 1,38E-124 | ENSG00000203880 | PCMTD2 | 16 | 14263 | 0 |
| rs6062359 | G | T | -23,5606 | 9,73E-123 | ENSG00000203880 | PCMTD2 | 16 | 14261 | 0 |
| rs6062682 | T | C | -23,4872 | 5,49E-122 | ENSG00000203880 | PCMTD2 | 14 | 13435 | 0 |
| rs1808056 | A | G | -23,4593 | 1,06E-121 | ENSG00000203880 | PCMTD2 | 14 | 13433 | 0 |
| rs6062678 | T | G | -23,452 | 1,26E-121 | ENSG00000203880 | PCMTD2 | 14 | 13428 | 0 |
| rs6062679 | C | T | -23,437 | 1,79E-121 | ENSG00000203880 | PCMTD2 | 14 | 13432 | 0 |
| rs6062683 | A | G | -23,4275 | 2,24E-121 | ENSG00000203880 | PCMTD2 | 14 | 13435 | 0 |
| rs6062681 | G | A | -23,4067 | 3,64E-121 | ENSG00000203880 | PCMTD2 | 14 | 13435 | 0 |
| rs1570520 | G | A | -19,878 | 6,28E-88 | ENSG00000203880 | PCMTD2 | 15 | 9188 | 0 |
| rs1570521 | T | G | -19,8584 | 9,29E-88 | ENSG00000203880 | PCMTD2 | 15 | 9186 | 0 |
| rs6090105 | A | C | -19,8476 | 1,16E-87 | ENSG00000203880 | PCMTD2 | 15 | 9187 | 0 |
| rs6090107 | T | C | -19,8404 | 1,33E-87 | ENSG00000203880 | PCMTD2 | 15 | 9187 | 0 |
| rs6089801 | G | T | -19,837 | 1,43E-87 | ENSG00000203880 | PCMTD2 | 15 | 9187 | 0 |
| rs6062688 | C | T | -19,836 | 1,45E-87 | ENSG00000203880 | PCMTD2 | 15 | 9187 | 0 |
| rs6062363 | A | G | -18,7697 | 1,33E-78 | ENSG00000203880 | PCMTD2 | 15 | 9188 | 0 |
| rs6062362 | G | A | -18,7374 | 2,44E-78 | ENSG00000203880 | PCMTD2 | 14 | 8672 | 0 |
| rs1806952 | A | T | -18,5037 | 1,92E-76 | ENSG00000203880 | PCMTD2 | 15 | 9182 | 0 |
| rs13043326 | A | C | -18,4845 | 2,75E-76 | ENSG00000203880 | PCMTD2 | 15 | 9184 | 0 |
| rs6062365 | A | G | -18,4528 | 4,93E-76 | ENSG00000203880 | PCMTD2 | 15 | 9187 | 0 |
| rs6062361 | G | A | -14,0516 | 7,53E-45 | ENSG00000203880 | PCMTD2 | 16 | 14260 | 0 |
| rs2427638 | T | C | -13,9315 | 4,07E-44 | ENSG00000203880 | PCMTD2 | 16 | 14262 | 0 |

| | | | | | | | | | |
|---|---|---|---|---|---|---|---|---|---|
| rs6089803 | A | G | -12,6117 | 1,82E-36 | ENSG00000203880 | PCMTD2 | 7 | 5437 | 0 |
| rs4809259 | C | T | -11,9384 | 7,45E-33 | ENSG00000203880 | PCMTD2 | 15 | 9185 | 0 |
| rs4809418 | G | A | -11,9055 | 1,11E-32 | ENSG00000203880 | PCMTD2 | 15 | 9184 | 0 |
| rs6062359 | G | T | -5,8819 | 4,05E-09 | ENSG00000125510 | OPRL1 | 34 | 30855 | 3,24E-05 |
| rs6062362 | G | A | -5,5292 | 3,21E-08 | ENSG00000125510 | OPRL1 | 34 | 25879 | 0,000134 |
| rs6090107 | T | C | -5,3549 | 8,56E-08 | ENSG00000125510 | OPRL1 | 33 | 25781 | 0,000309 |
| rs6062688 | C | T | -5,3507 | 8,76E-08 | ENSG00000125510 | OPRL1 | 33 | 25781 | 0,000309 |
| rs6090105 | A | C | -5,3414 | 9,22E-08 | ENSG00000125510 | OPRL1 | 33 | 25781 | 0,000309 |
| rs6089801 | G | T | -5,3411 | 9,23E-08 | ENSG00000125510 | OPRL1 | 33 | 25781 | 0,000309 |
| rs1570521 | T | G | -5,3058 | 1,12E-07 | ENSG00000125510 | OPRL1 | 33 | 25780 | 0,000358 |
| rs1570520 | G | A | -5,1469 | 2,65E-07 | ENSG00000125510 | OPRL1 | 34 | 25897 | 0,000834 |
| rs7270745 | G | C | -4,9613 | 7,00E-07 | ENSG00000125534 | PPDPF | 36 | 31567 | 0,002056 |
| rs6512309 | G | A | -4,9508 | 7,38E-07 | ENSG00000125534 | PPDPF | 37 | 31682 | 0,002184 |
| rs6062363 | A | G | -4,943 | 7,69E-07 | ENSG00000125510 | OPRL1 | 35 | 26395 | 0,002299 |
| rs6062682 | T | C | -4,9242 | 8,47E-07 | ENSG00000125534 | PPDPF | 34 | 30741 | 0,002488 |
| rs1808056 | A | G | -4,9184 | 8,72E-07 | ENSG00000125534 | PPDPF | 34 | 30739 | 0,002543 |
| rs6062679 | C | T | -4,8988 | 9,63E-07 | ENSG00000125534 | PPDPF | 34 | 30738 | 0,002785 |
| rs6062678 | T | G | -4,8959 | 9,78E-07 | ENSG00000125534 | PPDPF | 34 | 30734 | 0,002821 |
| rs6062683 | A | G | -4,8761 | 1,08E-06 | ENSG00000125534 | PPDPF | 34 | 30741 | 0,003063 |
| rs6062681 | G | A | -4,8691 | 1,12E-06 | ENSG00000125534 | PPDPF | 34 | 30741 | 0,003154 |
| rs1806952 | A | T | -4,8079 | 1,52E-06 | ENSG00000125510 | OPRL1 | 33 | 25776 | 0,004253 |
| rs6062359 | G | T | -4,8007 | 1,58E-06 | ENSG00000125534 | PPDPF | 35 | 31069 | 0,004343 |
| rs13043326 | A | C | -4,7801 | 1,75E-06 | ENSG00000125510 | OPRL1 | 33 | 25778 | 0,004821 |
| rs6062365 | A | G | -4,7647 | 1,89E-06 | ENSG00000125510 | OPRL1 | 33 | 25781 | 0,005133 |
| rs6062357 | T | C | -4,5757 | 4,74E-06 | ENSG00000125534 | PPDPF | 37 | 31684 | 0,012782 |
| rs2427638 | T | C | -4,4572 | 8,30E-06 | ENSG00000125510 | OPRL1 | 36 | 31469 | 0,021634 |

rsID, variant ID in dbSNP; FDR, false discovery rate.

**Supplementary Table S7a**. eQTLs reported in MetaBrain (cerebellum), for for the 31 variants on chromosome 20 (P-value < 1.0 x 10-5).

| SNP | Gene Symbol | SNP Effect Allele | SNP Effect Allele Frequency | Meta P-value | MetaP N | MetaP Z | Meta Beta | Meta SE | Nr Datasets | Dataset Correlation Coefficients.GTE.EUR.AMPAD.MAYO.V2.GTE.EUR.GTEx.GTE.EUR.TargetALS.GTE.EUR.UCLA_ASD. | Dataset Z Scores .GTE.EUR.AMPAD.MAYO.V2.GTE.EUR.GTEx.GTE.EUR.TargetALS.GTE.EUR.UCLA_ASD. | Dataset Sample Sizes.GTE.EUR.AMPAD.MAYO.V2.GTE.EUR.GTEx.GTE.EUR.TargetALS.GTE.EUR.UCLA_ASD. |
|---|---|---|---|---|---|---|---|---|---|---|---|---|
| 20:64283546:rs1806952:A_T | PCMTD2 | T | 0,628049 | 3,24E-12 | 492 | 6,966761 | 0,438393 | 0,062926 | 4 | 0.337248;0.265877;0.390208;0.125748 | 5.532493;2.909986;3.388473;0.832703 | 256;118;72;46 |
| 20:64281343:rs6062365:G_A | PCMTD2 | A | 0,371951 | 3,25E-12 | 492 | -6,966582 | -0,438383 | 0,062927 | 4 | -0.337248;-0.265877;-0.390208;-0.12566 | -5.532493;-2.909986;-3.388473;-0.832117 | 256;118;72;46 |
| 20:64282739:rs13043326:C_A | PCMTD2 | A | 0,370935 | 6,33E-12 | 492 | -6,872091 | -0,433204 | 0,063038 | 4 | -0.329705;-0.265877;-0.390208;-0.125748 | -5.40125;-2.909986;-3.388473;-0.832703 | 256;118;72;46 |
| 20:64281110:rs6062363:G_A | PCMTD2 | A | 0,380612 | 9,50E-12 | 490 | -6,813826 | -0,428447 | 0,062879 | 4 | -0.353105;-0.205083;-0.390208;-0.12566 | -5.787312;-2.227796;-3.388473;-0.832117 | 254;118;72;46 |
| 20:64257449:rs6062678:G_T | PCMTD2 | G | 0,557927 | 1,07E-10 | 492 | 6,456469 | 0,397925 | 0,061632 | 4 | 0.359052;0.176149;0.260711;0.200769 | 5.915142;1.908043;2.211896;1.337877 | 256;118;72;46 |
| 20:64258638:rs6062679:T_C | PCMTD2 | T | 0,558943 | 1,20E-10 | 492 | 6,439101 | 0,397034 | 0,06166 | 4 | 0.359052;0.176149;0.260711;0.192409 | 5.915142;1.908043;2.211896;1.281077 | 256;118;72;46 |
| 20:64260450:rs6062681:A_G | PCMTD2 | A | 0,558943 | 1,34E-10 | 492 | 6,422674 | 0,396099 | 0,061672 | 4 | 0.359052;0.176149;0.260711;0.184482 | 5.915142;1.908043;2.211896;1.227354 | 256;118;72;46 |
| 20:64261231:rs6512309:A_G | PCMTD2 | A | 0,558943 | 1,50E-10 | 492 | 6,405077 | 0,395098 | 0,061685 | 4 | 0.359052;0.176149;0.260711;0.175971 | 5.915142;1.908043;2.211896;1.169804 | 256;118;72;46 |
| 20:64261403:rs7270745:C_G | PCMTD2 | C | 0,558943 | 1,51E-10 | 492 | 6,404265 | 0,395051 | 0,061686 | 4 | 0.359052;0.176149;0.260711;0.175578 | 5.915142;1.908043;2.211896;1.167147 | 256;118;72;46 |
| 20:64259579:rs1808056:G_A | PCMTD2 | G | 0,561224 | 1,65E-10 | 490 | 6,390526 | 0,395231 | 0,061846 | 4 | 0.35293;0.188486;0.256336;0.187303 | 5.795716;2.035173;2.173475;1.246454 | 255;117;72;46 |
| 20:64260467:rs6062682:C_T | PCMTD2 | C | 0,560081 | 1,73E-10 | 491 | 6,383745 | 0,394361 | 0,061776 | 4 | 0.358139;0.176149;0.256336;0.183332 | 5.887364;1.908043;2.173475;1.219566 | 255;118;72;46 |
| 20:64260534:rs6062683:G_A | PCMTD2 | G | 0,558163 | 2,11E-10 | 490 | 6,353395 | 0,392818 | 0,061828 | 4 | 0.354876;0.176196;0.260711;0.18218 | 5.82993;1.900279;2.211896;1.211775 | 255;117;72;46 |
| 20:64279601:rs1570520:A_G | PCMTD2 | A | 0,583333 | 3,74E-10 | 492 | 6,264563 | 0,38983 | 0,062228 | 4 | 0.361295;0.113418;0.303028;0.186987 | 5.954787;1.222873;2.587419;1.244316 | 256;118;72;46 |
| 20:64280038:rs6089801:T_G | PCMTD2 | T | 0,583333 | 3,74E-10 | 492 | 6,264563 | 0,38983 | 0,062228 | 4 | 0.361295;0.113418;0.303028;0.186987 | 5.954787;1.222873;2.587419;1.244316 | 256;118;72;46 |
| 20:64281260:rs6062688:T_C | PCMTD2 | T | 0,583333 | 3,77E-10 | 492 | 6,263455 | 0,389767 | 0,062229 | 4 | 0.361295;0.113418;0.303028;0.186452 | 5.954787;1.222873;2.587419;1.240693 | 256;118;72;46 |
| 20:64281378:rs6090107:C_T | PCMTD2 | C | 0,583333 | 3,77E-10 | 492 | 6,263455 | 0,389767 | 0,062229 | 4 | 0.361295;0.113418;0.303028;0.186452 | 5.954787;1.222873;2.587419;1.240693 | 256;118;72;46 |
| 20:64281456:rs6089803:G_A | PCMTD2 | G | 0,576404 | 4,25E-10 | 445 | 6,244533 | 0,406187 | 0,065047 | 3 | 0.361295;0.124761;0.303028;- | 5.954787;1.340247;2.587419;- | 256;117;72;- |
| 20:64279666:rs1570521:G_T | PCMTD2 | G | 0,58435 | 6,82E-10 | 492 | 6,170147 | 0,384515 | 0,062319 | 4 | 0.353879;0.113418;0.303028;0.186987 | 5.823897;1.222873;2.587419;1.244316 | 256;118;72;46 |
| 20:64269027:rs6062359:T_G | PCMTD2 | T | 0,581301 | 7,47E-10 | 492 | 6,155793 | 0,383286 | 0,062264 | 4 | 0.35235;0.130971;0.277093;0.186987 | 5.796981;1.413657;2.356409;1.244316 | 256;118;72;46 |
| 20:64285790:rs6089804:T_C | PCMTD2 | C | 0,643293 | 7,58E-10 | 328 | 6,153584 | 0,474888 | 0,077173 | 2 | 0.332069;-;0.334505;- | 5.44232;-;2.871916;- | 256;-;72;- |
| 20:64261386:rs6062357:C_T | PCMTD2 | C | 0,551829 | 7,61E-10 | 492 | 6,152948 | 0,38007 | 0,06177 | 4 | 0.337859;0.176149;0.265766;0.175578 | 5.543147;1.908043;2.256379;1.167147 | 256;118;72;46 |
| 20:64279990:rs6090105:C_A | PCMTD2 | C | 0,58554 | 1,01E-09 | 491 | 6,107594 | 0,381412 | 0,062449 | 4 | 0.349742;0.113418;0.303028;0.186987 | 5.739791;1.222873;2.587419;1.244316 | 255;118;72;46 |
| 20:64274498:rs41279358:C_A | PCMTD2 | A | 0,160569 | 4,27E-06 | 492 | -4,598012 | -0,390943 | 0,085024 | 4 | -0.205637;-0.194152;-0.308545;-0.084278 | -3.309534;-2.10667;-2.636942;-0.55686 | 256;118;72;46 |
| 20:64269826:rs58586141:G_A | PCMTD2 | A | 0,162218 | 5,45E-06 | 487 | -4,546668 | -0,387054 | 0,085129 | 4 | -0.216377;-0.165221;-0.308545;-0.084737 | -3.458861;-1.780204;-2.636942;-0.559905 | 252;117;72;46 |

**Supplementary Table S7b**. eQTLs reported in MetaBrain (cortex), for for the 31 variants on chromosome 20 (P-value < 1.0 x 10-5).

| SNP | Gene Sym | SNP Effect Allele | SNP Effect Allele Frequenc | Meta P-value | MetaP N | MetaP Z | Meta Beta | Meta SE | Nr Dataset | Dataset Correlation Coefficients.GTE.EUR.AMPAD.MAYO.V2.GTE.EUR.AMPAD.MSBB.V2.GTE.EUR.AMPAD.ROSMAP.V2.GTE.EUR.BrainGVEX.V2.GTE.EUR.CMC.GTE.EUR.CMC_HBCC_set2.GTE.EUR.CMC_HBCC_set3.GTE.EUR.ENA.GTE.EUR.GTEx.GTE.EUR.GVEX.GTE.EUR.LIBD_1M.GTE.EUR.LIBD_h650.GTE.EUR.NABEC.H550.GTE.EUR.NABEC.H610.GTE.EUR.TargetALS.GTE.EUR.UCLA_ASD. | Dataset Z Scores.GTE.EUR.AMPAD.MAYO.V2.GTE.EUR.AMPAD.MSBB.V2.GTE.EUR.AMPAD.ROSMAP.V2.GTE.EUR.BrainGVEX.V2.GTE.EUR.CMC.GTE.EUR.CMC_HBCC_set2.GTE.EUR.CMC_HBCC_set3.GTE.EUR.ENA.GTE.EUR.GTEx.GTE.EUR.GVEX.GTE.EUR.LIBD_1M.GTE.EUR.LIBD_h650.GTE.EUR.NABEC.H550.GTE.EUR.NABEC.H610.GTE.EUR.TargetALS.GTE.EUR.UCLA_ASD. | Dataset Sample Sizes.GTE.EUR.AMPAD.MAYO.V2.GTE.EUR.AMPAD.MSBB.V2.GTE.EUR.AMPAD.ROSMAP.V2.GTE.EUR.BrainGVEX.V2.GTE.EUR.CMC.GTE.EUR.CMC_HBCC_set2.GTE.EUR.CMC_HBCC_set3.GTE.EUR.ENA.GTE.EUR.GTEx.GTE.EUR.GVEX.GTE.EUR.LIBD_1M.GTE.EUR.LIBD_h650.GTE.EUR.NABEC.H610.GTE.EUR.TargetALS.GTE.EUR.UCLA_ASD. |
|---|---|---|---|---|---|---|---|---|---|---|---|---|---|
| 20:64269826:rs58586141:G_A | PCMTD2 | A | 0,161423 | 6,38E-44 | 2670 | -13,8994 | -0,49923 | 0,035917 | 16 | -0.315251;-0.256005;-0.290437;-0.236066;-0.159282;-0.392399;-0.213995;-0.215787;-0.404192;-0.351368;-0.355308;-0.258127;-;-0.403748;-0.183156 | -5.089955;-3.593505;-6.952486;-2.756399;-3.391162;-2.788691;-1.271797;-3.386425;-4.636337;-4.115047;-4.668614;-1.671228;-;-3.542153;-1.363727 | 250;193;551;135;450;49;37;243;125;131;164;43;-;-;73;57 |
| 20:64274498:rs41279358:C_A | PCMTD2 | A | 0,162192 | 1,85E-43 | 2682 | -13,823 | -0,49468 | 0,035787 | 16 | -0.312177;-0.259628;-0.277008;-0.235203;-0.159468;-0.392521;-0.213995;-0.213318;-0.432198;-0.35006;-0.355481;-0.254842;-;-0.388977;-0.183354 | -5.078229;-3.67476;-6.629533;-2.746033;-3.395164;-2.789636;-1.271797;-3.346752;-5.033047;-4.098674;-4.671036;-1.649222;-;-3.425089;-1.365233 | 254;196;553;135;450;49;37;243;125;131;164;43;-;-;74;57 |
| 20:64283546:rs1806952:A_T | PCMTD2 | T | 0,608688 | 2,29E-29 | 2682 | 11,25091 | 0,307588 | 0,027339 | 16 | 0.289791;0.304212;0.249517;0.142961;0.093744;0.228541;0.177265;0.252738;0.27574;0.26145;0.196951;0.041986;-;-0.23495;0.030033 | 4.696899;4.33491;5.948708;1.654115;1.987465;1.579473;1.049592;3.984357;3.112467;3.016401;2.52772;0.267324;-;-2.015007;0.221769 | 254;196;553;135;450;49;37;243;125;131;164;43;-;-;74;57 |
| 20:64281343:rs6062365:G_A | PCMTD2 | A | 0,385762 | 3,49E-29 | 2683 | -11,2138 | -0,30737 | 0,027409 | 16 | -0.289791;-0.304212;-0.247103;-0.144356;-0.09326;-0.221205;-0.175593;-0.251862;-0.27574;-0.261506;-0.196959;-0.042023;-;-0.23495;-0.030046 | -4.696899;-4.33491;-5.894626;-1.670427;-1.977155;-1.52745;-1.039535;-3.970087;-3.112467;-3.017064;-2.527825;-0.267564;-;-2.015007;-0.221865 | 254;196;554;135;450;49;37;243;125;131;164;43;-;-;74;57 |
| 20:64282739:rs13043326:C_A | PCMTD2 | A | 0,38516 | 1,00E-28 | 2682 | -11,1199 | -0,30505 | 0,027433 | 16 | -0.282015;-0.299937;-0.243634;-0.144182;-0.093335;-0.226381;-0.17705;-0.252125;-0.27574;-0.261665;-0.196403;-0.041986;-;-0.23495;-0.030033 | -4.565412;-4.25996;-5.809283;-1.6684;-1.978746;-1.56414;-1.0483;-3.974371;-3.112467;-3.018968;-2.520547;-0.267324;-;-2.015007;-0.221769 | 254;195;554;135;450;49;37;243;125;131;164;43;-;-;74;57 |
| 20:64281110:rs6062363:G_A | PCMTD2 | A | 0,390672 | 1,40E-27 | 2680 | -10,882 | -0,29813 | 0,027397 | 16 | -0.282381;-0.282038;-0.247792;-0.143147;-0.097407;-0.22063;-0.175593;-0.232022;-0.203608;-0.271456;-0.196958;-0.042159;-;-0.23495;-0.030046 | -4.553385;-4.004894;-5.906236;-1.656293;-2.065471;-1.523384;-1.039535;-3.648131;-2.277448;-3.136289;-2.527825;-0.268431;-;-2.015007;-0.221865 | 252;196;553;135;450;49;37;243;125;131;164;43;-;-;74;57 |
| 20:64285790:rs6089804:T_C | PCMTD2 | C | 0,615814 | 7,49E-19 | 1075 | 8,867387 | 0,379535 | 0,042801 | 4 | 0.295501;0.297696;0.246647;-;-;-;-;-;-;-;-;-;-;-;-;0.234284;- | 4.79377;4.237564;5.867387;-;-;-;-;-;-;-;-;-;-;-;-;2.009135;- | 254;196;551;-;-;-;-;-;-;-;-;-;-;-;-;74;- |
| 20:64260534:rs6062683:G_A | PCMTD2 | A | 0,457106 | 6,39E-17 | 2681 | -8,35783 | -0,22619 | 0,027064 | 16 | -0.245167;-0.24361;-0.159501;-0.095239;-0.095213;-0.130957;-0.240493;-0.140266;-0.210692;-0.212452;-0.138289;-0.078624;-;-;-0.146163;-0.070134 | -3.940622;-3.440714;-3.769891;-1.098792;-2.018738;-0.896902;-1.433794;-2.186077;-2.348831;-2.436195;-1.765918;-0.501158;-;-;-1.242623;-0.518411 | 253;196;554;135;450;49;37;243;124;131;164;43;-;-;74;57 |
| 20:64261403:rs7270745:C_G | PCMTD2 | G | 0,456749 | 7,45E-17 | 2682 | -8,33962 | -0,22569 | 0,027062 | 16 | -0.237658;-0.24361;-0.161099;-0.095386;-0.09537;-0.130957;-0.239554;-0.141;-0.209485;-0.212938;-0.138049;-0.077678;-;-;-0.146163;-0.068749 | -3.823893;-3.440714;-3.804704;-1.100493;-2.022096;-0.896902;-1.428028;-2.197623;-2.344664;-2.441907;-1.762824;-0.495109;-;-;-1.242623;-0.508149 | 254;196;553;135;450;49;37;243;125;131;164;43;-;-;74;57 |
| 20:64257449:rs6062678:G_T | PCMTD2 | T | 0,457324 | 7,65E-17 | 2683 | -8,33653 | -0,22554 | 0,027054 | 16 | -0.237658;-0.24361;-0.1598;-0.094888;-0.095277;-0.128634;-0.240493;-0.141277;-0.209485;-0.213008;-0.139157;-0.080751;-;-;-0.146163;-0.072086 | -3.823893;-3.440714;-3.77706;-1.094723;-2.020114;-0.880857;-1.433794;-2.201985;-2.344664;-2.442724;-1.777105;-0.514756;-;-;-1.242623;-0.532875 | 254;196;554;135;450;49;37;243;125;131;164;43;-;-;74;57 |
| 20:64261231:rs6512309:A_G | PCMTD2 | G | 0,45709 | 1,04E-16 | 2680 | -8,30046 | -0,22472 | 0,027073 | 16 | -0.237658;-0.245057;-0.157453;-0.095299;-0.095276;-0.130957;-0.240493;-0.141011;-0.209485;-0.21297;-0.138049;-0.077244;-;-;-0.146163;-0.068846 | -3.823893;-3.452832;-3.714108;-1.099483;-2.020085;-0.896902;-1.433794;-2.197803;-2.344664;-2.442275;-1.762824;-0.492334;-;-;-1.242623;-0.508865 | 254;195;552;135;450;49;37;243;125;131;164;43;-;-;74;57 |
| 20:64260450:rs6062681:A_G | PCMTD2 | G | 0,456124 | 1,18E-16 | 2678 | -8,2847 | -0,22442 | 0,027089 | 16 | -0.237658;-0.24361;-0.15684;-0.095215;-0.095252;-0.130957;-0.240493;-0.140187;-0.209485;-0.212416;-0.138369;-0.079259;-;-;-0.146163;-0.071254 | -3.823893;-3.440714;-3.684589;-1.098506;-2.019578;-0.896902;-1.433794;-2.184832;-2.344664;-2.435776;-1.768945;-0.505219;-;-;-1.242623;-0.526706 | 254;196;549;135;450;49;37;243;125;131;164;43;-;-;74;57 |
| 20:64258638:rs6062679:T_C | PCMTD2 | C | 0,457122 | 1,34E-16 | 2682 | -8,27026 | -0,22384 | 0,027066 | 16 | -0.237658;-0.24361;-0.154527;-0.094849;-0.095219;-0.130957;-0.240493;-0.140372;-0.209485;-0.212644;-0.138765;-0.079554;-;-;-0.146163;-0.071471 | -3.823893;-3.440714;-3.647564;-1.094271;-2.018881;-0.896902;-1.433794;-2.187739;-2.344664;-2.438452;-1.772051;-0.507105;-;-;-1.242623;-0.528318 | 254;196;553;135;450;49;37;243;125;131;164;43;-;-;74;57 |
| 20:64260467:rs6062682:C_T | PCMTD2 | T | 0,456157 | 3,75E-16 | 2680 | -8,14632 | -0,22069 | 0,02709 | 16 | -0.224489;-0.24361;-0.158782;-0.095116;-0.095258;-0.130957;-0.196469;-0.128894;-0.209485;-0.212608;-0.138369;-0.079259;-;-;-0.138538;-0.07087 | -3.599071;-3.440714;-3.745871;-1.097365;-2.019702;-0.896902;-1.165457;-2.007282;-2.344664;-2.438027;-1.766945;-0.505219;-;-;-1.17715;-0.520284 | 253;196;552;135;450;49;37;243;125;131;164;43;-;-;74;57 |
| 20:64259579:rs1808056:G_A | PCMTD2 | A | 0,45653 | 4,22E-16 | 2680 | -8,13212 | -0,2203 | 0,02709 | 16 | -0.225535;-0.24361;-0.156656;-0.094021;-0.095154;-0.130835;-0.196469;-0.134844;-0.222875;-0.196042;-0.138135;-0.067723;-;-;-0.138538;-0.07042 | -3.61629;-3.440714;-3.69845;-1.084666;-2.017485;-0.896063;-1.165457;-2.102343;-2.488075;-2.244118;-1.763924;-0.431502;-;-;-1.17715;-0.520531 | 253;196;553;135;450;49;37;243;124;131;164;43;-;-;74;57 |
| 20:64261386:rs6062357:C_T | PCMTD2 | T | 0,462356 | 1,15E-14 | 2683 | -7,72121 | -0,2091 | 0,027081 | 16 | -0.211245;-0.235272;-0.145922;-0.090226;-0.093196;-0.105725;-0.133465;-0.133742;-0.209485;-0.197012;-0.104782;-0.077678;-;-;-0.188202;-0.068749 | -3.38841;-3.319461;-3.4453;-1.040708;-1.975796;-0.723;-0.787506;-2.083452;-2.344664;-2.255445;-1.335274;-0.495109;-;-;-1.605799;-0.508149 | 254;196;554;135;450;49;37;243;125;131;164;43;-;-;74;57 |
| 20:64269027:rs6062359:T_G | PCMTD2 | G | 0,436614 | 5,94E-14 | 2682 | -7,58036 | -0,20459 | 0,027245 | 16 | -0.224349;-0.245097;-0.151665;-0.112287;-0.063942;-0.151036;-0.115188;-0.11778;-0.189341;-0.239636;-0.126926;-0.077678;-;-;-0.151173;-0.014812 | -3.603943;-3.525092;-3.579191;-1.296631;-1.351887;-1.035917;-0.678879;-1.832921;-1.887931;-2.760314;-1.619572;-0.495109;-;-;-1.285704;-0.109358 | 254;196;553;135;450;49;37;243;125;131;164;43;-;-;74;57 |
| 20:64279601:rs1570520:A_G | PCMTD2 | G | 0,430063 | 5,75E-13 | 2681 | -7,20624 | -0,19688 | 0,027321 | 16 | -0.236847;-0.218186;-0.152505;-0.110594;-0.056523;-0.151036;-0.115188;-0.097587;-0.163598;-0.20147;-0.12688;-0.035261;-;-;-0.152295;-0.014812 | -3.810454;-3.056245;-3.60253;-1.276961;-1.196646;-1.035917;-0.678879;-1.517009;-1.823012;-2.307632;-1.618973;-0.224481;-;-;-1.295359;-0.109358 | 254;194;554;135;450;49;37;243;125;131;164;43;-;-;74;57 |
| 20:64280038:rs6089801:T_G | PCMTD2 | G | 0,430116 | 6,57E-13 | 2683 | -7,18814 | -0,19632 | 0,027312 | 16 | -0.236847;-0.211856;-0.152505;-0.110525;-0.056658;-0.151036;-0.115188;-0.097345;-0.163598;-0.202157;-0.126708;-0.034816;-;-;-0.152295;-0.014812 | -3.810454;-2.98093;-3.60253;-1.27616;-1.199515;-1.035917;-0.678879;-1.513235;-1.823012;-2.315576;-1.61677;-0.22164;-;-;-1.295359;-0.109358 | 254;196;554;135;450;49;37;243;125;131;164;43;-;-;74;57 |
| 20:64281260:rs6062688:T_C | PCMTD2 | C | 0,43025 | 6,81E-13 | 2681 | -7,18321 | -0,19625 | 0,027321 | 16 | -0.236847;-0.211856;-0.150478;-0.111916;-0.05825;-0.152424;-0.115188;-0.096155;-0.163598;-0.203175;-0.126912;-0.033774;-;-;-0.152295;-0.015427 | -3.810454;-2.98093;-3.547631;-1.292322;-1.23327;-1.045548;-0.678879;-1.49464;-1.823012;-2.327491;-1.619394;-0.215008;-;-;-1.295359;-0.113896 | 254;196;552;135;450;49;37;243;125;131;164;43;-;-;74;57 |
| 20:64281378:rs6090107:C_T | PCMTD2 | T | 0,429877 | 7,24E-13 | 2681 | -7,17482 | -0,19605 | 0,027324 | 16 | -0.230955;-0.211856;-0.152505;-0.111985;-0.058264;-0.153495;-0.115493;-0.096202;-0.163598;-0.203574;-0.126912;-0.033774;-;-;-0.152295;-0.015427 | -3.698195;-2.98093;-3.60253;-1.293124;-1.233587;-1.052985;-0.680689;-1.495381;-1.823012;-2.332161;-1.619394;-0.215008;-;-;-1.295359;-0.113896 | 252;196;554;135;450;49;37;243;125;131;164;43;-;-;74;57 |
| 20:64279990:rs6090105:C_A | PCMTD2 | A | 0,429877 | 9,44E-13 | 2681 | -7,13841 | -0,19507 | 0,027327 | 16 | -0.230898;-0.206045;-0.152505;-0.113371;-0.05663;-0.151036;-0.115188;-0.097626;-0.163598;-0.202361;-0.126708;-0.034816;-;-;-0.152295;-0.014812 | -3.70465;-2.889835;-3.60253;-1.309228;-1.198929;-1.035917;-0.678879;-1.517622;-1.823012;-2.31797;-1.61677;-0.22164;-;-;-1.295359;-0.109358 | 253;195;554;135;450;49;37;243;125;131;164;43;-;-;74;57 |
| 20:64279666:rs1570521:G_T | PCMTD2 | T | 0,430037 | 1,04E-12 | 2680 | -7,12458 | -0,19473 | 0,027332 | 16 | -0.228777;-0.204511;-0.152777;-0.113696;-0.056533;-0.151036;-0.115188;-0.09749;-0.163598;-0.202386;-0.126891;-0.034816;-;-;-0.152295;-0.014812 | -3.677007;-2.867851;-3.602483;-1.313001;-1.196875;-1.035917;-0.678879;-1.515497;-1.823012;-2.318259;-1.619119;-0.22164;-;-;-1.295359;-0.109358 | 254;195;552;135;450;49;37;243;125;131;164;43;-;-;74;57 |
| 20:64281456:rs6089803:G_A | PCMTD2 | A | 0,441764 | 2,00E-10 | 1202 | -6,36117 | -0,25697 | 0,040396 | 5 | -0.236847;-0.211856;-0.152505;-;-;-;-;-;-;-;0.178937;-;-;-;-;-;-;-0.152295;- | -3.810454;-2.98093;-3.60253;-;-;-;-;-;-;-;1.988461;-;-;-;-;-;-;1.295359;- | 254;196;554;-;-;-;-;124;-;-;-;-;-;74;- |

**Supplementary Table S8**. PheWAS results for the 31 variant on chromosome 20, across all UK Biobank phenotypes (*P* -value < 1.0 x $10^{-5}$). Data are sorted according to variant position.

| | tea intake * | | coffee intake * | |
|---|---|---|---|---|
| **variant ID** | ***P* -value** | **beta** | ***P* -value** | **beta** |
| 20:64257449:G:T | 5,7E-10 | 0,0435 | 1,6E-09 | 0,0112 |
| 20:64258638:T:C | 5E-10 | 0,0436 | 1,4E-09 | 0,0113 |
| 20:64259579:G:A | 4,8E-10 | 0,0436 | 1,1E-09 | 0,0113 |
| 20:64260450:A:G | 3,6E-10 | 0,0439 | 1,2E-09 | 0,0113 |
| 20:64260467:C:T | 4E-10 | 0,0438 | 9,3E-10 | 0,0114 |
| 20:64260534:G:A | 4,2E-10 | 0,0438 | 1,3E-09 | 0,0113 |
| 20:64261231:A:G | 4,1E-10 | 0,0438 | 1,3E-09 | 0,0113 |
| 20:64261386:C:T | 9,8E-10 | 0,043 | 1,2E-09 | 0,0113 |
| 20:64261403:C:G | 3,9E-10 | 0,0438 | 1,4E-09 | 0,0112 |
| 20:64261602:GT:G | 2,9E-10 | 0,0444 | 1,4E-09 | 0,0113 |
| 20:64269027:T:G | 3,40E-10 | 0,0437 | 1,50E-08 | 0,0104 |
| 20:64269364:C:T | 5,80E-08 | 0,0375 | >1.0E-05 | - |
| 20:64269826:G:A | 4,00E-11 | 0,0612 | >1.0E-05 | - |
| 20:64273189:A:G | 5,90E-08 | 0,0375 | >1.0E-05 | - |
| 20:64274498:C:A | 2,70E-11 | 0,0616 | >1.0E-05 | - |
| 20:64276336:ATAT:A | NA | NA | NA | NA |
| 20:64279601:A:G | 1,30E-08 | 0,0398 | 3,20E-08 | 0,0102 |
| 20:64279666:G:T | 1,20E-08 | 0,0398 | 3,30E-08 | 0,0102 |
| 20:64279876:A:G | 7,00E-09 | 0,0405 | 2,60E-08 | 0,0103 |
| 20:64279990:C:A | 1,20E-08 | 0,0398 | 3,20E-08 | 0,0102 |
| 20:64280038:T:G | 1,20E-08 | 0,0398 | 3,10E-08 | 0,0102 |
| 20:64281110:G:A | 9,00E-08 | 0,0378 | 2,90E-07 | 0,00961 |

| | | | | |
|---|---|---|---|---|
| 20:64281260:T:C | 1,50E-08 | 0,0396 | 2,20E-08 | 0,0104 |
| 20:64281343:G:A | 1,50E-07 | 0,0372 | 2,30E-07 | 0,0097 |
| 20:64281378:C:T | 1,40E-08 | 0,0396 | 2,20E-08 | 0,0104 |
| 20:64281456:G:A | 1,10E-08 | 0,0401 | 1,70E-08 | 0,0105 |
| 20:64281506:C:T | 1,20E-06 | -0,0336 | >1.0E-05 | - |
| 20:64282739:C:A | 1,80E-07 | 0,0369 | 2,30E-07 | 0,0097 |
| 20:64283546:A:T | 1,50E-07 | -0,0372 | 2,20E-07 | -0,00971 |
| 20:64283878:G:A | 3,10E-06 | -0,0323 | >1.0E-05 | - |
| 20:64285790:T:C | 6,20E-08 | -0,0386 | 1,90E-07 | -0,00985 |

* study IDs: NEALE2_1488_raw; NEALE2_1498, Author (year): UKB Neale v2 (2018)

NA, not available

**Supplementary Table S9**. Summary statistics from our GWAS of variants reported in the Human Pain Gene Database, sorted on the basis of their *P* -value of association with pain intensity in our study.

| rsID | Chromosome | Position (bp)* | Allele 0 | Allele 1 | frequency of allele 1 | BETA | SE | P-value | FDR | phenotype ^ | locus/gene ^ |
|---|---|---|---|---|---|---|---|---|---|---|---|
| rs143383 | 20 | 35438203 | G | A | 0,4905 | -0,0948 | 0,0291 | **0,0011** | 0,7333 | Neuraxial Pain, Arthritis | GDF5 |
| rs76340814 | 9 | 95559130 | G | A | 0,0435 | 0,2334 | 0,0726 | **0,0013** | 0,7333 | Post-operative pain | RP11-332M4.1 |
| rs143384 | 20 | 35437976 | G | A | 0,4302 | -0,0840 | 0,0291 | **0,0039** | 0,7333 | Musculoskeletal pain, Arthritis, Post-operativr pain | GDF5 |
| rs5335 | 4 | 147542688 | G | C | 0,4205 | 0,0831 | 0,0298 | **0,0053** | 0,7333 | Migraine | EDNRA |
| rs679987 | 6 | 154098920 | T | C | 0,0877 | -0,1466 | 0,0526 | **0,0053** | 0,7333 | Post-operative Pain | OPRM1 |
| rs2817032 | 6 | 35720842 | T | C | 0,3038 | 0,0863 | 0,0313 | **0,0059** | 0,7333 | Musculoskeletal Pain | FKBP5 |
| rs9394314 | 6 | 35715282 | G | A | 0,6894 | -0,0862 | 0,0313 | **0,0059** | 0,7333 | Musculoskeletal Pain | FKBP5 |
| rs11751591 | 6 | 33826438 | G | A | 0,1378 | -0,1142 | 0,0417 | **0,0062** | 0,7333 | Other Clinical Pain | |
| rs6438857 | 3 | 124838796 | T | C | 0,4395 | 0,0789 | 0,0292 | **0,0069** | 0,7333 | Migraine | ITGB5 |
| rs3993110 | 11 | 12772983 | A | C | 0,3894 | 0,0804 | 0,0300 | **0,0073** | 0,7333 | Arthritis | TEAD1 |
| rs11087273 | 20 | 1973945 | T | C | 0,1505 | -0,1115 | 0,0416 | **0,0074** | 0,7333 | Musculoskeletal Pain | PDYN-AS1 |
| rs11674595 | 2 | 101994530 | T | C | 0,2703 | 0,0879 | 0,0330 | **0,0077** | 0,7333 | Post-operative Pain | IL1R2 |
| rs1476413 | 1 | 11792243 | C | T | 0,2684 | -0,0866 | 0,0330 | **0,0087** | 0,7333 | Migraine | MTHFR |
| rs2299908 | 7 | 31098482 | G | A | 0,2584 | 0,0896 | 0,0342 | **0,0088** | 0,7333 | Migraine | ADCYAP1R1 |
| rs7667298 | 4 | 55125564 | T | C | 0,5331 | -0,0723 | 0,0289 | **0,0124** | 0,7600 | Cancer Pain | KDR |
| rs1542709 | 8 | 72584353 | A | G | 0,7368 | -0,0828 | 0,0333 | **0,0130** | 0,7600 | Migraine | KCNB2 |
| rs1431656 | 8 | 72578942 | G | A | 0,7227 | -0,0812 | 0,0328 | **0,0134** | 0,7600 | Migraine | KCNB2 |
| rs1861960 | 7 | 155492440 | T | G | 0,8068 | -0,0908 | 0,0376 | **0,0158** | 0,7600 | Migraine | SUV39H2 |
| rs12914479 | 15 | 98631599 | C | G | 0,3060 | 0,0744 | 0,0312 | **0,0169** | 0,7600 | Arthritis | RP11-35O15.1 |
| rs9380526 | 6 | 35690550 | C | T | 0,6544 | -0,0729 | 0,0305 | **0,0170** | 0,7600 | Musculoskeletal Pain | FKBP5 |
| rs7690766 | 4 | 130853053 | A | G | 0,2205 | 0,0839 | 0,0352 | **0,0171** | 0,7600 | Migraine | |
| rs2817040 | 6 | 35737829 | G | A | 0,2759 | 0,0763 | 0,0322 | **0,0179** | 0,7600 | Musculoskeletal Pain | ARMC12 |
| rs2014712 | 8 | 139628391 | C | T | 0,2329 | 0,0810 | 0,0345 | **0,0188** | 0,7600 | Post-operative Pain | KCNK9 |
| rs1801131 | 1 | 11794419 | T | G | 0,3077 | -0,0739 | 0,0317 | **0,0197** | 0,7600 | Migraine | MTHFR |
| rs80120866 | 8 | 95437202 | G | T | 0,0734 | -0,1315 | 0,0568 | **0,0205** | 0,7600 | Post-operative pain | CFAP418-AS1 |
| rs762551 | 15 | 74749576 | C | A | 0,6920 | -0,0716 | 0,0313 | **0,0222** | 0,7600 | Analgesia | CYP1A2 |
| rs11930554 | 4 | 130866227 | T | C | 0,2236 | 0,0794 | 0,0350 | **0,0234** | 0,7600 | Migraine | |
| rs11936003 | 4 | 130866937 | A | G | 0,2236 | 0,0794 | 0,0350 | **0,0234** | 0,7600 | Migraine | |
| rs1039325 | 5 | 30761314 | T | G | 0,5958 | -0,0677 | 0,0300 | **0,0239** | 0,7600 | Neuraxial pain | |
| rs1431659 | 8 | 72526835 | A | G | 0,7394 | -0,0748 | 0,0335 | **0,0255** | 0,7600 | Migraine | LOC105375897 |
| rs5007872 | 8 | 72534635 | G | A | 0,7404 | -0,0746 | 0,0335 | **0,0258** | 0,7600 | Migraine | |
| rs1065852 | 22 | 42130692 | G | A | 0,1915 | -0,0818 | 0,0368 | **0,0260** | 0,7600 | Analgesia | LOC112268294 |
| rs569207 | 15 | 78580777 | C | T | 0,2334 | 0,0767 | 0,0346 | **0,0263** | 0,7600 | Neuraxial pain | CHRNA5 |
| rs574584 | 8 | 26866167 | C | T | 0,9614 | -0,1654 | 0,0745 | **0,0265** | 0,7600 | Fibromyalgia | ADRA1A |
| rs11988795 | 8 | 72037366 | C | T | 0,3182 | -0,0674 | 0,0304 | **0,0268** | 0,7600 | Nociception, Neuorpathic pain | MSC-AS1 |
| rs7753746 | 6 | 35597645 | G | A | 0,8060 | -0,0802 | 0,0364 | **0,0274** | 0,7600 | Musculoskeletal Pain | FKBP5 |
| rs714588 | 7 | 34653614 | A | G | 0,4322 | -0,0648 | 0,0295 | **0,0282** | 0,7600 | Other Clinical Pain | NPSR1-AS1 |
| rs1383914 | 8 | 26865532 | T | C | 0,4874 | -0,0637 | 0,0291 | **0,0284** | 0,7600 | Fibromyalgia | ADRA1A |
| rs5333 | 4 | 147539885 | T | C | 0,2521 | -0,0739 | 0,0337 | **0,0284** | 0,7600 | Nociception, Migraine | EDNRA |

| | | | | | | | | | | | |
|---|---|---|---|---|---|---|---|---|---|---|---|
| rs9982601 | 21 | 34226827 | C | T | 0,1254 | 0,0985 | 0,0450 | **0,0285** | 0,7600 | Migraine | |
| rs11720013 | 3 | 38924745 | G | T | 0,1232 | -0,0977 | 0,0447 | **0,0287** | 0,7600 | Nociception | SCN11A |
| rs667282 | 15 | 78571130 | T | C | 0,2331 | 0,0750 | 0,0346 | **0,0301** | 0,7600 | Neuraxial pain | CHRNA5 |
| rs2506155 | 10 | 33214251 | C | A | 0,1682 | -0,0843 | 0,0391 | **0,0310** | 0,7600 | Migraine | SUV39H2 |
| rs6881648 | 5 | 75696024 | A | C | 0,3612 | 0,0642 | 0,0299 | **0,0316** | 0,7600 | Migraine | POC5 |
| rs920829 | 8 | 72065468 | C | T | 0,0992 | 0,1051 | 0,0491 | **0,0325** | 0,7600 | Nociception, Neuorpathic pain | TRPA1 |
| rs941601 | 14 | 94305204 | C | T | 0,1444 | 0,0890 | 0,0418 | **0,0331** | 0,7600 | Musculoskeletal Pain | SERPINA6 |
| rs2048894 | 4 | 147530682 | G | A | 0,2552 | -0,0713 | 0,0336 | **0,0337** | 0,7600 | Migraine | EDNRA |
| rs75361675 | 10 | 96372079 | C | A | 0,1108 | 0,0975 | 0,0459 | **0,0337** | 0,7600 | Post-operative pain | TLL2 |
| rs9524885 | 13 | 95283335 | T | C | 0,7081 | 0,0682 | 0,0321 | **0,0337** | 0,7600 | Cancer Pain | ABCC4 |
| rs1319339 | 6 | 154010049 | T | C | 0,1475 | 0,0870 | 0,0413 | **0,0354** | 0,7600 | Analgesia | OPRM1 |
| rs13017637 | 2 | 166303436 | C | T | 0,4285 | 0,0624 | 0,0298 | **0,0363** | 0,7600 | Post-operative Pain | SCN9A |
| rs3104767 | 16 | 52590826 | G | T | 0,4334 | -0,0617 | 0,0295 | **0,0365** | 0,7600 | Neuropathic pain | CASC16 |
| rs41270041 | 1 | 161191494 | G | C | 0,0749 | 0,1160 | 0,0555 | **0,0367** | 0,7600 | Neuraxial Pain | ADAMTS4 |
| rs851971 | 6 | 151656338 | C | T | 0,3080 | 0,0663 | 0,0318 | **0,0369** | 0,7600 | Migraine | ESR1 |
| rs851967 | 6 | 151660021 | C | T | 0,3080 | 0,0663 | 0,0318 | **0,0369** | 0,7600 | Migraine | ESR1 |
| rs1861881 | 9 | 116549977 | G | T | 0,3085 | 0,0668 | 0,0321 | **0,0375** | 0,7600 | Migraine | ASTN2 |
| rs1799724 | 6 | 31574705 | C | T | 0,0386 | 0,1556 | 0,0748 | **0,0376** | 0,7600 | Migraine | |
| rs776746 | 7 | 99672916 | T | C | 0,9191 | -0,1115 | 0,0537 | **0,0379** | 0,7600 | Post-operative pain | ZSCAN25 |
| rs573542 | 8 | 26866301 | C | T | 0,9628 | -0,1561 | 0,0758 | **0,0394** | 0,7600 | Fibromyalgia | ADRA1A |
| rs1800610 | 6 | 31576050 | G | A | 0,0369 | 0,1567 | 0,0763 | **0,0400** | 0,7600 | Cancer Pain | TNF |
| rs349335 | 8 | 72576736 | C | T | 0,8576 | -0,0856 | 0,0417 | **0,0401** | 0,7600 | Migraine | KCNB2 |
| rs1626492 | 6 | 12295270 | A | G | 0,6925 | -0,0640 | 0,0313 | **0,0411** | 0,7600 | Migraine | EDN1 |
| rs3782025 | 11 | 113936885 | G | A | 0,5438 | -0,0605 | 0,0297 | **0,0415** | 0,7600 | Analgesia | HTR3B |
| rs10494994 | 1 | 215188864 | G | A | 0,2353 | 0,0692 | 0,0340 | **0,0420** | 0,7600 | Migraine | KCNK2 |
| rs3815188 | 19 | 15192414 | G | A | 0,1490 | -0,0841 | 0,0416 | **0,0433** | 0,7600 | Migraine | NOTCH3 |
| rs851998 | 6 | 151662203 | G | A | 0,3072 | 0,0642 | 0,0318 | **0,0434** | 0,7600 | Migraine | ESR1 |
| rs2740574 | 7 | 99784473 | C | T | 0,9597 | -0,1518 | 0,0752 | **0,0435** | 0,7600 | Analgesia | |
| rs13093031 | 3 | 88809891 | A | G | 0,1636 | 0,0782 | 0,0392 | **0,0463** | 0,7964 | Analgesia | |
| rs4073 | 4 | 73740307 | A | T | 0,5532 | -0,0589 | 0,0297 | **0,0475** | 0,8053 | Cancer Pain | |
| rs1448239 | 16 | 10093578 | G | C | 0,1677 | -0,0760 | 0,0389 | 0,0505 | 0,8399 | Temporomandibular Disorder | GRIN2A |
| rs10465114 | 9 | 127155545 | G | A | 0,1928 | 0,0726 | 0,0372 | 0,0510 | 0,8399 | Arthritis | RALGPS1 |
| rs6754031 | 2 | 166298928 | T | G | 0,3804 | 0,0589 | 0,0304 | 0,0525 | 0,8451 | Fibromyalgia | SCN1A-AS1 |
| rs4880487 | 10 | 1200943 | C | T | 0,2589 | -0,0645 | 0,0333 | 0,0531 | 0,8451 | Migraine | SUV39H2 |
| rs6495306 | 15 | 78573551 | G | A | 0,6145 | 0,0579 | 0,0300 | 0,0536 | 0,8451 | Neuraxial pain | CHRNA5 |
| rs1042630 | 15 | 88858820 | A | G | 0,7550 | -0,0649 | 0,0338 | 0,0549 | 0,8451 | Neuraxial Pain | ACAN |
| rs588765 | 15 | 78573083 | T | C | 0,6145 | 0,0572 | 0,0300 | 0,0567 | 0,8451 | Neuraxial pain | CHRNA5 |
| rs349355 | 8 | 72543535 | A | G | 0,8303 | -0,0735 | 0,0386 | 0,0569 | 0,8451 | Migraine | KCNB2 |
| rs12339024 | 9 | 74782603 | T | C | 0,4208 | 0,0552 | 0,0291 | 0,0577 | 0,8451 | Migraine | TRPM6 |
| rs2276749 | 3 | 11601991 | T | C | 0,9477 | 0,1250 | 0,0660 | 0,0583 | 0,8451 | Post-operative pain | VGLL4 |
| rs680244 | 15 | 78578946 | T | C | 0,6125 | 0,0564 | 0,0300 | 0,0598 | 0,8451 | Neuraxial pain | CHRNA5 |
| rs7590387 | 2 | 237913557 | G | C | 0,5287 | 0,0552 | 0,0297 | 0,0626 | 0,8451 | Migraine | |

| | | | | | | | | | | | |
|---|---|---|---|---|---|---|---|---|---|---|---|
| rs6583954 | 10 | 94774506 | C | T | 0,1502 | 0,0756 | 0,0408 | 0,0640 | 0,8451 | Migraine | SUV39H2 |
| rs349358 | 8 | 72539240 | C | T | 0,8306 | -0,0713 | 0,0387 | 0,0652 | 0,8451 | Migraine | KCNB2 |
| rs767455 | 12 | 6341779 | T | C | 0,4302 | 0,0550 | 0,0299 | 0,0652 | 0,8451 | Neuraxial pain | TNFRSF1A |
| rs1835740 | 8 | 97154685 | T | C | 0,7832 | 0,0650 | 0,0353 | 0,0654 | 0,8451 | Migraine | LOC101927066 |
| rs3825994 | 15 | 88858384 | T | G | 0,7516 | -0,0621 | 0,0337 | 0,0656 | 0,8451 | Neuraxial Pain | ACAN |
| rs16851778 | 2 | 166204799 | A | G | 0,1806 | 0,0701 | 0,0381 | 0,0656 | 0,8451 | Nociception | SCN1A-AS1 |
| rs12765185 | 10 | 133163573 | T | A | 0,2866 | 0,0592 | 0,0322 | 0,0659 | 0,8451 | Other Clinical Pain | KNDC1 |
| rs3800373 | 6 | 35574699 | C | A | 0,7090 | -0,0585 | 0,0318 | 0,0659 | 0,8451 | Musculoskeletal Pain | FKBP5 |
| rs6478241 | 9 | 116490350 | A | G | 0,6286 | -0,0556 | 0,0303 | 0,0662 | 0,8451 | Migraine | ASTN2 |
| rs7834973 | 8 | 68727437 | T | G | 0,3965 | 0,0539 | 0,0294 | 0,0664 | 0,8451 | Neuraxial pain | C8orf34 |
| rs6966540 | 7 | 96098655 | T | C | 0,3646 | 0,0546 | 0,0298 | 0,0672 | 0,8451 | Other Clinical Pain | DYNC1I1 |
| rs2860216 | 14 | 76539665 | C | T | 0,7054 | -0,0594 | 0,0325 | 0,0674 | 0,8451 | Temporomandibular Disorder | ESRRB |
| rs56132153 | 5 | 68529306 | A | C | 0,3982 | -0,0544 | 0,0299 | 0,0683 | 0,8451 | Post-operative pain | CTC-537E7.1 |
| rs2211843 | 21 | 37811882 | G | T | 0,2394 | -0,0621 | 0,0342 | 0,0691 | 0,8451 | Analgesia | KCNJ6 |
| rs4986936 | 6 | 151842149 | A | G | 0,0401 | 0,1333 | 0,0737 | 0,0704 | 0,8451 | Analgesia | ESR1 |
| rs10160548 | 11 | 113985959 | G | T | 0,6585 | 0,0557 | 0,0308 | 0,0709 | 0,8451 | Neuropathic pain | HTR3A |
| rs2242480 | 7 | 99763843 | C | T | 0,1121 | 0,0846 | 0,0468 | 0,0710 | 0,8451 | Analgesia | CYP3A4 |
| rs1042713 | 5 | 148826877 | G | A | 0,3814 | 0,0535 | 0,0298 | 0,0721 | 0,8451 | Temporomandibular Disorder | ADRB2 |
| rs11958940 | 5 | 148821922 | A | T | 0,5885 | 0,0528 | 0,0294 | 0,0722 | 0,8451 | Temporomandibular Disorder | ADRB2 |
| rs1467847 | 21 | 34342245 | G | C | 0,5656 | -0,0528 | 0,0295 | 0,0731 | 0,8473 | Migraine | |
| rs1013063 | 21 | 34326090 | T | C | 0,5654 | -0,0531 | 0,0298 | 0,0742 | 0,8507 | Migraine | |
| rs1641025 | 16 | 8777531 | T | C | 0,7197 | -0,0569 | 0,0322 | 0,0773 | 0,8784 | Analgesia | ABAT |
| rs6845322 | 4 | 156962953 | A | G | 0,3381 | 0,0549 | 0,0312 | 0,0788 | 0,8867 | Cancer Pain | PDGFC |
| rs34811474 | 4 | 25407216 | G | A | 0,2071 | -0,0636 | 0,0364 | 0,0800 | 0,8867 | Other Clinical Pain | ANAPC4 |
| rs1799864 | 3 | 46357717 | G | A | 0,1060 | -0,0810 | 0,0464 | 0,0808 | 0,8867 | Migraine | CCR2 |
| rs1432623 | 5 | 148824445 | C | T | 0,5912 | 0,0512 | 0,0294 | 0,0811 | 0,8867 | Temporomandibular Disorder | ADRB2 |
| rs6907508 | 6 | 34624313 | A | G | 0,1084 | -0,0803 | 0,0463 | 0,0830 | 0,8987 | Other Clinical Pain | ILRUN |
| rs12494691 | 3 | 16658827 | G | A | 0,2827 | 0,0550 | 0,0318 | 0,0837 | 0,8989 | Analgesia | |
| rs6279 | 11 | 113410351 | G | C | 0,7120 | -0,0555 | 0,0324 | 0,0866 | 0,9163 | Migraine | DRD2 |
| rs9981629 | 21 | 37594103 | C | G | 0,5875 | -0,0502 | 0,0293 | 0,0869 | 0,9163 | Analgesia | |
| rs3740129 | 10 | 72008101 | G | A | 0,4509 | 0,0497 | 0,0292 | 0,0887 | 0,9222 | Post-operative pain | CHST3 |
| rs1800470 | 19 | 41353016 | G | A | 0,5873 | 0,0496 | 0,0292 | 0,0895 | 0,9222 | Migraine | TGFB1 |
| rs12948783 | 17 | 76503318 | G | A | 0,1682 | 0,0660 | 0,0391 | 0,0914 | 0,9222 | Analgesia | |
| rs2756109 | 10 | 99798989 | G | T | 0,5848 | -0,0498 | 0,0295 | 0,0914 | 0,9222 | Cancer Pain | ABCC2 |
| rs7294636 | 12 | 14901082 | G | A | 0,3838 | 0,0498 | 0,0295 | 0,0914 | 0,9222 | Arthritis | C12orf60 |
| rs144017103 | 20 | 32041179 | C | T | 0,0211 | 0,1727 | 0,1028 | 0,0931 | 0,9222 | Migraine | |
| rs12654778 | 5 | 148826178 | G | A | 0,3824 | 0,0500 | 0,0298 | 0,0935 | 0,9222 | Musculoskeletal Pain | |
| rs1913707 | 4 | 13037816 | A | G | 0,3751 | 0,0504 | 0,0302 | 0,0945 | 0,9222 | Arthritis | RNU6-962P |
| rs10459853 | 16 | 84383036 | C | G | 0,1235 | 0,0748 | 0,0448 | 0,0949 | 0,9222 | Migraine | ATP2C2 |
| rs1045280 | 17 | 4719343 | C | T | 0,6818 | -0,0523 | 0,0315 | 0,0970 | 0,9222 | Analgesia | ARRB2 |
| rs1432622 | 5 | 148824199 | T | C | 0,5914 | 0,0487 | 0,0294 | 0,0971 | 0,9222 | Temporomandibular Disorder | ADRB2 |
| rs6275 | 11 | 113412755 | A | G | 0,7127 | -0,0537 | 0,0324 | 0,0975 | 0,9222 | Migraine | DRD2 |
| rs1042714 | 5 | 148826910 | G | C | 0,5950 | 0,0485 | 0,0293 | 0,0978 | 0,9222 | Temporomandibular Disorder | ADRB2 |
| rs8065080 | 17 | 3577153 | T | C | 0,3926 | -0,0493 | 0,0299 | 0,0990 | 0,9222 | Nociception | TRPV1 |
| rs2073618 | 8 | 118951813 | G | C | 0,4669 | -0,0484 | 0,0294 | 0,0993 | 0,9222 | Cancer Pain | TNFRSF11B |
| rs302680 | 2 | 237882754 | G | A | 0,8279 | -0,0631 | 0,0385 | 0,1010 | 0,9303 | Migraine | RAMP1 |

| | | | | | | | | | | | |
|---|---|---|---|---|---|---|---|---|---|---|---|
| rs13078967 | 3 | 154572157 | A | C | 0,0331 | 0,1310 | 0,0808 | 0,1049 | 0,9527 | Migraine | |
| rs1672717 | 11 | 113942011 | G | A | 0,6101 | -0,0489 | 0,0302 | 0,1051 | 0,9527 | Analgesia | HTR3B |
| rs6685551 | 1 | 61744809 | G | A | 0,2693 | -0,0534 | 0,0330 | 0,1059 | 0,9527 | Temporomandibular Disorder | PATJ |
| rs2293489 | 7 | 73692949 | C | T | 0,3099 | 0,0497 | 0,0310 | 0,1086 | 0,9545 | Migraine | BUD23 |
| rs2400707 | 5 | 148825489 | A | G | 0,5919 | 0,0469 | 0,0293 | 0,1100 | 0,9545 | Neuropathic pain | |
| rs59898460 | 1 | 150520528 | T | C | 0,4006 | -0,0466 | 0,0292 | 0,1110 | 0,9545 | Other Clinical Pain | |
| rs12365397 | 11 | 43214511 | A | G | 0,3128 | 0,0505 | 0,0319 | 0,1133 | 0,9545 | Migraine | SUV39H2 |
| rs638416 | 17 | 18363661 | G | C | 0,6164 | 0,0476 | 0,0300 | 0,1134 | 0,9545 | Temporomandibular Disorder | |
| rs11127292 | 2 | 2026171 | C | T | 0,1091 | 0,0727 | 0,0460 | 0,1139 | 0,9545 | Fibromyalgia | MYT1L |
| rs17615906 | 5 | 128682720 | T | C | 0,1473 | 0,0660 | 0,0418 | 0,1144 | 0,9545 | Arthritis | SLC27A6 |
| rs28451064 | 21 | 34221526 | G | A | 0,1167 | 0,0725 | 0,0460 | 0,1148 | 0,9545 | Migraine | |
| rs4663804 | 2 | 237903394 | C | T | 0,3918 | -0,0468 | 0,0298 | 0,1162 | 0,9545 | Migraine | RAMP1 |
| rs2271933 | 1 | 31626924 | A | G | 0,6201 | 0,0478 | 0,0305 | 0,1171 | 0,9545 | Migraine | HCRTR1 |
| rs11777116 | 8 | 24186788 | C | T | 0,0802 | -0,0836 | 0,0534 | 0,1176 | 0,9545 | Migraine | LOC107986931 |
| rs2053044 | 5 | 148825809 | A | G | 0,5921 | 0,0459 | 0,0293 | 0,1180 | 0,9545 | Musculoskeletal Pain | |
| rs75213074 | 17 | 5709320 | C | T | 0,0377 | -0,1195 | 0,0768 | 0,1194 | 0,9545 | Migraine | |
| rs4846048 | 1 | 11786195 | G | A | 0,7008 | 0,0502 | 0,0322 | 0,1198 | 0,9545 | Migraine | MTHFR |
| rs1024905 | 12 | 4408974 | G | C | 0,5547 | 0,0447 | 0,0288 | 0,1206 | 0,9545 | Migraine | |
| rs698621 | 15 | 88859365 | T | G | 0,6388 | -0,0473 | 0,0305 | 0,1212 | 0,9545 | Neuraxial Pain | ACAN |
| rs7033149 | 9 | 32398236 | G | T | 0,8653 | 0,0658 | 0,0425 | 0,1217 | 0,9545 | Neuropathic Pain | ACO1 |
| rs1061622 | 1 | 12192898 | T | G | 0,2309 | -0,0531 | 0,0347 | 0,1253 | 0,9545 | Cancer Pain | TNFRSF1B |
| rs745011 | 14 | 76450932 | T | C | 0,3267 | 0,0474 | 0,0309 | 0,1257 | 0,9545 | Temporomandibular Disorder | ESRRB |
| rs4880 | 6 | 159692840 | A | G | 0,5044 | 0,0447 | 0,0292 | 0,1261 | 0,9545 | Migraine | SOD2 |
| rs11720988 | 3 | 38865054 | G | A | 0,2360 | -0,0527 | 0,0345 | 0,1269 | 0,9545 | Nociception | SCN11A |
| rs2023239 | 6 | 88150763 | T | C | 0,1677 | -0,0595 | 0,0392 | 0,1289 | 0,9545 | Migraine | CNR1 |
| rs58973023 | 13 | 42384997 | A | T | 0,4694 | -0,0443 | 0,0292 | 0,1301 | 0,9545 | Arthritis | FABP3P2 |
| rs533123 | 1 | 28814643 | G | A | 0,8175 | -0,0575 | 0,0381 | 0,1305 | 0,9545 | Analgesia | OPRD1 |
| rs3737240 | 1 | 150510879 | C | T | 0,3950 | -0,0442 | 0,0293 | 0,1311 | 0,9545 | Musculoskeletal pain | ECM1 |
| rs10037055 | 5 | 177264278 | T | G | 0,8391 | 0,0604 | 0,0400 | 0,1312 | 0,9545 | Migraine | SUV39H2 |
| rs35283004 | 5 | 148819704 | A | G | 0,3833 | 0,0450 | 0,0299 | 0,1325 | 0,9545 | Temporomandibular Disorder | ADRB2 |
| rs2834462 | 21 | 34344892 | T | C | 0,6702 | -0,0467 | 0,0311 | 0,1332 | 0,9545 | Migraine | |
| rs3773679 | 3 | 114150488 | C | T | 0,3768 | 0,0452 | 0,0301 | 0,1333 | 0,9545 | Nociception | DRD3 |
| rs2243248 | 5 | 132672952 | T | G | 0,0627 | -0,0899 | 0,0599 | 0,1336 | 0,9545 | Other Clinical Pain | |
| rs2856821 | 6 | 33078965 | T | C | 0,1903 | -0,0557 | 0,0371 | 0,1336 | 0,9545 | Arthritis | HLA-DPA1 |
| rs4387806 | 2 | 166294304 | T | C | 0,6719 | 0,0465 | 0,0312 | 0,1361 | 0,9545 | Analgesia | SCN1A-AS1 |
| rs17289394 | 13 | 46899085 | G | A | 0,3456 | 0,0447 | 0,0301 | 0,1375 | 0,9545 | Musculoskeletal Pain | |
| rs2006281 | 14 | 103861395 | C | T | 0,5173 | 0,0424 | 0,0286 | 0,1379 | 0,9545 | Other Clinical Pain | |
| rs1535255 | 6 | 88151489 | T | G | 0,1670 | -0,0580 | 0,0393 | 0,1393 | 0,9545 | Migraine | CNR1 |
| rs11120499 | 1 | 215125465 | T | G | 0,6390 | -0,0444 | 0,0302 | 0,1411 | 0,9545 | Migraine | KCNK2 |
| rs9383939 | 6 | 151685043 | G | A | 0,0676 | 0,0869 | 0,0592 | 0,1422 | 0,9545 | Migraine | ESR1 |
| rs10877969 | 12 | 63153459 | T | C | 0,1298 | -0,0637 | 0,0436 | 0,1437 | 0,9545 | Nociception | |
| rs5760405 | 22 | 24417873 | C | T | 0,2132 | -0,0522 | 0,0357 | 0,1437 | 0,9545 | Migraine | ADORA2A-AS1 |
| rs7578855 | 2 | 237892655 | C | T | 0,6079 | -0,0439 | 0,0300 | 0,1443 | 0,9545 | Migraine | RAMP1 |
| rs941298 | 7 | 73710933 | G | A | 0,3114 | 0,0453 | 0,0310 | 0,1444 | 0,9545 | Migraine | LOC105375350 |
| rs4646 | 15 | 51210647 | A | C | 0,7387 | 0,0479 | 0,0329 | 0,1450 | 0,9545 | Migraine | CYP19A1 |
| rs13421094 | 2 | 157185290 | A | G | 0,1624 | -0,0571 | 0,0392 | 0,1451 | 0,9545 | Analgesia | |

| | | | | | | | | | | | |
|---|---|---|---|---|---|---|---|---|---|---|---|
| rs17301853 | 1 | 174583673 | C | T | 0,1407 | -0,0607 | 0,0417 | 0,1454 | 0,9545 | Migraine | SUV39H2 |
| rs8129919 | 21 | 37882237 | G | A | 0,4363 | -0,0427 | 0,0294 | 0,1460 | 0,9545 | Cancer Pain | KCNJ6 |
| rs12567520 | 1 | 215155924 | G | A | 0,1842 | 0,0540 | 0,0372 | 0,1471 | 0,9545 | Migraine | KCNK2 |
| rs6500609 | 16 | 4465333 | C | G | 0,9018 | 0,0711 | 0,0491 | 0,1473 | 0,9545 | Arthritis | NMRAL1 |
| rs2877098 | 7 | 41703696 | T | C | 0,6767 | 0,0454 | 0,0313 | 0,1477 | 0,9545 | Migraine | SUV39H2 |
| rs10826566 | 10 | 29075768 | G | A | 0,1770 | -0,0563 | 0,0389 | 0,1477 | 0,9545 | Migraine | SUV39H2 |
| rs2882676 | 15 | 88857108 | A | C | 0,6429 | -0,0442 | 0,0305 | 0,1478 | 0,9545 | Neuraxial Pain | ACAN |
| rs2351491 | 15 | 88854874 | C | T | 0,6420 | -0,0440 | 0,0306 | 0,1500 | 0,9545 | Neuraxial Pain | ACAN |
| rs429358 | 19 | 44908684 | T | C | 0,1179 | 0,0653 | 0,0454 | 0,1504 | 0,9545 | Fibromyalgia | APOE |
| rs938609 | 15 | 88855400 | T | A | 0,6424 | -0,0439 | 0,0305 | 0,1510 | 0,9545 | Neuraxial Pain | ACAN |
| rs614230 | 16 | 57385374 | C | T | 0,6398 | 0,0444 | 0,0310 | 0,1520 | 0,9545 | Post-operative pain | |
| rs12705966 | 7 | 114608796 | A | G | 0,3807 | -0,0425 | 0,0297 | 0,1528 | 0,9545 | Musculoskeletal pain | FOXP2 |
| rs6277 | 11 | 113412737 | G | A | 0,5751 | -0,0418 | 0,0293 | 0,1533 | 0,9545 | Neuropathic Pain | DRD2 |
| rs17723231 | 7 | 31067832 | C | T | 0,2783 | 0,0465 | 0,0327 | 0,1546 | 0,9545 | Migraine | ADCYAP1R1 |
| rs1979572 | 17 | 30184960 | G | A | 0,4820 | 0,0421 | 0,0296 | 0,1554 | 0,9545 | Migraine | NSRP1 |
| rs12143625 | 1 | 215218497 | C | T | 0,7613 | -0,0484 | 0,0343 | 0,1579 | 0,9545 | Migraine | KCNK2 |
| rs17428041 | 8 | 21853920 | T | C | 0,2416 | 0,0485 | 0,0344 | 0,1589 | 0,9545 | Neuropathic Pain | LOC105379318 |
| rs2835930 | 21 | 37749198 | C | A | 0,2620 | -0,0474 | 0,0337 | 0,1591 | 0,9545 | Analgesia | KCNJ6 |
| rs2070699 | 6 | 12292539 | G | T | 0,4465 | -0,0408 | 0,0290 | 0,1602 | 0,9545 | Migraine | EDN1 |
| rs2834442 | 21 | 34318486 | T | A | 0,6704 | -0,0443 | 0,0316 | 0,1610 | 0,9545 | Migraine | |
| rs12641989 | 4 | 3418113 | G | A | 0,0890 | -0,0726 | 0,0519 | 0,1623 | 0,9545 | Migraine | RGS12 |
| rs3904512 | 13 | 37783334 | G | A | 0,4239 | 0,0419 | 0,0300 | 0,1623 | 0,9545 | Migraine | TRPC4 |
| rs7218756 | 17 | 3515353 | G | A | 0,4789 | -0,0411 | 0,0295 | 0,1633 | 0,9545 | Migraine | TRPV3 |
| rs4760820 | 12 | 72003216 | C | G | 0,4341 | 0,0403 | 0,0290 | 0,1635 | 0,9545 | Migraine | TPH2 |
| rs1050316 | 1 | 156464911 | G | T | 0,6872 | -0,0435 | 0,0312 | 0,1636 | 0,9545 | Migraine | MEF2D |
| rs2274316 | 1 | 156476450 | C | A | 0,6872 | -0,0435 | 0,0312 | 0,1636 | 0,9545 | Migraine | MEF2D |
| rs2770293 | 13 | 46864839 | C | T | 0,3916 | 0,0406 | 0,0293 | 0,1662 | 0,9545 | Cancer Pain | HTR2A |
| rs12994338 | 2 | 166303519 | T | C | 0,7231 | 0,0455 | 0,0329 | 0,1670 | 0,9545 | Analgesia | SCN9A |
| rs5277 | 1 | 186679065 | C | G | 0,1648 | -0,0540 | 0,0391 | 0,1675 | 0,9545 | Cancer Pain | PTGS2 |
| rs2072100 | 7 | 97732472 | C | T | 0,5231 | -0,0402 | 0,0291 | 0,1677 | 0,9545 | Temporomandibular Disorder | TAC1 |
| rs1925950 | 1 | 156480948 | G | A | 0,6874 | -0,0430 | 0,0312 | 0,1681 | 0,9545 | Migraine | MEF2D |
| rs4852567 | 2 | 80476254 | A | G | 0,3092 | 0,0437 | 0,0317 | 0,1688 | 0,9545 | Other Clinical Pain | CTNNA2 |
| rs3790455 | 1 | 156486509 | C | T | 0,6886 | -0,0430 | 0,0313 | 0,1690 | 0,9545 | Migraine | MEF2D |
| rs10820447 | 9 | 96369762 | C | T | 0,1706 | 0,0527 | 0,0387 | 0,1736 | 0,9545 | Migraine | SUV39H2 |
| rs12310519 | 12 | 23822285 | C | T | 0,1245 | -0,0600 | 0,0441 | 0,1738 | 0,9545 | Neuraxial pain | SOX5 |
| rs1998056 | 14 | 94323158 | C | G | 0,5695 | -0,0392 | 0,0291 | 0,1778 | 0,9545 | Musculoskeletal Pain | SERPINA6 |
| rs561561 | 11 | 133959811 | A | T | 0,1145 | -0,0612 | 0,0458 | 0,1822 | 0,9545 | Migraine | |
| rs2274319 | 1 | 156481081 | T | C | 0,6881 | -0,0416 | 0,0312 | 0,1828 | 0,9545 | Migraine | MEF2D |
| rs3782221 | 12 | 117358076 | G | A | 0,2268 | 0,0468 | 0,0353 | 0,1852 | 0,9545 | Temporomandibular Disorder | NOS1 |
| rs11079993 | 17 | 52224192 | G | T | 0,3782 | -0,0404 | 0,0306 | 0,1875 | 0,9545 | Other Clinical Pain | |
| rs9341066 | 6 | 152098391 | G | A | 0,0445 | -0,0928 | 0,0705 | 0,1877 | 0,9545 | Migraine | ESR1 |
| rs9576354 | 13 | 37788657 | T | C | 0,4283 | 0,0386 | 0,0294 | 0,1886 | 0,9545 | Migraine | TRPC4 |
| rs7085387 | 10 | 58444842 | G | A | 0,7688 | -0,0452 | 0,0343 | 0,1886 | 0,9545 | Migraine | SUV39H2 |
| rs1042173 | 17 | 30197993 | A | C | 0,4757 | 0,0389 | 0,0296 | 0,1895 | 0,9545 | Arthritis | SLC6A4 |
| rs2836050 | 21 | 37912532 | C | T | 0,1670 | 0,0510 | 0,0389 | 0,1897 | 0,9545 | Cancer Pain | KCNJ6 |
| rs883248 | 10 | 1204244 | C | T | 0,5975 | 0,0387 | 0,0296 | 0,1898 | 0,9545 | Migraine | ADARB2 |

| | | | | | | | | | | | |
|---|---|---|---|---|---|---|---|---|---|---|---|
| rs4559 | 12 | 57095865 | C | T | 0,6500 | 0,0403 | 0,0308 | 0,1901 | 0,9545 | Migraine | STAT6 |
| rs7131056 | 11 | 113459052 | A | C | 0,6133 | -0,0391 | 0,0298 | 0,1903 | 0,9545 | Migraine | DRD2 |
| rs2223089 | 10 | 122450644 | G | C | 0,0688 | 0,0773 | 0,0591 | 0,1904 | 0,9545 | Migraine | LOC105378525 |
| rs3774354 | 3 | 52783659 | G | A | 0,3918 | 0,0393 | 0,0300 | 0,1910 | 0,9545 | Post-operative pain | ITIH1 |
| rs4363087 | 7 | 73703866 | T | C | 0,3568 | 0,0385 | 0,0298 | 0,1956 | 0,9545 | Migraine | BUD23 |
| rs4325622 | 17 | 30199457 | T | C | 0,4750 | 0,0382 | 0,0296 | 0,1970 | 0,9545 | Cancer Pain | SLC6A4 |
| rs2835925 | 21 | 37747000 | A | G | 0,1930 | -0,0469 | 0,0365 | 0,1982 | 0,9545 | Analgesia | KCNJ6 |
| rs3884606 | 5 | 171444070 | G | A | 0,5440 | 0,0387 | 0,0301 | 0,1983 | 0,9545 | Arthritis | FGF18 |
| rs12453010 | 17 | 52238771 | C | T | 0,3875 | -0,0391 | 0,0305 | 0,1998 | 0,9545 | Musculoskeletal pain | |
| rs6717794 | 2 | 237902121 | G | A | 0,6915 | -0,0404 | 0,0317 | 0,2018 | 0,9545 | Migraine | RAMP1 |
| rs6756590 | 2 | 216343848 | C | T | 0,4353 | -0,0377 | 0,0296 | 0,2026 | 0,9545 | Migraine | MARCHF4 |
| rs13136239 | 4 | 139987601 | G | A | 0,3257 | -0,0402 | 0,0315 | 0,2027 | 0,9545 | Other Clinical Pain | MAML3 |
| rs165599 | 22 | 19969258 | G | A | 0,7003 | 0,0404 | 0,0317 | 0,2028 | 0,9545 | Other Clinical Pain | ARVCF |
| rs9311195 | 3 | 38639727 | C | G | 0,1957 | -0,0460 | 0,0362 | 0,2032 | 0,9545 | Migraine | SCN5A |
| rs8008129 | 14 | 58362314 | T | C | 0,3077 | -0,0400 | 0,0315 | 0,2038 | 0,9545 | Migraine | ARID4A |
| rs10512405 | 9 | 110474517 | T | C | 0,3204 | -0,0394 | 0,0311 | 0,2049 | 0,9545 | Migraine | SVEP1 |
| rs1787337 | 21 | 37783651 | G | A | 0,4025 | -0,0386 | 0,0305 | 0,2052 | 0,9545 | Analgesia | KCNJ6 |
| rs1485395 | 12 | 53601293 | T | C | 0,1629 | -0,0499 | 0,0394 | 0,2058 | 0,9545 | Migraine | SUV39H2 |
| rs1048483 | 17 | 2063163 | C | T | 0,5105 | -0,0373 | 0,0295 | 0,2064 | 0,9545 | Migraine | HIC1 |
| rs7142517 | 14 | 54840086 | C | A | 0,3454 | -0,0392 | 0,0311 | 0,2067 | 0,9545 | Neuraxial Pain | GCH1 |
| rs3020343 | 6 | 151733228 | C | T | 0,5685 | -0,0372 | 0,0295 | 0,2074 | 0,9545 | Migraine | ESR1 |
| rs4883544 | 12 | 132625361 | T | C | 0,5914 | 0,0376 | 0,0299 | 0,2077 | 0,9545 | Temporomandibular Disorder | POLE |
| rs2386592 | 5 | 10174546 | A | G | 0,4336 | -0,0376 | 0,0299 | 0,2093 | 0,9545 | Musculoskeletal Pain | |
| rs10835649 | 11 | 30307628 | A | G | 0,1568 | 0,0512 | 0,0407 | 0,2093 | 0,9545 | Migraine | ARL14EP-DT |
| rs3777747 | 6 | 35611225 | A | G | 0,4669 | -0,0364 | 0,0292 | 0,2114 | 0,9545 | Musculoskeletal Pain | LOC112267956 |
| rs12720071 | 6 | 88141462 | T | C | 0,0885 | 0,0636 | 0,0510 | 0,2122 | 0,9545 | Migraine | CNR1 |
| rs216175 | 17 | 2264396 | A | C | 0,1621 | 0,0498 | 0,0400 | 0,2129 | 0,9545 | Arthritis | SMG6 |
| rs2110726 | 2 | 102177822 | G | A | 0,3763 | 0,0371 | 0,0299 | 0,2136 | 0,9545 | Cancer Pain | IL1R1 |
| rs7374540 | 3 | 38592651 | C | A | 0,6070 | 0,0380 | 0,0306 | 0,2139 | 0,9545 | Migraine | SCN5A |
| rs6770476 | 3 | 136355078 | C | T | 0,3014 | 0,0404 | 0,0325 | 0,2140 | 0,9545 | Other Clinical Pain | STAG1 |
| rs928723 | 21 | 37598364 | A | C | 0,5107 | -0,0365 | 0,0294 | 0,2144 | 0,9545 | Analgesia | |
| rs7819749 | 8 | 72063566 | T | G | 0,5955 | -0,0367 | 0,0295 | 0,2145 | 0,9545 | Migraine | TRPA1 |
| rs13361160 | 5 | 10169711 | T | C | 0,4339 | -0,0372 | 0,0299 | 0,2147 | 0,9545 | Musculoskeletal pain | |
| rs13072552 | 3 | 149195339 | G | T | 0,0754 | -0,0684 | 0,0552 | 0,2155 | 0,9545 | Neuropathic Pain | CP |
| rs7833174 | 8 | 129706526 | T | C | 0,2380 | 0,0422 | 0,0341 | 0,2162 | 0,9545 | Neuraxial pain | GSDMC |
| rs9383938 | 6 | 151666222 | G | T | 0,0926 | 0,0629 | 0,0509 | 0,2172 | 0,9545 | Migraine | ESR1 |
| rs6432896 | 2 | 166304910 | G | A | 0,5314 | -0,0369 | 0,0299 | 0,2173 | 0,9545 | Arthritis | SCN9A |
| rs1901531 | 15 | 44713183 | T | C | 0,1716 | 0,0479 | 0,0389 | 0,2182 | 0,9545 | Neuropathic Pain | B2M |
| rs4499491 | 20 | 45092778 | C | A | 0,3741 | -0,0370 | 0,0300 | 0,2183 | 0,9545 | Neuropathic Pain | KCNS1 |
| rs10218452 | 1 | 3159033 | A | G | 0,2637 | 0,0407 | 0,0331 | 0,2191 | 0,9545 | Migraine | PRDM16 |
| rs17841327 | 16 | 55660341 | A | C | 0,6650 | 0,0379 | 0,0309 | 0,2198 | 0,9545 | Neuropathic pain | SLC6A2 |
| rs12363824 | 11 | 30320603 | G | A | 0,1575 | 0,0498 | 0,0407 | 0,2210 | 0,9545 | Migraine | ARL14EP-DT |
| rs182637 | 17 | 3606538 | C | T | 0,4458 | 0,0358 | 0,0293 | 0,2219 | 0,9545 | Migraine | TRPV1 |
| rs2249714 | 7 | 31071801 | T | C | 0,6621 | -0,0382 | 0,0313 | 0,2221 | 0,9545 | Migraine | ADCYAP1R1 |
| rs9547988 | 13 | 37636094 | T | G | 0,3418 | 0,0379 | 0,0310 | 0,2222 | 0,9545 | Migraine | TRPC4 |
| rs2151438 | 13 | 37784293 | C | T | 0,5464 | -0,0363 | 0,0299 | 0,2242 | 0,9545 | Migraine | TRPC4 |

| | | | | | | | | | | | |
|---|---|---|---|---|---|---|---|---|---|---|---|
| rs12211463 | 6 | 92757440 | T | G | 0,2151 | -0,0433 | 0,0356 | 0,2243 | 0,9545 | Analgesia | |
| rs6927800 | 6 | 118282959 | C | G | 0,4750 | -0,0364 | 0,0300 | 0,2251 | 0,9545 | Neuraxial pain | CHRNA5 |
| rs733080 | 17 | 3597317 | T | C | 0,2703 | 0,0399 | 0,0329 | 0,2252 | 0,9545 | Migraine | TRPV1 |
| rs4448731 | 12 | 71935326 | T | C | 0,5119 | 0,0355 | 0,0293 | 0,2255 | 0,9545 | Migraine | TPH2 |
| rs12223987 | 11 | 30374324 | C | T | 0,1663 | 0,0480 | 0,0396 | 0,2257 | 0,9545 | Migraine | |
| rs3858429 | 11 | 30322210 | C | T | 0,1573 | 0,0493 | 0,0407 | 0,2260 | 0,9545 | Migraine | ARL14EP-DT |
| rs4071558 | 11 | 30323044 | C | T | 0,1573 | 0,0493 | 0,0407 | 0,2260 | 0,9545 | Migraine | |
| rs4071559 | 11 | 30323178 | C | T | 0,1573 | 0,0493 | 0,0407 | 0,2260 | 0,9545 | Migraine | ARL14EP |
| rs2243250 | 5 | 132673462 | C | T | 0,1439 | 0,0503 | 0,0416 | 0,2264 | 0,9545 | Neuraxial pain | |
| rs1800469 | 19 | 41354391 | A | G | 0,6607 | 0,0367 | 0,0304 | 0,2279 | 0,9545 | Migraine | |
| rs6869446 | 5 | 66274779 | T | C | 0,3875 | 0,0363 | 0,0302 | 0,2281 | 0,9545 | Other Clinical Pain | |
| rs12278989 | 11 | 30295275 | A | G | 0,1568 | 0,0491 | 0,0407 | 0,2284 | 0,9545 | Migraine | ARL14EP-DT |
| rs11031040 | 11 | 30296186 | T | G | 0,1568 | 0,0491 | 0,0407 | 0,2284 | 0,9545 | Migraine | ARL14EP-DT |
| rs12271187 | 11 | 30297712 | G | A | 0,1568 | 0,0491 | 0,0407 | 0,2284 | 0,9545 | Migraine | ARL14EP-DT |
| rs12271300 | 11 | 30297886 | G | A | 0,1568 | 0,0491 | 0,0407 | 0,2284 | 0,9545 | Migraine | ARL14EP-DT |
| rs4861775 | 4 | 179395497 | A | C | 0,2081 | -0,0437 | 0,0364 | 0,2304 | 0,9545 | Migraine | |
| rs11031047 | 11 | 30315976 | C | T | 0,1573 | 0,0488 | 0,0407 | 0,2305 | 0,9545 | Migraine | ARL14EP-DT |
| rs1543754 | 21 | 37721804 | G | C | 0,5428 | 0,0349 | 0,0292 | 0,2320 | 0,9545 | Analgesia | KCNJ6 |
| rs3020348 | 6 | 151736779 | C | A | 0,5700 | -0,0352 | 0,0295 | 0,2327 | 0,9545 | Migraine | ESR1 |
| rs685550 | 1 | 239761108 | G | A | 0,7543 | 0,0391 | 0,0328 | 0,2328 | 0,9545 | Analgesia | CHRM3 |
| rs2272023 | 15 | 88847929 | C | A | 0,7708 | -0,0414 | 0,0348 | 0,2336 | 0,9545 | Neuraxial Pain | ACAN |
| rs7858755 | 9 | 74792820 | A | G | 0,2523 | 0,0399 | 0,0335 | 0,2343 | 0,9545 | Migraine | TRPM6 |
| rs1149620 | 11 | 76795528 | T | A | 0,4473 | -0,0345 | 0,0290 | 0,2352 | 0,9545 | Arthritis | TSKU |
| rs8904 | 14 | 35402011 | G | A | 0,3887 | 0,0354 | 0,0299 | 0,2363 | 0,9545 | Cancer Pain | NFKBIA |
| rs10453201 | 9 | 34050347 | C | T | 0,2428 | -0,0400 | 0,0338 | 0,2366 | 0,9545 | Arthritis | UBAP2 |
| rs4939879 | 18 | 49619613 | A | G | 0,5265 | -0,0339 | 0,0288 | 0,2397 | 0,9637 | Migraine | LOC105372112 |
| rs2284015 | 22 | 36700528 | C | G | 0,2423 | -0,0400 | 0,0341 | 0,2418 | 0,9674 | Cancer Pain | CACNG2 |
| rs7006287 | 8 | 72932080 | A | G | 0,4310 | -0,0349 | 0,0299 | 0,2432 | 0,9674 | Migraine | KCNB2 |
| rs6686529 | 1 | 215236763 | G | C | 0,7654 | -0,0402 | 0,0345 | 0,2435 | 0,9674 | Migraine | KCNK2 |
| rs4820242 | 22 | 36586628 | G | A | 0,6201 | 0,0353 | 0,0303 | 0,2439 | 0,9674 | Cancer Pain | CACNG2 |
| rs2834167 | 21 | 33268483 | A | G | 0,2871 | 0,0370 | 0,0321 | 0,2484 | 0,9767 | Cancer Pain | IL10RB |
| rs9650767 | 9 | 74735440 | G | A | 0,3709 | 0,0345 | 0,0299 | 0,2493 | 0,9767 | Migraine | TRPM6 |
| rs10405617 | 19 | 10642292 | A | G | 0,6621 | -0,0354 | 0,0308 | 0,2493 | 0,9767 | Arthritis | SLC44A2 |
| rs7776341 | 6 | 154027470 | A | C | 0,0335 | 0,0948 | 0,0826 | 0,2509 | 0,9767 | Analgesia | OPRM1 |
| rs1256049 | 14 | 64257333 | C | T | 0,0263 | 0,1061 | 0,0927 | 0,2524 | 0,9767 | Temporomandibular disorders | ESR2 |
| rs13107066 | 4 | 47376678 | G | T | 0,5987 | 0,0342 | 0,0299 | 0,2530 | 0,9767 | Neuraxial Pain | GABRB1 |
| rs505738 | 1 | 181473340 | A | C | 0,4774 | -0,0333 | 0,0293 | 0,2557 | 0,9767 | Migraine | CACNA1E |
| rs3777567 | 6 | 45932829 | G | A | 0,2876 | -0,0365 | 0,0321 | 0,2557 | 0,9767 | Migraine | CLIC5 |
| rs10831475 | 11 | 96063743 | A | G | 0,1903 | -0,0417 | 0,0368 | 0,2567 | 0,9767 | Post-operative pain | MAML2 |
| rs10831476 | 11 | 96063746 | A | C | 0,1903 | -0,0417 | 0,0368 | 0,2567 | 0,9767 | Arthritis | MAML2 |
| rs10831477 | 11 | 96063947 | T | G | 0,1903 | -0,0417 | 0,0368 | 0,2567 | 0,9767 | Arthritis | MAML2 |
| rs4985445 | 16 | 69833932 | A | G | 0,4490 | -0,0333 | 0,0294 | 0,2579 | 0,9767 | Musculoskeletal pain | WWP2 |
| rs6813436 | 4 | 47388803 | G | A | 0,1121 | -0,0535 | 0,0473 | 0,2580 | 0,9767 | Neuraxial Pain | GABRB1 |
| rs9940278 | 16 | 53766288 | C | T | 0,4429 | -0,0331 | 0,0292 | 0,2581 | 0,9767 | Arthritis | FTO |
| rs4478147 | 4 | 86552623 | G | A | 0,5243 | -0,0332 | 0,0295 | 0,2594 | 0,9767 | Migraine | SUV39H2 |
| rs1801253 | 10 | 114045297 | G | C | 0,7086 | 0,0366 | 0,0325 | 0,2601 | 0,9767 | Analgesia | ADRB1 |

| | | | | | | | | | | | |
|---|---|---|---|---|---|---|---|---|---|---|---|
| rs10895837 | 11 | 105577727 | T | C | 0,8816 | -0,0498 | 0,0443 | 0,2605 | 0,9767 | Fibromyalgia | |
| rs3851738 | 16 | 75353635 | G | C | 0,5851 | 0,0332 | 0,0297 | 0,2642 | 0,9804 | Migraine | CFDP1 |
| rs1352250 | 12 | 72004004 | A | G | 0,5902 | 0,0330 | 0,0296 | 0,2648 | 0,9804 | Migraine | TPH2 |
| rs806379 | 6 | 88151548 | A | T | 0,4667 | -0,0326 | 0,0293 | 0,2657 | 0,9804 | Migraine | CNR1 |
| rs731236 | 12 | 47844974 | A | G | 0,4071 | -0,0330 | 0,0297 | 0,2668 | 0,9804 | Migraine | VDR |
| rs1517572 | 11 | 28808335 | A | C | 0,5807 | 0,0333 | 0,0302 | 0,2692 | 0,9804 | Arthritis | RP11-115J23.1 |
| rs1946247 | 5 | 161409614 | T | G | 0,8422 | 0,0441 | 0,0399 | 0,2695 | 0,9804 | Other Clinical Pain | GABRB2 |
| rs1799983 | 7 | 150999023 | T | G | 0,6650 | 0,0346 | 0,0315 | 0,2708 | 0,9804 | Migraine | NOS3 |
| rs3804452 | 6 | 36109157 | G | A | 0,1147 | 0,0507 | 0,0461 | 0,2710 | 0,9804 | Temporomandibular Disorder | MAPK14 |
| rs4906902 | 15 | 26774621 | A | G | 0,1748 | 0,0422 | 0,0383 | 0,2714 | 0,9804 | Fibromyalgia | |
| rs7595255 | 2 | 166226468 | T | C | 0,8614 | 0,0469 | 0,0427 | 0,2715 | 0,9804 | Nociception | SCN1A-AS1 |
| rs4888408 | 16 | 75398926 | G | A | 0,5841 | 0,0327 | 0,0297 | 0,2715 | 0,9804 | Migraine | CFDP1 |
| rs10484919 | 6 | 151653287 | C | T | 0,0955 | 0,0549 | 0,0499 | 0,2720 | 0,9804 | Migraine | ESR1 |
| rs10504861 | 8 | 88535703 | C | T | 0,1864 | -0,0408 | 0,0373 | 0,2737 | 0,9804 | Migraine | LOC105375629 |
| rs2236225 | 14 | 64442127 | G | A | 0,4458 | 0,0313 | 0,0286 | 0,2741 | 0,9804 | Temporomandibular Disorder | MTHFD1 |
| rs644796 | 1 | 181466918 | T | C | 0,4806 | -0,0321 | 0,0294 | 0,2745 | 0,9804 | Migraine | CACNA1E |
| rs1043994 | 19 | 15192033 | T | C | 0,8724 | -0,0475 | 0,0436 | 0,2765 | 0,9804 | Migraine | NOTCH3 |
| rs910079 | 20 | 1979552 | A | G | 0,2742 | -0,0362 | 0,0333 | 0,2774 | 0,9804 | Musculoskeletal Pain | PDYN |
| rs3729618 | 6 | 45920336 | A | G | 0,3077 | -0,0341 | 0,0315 | 0,2782 | 0,9804 | Migraine | CLIC5 |
| rs2857605 | 6 | 31557074 | C | T | 0,9137 | 0,0559 | 0,0516 | 0,2782 | 0,9804 | Neuropathic Pain | LOC100287329 |
| rs1401795 | 17 | 56762291 | A | G | 0,5143 | 0,0319 | 0,0295 | 0,2792 | 0,9804 | Arthritis | C17orf67 |
| rs1416167 | 6 | 45919684 | A | T | 0,3080 | -0,0340 | 0,0315 | 0,2802 | 0,9804 | Migraine | CLIC5 |
| rs217693 | 14 | 61936083 | A | G | 0,7667 | -0,0377 | 0,0350 | 0,2804 | 0,9804 | Migraine | SYT16 |
| rs2070874 | 5 | 132674018 | C | T | 0,1390 | 0,0457 | 0,0424 | 0,2816 | 0,9804 | Neuraxial pain | IL4 |
| rs7105462 | 11 | 113041326 | G | A | 0,5870 | 0,0322 | 0,0299 | 0,2823 | 0,9804 | Neuraxial pain | NCAM1 |
| rs6166 | 2 | 48962782 | C | T | 0,5352 | 0,0317 | 0,0295 | 0,2826 | 0,9804 | Migraine | ESR1 |
| rs3817428 | 15 | 88872016 | C | G | 0,2623 | -0,0356 | 0,0332 | 0,2832 | 0,9804 | Neuraxial Pain | ACAN |
| rs10786156 | 10 | 94254865 | C | G | 0,4565 | 0,0313 | 0,0294 | 0,2865 | 0,9823 | Migraine | PLCE1 |
| rs4713902 | 6 | 35646249 | T | C | 0,2927 | -0,0341 | 0,0320 | 0,2873 | 0,9823 | Musculoskeletal Pain | FKBP5 |
| rs11709492 | 3 | 38904493 | C | T | 0,2166 | -0,0381 | 0,0360 | 0,2896 | 0,9823 | Nociception | SCN11A |
| rs2070697 | 14 | 24574883 | C | T | 0,2878 | 0,0344 | 0,0325 | 0,2897 | 0,9823 | Post-operative Pain | CTSG |
| rs480760 | 3 | 196071387 | T | C | 0,9575 | 0,0741 | 0,0700 | 0,2898 | 0,9823 | Neuropathic Pain | TFRC |
| rs6746030 | 2 | 166242648 | A | G | 0,8619 | 0,0451 | 0,0427 | 0,2909 | 0,9823 | Neuraxial Pain | SCN1A-AS1 |
| rs2095771 | 6 | 45936895 | C | A | 0,2783 | -0,0343 | 0,0325 | 0,2910 | 0,9823 | Migraine | CLIC5 |
| rs1268083 | 6 | 125727894 | T | C | 0,4835 | 0,0314 | 0,0298 | 0,2916 | 0,9823 | Migraine | LOC105377986 |
| rs2813550 | 6 | 152120452 | C | A | 0,7365 | 0,0345 | 0,0329 | 0,2932 | 0,9823 | Migraine | ESR1 |
| rs2813544 | 6 | 152104447 | A | G | 0,1983 | -0,0383 | 0,0366 | 0,2960 | 0,9823 | Migraine | ESR1 |
| rs267206 | 6 | 7860582 | C | T | 0,7995 | -0,0375 | 0,0359 | 0,2965 | 0,9823 | Neuropathic Pain | BMP6 |
| rs1143634 | 2 | 112832813 | G | A | 0,2394 | 0,0357 | 0,0342 | 0,2971 | 0,9823 | Migraine | IL1B |
| rs10870267 | 10 | 132154559 | C | T | 0,5139 | -0,0304 | 0,0292 | 0,2973 | 0,9823 | Neuraxial pain | JAKMIP3 |
| rs6107848 | 20 | 6610469 | A | G | 0,6415 | -0,0315 | 0,0303 | 0,2997 | 0,9823 | Migraine | |
| rs34612513 | 3 | 137822243 | T | A | 0,1106 | -0,0484 | 0,0469 | 0,3026 | 0,9823 | Temporomandibular disorders | |
| rs13080116 | 3 | 38865732 | T | C | 0,2450 | -0,0352 | 0,0342 | 0,3032 | 0,9823 | Analgesia | SCN11A |
| rs57866767 | 10 | 94263320 | T | C | 0,4567 | 0,0301 | 0,0294 | 0,3055 | 0,9823 | Migraine | PLCE1 |
| rs4493873 | 8 | 91063415 | A | C | 0,6381 | 0,0310 | 0,0304 | 0,3084 | 0,9823 | Migraine | SUV39H2 |
| rs324419 | 1 | 46406314 | T | C | 0,8381 | -0,0405 | 0,0398 | 0,3086 | 0,9823 | Other Clinical Pain | FAAH |

| | | | | | | | | | | | |
|---|---|---|---|---|---|---|---|---|---|---|---|
| rs10925250 | 1 | 236858830 | A | G | 0,1711 | -0,0390 | 0,0384 | 0,3098 | 0,9823 | Migraine | MTR |
| rs1045642 | 7 | 87509329 | A | G | 0,4793 | 0,0300 | 0,0296 | 0,3100 | 0,9823 | Analgesia | ABCB1 |
| rs6746771 | 2 | 237893144 | A | G | 0,1101 | -0,0477 | 0,0470 | 0,3101 | 0,9823 | Migraine | RAMP1 |
| rs10155855 | 7 | 111688341 | A | T | 0,0683 | -0,0591 | 0,0583 | 0,3106 | 0,9823 | Migraine | |
| rs2284017 | 22 | 36700882 | T | C | 0,5661 | 0,0299 | 0,0296 | 0,3114 | 0,9823 | Cancer Pain, Post-operative pain | CACNG2 |
| rs3777585 | 6 | 45951232 | C | T | 0,2270 | -0,0349 | 0,0346 | 0,3129 | 0,9823 | Migraine | CLIC5 |
| rs17568951 | 2 | 47580354 | T | C | 0,1974 | 0,0373 | 0,0371 | 0,3139 | 0,9823 | Migraine | MSH2 |
| rs11164653 | 1 | 102998654 | T | C | 0,5924 | 0,0299 | 0,0298 | 0,3162 | 0,9823 | Arthritis | COL11A1 |
| rs2069845 | 7 | 22730530 | G | A | 0,6048 | 0,0291 | 0,0291 | 0,3187 | 0,9823 | Cancer Pain | IL6 |
| rs10733092 | 1 | 91160992 | A | G | 0,2628 | -0,0335 | 0,0336 | 0,3192 | 0,9823 | Migraine | |
| rs12282928 | 11 | 48310476 | A | G | 0,2642 | -0,0332 | 0,0334 | 0,3208 | 0,9823 | Migraine | SUV39H2 |
| rs9861643 | 3 | 38655848 | C | T | 0,1823 | -0,0372 | 0,0375 | 0,3213 | 0,9823 | Migraine | |
| rs3787441 | 20 | 4224413 | T | C | 0,2623 | -0,0326 | 0,0329 | 0,3213 | 0,9823 | Cancer Pain | ADRA1D |
| rs8022616 | 14 | 94307608 | A | G | 0,1060 | -0,0472 | 0,0477 | 0,3217 | 0,9823 | Musculoskeletal Pain | SERPINA6 |
| rs11179000 | 12 | 71944848 | A | T | 0,2236 | -0,0349 | 0,0352 | 0,3217 | 0,9823 | Neuropathic pain | TPH2 |
| rs11071366 | 15 | 58042046 | A | T | 0,3525 | 0,0304 | 0,0308 | 0,3229 | 0,9823 | Arthritis | ALDH1A2 |
| rs694539 | 11 | 114262697 | C | T | 0,1779 | -0,0376 | 0,0381 | 0,3231 | 0,9823 | Migraine | NNMT |
| rs35072907 | 1 | 50723884 | G | C | 0,3367 | 0,0306 | 0,0310 | 0,3238 | 0,9823 | Other Clinical Pain | FAF1 |
| rs2525570 | 17 | 31354227 | A | G | 0,6118 | -0,0298 | 0,0303 | 0,3251 | 0,9823 | Migraine | NF1 |
| rs4977338 | 9 | 18718088 | G | T | 0,1619 | -0,0393 | 0,0400 | 0,3255 | 0,9823 | Migraine | ADAMTSL1 |
| rs9534511 | 13 | 46894445 | T | C | 0,5515 | -0,0290 | 0,0296 | 0,3269 | 0,9823 | Musculoskeletal Pain | HTR2A |
| rs13267466 | 8 | 132327150 | A | C | 0,1915 | 0,0362 | 0,0369 | 0,3270 | 0,9823 | Migraine | KCNQ3 |
| rs1186902 | 6 | 89217243 | T | C | 0,2632 | -0,0328 | 0,0335 | 0,3271 | 0,9823 | Migraine | GABRR1 |
| rs6265 | 11 | 27658369 | C | T | 0,2010 | -0,0357 | 0,0365 | 0,3283 | 0,9823 | Musculoskeletal pain | BDNF |
| rs4986790 | 9 | 117713024 | A | G | 0,0489 | 0,0671 | 0,0686 | 0,3284 | 0,9823 | Migraine | TLR4 |
| rs2273206 | 6 | 152061176 | G | T | 0,1152 | 0,0448 | 0,0459 | 0,3285 | 0,9823 | Temporomandibular Disorder | ESR1 |
| rs222747 | 17 | 3589906 | C | G | 0,7402 | 0,0326 | 0,0335 | 0,3308 | 0,9823 | Nociception | TRPV1 |
| rs3766694 | 1 | 175174071 | T | C | 0,5647 | -0,0284 | 0,0292 | 0,3309 | 0,9823 | Migraine | KIAA0040 |
| rs7104613 | 11 | 14058384 | C | T | 0,0685 | 0,0561 | 0,0578 | 0,3317 | 0,9823 | Analgesia | SPON1 |
| rs2070762 | 11 | 2165105 | A | G | 0,4998 | 0,0280 | 0,0289 | 0,3328 | 0,9823 | Cancer Pain | TH |
| rs1374111 | 2 | 136676332 | G | A | 0,6009 | 0,0284 | 0,0293 | 0,3329 | 0,9823 | Migraine | |
| rs12550268 | 8 | 72523859 | A | G | 0,5671 | -0,0287 | 0,0296 | 0,3329 | 0,9823 | Migraine | LOC105375897 |
| rs1801132 | 6 | 151944387 | G | C | 0,7730 | -0,0341 | 0,0353 | 0,3340 | 0,9823 | Migraine | ESR1 |
| rs162502 | 21 | 26960687 | C | T | 0,2154 | -0,0347 | 0,0360 | 0,3351 | 0,9823 | Neuraxial Pain | ADAMTS5 |
| rs3918242 | 20 | 46007337 | C | T | 0,1376 | -0,0402 | 0,0418 | 0,3359 | 0,9823 | Temporomandibular Disorder | |
| rs3845446 | 1 | 181797301 | T | C | 0,0486 | 0,0647 | 0,0677 | 0,3390 | 0,9823 | Analgesia | CACNA1E |
| rs5030977 | 3 | 50379070 | C | T | 0,1101 | 0,0440 | 0,0460 | 0,3390 | 0,9823 | Analgesia | CACNA2D2 |
| rs302679 | 2 | 237880402 | G | T | 0,7790 | -0,0331 | 0,0348 | 0,3421 | 0,9823 | Migraine | RAMP1 |
| rs229052 | 21 | 26943889 | G | A | 0,7127 | -0,0309 | 0,0326 | 0,3424 | 0,9823 | Neuraxial Pain | ADAMTS5 |
| rs10983775 | 9 | 117758822 | C | T | 0,5540 | -0,0274 | 0,0290 | 0,3437 | 0,9823 | Arthritis | RP11-281A20.2 |
| rs429313 | 16 | 84464239 | C | A | 0,2010 | -0,0345 | 0,0366 | 0,3454 | 0,9823 | Migraine | ATP2C2 |
| rs516243 | 1 | 10690375 | A | G | 0,5131 | 0,0271 | 0,0288 | 0,3464 | 0,9823 | Migraine | SUV39H2 |
| rs12439516 | 15 | 66411138 | A | T | 0,0826 | -0,0496 | 0,0527 | 0,3466 | 0,9823 | Temporomandibular Disorder | MAP2K1 |
| rs6971 | 22 | 43162920 | A | G | 0,6969 | 0,0300 | 0,0319 | 0,3469 | 0,9823 | Neuraxial Pain | TSPO |
| rs2298771 | 2 | 166036278 | C | T | 0,6595 | 0,0287 | 0,0306 | 0,3473 | 0,9823 | Musculoskeletal Pain | LOC102724058 |
| rs6432860 | 2 | 166041354 | A | G | 0,6595 | 0,0287 | 0,0306 | 0,3473 | 0,9823 | Musculoskeletal Pain | SCN1A |

| | | | | | | | | | | | |
|---|---|---|---|---|---|---|---|---|---|---|---|
| rs1461193 | 2 | 166047836 | G | A | 0,6595 | 0,0287 | 0,0306 | 0,3473 | 0,9823 | Musculoskeletal Pain | SCN1A |
| rs8112559 | 19 | 45887197 | C | G | 0,1196 | 0,0435 | 0,0464 | 0,3490 | 0,9823 | Arthritis | IRF2BP1 |
| rs10062749 | 5 | 142425523 | G | T | 0,2786 | -0,0310 | 0,0332 | 0,3510 | 0,9823 | Arthritis | AC005592.2 |
| rs7350833 | 16 | 84380558 | G | C | 0,3051 | -0,0292 | 0,0313 | 0,3514 | 0,9823 | Migraine | ATP2C2 |
| rs9332377 | 22 | 19968169 | C | T | 0,1633 | -0,0373 | 0,0401 | 0,3520 | 0,9823 | Temporomandibular disorders | ARVCF |
| rs1801133 | 1 | 11796321 | G | A | 0,3845 | 0,0278 | 0,0299 | 0,3539 | 0,9823 | Migraine | MTHFR |
| rs11588850 | 1 | 227739541 | A | G | 0,1325 | -0,0402 | 0,0437 | 0,3576 | 0,9823 | Arthritis | SNAP47 |
| rs7604448 | 2 | 166256134 | A | C | 0,8563 | 0,0386 | 0,0420 | 0,3592 | 0,9823 | Arthritis | SCN1A-AS1 |
| rs2499797 | 6 | 96400793 | G | A | 0,8153 | -0,0349 | 0,0382 | 0,3607 | 0,9823 | Migraine | UFL1-AS1 |
| rs4986938 | 14 | 64233098 | C | T | 0,3807 | -0,0281 | 0,0308 | 0,3610 | 0,9823 | Migraine | ESR1 |
| rs2183271 | 10 | 21668300 | T | C | 0,3879 | 0,0273 | 0,0299 | 0,3624 | 0,9823 | Other Clinical Pain | MLLT10 |
| rs543844 | 6 | 44457063 | A | G | 0,3853 | -0,0274 | 0,0301 | 0,3633 | 0,9823 | Migraine | SUV39H2 |
| rs2813554 | 6 | 152121203 | G | A | 0,1976 | -0,0332 | 0,0366 | 0,3646 | 0,9823 | Migraine | ESR1 |
| rs4677830 | 3 | 195339614 | C | T | 0,8160 | -0,0340 | 0,0376 | 0,3655 | 0,9823 | Analgesia | OPRM1 |
| rs390208 | 16 | 84474211 | G | A | 0,1988 | -0,0333 | 0,0369 | 0,3665 | 0,9823 | Migraine | |
| rs2438224 | 8 | 97679242 | A | G | 0,0724 | 0,0508 | 0,0564 | 0,3677 | 0,9823 | Migraine | MTDH |
| rs7583431 | 2 | 175057654 | A | C | 0,3841 | 0,0267 | 0,0297 | 0,3693 | 0,9823 | Analgesia | |
| rs2049604 | 7 | 114350297 | C | T | 0,3923 | -0,0268 | 0,0299 | 0,3704 | 0,9823 | Musculoskeletal pain | FOXP2 |
| rs10888075 | 8 | 13902910 | T | G | 0,8393 | -0,0356 | 0,0398 | 0,3709 | 0,9823 | Migraine | |
| rs1556832 | 20 | 4234910 | C | T | 0,5051 | -0,0257 | 0,0288 | 0,3716 | 0,9823 | Temporomandibular Disorder | ADRA1D |
| rs569356 | 1 | 28810174 | A | G | 0,1174 | 0,0408 | 0,0456 | 0,3717 | 0,9823 | Post-operative pain | |
| rs11668962 | 19 | 49215291 | G | A | 0,4577 | -0,0262 | 0,0295 | 0,3729 | 0,9823 | Migraine | |
| rs2723279 | 12 | 117835066 | C | A | 0,2807 | 0,0287 | 0,0322 | 0,3733 | 0,9823 | Migraine | SUV39H2 |
| rs699947 | 6 | 43768652 | A | C | 0,5338 | -0,0260 | 0,0294 | 0,3761 | 0,9823 | Migraine | POLR1C |
| rs12633508 | 3 | 88765985 | T | C | 0,2467 | 0,0300 | 0,0340 | 0,3765 | 0,9823 | Analgesia | |
| rs11705555 | 22 | 27810924 | A | C | 0,2691 | -0,0292 | 0,0331 | 0,3782 | 0,9823 | Arthritis | MN1 |
| rs2052129 | 7 | 150851884 | G | T | 0,2368 | -0,0310 | 0,0352 | 0,3791 | 0,9823 | Migraine | LOC105375567 |
| rs1295686 | 5 | 132660151 | T | C | 0,8024 | -0,0328 | 0,0373 | 0,3798 | 0,9823 | Cancer Pain | IL13 |
| rs743506 | 7 | 151009827 | G | A | 0,7299 | -0,0288 | 0,0328 | 0,3805 | 0,9823 | Migraine | NOS3 |
| rs1631174 | 11 | 47952821 | A | C | 0,6808 | 0,0272 | 0,0310 | 0,3807 | 0,9823 | Arthritis | PTPRJ |
| rs2026739 | 9 | 32418239 | G | T | 0,7137 | 0,0286 | 0,0327 | 0,3826 | 0,9823 | Neuropathic Pain | ACO1 |
| rs10178489 | 2 | 17871407 | C | G | 0,3002 | 0,0274 | 0,0315 | 0,3829 | 0,9823 | Migraine | |
| rs4081947 | 16 | 87546264 | A | G | 0,3141 | -0,0273 | 0,0313 | 0,3832 | 0,9823 | Migraine | |
| rs1077430 | 14 | 76431334 | T | C | 0,3133 | 0,0275 | 0,0317 | 0,3860 | 0,9823 | Temporomandibular Disorder | ESRRB |
| rs394533 | 16 | 84470981 | C | T | 0,2499 | -0,0292 | 0,0337 | 0,3865 | 0,9823 | Migraine | |
| rs1805087 | 1 | 236885200 | A | G | 0,1709 | -0,0332 | 0,0383 | 0,3866 | 0,9823 | Migraine | MTR |
| rs1572668 | 1 | 73434059 | A | G | 0,4584 | -0,0258 | 0,0298 | 0,3867 | 0,9823 | Migraine | |
| rs167769 | 12 | 57109992 | C | T | 0,3515 | 0,0260 | 0,0301 | 0,3873 | 0,9823 | Analgesia | STAT6 |
| rs4807347 | 19 | 2857289 | A | C | 0,8359 | -0,0344 | 0,0398 | 0,3878 | 0,9823 | Migraine | ZNF555 |
| rs11031122 | 11 | 30525891 | T | C | 0,2453 | -0,0291 | 0,0337 | 0,3885 | 0,9823 | Migraine | MPPED2 |
| rs1143627 | 2 | 112836810 | G | A | 0,6687 | 0,0272 | 0,0317 | 0,3906 | 0,9823 | Cancer Pain | IL1B |
| rs2473967 | 6 | 113158133 | G | T | 0,9397 | -0,0536 | 0,0626 | 0,3916 | 0,9823 | Analgesia | |
| rs13946 | 9 | 134842386 | C | T | 0,7555 | -0,0294 | 0,0343 | 0,3921 | 0,9823 | Other Clinical Pain | LOC101448202 |
| rs16851799 | 2 | 166229904 | C | T | 0,3804 | -0,0256 | 0,0300 | 0,3932 | 0,9823 | Analgesia | SCN1A-AS1 |
| rs8133052 | 21 | 36135203 | G | A | 0,4623 | 0,0251 | 0,0294 | 0,3933 | 0,9823 | Cancer Pain | CBR3-AS1 |
| rs1577007 | 13 | 37729549 | C | T | 0,5814 | 0,0250 | 0,0295 | 0,3961 | 0,9823 | Migraine | TRPC4 |

| | | | | | | | | | | | |
|---|---|---|---|---|---|---|---|---|---|---|---|
| rs10925257 | 1 | 236882860 | A | G | 0,1714 | -0,0320 | 0,0384 | 0,4034 | 0,9823 | Migraine | MTR |
| rs16944 | 2 | 112837290 | A | G | 0,6689 | 0,0264 | 0,0317 | 0,4038 | 0,9823 | Musculoskeletal Pain | IL1B |
| rs75621460 | 19 | 41327879 | G | A | 0,0228 | 0,0827 | 0,0991 | 0,4040 | 0,9823 | Post-operative pain | TGFB1 |
| rs6951030 | 7 | 73718911 | T | G | 0,1860 | 0,0311 | 0,0374 | 0,4055 | 0,9823 | Migraine | BUD23 |
| rs10275320 | 7 | 20142431 | G | A | 0,1383 | -0,0349 | 0,0422 | 0,4086 | 0,9823 | Migraine | MACC1-AS1 |
| rs2229094 | 6 | 31572779 | T | C | 0,1458 | -0,0339 | 0,0411 | 0,4094 | 0,9823 | Musculoskeletal Pain | LTA |
| rs13107325 | 4 | 102267552 | C | T | 0,0671 | -0,0483 | 0,0587 | 0,4106 | 0,9823 | Musculoskeletal pain | SLC39A8 |
| rs895572 | 2 | 237906610 | C | T | 0,5374 | -0,0242 | 0,0296 | 0,4129 | 0,9823 | Migraine | RAMP1 |
| rs1643821 | 6 | 151862416 | G | A | 0,4071 | 0,0244 | 0,0300 | 0,4158 | 0,9823 | Temporomandibular Disorder | ESR1 |
| rs1800783 | 7 | 150992309 | A | T | 0,5892 | 0,0243 | 0,0299 | 0,4162 | 0,9823 | Cancer Pain | NOS3 |
| rs10259354 | 7 | 3447782 | G | A | 0,6971 | -0,0253 | 0,0313 | 0,4189 | 0,9823 | Other Clinical Pain | SDK1 |
| rs1409202 | 10 | 18474754 | C | A | 0,1237 | 0,0357 | 0,0442 | 0,4190 | 0,9823 | Migraine | CACNB2 |
| rs10809907 | 9 | 13134433 | C | G | 0,6682 | 0,0244 | 0,0304 | 0,4214 | 0,9823 | Nociception | MPDZ |
| rs3782202 | 12 | 117282575 | G | A | 0,7905 | -0,0291 | 0,0362 | 0,4218 | 0,9823 | Temporomandibular Disorder | NOS1 |
| rs1544325 | 22 | 19944145 | A | G | 0,5885 | 0,0234 | 0,0292 | 0,4240 | 0,9823 | Temporomandibular Disorder | COMT |
| rs1928040 | 13 | 46873101 | G | A | 0,5010 | -0,0233 | 0,0291 | 0,4248 | 0,9823 | Cancer Pain | HTR2A |
| rs926849 | 6 | 161740587 | C | T | 0,6906 | -0,0248 | 0,0311 | 0,4248 | 0,9823 | Neuraxial Pain | PRKN |
| rs17288390 | 6 | 45416281 | T | C | 0,3503 | 0,0248 | 0,0311 | 0,4253 | 0,9823 | Post-operative pain | RUNX2 |
| rs11890824 | 2 | 166314399 | A | T | 0,6135 | -0,0242 | 0,0304 | 0,4258 | 0,9823 | Migraine | SCN9A |
| rs12584920 | 13 | 46890902 | G | T | 0,1745 | 0,0308 | 0,0387 | 0,4259 | 0,9823 | Musculoskeletal Pain | HTR2A |
| rs1563826 | 4 | 74369807 | T | A | 0,7827 | -0,0280 | 0,0353 | 0,4271 | 0,9823 | Temporomandibular Disorder | EREG |
| rs11596974 | 10 | 18131455 | G | A | 0,2477 | -0,0264 | 0,0334 | 0,4292 | 0,9823 | Migraine | |
| rs2195450 | 5 | 153491449 | G | A | 0,2392 | 0,0275 | 0,0349 | 0,4297 | 0,9823 | Migraine | GRIA1 |
| rs10888692 | 1 | 50525801 | C | G | 0,3755 | -0,0238 | 0,0302 | 0,4307 | 0,9823 | Other Clinical Pain | FAF1 |
| rs4708592 | 6 | 169109450 | C | T | 0,9317 | -0,0459 | 0,0585 | 0,4324 | 0,9823 | Neuraxial Pain | |
| rs2234918 | 1 | 28863085 | C | T | 0,5425 | 0,0224 | 0,0286 | 0,4343 | 0,9823 | Analgesia | OPRD1 |
| rs8007201 | 14 | 54858130 | A | G | 0,3063 | 0,0249 | 0,0319 | 0,4352 | 0,9823 | Neuraxial Pain | GCH1 |
| rs247889 | 16 | 84449625 | G | A | 0,2803 | -0,0249 | 0,0321 | 0,4368 | 0,9823 | Migraine | ATP2C2 |
| rs672931 | 11 | 30899350 | T | C | 0,6152 | -0,0229 | 0,0294 | 0,4370 | 0,9823 | Migraine | DCDC1 |
| rs2097629 | 9 | 133654578 | A | G | 0,3884 | 0,0236 | 0,0304 | 0,4372 | 0,9823 | Migraine | DBH |
| rs11976703 | 7 | 24509907 | C | A | 0,0600 | 0,0481 | 0,0621 | 0,4387 | 0,9823 | Nociception | |
| rs1946225 | 5 | 152428403 | T | G | 0,1779 | -0,0299 | 0,0386 | 0,4389 | 0,9823 | Migraine | |
| rs871385 | 5 | 136233776 | C | T | 0,4599 | -0,0228 | 0,0294 | 0,4391 | 0,9823 | Migraine | TRPC7-AS2 |
| rs9981408 | 21 | 38645522 | G | T | 0,2027 | 0,0282 | 0,0365 | 0,4396 | 0,9823 | Post-operative pain | ERG |
| rs5748489 | 22 | 19939623 | A | C | 0,5890 | 0,0225 | 0,0291 | 0,4399 | 0,9823 | Temporomandibular Disorder | TXNRD2 |
| rs2075507 | 22 | 19940569 | G | A | 0,5887 | 0,0224 | 0,0291 | 0,4407 | 0,9823 | Neuraxial Pain | COMT |
| rs12901499 | 15 | 67078107 | G | A | 0,4397 | 0,0227 | 0,0295 | 0,4414 | 0,9823 | Arthritis | SMAD3 |
| rs165656 | 22 | 19961340 | G | C | 0,5090 | -0,0226 | 0,0294 | 0,4426 | 0,9823 | Temporomandibular Disorder, Neuraxial Pain, Cancer | COMT |
| rs6574293 | 14 | 76404257 | A | G | 0,9385 | 0,0461 | 0,0603 | 0,4444 | 0,9823 | Temporomandibular Disorder | ESRRB |
| rs2305948 | 4 | 55113391 | C | T | 0,0904 | 0,0394 | 0,0516 | 0,4452 | 0,9823 | Cancer Pain | KDR |
| rs10483636 | 14 | 54334127 | A | G | 0,0318 | 0,0641 | 0,0840 | 0,4454 | 0,9823 | Analgesia | GCH1 |
| rs1550798 | 2 | 154822325 | A | T | 0,5311 | -0,0226 | 0,0298 | 0,4494 | 0,9823 | Temporomandibular Disorder | KCNJ3 |
| rs1800795 | 7 | 22727026 | C | G | 0,6201 | 0,0222 | 0,0293 | 0,4494 | 0,9823 | Analgesia | IL6 |
| rs7798894 | 7 | 21513377 | A | T | 0,7144 | -0,0246 | 0,0326 | 0,4499 | 0,9823 | Other Clinical Pain | SP4 |
| rs11898284 | 2 | 166325017 | A | G | 0,1386 | -0,0323 | 0,0430 | 0,4515 | 0,9823 | Migraine | SCN9A |
| rs858035 | 21 | 37726888 | G | A | 0,7107 | 0,0242 | 0,0321 | 0,4516 | 0,9823 | Analgesia | KCNJ6 |

| | | | | | | | | | | | |
|---|---|---|---|---|---|---|---|---|---|---|---|
| rs858339 | 6 | 131832757 | T | A | 0,2876 | -0,0243 | 0,0323 | 0,4516 | 0,9823 | Temporomandibular Disorder | ENPP1 |
| rs922772 | 8 | 72941326 | C | T | 0,5853 | -0,0223 | 0,0298 | 0,4538 | 0,9823 | Migraine | KCNB2 |
| rs67924081 | 11 | 65575510 | A | G | 0,2491 | 0,0257 | 0,0344 | 0,4542 | 0,9823 | Post-operative pain | EHBP1L1 |
| rs72793414 | 5 | 152448862 | G | A | 0,1779 | -0,0288 | 0,0386 | 0,4559 | 0,9823 | Migraine | |
| rs1391950 | 3 | 7016730 | T | C | 0,4859 | -0,0216 | 0,0290 | 0,4579 | 0,9823 | Migraine | GRM7 |
| rs3211371 | 19 | 41016810 | C | T | 0,1053 | -0,0348 | 0,0469 | 0,4583 | 0,9823 | Cancer Pain | CYP2B6 |
| rs4910165 | 11 | 10652497 | C | G | 0,6621 | 0,0229 | 0,0309 | 0,4584 | 0,9823 | Migraine | IRAG1 |
| rs140174 | 22 | 23580796 | A | G | 0,2730 | -0,0245 | 0,0331 | 0,4590 | 0,9823 | Migraine | |
| rs464049 | 5 | 1423790 | A | G | 0,4315 | -0,0216 | 0,0293 | 0,4594 | 0,9823 | Neuropathic pain | SLC6A3 |
| rs963218 | 7 | 34672157 | G | A | 0,4587 | -0,0217 | 0,0296 | 0,4629 | 0,9823 | Other Clinical Pain | NPSR1 |
| rs10194315 | 2 | 219980900 | C | T | 0,3454 | 0,0226 | 0,0308 | 0,4630 | 0,9823 | Post-operative pain | LOC105373891 |
| rs10814130 | 9 | 34637994 | C | A | 0,1677 | 0,0284 | 0,0387 | 0,4630 | 0,9823 | Nociception | |
| rs400922 | 16 | 84472761 | C | G | 0,2003 | -0,0271 | 0,0370 | 0,4641 | 0,9823 | Migraine | |
| rs1718119 | 12 | 121177300 | G | A | 0,3790 | 0,0214 | 0,0293 | 0,4661 | 0,9823 | Neuropathic Pain | P2RX7 |
| rs5498 | 19 | 10285007 | A | G | 0,4341 | 0,0215 | 0,0295 | 0,4663 | 0,9823 | Migraine | ICAM1 |
| rs1406846 | 6 | 45433203 | T | A | 0,4925 | -0,0215 | 0,0295 | 0,4666 | 0,9823 | Arthritis | RUNX2 |
| rs10774912 | 12 | 109825003 | T | C | 0,2749 | 0,0235 | 0,0323 | 0,4674 | 0,9823 | Migraine | TRPV4 |
| rs10797923 | 1 | 183932832 | T | C | 0,2825 | -0,0233 | 0,0322 | 0,4687 | 0,9823 | Post-operative pain | COLGALT2 |
| rs4957810 | 5 | 109338561 | C | T | 0,1274 | -0,0314 | 0,0434 | 0,4700 | 0,9823 | Post-operative pain | PJA2 |
| rs10925252 | 1 | 236859062 | T | C | 0,4020 | 0,0216 | 0,0300 | 0,4719 | 0,9823 | Migraine | MTR |
| rs174697 | 22 | 19966309 | A | G | 0,9614 | 0,0547 | 0,0761 | 0,4723 | 0,9823 | Temporomandibular Disorder | COMT |
| rs12622743 | 2 | 166337881 | A | G | 0,1393 | -0,0308 | 0,0428 | 0,4725 | 0,9823 | Migraine | SCN9A |
| rs111844273 | 7 | 18396714 | G | A | 0,0236 | 0,0694 | 0,0968 | 0,4737 | 0,9823 | Arthritis | HDAC9 |
| rs10950641 | 7 | 2294751 | G | A | 0,0408 | -0,0530 | 0,0748 | 0,4782 | 0,9823 | Neuropathic pain | SNX8 |
| rs1799964 | 6 | 31574531 | T | C | 0,1060 | -0,0333 | 0,0470 | 0,4787 | 0,9823 | Cancer Pain | |
| rs1048101 | 8 | 26770511 | A | G | 0,4446 | 0,0206 | 0,0290 | 0,4789 | 0,9823 | Fibromyalgia | ADRA1A |
| rs2363561 | 1 | 215081964 | T | C | 0,5788 | 0,0205 | 0,0289 | 0,4789 | 0,9823 | Temporomandibular Disorder | KCNK2 |
| rs10132091 | 14 | 76404475 | T | C | 0,3785 | 0,0213 | 0,0301 | 0,4799 | 0,9823 | Temporomandibular Disorder | ESRRB |
| rs2275565 | 1 | 236885376 | G | T | 0,1959 | -0,0257 | 0,0366 | 0,4828 | 0,9823 | Migraine | MTR |
| rs3918226 | 7 | 150993088 | C | T | 0,0877 | -0,0370 | 0,0528 | 0,4829 | 0,9823 | Migraine | NOS3 |
| rs6853 | 3 | 38142879 | A | G | 0,1422 | 0,0291 | 0,0416 | 0,4840 | 0,9823 | Analgesia | MYD88 |
| rs138556413 | 2 | 202968144 | C | T | 0,0401 | -0,0518 | 0,0740 | 0,4843 | 0,9823 | Migraine | CARF |
| rs66989638 | 2 | 106073280 | G | A | 0,1279 | -0,0308 | 0,0442 | 0,4860 | 0,9823 | Post-operative pain | C2orf40 |
| rs934287 | 2 | 202843584 | A | G | 0,8257 | -0,0267 | 0,0384 | 0,4863 | 0,9823 | Migraine | ICA1L |
| rs60249166 | 13 | 31510764 | C | T | 0,1767 | -0,0267 | 0,0384 | 0,4870 | 0,9823 | Temporomandibular Disorder | |
| rs13260 | 13 | 110149776 | G | T | 0,1026 | 0,0336 | 0,0484 | 0,4873 | 0,9823 | Migraine | COL4A1 |
| rs2651899 | 1 | 3167148 | T | C | 0,4436 | 0,0204 | 0,0294 | 0,4873 | 0,9823 | Migraine | LOC105378606 |
| rs13290757 | 9 | 126166159 | C | T | 0,1298 | -0,0297 | 0,0429 | 0,4889 | 0,9823 | Migraine | |
| rs4633 | 22 | 19962712 | C | T | 0,5044 | -0,0203 | 0,0293 | 0,4891 | 0,9823 | Nociception, Temporomandibular Disorder, Fibromya | COMT |
| rs7412 | 19 | 44908822 | C | T | 0,0668 | 0,0403 | 0,0584 | 0,4900 | 0,9823 | Fibromyalgia | APOE |
| rs17172526 | 7 | 35944418 | G | A | 0,0846 | -0,0365 | 0,0528 | 0,4900 | 0,9823 | Migraine | |
| rs7814941 | 8 | 129706613 | A | G | 0,1930 | 0,0255 | 0,0369 | 0,4901 | 0,9823 | Neuraxial pain | GSDMC |
| rs7753655 | 6 | 49568851 | A | G | 0,2795 | -0,0225 | 0,0327 | 0,4907 | 0,9823 | Migraine | |
| rs10850830 | 12 | 109834094 | C | T | 0,4937 | -0,0202 | 0,0294 | 0,4920 | 0,9823 | Migraine | TRPV4 |
| rs734784 | 20 | 45094986 | T | C | 0,4592 | 0,0204 | 0,0297 | 0,4925 | 0,9823 | Neuropathic Pain | KCNS1 |
| rs2530566 | 7 | 34665211 | A | G | 0,4908 | -0,0200 | 0,0292 | 0,4925 | 0,9823 | Other Clinical Pain | NPSR1-AS1 |

| | | | | | | | | | | | |
|---|---|---|---|---|---|---|---|---|---|---|---|
| rs7911 | 1 | 89052437 | A | G | 0,3712 | -0,0206 | 0,0301 | 0,4931 | 0,9823 | Fibromyalgia | LOC105378841 |
| rs62327819 | 4 | 146289989 | C | T | 0,6818 | 0,0220 | 0,0321 | 0,4932 | 0,9823 | Neuraxial pain | SLC10A7 |
| rs6336 | 1 | 156879126 | C | T | 0,0510 | 0,0451 | 0,0660 | 0,4939 | 0,9823 | Post-operative Pain | NTRK1 |
| rs2383515 | 1 | 186683820 | G | T | 0,1825 | -0,0259 | 0,0378 | 0,4941 | 0,9823 | Other Clinical Pain | PTGS2 |
| rs11599236 | 10 | 104694914 | T | C | 0,4699 | -0,0195 | 0,0286 | 0,4943 | 0,9823 | Other Clinical Pain | SORCS3 |
| rs2203834 | 8 | 12967384 | A | C | 0,8690 | -0,0297 | 0,0435 | 0,4952 | 0,9823 | Migraine | TRMT9B |
| rs1611115 | 9 | 133635393 | T | C | 0,7778 | 0,0238 | 0,0350 | 0,4954 | 0,9823 | Migraine | |
| rs10770367 | 12 | 18510988 | C | A | 0,3398 | 0,0210 | 0,0309 | 0,4959 | 0,9823 | Cancer Pain | PIK3C2G |
| rs74676797 | 2 | 633063 | G | A | 0,8257 | -0,0257 | 0,0378 | 0,4961 | 0,9823 | Arthritis | TMEM18 |
| rs12415832 | 10 | 119352815 | C | A | 0,0202 | -0,0714 | 0,1051 | 0,4968 | 0,9823 | Temporomandibular Disorder | GRK5 |
| rs11849538 | 14 | 95709641 | C | G | 0,1145 | -0,0308 | 0,0455 | 0,4979 | 0,9823 | Musculoskeletal Pain | TCL1A |
| rs6473799 | 8 | 53240563 | A | G | 0,2649 | 0,0221 | 0,0326 | 0,4980 | 0,9823 | Nociception | OPRK1 |
| rs12667224 | 7 | 114384261 | G | A | 0,5649 | -0,0198 | 0,0293 | 0,4997 | 0,9823 | Arthritis | FOXP2 |
| rs1800866 | 9 | 34637693 | T | G | 0,1689 | 0,0260 | 0,0387 | 0,5015 | 0,9823 | Nociception | SIGMAR1 |
| rs887797 | 17 | 66583327 | G | A | 0,3330 | 0,0205 | 0,0306 | 0,5033 | 0,9823 | Neuropathic Pain | PRKCA |
| rs3754255 | 1 | 236846557 | C | T | 0,4273 | 0,0199 | 0,0298 | 0,5043 | 0,9823 | Migraine | MTR |
| rs5993875 | 22 | 19927803 | A | G | 0,5877 | 0,0195 | 0,0292 | 0,5045 | 0,9823 | Temporomandibular Disorder | TXNRD2 |
| rs13263568 | 8 | 71535183 | T | G | 0,0836 | 0,0349 | 0,0524 | 0,5053 | 0,9823 | Migraine | SUV39H2 |
| rs11984666 | 8 | 129718034 | C | A | 0,1915 | 0,0247 | 0,0371 | 0,5056 | 0,9823 | Post-operative pain | RP11-274M4.1 |
| rs151058 | 21 | 26939253 | T | C | 0,8286 | -0,0261 | 0,0394 | 0,5086 | 0,9823 | Neuraxial Pain | ADAMTS5 |
| rs34884997 | 1 | 161191082 | T | C | 0,1519 | 0,0272 | 0,0411 | 0,5090 | 0,9823 | Neuraxial Pain | ADAMTS4 |
| rs3094117 | 6 | 30769709 | A | C | 0,1242 | 0,0294 | 0,0446 | 0,5096 | 0,9823 | Migraine | SUV39H2 |
| rs2542424 | 8 | 139620258 | T | C | 0,4358 | 0,0195 | 0,0296 | 0,5101 | 0,9823 | Post-operative Pain | KCNK9 |
| rs634479 | 6 | 154043305 | A | G | 0,2139 | -0,0232 | 0,0352 | 0,5103 | 0,9823 | Post-operative Pain | OPRM1 |
| rs4680 | 22 | 19963748 | G | A | 0,5032 | -0,0193 | 0,0294 | 0,5103 | 0,9823 | Nociception, Temporomandibular Disorder, Analgesia | COMT |
| rs1076292 | 7 | 30673085 | C | G | 0,6245 | -0,0201 | 0,0306 | 0,5107 | 0,9823 | Temporomandibular Disorder | CRHR2 |
| rs7322347 | 13 | 46835968 | T | A | 0,4584 | 0,0191 | 0,0290 | 0,5113 | 0,9823 | Cancer Pain | HTR2A |
| rs165722 | 22 | 19961490 | C | T | 0,5058 | -0,0193 | 0,0294 | 0,5116 | 0,9823 | Analgesia, Temporomandibular Disorder | COMT |
| rs11846556 | 14 | 41713822 | G | A | 0,4932 | -0,0190 | 0,0290 | 0,5124 | 0,9823 | Other Clinical Pain | LRFN5 |
| rs4814864 | 20 | 19489173 | G | C | 0,2703 | -0,0215 | 0,0328 | 0,5136 | 0,9823 | Migraine | SLC24A3 |
| rs7640543 | 3 | 30420911 | G | A | 0,3077 | -0,0205 | 0,0315 | 0,5146 | 0,9823 | Migraine | LOC105377013 |
| rs17376373 | 7 | 120360431 | T | G | 0,2455 | -0,0219 | 0,0337 | 0,5147 | 0,9823 | Post-operative Pain | KCND2 |
| rs900414 | 15 | 101314378 | A | G | 0,3284 | -0,0198 | 0,0304 | 0,5150 | 0,9823 | Musculoskeletal Pain | PCSK6 |
| rs3180 | 10 | 72060864 | A | G | 0,5605 | 0,0196 | 0,0301 | 0,5158 | 0,9823 | Neuraxial pain | SPOCK2 |
| rs1176744 | 11 | 113932306 | A | C | 0,3294 | -0,0204 | 0,0315 | 0,5169 | 0,9823 | Analgesia | HTR3B |
| rs12537376 | 7 | 114384998 | A | G | 0,4334 | -0,0189 | 0,0293 | 0,5176 | 0,9823 | Other Clinical Pain | FOXP2 |
| rs6670661 | 1 | 215227100 | G | A | 0,5544 | -0,0188 | 0,0291 | 0,5181 | 0,9823 | Migraine | KCNK2 |
| rs13276133 | 8 | 72943025 | A | C | 0,3712 | -0,0198 | 0,0306 | 0,5182 | 0,9823 | Migraine | KCNB2 |
| rs16023 | 19 | 13298658 | T | A | 0,1670 | -0,0254 | 0,0393 | 0,5182 | 0,9823 | Migraine | CACNA1A |
| rs3024498 | 1 | 206768184 | T | C | 0,2195 | 0,0225 | 0,0349 | 0,5190 | 0,9823 | Post-operative Pain | IL19 |
| rs4300189 | 1 | 215113078 | A | G | 0,7506 | -0,0211 | 0,0328 | 0,5207 | 0,9823 | Migraine | KCNK2 |
| rs1128503 | 7 | 87550285 | A | G | 0,5707 | 0,0191 | 0,0299 | 0,5226 | 0,9823 | Analgesia | ABCB1 |
| rs7867868 | 9 | 74831958 | C | T | 0,3670 | 0,0190 | 0,0300 | 0,5251 | 0,9823 | Migraine | TRPM6 |
| rs7217270 | 17 | 3518181 | A | G | 0,5372 | 0,0188 | 0,0296 | 0,5262 | 0,9823 | Migraine | TRPV3 |
| rs344781 | 19 | 43670636 | C | T | 0,7611 | 0,0216 | 0,0341 | 0,5264 | 0,9823 | Migraine | |
| rs9835230 | 3 | 190017672 | G | A | 0,2426 | -0,0215 | 0,0340 | 0,5265 | 0,9823 | Arthritis | LEPREL1 |

| | | | | | | | | | | | |
|---|---|---|---|---|---|---|---|---|---|---|---|
| rs11563056 | 2 | 233992526 | T | G | 0,3393 | 0,0196 | 0,0309 | 0,5270 | 0,9823 | Migraine | TRPM8 |
| rs12722 | 9 | 134842570 | C | T | 0,5836 | 0,0187 | 0,0296 | 0,5272 | 0,9823 | Other Clinical Pain | LOC101448202 |
| rs3804100 | 4 | 153704257 | T | C | 0,0651 | -0,0375 | 0,0594 | 0,5279 | 0,9823 | Analgesia | TLR2 |
| rs11166921 | 8 | 139695512 | A | C | 0,6135 | 0,0191 | 0,0303 | 0,5281 | 0,9823 | Cancer Pain | KCNK9 |
| rs3741559 | 12 | 49951193 | G | A | 0,1937 | -0,0231 | 0,0367 | 0,5285 | 0,9823 | Temporomandibular disorders | AQP2 |
| rs6795970 | 3 | 38725184 | A | G | 0,5839 | 0,0184 | 0,0292 | 0,5290 | 0,9823 | Nociception | SCN10A |
| rs226794 | 21 | 26930036 | A | G | 0,8957 | 0,0298 | 0,0474 | 0,5300 | 0,9823 | Neuraxial Pain | ADAMTS5 |
| rs6572493 | 14 | 22503969 | A | G | 0,5907 | -0,0186 | 0,0296 | 0,5306 | 0,9823 | Cancer Pain | LOC112267867 |
| rs7439087 | 4 | 47394983 | T | C | 0,3461 | -0,0196 | 0,0312 | 0,5306 | 0,9823 | Neuraxial Pain | GABRB1 |
| rs11782118 | 8 | 72937968 | G | A | 0,3945 | -0,0189 | 0,0303 | 0,5314 | 0,9823 | Migraine | KCNB2 |
| rs1042114 | 1 | 28812463 | G | T | 0,8824 | -0,0284 | 0,0457 | 0,5337 | 0,9823 | Nociception | OPRD1 |
| rs3769671 | 2 | 25167284 | A | C | 0,0335 | 0,0507 | 0,0817 | 0,5345 | 0,9823 | Musculoskeletal Pain | POMC |
| rs11594111 | 10 | 14903407 | A | G | 0,1264 | 0,0270 | 0,0435 | 0,5348 | 0,9823 | Migraine | SUV39H2 |
| rs7965399 | 12 | 102497908 | T | C | 0,0428 | 0,0450 | 0,0726 | 0,5353 | 0,9823 | Cancer Pain | LOC105369944 |
| rs4694846 | 4 | 47366781 | T | C | 0,4490 | 0,0181 | 0,0293 | 0,5353 | 0,9823 | Neuraxial Pain | GABRB1 |
| rs20417 | 1 | 186681189 | C | G | 0,1828 | -0,0234 | 0,0378 | 0,5357 | 0,9823 | Migraine | PACERR |
| rs2078371 | 1 | 115134562 | T | C | 0,1053 | -0,0293 | 0,0474 | 0,5361 | 0,9823 | Migraine | |
| rs9952528 | 18 | 6453862 | T | C | 0,8393 | -0,0241 | 0,0392 | 0,5389 | 0,9823 | Other Clinical Pain | |
| rs10413396 | 19 | 44309549 | G | T | 0,0457 | 0,0424 | 0,0690 | 0,5394 | 0,9823 | Analgesia | |
| rs12908498 | 15 | 67074150 | C | G | 0,4473 | 0,0181 | 0,0296 | 0,5395 | 0,9823 | Arthritis | SMAD3 |
| rs1560080 | 5 | 116003035 | G | A | 0,8021 | -0,0222 | 0,0362 | 0,5400 | 0,9823 | Arthritis | AQPEP |
| rs974819 | 11 | 103789839 | T | C | 0,6998 | 0,0197 | 0,0322 | 0,5405 | 0,9823 | Migraine | |
| rs548294 | 5 | 153488877 | T | C | 0,5994 | -0,0184 | 0,0301 | 0,5414 | 0,9823 | Migraine | |
| rs6668344 | 1 | 236838026 | C | T | 0,4045 | 0,0183 | 0,0300 | 0,5423 | 0,9823 | Migraine | MTR |
| rs4663994 | 2 | 233982284 | C | G | 0,3534 | 0,0188 | 0,0308 | 0,5424 | 0,9823 | Migraine | TRPM8 |
| rs3745274 | 19 | 41006936 | G | T | 0,2547 | 0,0207 | 0,0340 | 0,5437 | 0,9823 | Cancer Pain | CYP2B6 |
| rs2070744 | 7 | 150992991 | C | T | 0,5909 | 0,0182 | 0,0299 | 0,5437 | 0,9823 | Neuraxial Pain | NOS3 |
| rs2229741 | 21 | 14967968 | C | T | 0,4220 | -0,0180 | 0,0297 | 0,5439 | 0,9823 | Migraine | NRIP1 |
| rs3750625 | 10 | 111079843 | C | A | 0,0554 | 0,0384 | 0,0634 | 0,5449 | 0,9823 | Musculoskeletal Pain | ADRA2A |
| rs1801252 | 10 | 114044277 | A | G | 0,1300 | -0,0259 | 0,0427 | 0,5449 | 0,9823 | Analgesia | ADRB1 |
| rs302673 | 2 | 237886960 | A | G | 0,6495 | -0,0183 | 0,0303 | 0,5468 | 0,9823 | Migraine | RAMP1 |
| rs854560 | 7 | 95316772 | A | T | 0,3556 | -0,0185 | 0,0308 | 0,5471 | 0,9823 | Migraine | PON1 |
| rs7757130 | 6 | 112996060 | C | A | 0,0676 | 0,0352 | 0,0587 | 0,5486 | 0,9823 | Analgesia | LOC105377951 |
| rs8128316 | 21 | 34349261 | C | T | 0,4759 | -0,0176 | 0,0293 | 0,5494 | 0,9823 | Migraine | |
| rs806368 | 6 | 88140381 | T | C | 0,2163 | 0,0207 | 0,0346 | 0,5495 | 0,9823 | Migraine | CNR1 |
| rs1678626 | 10 | 72066577 | T | C | 0,5481 | 0,0179 | 0,0299 | 0,5502 | 0,9823 | Neuraxial pain | SPOCK2 |
| rs2562456 | 19 | 21483408 | C | T | 0,7557 | -0,0202 | 0,0339 | 0,5503 | 0,9823 | Analgesia | |
| rs11598027 | 10 | 18471706 | C | T | 0,1225 | 0,0265 | 0,0444 | 0,5504 | 0,9823 | Migraine | CACNB2 |
| rs6426929 | 1 | 154778513 | G | A | 0,4939 | 0,0174 | 0,0292 | 0,5510 | 0,9823 | Migraine | KCNN3 |
| rs1042838 | 11 | 101062681 | C | A | 0,1471 | 0,0243 | 0,0408 | 0,5513 | 0,9823 | Migraine | PGR |
| rs1465040 | 4 | 122007101 | T | C | 0,7210 | 0,0194 | 0,0326 | 0,5517 | 0,9823 | Analgesia | |
| rs11758298 | 6 | 45917961 | C | T | 0,1373 | 0,0252 | 0,0424 | 0,5521 | 0,9823 | Migraine | LOC105375078 |
| rs909253 | 6 | 31572536 | A | G | 0,2005 | -0,0213 | 0,0360 | 0,5530 | 0,9823 | Migraine | LOC100287329 |
| rs946188 | 20 | 4234669 | A | G | 0,2608 | -0,0193 | 0,0326 | 0,5540 | 0,9823 | Temporomandibular Disorder | ADRA1D |
| rs12138911 | 1 | 236813843 | T | C | 0,1723 | -0,0227 | 0,0384 | 0,5540 | 0,9823 | Migraine | MTR |
| rs55933916 | 21 | 26966104 | C | G | 0,2005 | 0,0213 | 0,0360 | 0,5542 | 0,9823 | Neuraxial Pain | ADAMTS5 |

| | | | | | | | | | | | |
|---|---|---|---|---|---|---|---|---|---|---|---|
| rs247820 | 16 | 84411831 | T | C | 0,4514 | 0,0173 | 0,0292 | 0,5546 | 0,9823 | Migraine | ATP2C2 |
| rs12229394 | 12 | 71999134 | G | A | 0,2513 | -0,0198 | 0,0335 | 0,5546 | 0,9823 | Migraine | TPH2 |
| rs3856087 | 1 | 181455397 | G | A | 0,3673 | -0,0179 | 0,0304 | 0,5556 | 0,9823 | Migraine | CACNA1E |
| rs7577262 | 2 | 233910224 | G | A | 0,1162 | 0,0272 | 0,0462 | 0,5562 | 0,9823 | Migraine | |
| rs2779249 | 17 | 27801555 | C | A | 0,3247 | -0,0182 | 0,0310 | 0,5567 | 0,9823 | Migraine | NOS2 |
| rs361525 | 6 | 31575324 | G | A | 0,0202 | 0,0616 | 0,1050 | 0,5572 | 0,9823 | Other Clinical Pain | |
| rs179971 | 6 | 16362511 | C | T | 0,7341 | -0,0191 | 0,0326 | 0,5583 | 0,9823 | Analgesia | ATXN1 |
| rs2363556 | 1 | 215158420 | G | C | 0,7526 | -0,0193 | 0,0329 | 0,5587 | 0,9823 | Migraine | KCNK2 |
| rs222749 | 17 | 3592080 | G | A | 0,0496 | 0,0396 | 0,0677 | 0,5590 | 0,9823 | Migraine | TRPV1 |
| rs10895275 | 11 | 102212877 | T | A | 0,3408 | 0,0181 | 0,0311 | 0,5606 | 0,9823 | Migraine | YAP1 |
| rs1611131 | 9 | 133657065 | A | G | 0,3007 | 0,0187 | 0,0322 | 0,5615 | 0,9823 | Migraine | DBH-AS1 |
| rs4286289 | 2 | 166305201 | C | A | 0,7273 | -0,0191 | 0,0331 | 0,5626 | 0,9823 | Analgesia | SCN9A |
| rs7824175 | 8 | 53231614 | C | G | 0,0897 | 0,0300 | 0,0518 | 0,5629 | 0,9823 | Nociception | OPRK1 |
| rs1443914 | 13 | 53343095 | T | C | 0,5224 | 0,0170 | 0,0295 | 0,5641 | 0,9823 | Other Clinical Pain | |
| rs72979233 | 11 | 74644478 | A | G | 0,2491 | -0,0194 | 0,0336 | 0,5643 | 0,9823 | Post-operative pain | POLD3 |
| rs6796803 | 3 | 186746318 | T | C | 0,7450 | 0,0187 | 0,0327 | 0,5676 | 0,9823 | Neuropathic pain | |
| rs9671371 | 14 | 54861917 | C | T | 0,2842 | 0,0185 | 0,0326 | 0,5695 | 0,9823 | Neuraxial Pain | GCH1 |
| rs887200 | 22 | 19976143 | C | T | 0,8952 | 0,0268 | 0,0472 | 0,5697 | 0,9823 | Nociception | ARVCF |
| rs7068341 | 10 | 16592300 | C | T | 0,1138 | 0,0262 | 0,0461 | 0,5705 | 0,9823 | Migraine | SUV39H2 |
| rs5443 | 12 | 6845711 | C | T | 0,3177 | 0,0179 | 0,0316 | 0,5716 | 0,9823 | Other Clinical Pain | CDCA3 |
| rs806369 | 6 | 88146459 | T | C | 0,6646 | -0,0175 | 0,0310 | 0,5725 | 0,9823 | Migraine | CNR1 |
| rs2275913 | 6 | 52186235 | G | A | 0,3323 | -0,0174 | 0,0308 | 0,5729 | 0,9823 | Arthritis | |
| rs1879234 | 19 | 21521677 | T | G | 0,7635 | -0,0194 | 0,0347 | 0,5750 | 0,9823 | Analgesia | ZNF429 |
| rs2562408 | 19 | 21527079 | C | G | 0,7635 | -0,0194 | 0,0347 | 0,5750 | 0,9823 | Analgesia | ZNF429 |
| rs2562466 | 19 | 21531402 | C | T | 0,7635 | -0,0194 | 0,0347 | 0,5750 | 0,9823 | Analgesia | |
| rs1420100 | 2 | 102420542 | C | A | 0,5041 | -0,0164 | 0,0293 | 0,5751 | 0,9823 | Neuraxial Pain | IL18RAP |
| rs2276008 | 22 | 21759747 | G | C | 0,0416 | -0,0403 | 0,0719 | 0,5756 | 0,9823 | Temporomandibular Disorder | MAPK1 |
| rs174680 | 22 | 19947476 | T | C | 0,7265 | -0,0184 | 0,0329 | 0,5758 | 0,9823 | Analgesia | COMT |
| rs1800629 | 6 | 31575254 | G | A | 0,0788 | -0,0298 | 0,0533 | 0,5760 | 0,9823 | Migraine | |
| rs17461905 | 4 | 47367048 | T | C | 0,1245 | 0,0247 | 0,0442 | 0,5761 | 0,9823 | Neuraxial Pain | GABRB1 |
| rs6280 | 3 | 114171968 | C | T | 0,6677 | -0,0175 | 0,0313 | 0,5764 | 0,9823 | Nociception | DRD3 |
| rs6035355 | 20 | 19484445 | T | A | 0,2914 | -0,0179 | 0,0321 | 0,5778 | 0,9823 | Migraine | SLC24A3 |
| rs6986153 | 8 | 107059816 | G | A | 0,7790 | 0,0197 | 0,0354 | 0,5778 | 0,9823 | Neuropathic Pain | |
| rs2066928 | 5 | 30843680 | A | G | 0,5160 | -0,0162 | 0,0292 | 0,5786 | 0,9823 | Arthritis | RPL19P11 |
| rs4903419 | 14 | 76518312 | A | G | 0,1330 | 0,0239 | 0,0431 | 0,5793 | 0,9823 | Temporomandibular Disorder | ESRRB |
| rs228648 | 1 | 7853370 | G | A | 0,6009 | 0,0163 | 0,0294 | 0,5793 | 0,9823 | Migraine | UTS2 |
| rs1556905 | 1 | 215188249 | C | A | 0,4356 | 0,0159 | 0,0288 | 0,5801 | 0,9823 | Migraine | KCNK2 |
| rs12996816 | 2 | 17863421 | C | T | 0,1386 | 0,0232 | 0,0420 | 0,5801 | 0,9823 | Migraine | |
| rs1531554 | 17 | 81406747 | T | C | 0,5350 | 0,0163 | 0,0295 | 0,5803 | 0,9823 | Temporomandibular Disorder | BAHCC1 |
| rs255097 | 7 | 30687343 | G | A | 0,5868 | -0,0163 | 0,0297 | 0,5830 | 0,9823 | Temporomandibular Disorder | CRHR2 |
| rs1105794 | 18 | 6451335 | G | A | 0,8401 | -0,0214 | 0,0393 | 0,5858 | 0,9823 | Other Clinical Pain | |
| rs4479336 | 18 | 6451516 | C | T | 0,8401 | -0,0214 | 0,0393 | 0,5858 | 0,9823 | Other Clinical Pain | |
| rs6506387 | 18 | 6451940 | C | T | 0,8401 | -0,0214 | 0,0393 | 0,5858 | 0,9823 | Other Clinical Pain | |
| rs4798443 | 18 | 6452945 | C | T | 0,8401 | -0,0214 | 0,0393 | 0,5858 | 0,9823 | Other Clinical Pain | |
| rs10282983 | 8 | 68678319 | C | T | 0,2389 | -0,0184 | 0,0339 | 0,5869 | 0,9823 | Post-operative pain | C8orf34 |
| rs499796 | 6 | 154051557 | A | G | 0,2156 | -0,0190 | 0,0351 | 0,5874 | 0,9823 | Post-operative Pain | OPRM1 |

| | | | | | | | | | | | |
|---|---|---|---|---|---|---|---|---|---|---|---|
| rs419335 | 1 | 28825332 | A | G | 0,3595 | 0,0162 | 0,0300 | 0,5892 | 0,9823 | Analgesia | OPRD1 |
| rs13135092 | 4 | 102276925 | A | G | 0,0771 | -0,0296 | 0,0549 | 0,5897 | 0,9823 | Other Clinical Pain | SLC39A8 |
| rs7287604 | 22 | 19928157 | C | T | 0,2005 | -0,0195 | 0,0363 | 0,5910 | 0,9823 | Temporomandibular Disorder | TXNRD2 |
| rs7290448 | 22 | 19928416 | G | A | 0,2005 | -0,0195 | 0,0363 | 0,5910 | 0,9823 | Temporomandibular Disorder | TXNRD2 |
| rs4380013 | 15 | 50467231 | G | A | 0,2234 | 0,0188 | 0,0352 | 0,5925 | 0,9823 | Arthritis | USP8 |
| rs2097903 | 7 | 10642782 | A | T | 0,4903 | 0,0155 | 0,0289 | 0,5929 | 0,9823 | Fibromyalgia | MGC4859 |
| rs10843013 | 12 | 27872263 | A | C | 0,2071 | -0,0190 | 0,0356 | 0,5929 | 0,9823 | Post-operative pain | RP11-993B23.1 |
| rs8060725 | 16 | 84780547 | C | A | 0,3004 | 0,0169 | 0,0316 | 0,5933 | 0,9823 | Migraine | |
| rs11030064 | 11 | 27596469 | C | T | 0,5297 | 0,0155 | 0,0290 | 0,5936 | 0,9823 | Neuraxial pain | BDNF-AS |
| rs6479874 | 10 | 51029595 | T | C | 0,8634 | -0,0232 | 0,0434 | 0,5938 | 0,9823 | Migraine | SUV39H2 |
| rs11214796 | 11 | 113983957 | C | T | 0,7812 | 0,0190 | 0,0356 | 0,5940 | 0,9823 | Cancer Pain | HTR3A |
| rs2963155 | 5 | 143376439 | A | G | 0,2200 | 0,0186 | 0,0349 | 0,5946 | 0,9823 | Temporomandibular Disorder | NR3C1 |
| rs10997517 | 10 | 67120045 | T | C | 0,1429 | -0,0216 | 0,0406 | 0,5948 | 0,9823 | Migraine | SUV39H2 |
| rs5993883 | 22 | 19950115 | T | G | 0,5571 | 0,0153 | 0,0288 | 0,5951 | 0,9823 | Temporomandibular Disorder | COMT |
| rs8136867 | 22 | 21850504 | G | A | 0,5727 | -0,0156 | 0,0295 | 0,5958 | 0,9823 | Cancer Pain | MAPK1 |
| rs12260159 | 10 | 98942980 | G | A | 0,0994 | 0,0255 | 0,0480 | 0,5959 | 0,9823 | Migraine | HPSE2 |
| rs6598163 | 12 | 131840694 | G | A | 0,5000 | 0,0151 | 0,0286 | 0,5969 | 0,9823 | Migraine | MMP17 |
| rs12071912 | 1 | 243078312 | C | T | 0,3333 | -0,0160 | 0,0303 | 0,5976 | 0,9823 | Other Clinical Pain | LINC01347 |
| rs2367707 | 4 | 74382717 | A | G | 0,7985 | -0,0192 | 0,0365 | 0,5980 | 0,9823 | Temporomandibular Disorder | EREG |
| rs7894047 | 10 | 16803854 | A | T | 0,0335 | -0,0416 | 0,0796 | 0,6012 | 0,9823 | Post-operative pain | RSU1 |
| rs12160491 | 22 | 37799789 | A | G | 0,3330 | -0,0162 | 0,0310 | 0,6018 | 0,9823 | Arthritis, Post-operative pain | H1F0 |
| rs2506142 | 10 | 33179196 | A | G | 0,1940 | -0,0193 | 0,0373 | 0,6054 | 0,9823 | Migraine | NRP1 |
| rs7532286 | 1 | 154778340 | C | A | 0,4949 | 0,0151 | 0,0293 | 0,6055 | 0,9823 | Migraine | KCNN3 |
| rs5751862 | 22 | 24406596 | G | A | 0,4545 | -0,0152 | 0,0294 | 0,6063 | 0,9823 | Migraine | ADORA2A-AS1 |
| rs7212908 | 17 | 61577232 | A | G | 0,2154 | 0,0179 | 0,0351 | 0,6100 | 0,9823 | Post-operative pain | NACA2 |
| rs224446 | 12 | 50987935 | C | T | 0,1573 | -0,0204 | 0,0400 | 0,6105 | 0,9823 | Neuropathic Pain | SLC11A2 |
| rs9646772 | 2 | 166306689 | A | T | 0,6332 | -0,0157 | 0,0309 | 0,6106 | 0,9823 | Post-operative Pain | SCN9A |
| rs2151423 | 9 | 74791089 | A | G | 0,4220 | -0,0152 | 0,0298 | 0,6110 | 0,9823 | Migraine | TRPM6 |
| rs11031005 | 11 | 30204809 | T | C | 0,1422 | 0,0214 | 0,0424 | 0,6131 | 0,9823 | Migraine | ARL14EP-DT |
| rs11031006 | 11 | 30204981 | G | A | 0,1422 | 0,0214 | 0,0424 | 0,6131 | 0,9823 | Migraine | ARL14EP-DT |
| rs1321917 | 9 | 116562650 | G | C | 0,4042 | 0,0150 | 0,0296 | 0,6135 | 0,9823 | Post-operative pain | ASTN2 |
| rs2531840 | 7 | 34678911 | G | A | 0,4047 | -0,0152 | 0,0301 | 0,6138 | 0,9823 | Other Clinical Pain | NPSR1 |
| rs1051312 | 20 | 10306440 | T | C | 0,2703 | 0,0166 | 0,0330 | 0,6150 | 0,9823 | Fibromyalgia | SNAP25 |
| rs1566652 | 16 | 55697663 | G | T | 0,3717 | -0,0153 | 0,0304 | 0,6155 | 0,9823 | Neuropathic pain | SLC6A2 |
| rs7696139 | 4 | 3774521 | G | C | 0,7611 | 0,0174 | 0,0348 | 0,6164 | 0,9823 | Temporomandibular Disorder | |
| rs12134493 | 1 | 115135325 | C | A | 0,1045 | -0,0237 | 0,0475 | 0,6182 | 0,9823 | Migraine | |
| rs2052692 | 11 | 10646094 | A | G | 0,6619 | 0,0154 | 0,0310 | 0,6183 | 0,9823 | Migraine | IRAG1 |
| rs1518111 | 1 | 206771300 | T | C | 0,7722 | -0,0173 | 0,0347 | 0,6184 | 0,9823 | Post-operative Pain | IL19 |
| rs1518110 | 1 | 206771516 | A | C | 0,7722 | -0,0173 | 0,0347 | 0,6184 | 0,9823 | Post-operative Pain | IL19 |
| rs6290 | 4 | 47406821 | C | T | 0,0727 | 0,0281 | 0,0565 | 0,6185 | 0,9823 | Neuraxial Pain | GABRB1 |
| rs4778889 | 15 | 81296654 | T | C | 0,2032 | -0,0178 | 0,0358 | 0,6185 | 0,9823 | Other Clinical Pain | IL16 |
| rs165728 | 22 | 19969500 | C | T | 0,9597 | 0,0369 | 0,0742 | 0,6191 | 0,9823 | Analgesia | COMT |
| rs6017486 | 20 | 45096238 | G | A | 0,2817 | 0,0160 | 0,0323 | 0,6192 | 0,9823 | Neuropathic Pain | KCNS1 |
| rs3820571 | 1 | 236897133 | G | T | 0,5946 | 0,0147 | 0,0296 | 0,6205 | 0,9823 | Migraine | MTR |
| rs1800532 | 11 | 18026269 | G | T | 0,4020 | -0,0149 | 0,0301 | 0,6209 | 0,9823 | Migraine | TPH1 |
| rs6025 | 1 | 169549811 | C | T | 0,0221 | -0,0497 | 0,1007 | 0,6215 | 0,9823 | Migraine | F5 |

| | | | | | | | | | | | |
|---|---|---|---|---|---|---|---|---|---|---|---|
| rs16909443 | 11 | 6171232 | T | C | 0,0617 | -0,0298 | 0,0608 | 0,6234 | 0,9823 | Other Clinical Pain | RP11-290F24.3 |
| rs7687621 | 4 | 74384109 | T | C | 0,7980 | -0,0179 | 0,0364 | 0,6235 | 0,9823 | Temporomandibular Disorder | EREG |
| rs2650825 | 19 | 21516423 | C | T | 0,7640 | -0,0170 | 0,0346 | 0,6240 | 0,9823 | Analgesia | ZNF429 |
| rs7287550 | 22 | 19944453 | T | C | 0,2739 | 0,0160 | 0,0328 | 0,6254 | 0,9823 | Analgesia | COMT |
| rs9396861 | 6 | 18403902 | C | A | 0,5751 | -0,0142 | 0,0292 | 0,6267 | 0,9823 | Arthritis | RNF144B |
| rs9851381 | 3 | 142803548 | G | A | 0,1736 | -0,0187 | 0,0386 | 0,6277 | 0,9823 | Migraine | TRPC1 |
| rs12435797 | 14 | 73330961 | G | T | 0,2555 | 0,0160 | 0,0332 | 0,6294 | 0,9823 | Other Clinical Pain | NUMB |
| rs12875271 | 13 | 110140396 | A | G | 0,1045 | 0,0232 | 0,0482 | 0,6300 | 0,9823 | Migraine | |
| rs3771501 | 2 | 70490521 | A | G | 0,5105 | 0,0142 | 0,0294 | 0,6301 | 0,9823 | Arthritis | TGFA |
| rs2672596 | 10 | 122467277 | G | A | 0,2292 | 0,0168 | 0,0350 | 0,6305 | 0,9823 | Neuraxial pain | HTRA1 |
| rs4141964 | 1 | 46399368 | T | C | 0,6524 | -0,0146 | 0,0305 | 0,6317 | 0,9823 | Nociception | FAAH |
| rs165774 | 22 | 19965038 | G | A | 0,3221 | -0,0151 | 0,0316 | 0,6322 | 0,9823 | Nociception, Temporomandibular Disorder, Cancer P | COMT |
| rs7958311 | 12 | 121167552 | G | A | 0,2713 | 0,0156 | 0,0326 | 0,6332 | 0,9823 | Musculoskeletal Pain | LOC105370032 |
| rs6967334 | 7 | 82432452 | G | C | 0,3634 | 0,0144 | 0,0301 | 0,6333 | 0,9823 | Temporomandibular Disorder | CACNA2D1 |
| rs11030104 | 11 | 27662970 | A | G | 0,2270 | -0,0167 | 0,0352 | 0,6346 | 0,9823 | Neuraxial pain | BDNF-AS |
| rs10483639 | 14 | 54839739 | G | C | 0,1974 | 0,0175 | 0,0368 | 0,6350 | 0,9823 | Nociception | |
| rs7943316 | 11 | 34438925 | A | T | 0,6650 | 0,0146 | 0,0312 | 0,6391 | 0,9823 | Migraine | |
| rs12060570 | 1 | 236825769 | G | C | 0,4020 | 0,0141 | 0,0300 | 0,6394 | 0,9823 | Migraine | MTR |
| rs1806505 | 1 | 236833275 | C | T | 0,4020 | 0,0141 | 0,0300 | 0,6394 | 0,9823 | Migraine | MTR |
| rs7767143 | 6 | 151774559 | A | G | 0,1830 | 0,0174 | 0,0373 | 0,6414 | 0,9823 | Migraine | ESR1 |
| rs4663 | 12 | 76060186 | G | A | 0,5902 | -0,0135 | 0,0293 | 0,6442 | 0,9823 | Neuropathic pain | COMT |
| rs2267730 | 7 | 31083015 | C | T | 0,4655 | 0,0135 | 0,0293 | 0,6456 | 0,9823 | Migraine | ADCYAP1R1 |
| rs13075921 | 3 | 149197841 | T | C | 0,0975 | -0,0232 | 0,0506 | 0,6470 | 0,9823 | Neuropathic Pain | CP |
| rs2069762 | 4 | 122456825 | A | C | 0,3204 | -0,0143 | 0,0313 | 0,6472 | 0,9823 | Neuraxial pain | |
| rs10767664 | 11 | 27704439 | T | A | 0,7640 | 0,0158 | 0,0348 | 0,6494 | 0,9823 | Neuraxial pain | BDNF |
| rs72663521 | 1 | 39540231 | G | A | 0,1804 | -0,0171 | 0,0377 | 0,6502 | 0,9823 | Migraine | |
| rs6073643 | 20 | 45099429 | T | C | 0,2834 | 0,0146 | 0,0323 | 0,6507 | 0,9823 | Neuropathic Pain | KCNS1 |
| rs10824456 | 10 | 76855700 | C | G | 0,3673 | -0,0132 | 0,0293 | 0,6511 | 0,9823 | Post-operative pain | KCNMA1 |
| rs1893047 | 11 | 69811704 | A | G | 0,5248 | -0,0133 | 0,0293 | 0,6512 | 0,9823 | Temporomandibular disorders | FGF3 |
| rs4941573 | 13 | 46890722 | A | G | 0,4531 | -0,0133 | 0,0294 | 0,6517 | 0,9823 | Cancer Pain | HTR2A |
| rs1491850 | 11 | 27728178 | T | C | 0,4239 | -0,0135 | 0,0299 | 0,6524 | 0,9823 | Post-operative Pain | |
| rs758275 | 2 | 233929375 | A | G | 0,2010 | 0,0166 | 0,0369 | 0,6525 | 0,9823 | Migraine | TRPM8 |
| rs1979277 | 17 | 18328782 | G | A | 0,2854 | 0,0147 | 0,0328 | 0,6534 | 0,9823 | Temporomandibular Disorder | SHMT1 |
| rs4909945 | 11 | 10652192 | T | C | 0,6653 | 0,0139 | 0,0310 | 0,6535 | 0,9823 | Migraine | SUV39H2 |
| rs1072198 | 7 | 120687295 | C | T | 0,6796 | -0,0139 | 0,0310 | 0,6539 | 0,9823 | Post-operative Pain | KCND2 |
| rs6295 | 5 | 63962738 | C | G | 0,5005 | -0,0133 | 0,0296 | 0,6541 | 0,9823 | Migraine | |
| rs1042615 | 12 | 63150429 | A | G | 0,5768 | 0,0133 | 0,0297 | 0,6544 | 0,9823 | Nociception | AVPR1A |
| rs10046 | 15 | 51210789 | G | A | 0,5090 | 0,0131 | 0,0293 | 0,6548 | 0,9823 | Migraine | CYP19A1 |
| rs40184 | 5 | 1394962 | C | T | 0,4810 | -0,0128 | 0,0293 | 0,6608 | 0,9823 | Migraine | SLC6A3 |
| rs1800797 | 7 | 22726602 | A | G | 0,6305 | 0,0130 | 0,0296 | 0,6613 | 0,9823 | Neuraxial Pain | IL6-AS1 |
| rs7734804 | 5 | 164919530 | G | T | 0,0221 | -0,0420 | 0,0964 | 0,6631 | 0,9823 | Neuropathic Pain | LOC105377703 |
| rs3756612 | 5 | 111367789 | A | G | 0,2042 | -0,0159 | 0,0365 | 0,6637 | 0,9823 | Temporomandibular Disorder | CAMK4 |
| rs28865059 | 3 | 137968557 | G | C | 0,1101 | -0,0204 | 0,0470 | 0,6639 | 0,9823 | Temporomandibular disorders | |
| rs13078961 | 3 | 137968843 | G | C | 0,1101 | -0,0204 | 0,0470 | 0,6639 | 0,9823 | Temporomandibular disorders | |
| rs2884129 | 10 | 17543150 | T | G | 0,2056 | 0,0158 | 0,0364 | 0,6642 | 0,9823 | Analgesia | |
| rs2236742 | 14 | 24575924 | C | T | 0,1655 | -0,0172 | 0,0396 | 0,6643 | 0,9823 | Post-operative Pain | CTSG |

| | | | | | | | | | | | |
|---|---|---|---|---|---|---|---|---|---|---|---|
| rs2070995 | 21 | 37714662 | T | C | 0,7922 | -0,0160 | 0,0368 | 0,6647 | 0,9823 | Analgesia | KCNJ6 |
| rs4792311 | 17 | 13011692 | G | A | 0,3048 | -0,0136 | 0,0315 | 0,6651 | 0,9823 | Fibromyalgia | ELAC2 |
| rs11858956 | 15 | 69968889 | T | C | 0,6801 | -0,0136 | 0,0313 | 0,6652 | 0,9823 | Migraine | |
| rs1327123 | 1 | 184045459 | G | C | 0,3245 | 0,0135 | 0,0313 | 0,6663 | 0,9823 | Post-operative pain | TSEN15 |
| rs1976423 | 5 | 104706942 | A | C | 0,4650 | 0,0129 | 0,0299 | 0,6664 | 0,9823 | Other Clinical Pain | LOC105379109 |
| rs1332844 | 6 | 12888772 | C | T | 0,6152 | -0,0128 | 0,0297 | 0,6672 | 0,9823 | Migraine | PHACTR1 |
| rs11871043 | 17 | 45095481 | T | C | 0,5535 | 0,0127 | 0,0297 | 0,6681 | 0,9823 | Other Clinical Pain | NMT1 |
| rs10974438 | 9 | 4291928 | A | C | 0,3802 | -0,0130 | 0,0304 | 0,6690 | 0,9823 | Arthritis | GLIS3 |
| rs9544636 | 13 | 77925434 | C | T | 0,0933 | 0,0214 | 0,0502 | 0,6698 | 0,9823 | Migraine | EDNRB |
| rs1561836 | 5 | 22794548 | A | G | 0,1254 | 0,0189 | 0,0446 | 0,6712 | 0,9823 | Migraine | CDH12 |
| rs985933 | 13 | 46881728 | A | G | 0,6247 | 0,0130 | 0,0307 | 0,6715 | 0,9823 | Musculoskeletal Pain | HTR2A |
| rs1049353 | 6 | 88143916 | C | T | 0,2426 | -0,0142 | 0,0335 | 0,6720 | 0,9823 | Migraine | CNR1 |
| rs8659 | 5 | 7900720 | T | A | 0,6417 | -0,0129 | 0,0305 | 0,6728 | 0,9823 | Migraine | MTRR |
| rs10502966 | 18 | 53222129 | A | G | 0,4336 | 0,0123 | 0,0292 | 0,6734 | 0,9823 | Neuraxial pain | DCC |
| rs4384683 | 18 | 52852662 | G | A | 0,5321 | 0,0122 | 0,0290 | 0,6743 | 0,9823 | Neuraxial pain | DCC |
| rs4818 | 22 | 19963684 | C | G | 0,4203 | 0,0124 | 0,0295 | 0,6747 | 0,9823 | Nociception, Temporomandibular Disorder, Fibromya | COMT |
| rs2095019 | 6 | 169164779 | A | C | 0,8055 | -0,0153 | 0,0366 | 0,6760 | 0,9823 | Neuraxial Pain | |
| rs72760655 | 9 | 114153934 | C | A | 0,3019 | -0,0131 | 0,0313 | 0,6762 | 0,9823 | Arthritis | COL27A1 |
| rs17171710 | 7 | 40400634 | C | T | 0,0994 | -0,0206 | 0,0493 | 0,6771 | 0,9823 | Migraine | SUGCT |
| rs7639403 | 3 | 142795831 | C | T | 0,1915 | -0,0153 | 0,0368 | 0,6774 | 0,9823 | Migraine | TRPC1 |
| rs9349379 | 6 | 12903725 | A | G | 0,3933 | -0,0122 | 0,0294 | 0,6792 | 0,9823 | Migraine | PHACTR1 |
| rs4646312 | 22 | 19960814 | T | C | 0,4208 | 0,0122 | 0,0295 | 0,6800 | 0,9823 | Nociception | COMT |
| rs3766246 | 1 | 46399999 | A | G | 0,6526 | -0,0126 | 0,0305 | 0,6800 | 0,9823 | Nociception | FAAH |
| rs4845663 | 1 | 154719612 | T | C | 0,4110 | 0,0122 | 0,0296 | 0,6801 | 0,9823 | Migraine | KCNN3 |
| rs841 | 14 | 54843774 | G | A | 0,1959 | 0,0151 | 0,0369 | 0,6820 | 0,9823 | Fibromyalgia | GCH1 |
| rs752688 | 14 | 54844851 | C | T | 0,1959 | 0,0151 | 0,0369 | 0,6820 | 0,9823 | Neuraxial Pain | GCH1 |
| rs4411417 | 14 | 54853845 | T | C | 0,1959 | 0,0151 | 0,0369 | 0,6820 | 0,9823 | Neuraxial Pain | GCH1 |
| rs4803455 | 19 | 41345604 | C | A | 0,4652 | 0,0121 | 0,0295 | 0,6822 | 0,9823 | Migraine | SUV39H2 |
| rs1129235 | 17 | 16422691 | A | C | 0,3845 | -0,0124 | 0,0304 | 0,6831 | 0,9823 | Fibromyalgia | TRPV2 |
| rs17862920 | 2 | 233919350 | C | T | 0,1150 | 0,0189 | 0,0464 | 0,6841 | 0,9823 | Migraine | TRPM8 |
| rs34195470 | 16 | 69921787 | A | G | 0,5771 | -0,0118 | 0,0290 | 0,6845 | 0,9823 | Arthritis | WWP2 |
| rs2069885 | 5 | 135892476 | G | A | 0,1356 | -0,0173 | 0,0426 | 0,6846 | 0,9823 | Migraine | IL9 |
| rs12073221 | 1 | 181444938 | G | C | 0,3585 | -0,0123 | 0,0306 | 0,6884 | 0,9823 | Migraine | CACNA1E |
| rs11759769 | 6 | 96617336 | G | A | 0,2421 | 0,0138 | 0,0345 | 0,6889 | 0,9823 | Migraine | FHL5 |
| rs11906854 | 20 | 35795712 | A | G | 0,0754 | -0,0221 | 0,0554 | 0,6893 | 0,9823 | Migraine | SUV39H2 |
| rs4645978 | 1 | 15525539 | C | T | 0,5318 | -0,0115 | 0,0289 | 0,6897 | 0,9823 | Neuraxial Pain | |
| rs1271309 | 12 | 124336159 | A | G | 0,8379 | 0,0158 | 0,0397 | 0,6898 | 0,9823 | Migraine | NCOR2 |
| rs10490825 | 3 | 130977539 | G | A | 0,1167 | -0,0179 | 0,0451 | 0,6905 | 0,9823 | Musculoskeletal Pain | ATP2C1 |
| rs7574878 | 2 | 154750636 | T | G | 0,4857 | -0,0118 | 0,0297 | 0,6907 | 0,9823 | Cancer Pain | KCNJ3 |
| rs6790925 | 3 | 30438593 | C | T | 0,3724 | -0,0120 | 0,0304 | 0,6925 | 0,9823 | Migraine | LOC101927995 |
| rs973009 | 19 | 38683692 | G | A | 0,8678 | -0,0171 | 0,0432 | 0,6930 | 0,9823 | Migraine | SUV39H2 |
| rs2230365 | 6 | 31557671 | C | T | 0,0732 | -0,0223 | 0,0567 | 0,6939 | 0,9823 | Neuropathic Pain | LOC100287329 |
| rs1050993 | 1 | 236899005 | A | G | 0,5980 | 0,0116 | 0,0297 | 0,6955 | 0,9823 | Migraine | MTR |
| rs1571138 | 1 | 46429969 | A | G | 0,8230 | 0,0147 | 0,0378 | 0,6967 | 0,9823 | Nociception | |
| rs9862 | 22 | 32857293 | T | C | 0,5007 | 0,0115 | 0,0297 | 0,6979 | 0,9823 | Neuraxial Pain, Migraine | SYN3 |
| rs62053992 | 16 | 72355973 | A | G | 0,1449 | -0,0165 | 0,0427 | 0,6994 | 0,9823 | Musculoskeletal pain | LINC01572 |

| | | | | | | | | | | | |
|---|---|---|---|---|---|---|---|---|---|---|---|
| rs5275 | 1 | 186673926 | A | G | 0,3447 | -0,0120 | 0,0311 | 0,7005 | 0,9823 | Cancer Pain | PTGS2 |
| rs932816 | 1 | 46394077 | G | A | 0,2929 | -0,0125 | 0,0325 | 0,7006 | 0,9823 | Nociception | |
| rs8121 | 17 | 16422654 | A | G | 0,3850 | -0,0117 | 0,0304 | 0,7010 | 0,9823 | Fibromyalgia | TRPV2 |
| rs11726563 | 4 | 46821617 | A | C | 0,1189 | -0,0173 | 0,0451 | 0,7013 | 0,9823 | Migraine | SUV39H2 |
| rs6449693 | 5 | 63960191 | G | A | 0,5024 | -0,0113 | 0,0296 | 0,7016 | 0,9823 | Cancer Pain | HTR1A |
| rs10802569 | 1 | 236892005 | G | C | 0,5933 | 0,0112 | 0,0296 | 0,7051 | 0,9823 | Migraine | MTR |
| rs2239393 | 22 | 19962905 | A | G | 0,4273 | 0,0111 | 0,0295 | 0,7054 | 0,9823 | Analgesia | COMT |
| rs2295633 | 1 | 46408711 | A | G | 0,6607 | -0,0116 | 0,0307 | 0,7067 | 0,9823 | Nociception | FAAH |
| rs62578126 | 9 | 126613059 | C | T | 0,3743 | 0,0112 | 0,0299 | 0,7087 | 0,9823 | Post-operative pain | RP11-123K19.1 |
| rs378363 | 9 | 9020223 | T | C | 0,2368 | -0,0130 | 0,0349 | 0,7088 | 0,9823 | Migraine | SUV39H2 |
| rs161393 | 17 | 3586220 | T | C | 0,3632 | -0,0114 | 0,0305 | 0,7091 | 0,9823 | Migraine | TRPV1 |
| rs12308843 | 12 | 23821470 | G | C | 0,2173 | -0,0132 | 0,0354 | 0,7103 | 0,9823 | Neuraxial pain | SOX5 |
| rs9908234 | 17 | 49499986 | A | G | 0,0705 | 0,0211 | 0,0570 | 0,7105 | 0,9823 | Migraine | NGFR |
| rs7016778 | 8 | 53237545 | A | T | 0,1213 | 0,0165 | 0,0447 | 0,7111 | 0,9823 | Nociception | OPRK1 |
| rs17110477 | 12 | 71950083 | T | A | 0,2256 | -0,0128 | 0,0347 | 0,7131 | 0,9823 | Migraine | TPH2 |
| rs10495386 | 1 | 236869508 | G | A | 0,0231 | 0,0358 | 0,0976 | 0,7133 | 0,9823 | Migraine | MTR |
| rs7739181 | 6 | 12934455 | G | A | 0,3474 | -0,0111 | 0,0303 | 0,7134 | 0,9823 | Migraine | PHACTR1 |
| rs2386584 | 15 | 90996342 | T | G | 0,4001 | 0,0109 | 0,0297 | 0,7143 | 0,9823 | Other Clinical Pain | |
| rs881 | 2 | 75049302 | C | G | 0,1680 | -0,0143 | 0,0391 | 0,7150 | 0,9823 | Other Clinical Pain | TACR1 |
| rs4379368 | 7 | 40426601 | C | T | 0,0997 | -0,0180 | 0,0493 | 0,7157 | 0,9823 | Migraine | SUGCT |
| rs9608416 | 22 | 25715051 | G | A | 0,6021 | 0,0111 | 0,0306 | 0,7166 | 0,9823 | Neuropathic pain, Cancer Pain | GRK3 |
| rs1364402 | 7 | 136899616 | T | C | 0,0877 | 0,0186 | 0,0512 | 0,7172 | 0,9823 | Migraine | SUV39H2 |
| rs2808772 | 9 | 114151514 | A | G | 0,4781 | -0,0103 | 0,0286 | 0,7178 | 0,9823 | Musculoskeletal pain | LOC105376225 |
| rs7953280 | 12 | 93742233 | G | C | 0,4752 | 0,0105 | 0,0292 | 0,7196 | 0,9823 | Arthritis | CRADD |
| rs13208321 | 6 | 96412478 | A | G | 0,7613 | -0,0124 | 0,0346 | 0,7206 | 0,9823 | Migraine | UFL1-AS1 |
| rs10459710 | 15 | 93137328 | C | T | 0,1940 | 0,0130 | 0,0364 | 0,7217 | 0,9823 | Post-operative pain | LOC101927025 |
| rs3816527 | 3 | 157437525 | C | A | 0,5654 | -0,0104 | 0,0294 | 0,7226 | 0,9823 | Migraine | VEPH1 |
| rs6313 | 13 | 46895805 | G | A | 0,4560 | -0,0104 | 0,0293 | 0,7230 | 0,9823 | Fibromyalgia | HTR2A |
| rs1985242 | 11 | 113977551 | A | T | 0,6825 | -0,0111 | 0,0316 | 0,7255 | 0,9823 | Cancer Pain | HTR3A |
| rs2327621 | 6 | 12922457 | G | A | 0,6437 | 0,0106 | 0,0304 | 0,7259 | 0,9823 | Migraine | PHACTR1 |
| rs162036 | 5 | 7885846 | A | G | 0,1174 | 0,0158 | 0,0452 | 0,7274 | 0,9823 | Migraine | MTRR |
| rs224222 | 16 | 3254463 | C | T | 0,2645 | -0,0113 | 0,0326 | 0,7289 | 0,9823 | Fibromyalgia | MEFV |
| rs9371601 | 6 | 152469438 | G | T | 0,3583 | 0,0105 | 0,0304 | 0,7290 | 0,9823 | Migraine | SYNE1 |
| rs12454023 | 18 | 58342372 | C | T | 0,4842 | 0,0100 | 0,0291 | 0,7313 | 0,9823 | Migraine | SUV39H2 |
| rs2860174 | 19 | 7130707 | A | T | 0,1750 | -0,0133 | 0,0388 | 0,7328 | 0,9823 | Migraine | INSR |
| rs12209223 | 6 | 75454873 | C | A | 0,0919 | -0,0172 | 0,0503 | 0,7330 | 0,9823 | Arthritis | FILIP1 |
| rs917997 | 2 | 102454108 | T | C | 0,7868 | -0,0121 | 0,0355 | 0,7335 | 0,9823 | Neuraxial Pain | IL18RAP |
| rs10504152 | 8 | 53217555 | G | A | 0,1356 | 0,0142 | 0,0418 | 0,7336 | 0,9823 | Musculoskeletal Pain | LOC105375836 |
| rs3745367 | 19 | 7669625 | G | A | 0,2270 | 0,0116 | 0,0341 | 0,7349 | 0,9823 | Post-operative pain | RETN |
| rs324420 | 1 | 46405089 | C | A | 0,1770 | -0,0128 | 0,0378 | 0,7356 | 0,9823 | Analgesia | FAAH |
| rs10456100 | 6 | 39215694 | C | T | 0,2795 | 0,0110 | 0,0327 | 0,7357 | 0,9823 | Migraine | KCNK5 |
| rs12465950 | 2 | 233990798 | C | T | 0,3131 | 0,0108 | 0,0320 | 0,7361 | 0,9823 | Migraine | TRPM8 |
| rs2282652 | 11 | 102226584 | T | C | 0,3403 | 0,0104 | 0,0310 | 0,7363 | 0,9823 | Migraine | YAP1 |
| rs8004445 | 14 | 54883948 | G | T | 0,1113 | 0,0154 | 0,0461 | 0,7377 | 0,9823 | Neuraxial Pain | GCH1 |
| rs2391333 | 13 | 106514346 | C | T | 0,3734 | 0,0101 | 0,0301 | 0,7378 | 0,9823 | Neuraxial Pain | EFNB2 |
| rs2228480 | 6 | 152098960 | G | A | 0,1539 | 0,0135 | 0,0402 | 0,7382 | 0,9823 | Migraine | ESR1 |

| | | | | | | | | | | | |
|---|---|---|---|---|---|---|---|---|---|---|---|
| rs7975232 | 12 | 47845054 | C | A | 0,5527 | -0,0096 | 0,0289 | 0,7390 | 0,9823 | Neuraxial Pain | VDR |
| rs17857135 | 17 | 80288362 | T | C | 0,1461 | 0,0138 | 0,0414 | 0,7390 | 0,9823 | Migraine | RNF213 |
| rs11627241 | 14 | 94319114 | T | C | 0,7484 | -0,0109 | 0,0328 | 0,7399 | 0,9823 | Musculoskeletal Pain | SERPINA6 |
| rs6791480 | 3 | 30439067 | C | T | 0,3041 | -0,0105 | 0,0317 | 0,7406 | 0,9823 | Migraine | LOC101927995 |
| rs1491985 | 3 | 49702074 | G | C | 0,7866 | -0,0117 | 0,0353 | 0,7406 | 0,9823 | Musculoskeletal Pain | RNF123 |
| rs7628207 | 3 | 49717537 | T | C | 0,7866 | -0,0117 | 0,0353 | 0,7406 | 0,9823 | Musculoskeletal Pain | AMIGO3 |
| rs1146161 | 1 | 115116155 | A | C | 0,8403 | 0,0130 | 0,0396 | 0,7422 | 0,9823 | Migraine | |
| rs34560402 | 11 | 67104849 | C | T | 0,0561 | -0,0205 | 0,0628 | 0,7440 | 0,9823 | Arthritis | KDM2A |
| rs13043825 | 20 | 45098514 | C | T | 0,2803 | 0,0106 | 0,0324 | 0,7445 | 0,9823 | Neuropathic Pain | KCNS1 |
| rs1553005 | 11 | 14972944 | G | C | 0,3187 | 0,0102 | 0,0312 | 0,7446 | 0,9823 | Migraine | |
| rs3781719 | 11 | 14972978 | A | G | 0,3187 | 0,0102 | 0,0312 | 0,7446 | 0,9823 | Migraine | |
| rs1712517 | 10 | 103273258 | C | T | 0,5265 | -0,0096 | 0,0297 | 0,7465 | 0,9823 | Migraine | |
| rs10925235 | 1 | 236799475 | T | C | 0,6004 | -0,0096 | 0,0297 | 0,7469 | 0,9823 | Migraine | MTR |
| rs2835859 | 21 | 37645860 | T | C | 0,0814 | 0,0166 | 0,0522 | 0,7503 | 0,9823 | Analgesia | KCNJ6 |
| rs11713183 | 3 | 7036492 | T | C | 0,5421 | -0,0093 | 0,0293 | 0,7509 | 0,9823 | Migraine | GRM7 |
| rs400824 | 8 | 80445467 | C | T | 0,3238 | -0,0099 | 0,0313 | 0,7513 | 0,9823 | Migraine | SUV39H2 |
| rs28455731 | 6 | 121524892 | G | T | 0,1590 | -0,0128 | 0,0403 | 0,7515 | 0,9823 | Migraine | |
| rs210993 | 5 | 162192498 | G | A | 0,3607 | -0,0097 | 0,0305 | 0,7515 | 0,9823 | Migraine | |
| rs16022 | 19 | 13298882 | C | G | 0,1641 | -0,0124 | 0,0395 | 0,7528 | 0,9823 | Migraine | CACNA1A |
| rs4646310 | 22 | 19941283 | G | A | 0,1974 | -0,0115 | 0,0364 | 0,7529 | 0,9823 | Temporomandibular Disorder | TXNRD2 |
| rs222741 | 17 | 3605586 | G | A | 0,7353 | 0,0104 | 0,0330 | 0,7530 | 0,9823 | Migraine | TRPV1 |
| rs4822492 | 22 | 24447626 | C | G | 0,5452 | -0,0092 | 0,0294 | 0,7535 | 0,9823 | Migraine | ADORA2A-AS1 |
| rs4903399 | 14 | 76308859 | C | T | 0,2018 | 0,0114 | 0,0364 | 0,7539 | 0,9823 | Temporomandibular Disorder | ESRRB |
| rs174699 | 22 | 19966935 | C | T | 0,9579 | 0,0224 | 0,0720 | 0,7555 | 0,9823 | Analgesia | COMT |
| rs467323 | 12 | 49955982 | C | T | 0,7086 | 0,0099 | 0,0318 | 0,7556 | 0,9823 | Temporomandibular disorders | AQP5-AS1 |
| rs2770298 | 13 | 46872712 | C | T | 0,7168 | -0,0102 | 0,0329 | 0,7567 | 0,9823 | Cancer Pain | HTR2A |
| rs2622873 | 1 | 103000497 | T | C | 0,1281 | -0,0135 | 0,0435 | 0,7568 | 0,9823 | Arthritis | COL11A1 |
| rs4766311 | 12 | 4913272 | C | T | 0,5005 | -0,0091 | 0,0293 | 0,7570 | 0,9823 | Post-operative Pain | KCNA1 |
| rs3787535 | 20 | 62722169 | G | A | 0,2951 | 0,0098 | 0,0317 | 0,7581 | 0,9823 | Temporomandibular Disorder | NTSR1 |
| rs7492600 | 14 | 54870157 | G | T | 0,1116 | 0,0141 | 0,0461 | 0,7600 | 0,9823 | Neuraxial Pain | GCH1 |
| rs12147422 | 14 | 54877297 | T | C | 0,1116 | 0,0141 | 0,0461 | 0,7600 | 0,9823 | Neuraxial Pain | GCH1 |
| rs1800872 | 1 | 206773062 | T | G | 0,7547 | -0,0103 | 0,0340 | 0,7612 | 0,9823 | Neuraxial pain | IL19 |
| rs1800871 | 1 | 206773289 | A | G | 0,7547 | -0,0103 | 0,0340 | 0,7612 | 0,9823 | Neuraxial pain | IL19 |
| rs927544 | 13 | 46881916 | G | A | 0,7297 | 0,0101 | 0,0334 | 0,7622 | 0,9823 | Musculoskeletal Pain | HTR2A |
| rs2718796 | 3 | 133760356 | G | C | 0,9672 | -0,0251 | 0,0830 | 0,7626 | 0,9823 | Neuropathic Pain | TF |
| rs17641121 | 2 | 154809240 | T | C | 0,3420 | -0,0093 | 0,0307 | 0,7633 | 0,9823 | Post-operative Pain | KCNJ3 |
| rs6425412 | 1 | 177104591 | A | G | 0,0537 | -0,0195 | 0,0649 | 0,7637 | 0,9823 | Migraine | ASTN1 |
| rs6758653 | 2 | 234004155 | G | A | 0,3384 | 0,0093 | 0,0308 | 0,7637 | 0,9823 | Migraine | TRPM8 |
| rs2971603 | 6 | 96587542 | C | T | 0,2465 | 0,0103 | 0,0344 | 0,7642 | 0,9823 | Migraine | FHL5 |
| rs3816893 | 3 | 149209924 | A | T | 0,0960 | -0,0151 | 0,0507 | 0,7661 | 0,9823 | Neuropathic Pain | CP |
| rs73581580 | 9 | 137357006 | G | A | 0,1099 | 0,0136 | 0,0458 | 0,7661 | 0,9823 | Musculoskeletal pain | EXD3 |
| rs7767277 | 6 | 32885265 | C | A | 0,0462 | 0,0207 | 0,0701 | 0,7674 | 0,9823 | Neuraxial Pain | |
| rs1799971 | 6 | 154039662 | A | G | 0,1393 | -0,0124 | 0,0422 | 0,7687 | 0,9823 | Analgesia | OPRM1 |
| rs806366 | 6 | 88137870 | C | T | 0,4733 | 0,0084 | 0,0285 | 0,7693 | 0,9823 | Migraine | CNR1 |
| rs2983896 | 6 | 96581995 | G | A | 0,2397 | 0,0101 | 0,0347 | 0,7707 | 0,9823 | Migraine | FHL5 |
| rs41268673 | 2 | 166284599 | G | T | 0,0338 | 0,0235 | 0,0808 | 0,7708 | 0,9823 | Nociception | SCN1A-AS1 |

| | | | | | | | | | | | |
|---|---|---|---|---|---|---|---|---|---|---|---|
| rs1080519 | 2 | 237907559 | C | T | 0,2346 | 0,0101 | 0,0349 | 0,7729 | 0,9823 | Migraine | RAMP1 |
| rs6269 | 22 | 19962429 | A | G | 0,4276 | 0,0085 | 0,0295 | 0,7730 | 0,9823 | Nociception, Temporomandibular Disorder, Fibromya | COMT |
| rs62182810 | 2 | 203522759 | G | A | 0,5627 | 0,0084 | 0,0290 | 0,7731 | 0,9823 | Arthritis | RAPH1 |
| rs7079024 | 10 | 3403476 | C | T | 0,6060 | -0,0086 | 0,0297 | 0,7732 | 0,9823 | Migraine | LOC105376360 |
| rs2591172 | 2 | 154765665 | T | G | 0,3138 | 0,0090 | 0,0314 | 0,7734 | 0,9823 | Cancer Pain | KCNJ3 |
| rs9475400 | 6 | 55773460 | C | T | 0,1084 | -0,0135 | 0,0470 | 0,7735 | 0,9823 | Post-operative pain | BMP5 |
| rs12619987 | 2 | 166301463 | G | A | 0,1104 | 0,0133 | 0,0463 | 0,7739 | 0,9823 | Post-operative Pain | SCN1A-AS1 |
| rs5751876 | 22 | 24441333 | T | C | 0,5676 | -0,0085 | 0,0295 | 0,7741 | 0,9823 | Migraine | ADORA2A-AS1 |
| rs403636 | 5 | 1438239 | A | C | 0,8576 | 0,0120 | 0,0419 | 0,7744 | 0,9823 | Neuropathic pain | SLC6A3 |
| rs2297518 | 17 | 27769571 | G | A | 0,2110 | 0,0102 | 0,0358 | 0,7761 | 0,9823 | Migraine | NOS2 |
| rs4129256 | 6 | 132623858 | G | A | 0,2166 | -0,0101 | 0,0355 | 0,7772 | 0,9823 | Fibromyalgia | TAAR2 |
| rs7800170 | 7 | 136939573 | C | A | 0,4871 | -0,0082 | 0,0289 | 0,7773 | 0,9823 | Temporomandibular Disorder | CHRM2 |
| rs12995382 | 2 | 154775781 | T | C | 0,3872 | -0,0085 | 0,0303 | 0,7779 | 0,9823 | Post-operative Pain | KCNJ3 |
| rs1800587 | 2 | 112785383 | G | A | 0,2895 | -0,0092 | 0,0327 | 0,7781 | 0,9823 | Migraine | |
| rs227732 | 17 | 56692529 | C | T | 0,2603 | -0,0095 | 0,0339 | 0,7782 | 0,9823 | Post-operative pain | NOG |
| rs2187689 | 6 | 32884870 | T | C | 0,0462 | 0,0197 | 0,0701 | 0,7783 | 0,9823 | Neuraxial Pain | |
| rs10930214 | 2 | 166249343 | C | G | 0,7022 | -0,0090 | 0,0323 | 0,7802 | 0,9823 | Arthritis | SCN1A-AS1 |
| rs9324918 | 5 | 143387595 | T | C | 0,1327 | -0,0119 | 0,0425 | 0,7803 | 0,9823 | Temporomandibular Disorder | NR3C1 |
| rs2329047 | 13 | 77927515 | T | G | 0,6441 | -0,0085 | 0,0307 | 0,7804 | 0,9823 | Migraine | EDNRB |
| rs1420106 | 2 | 102418584 | A | G | 0,7856 | -0,0099 | 0,0357 | 0,7805 | 0,9823 | Neuraxial Pain | IL18RAP |
| rs7932320 | 11 | 69810743 | T | C | 0,4891 | 0,0080 | 0,0292 | 0,7833 | 0,9823 | Temporomandibular disorders | FGF3 |
| rs4776783 | 15 | 66369769 | A | G | 0,1461 | 0,0114 | 0,0415 | 0,7842 | 0,9823 | Temporomandibular Disorder | TIPIN |
| rs10914731 | 1 | 33469223 | A | G | 0,1463 | -0,0112 | 0,0412 | 0,7855 | 0,9823 | Neuropathic Pain | |
| rs10485171 | 6 | 88133671 | A | G | 0,4084 | -0,0079 | 0,0292 | 0,7874 | 0,9823 | Fibromyalgia | |
| rs35737760 | 1 | 181732663 | T | A | 0,1381 | 0,0114 | 0,0424 | 0,7881 | 0,9823 | Migraine | CACNA1E |
| rs36017 | 16 | 55684906 | G | C | 0,4730 | -0,0079 | 0,0295 | 0,7886 | 0,9823 | Cancer Pain | SLC6A2 |
| rs1800796 | 7 | 22726627 | G | C | 0,0625 | -0,0160 | 0,0599 | 0,7896 | 0,9823 | Neuraxial Pain | IL6-AS1 |
| rs2206593 | 1 | 186673297 | A | G | 0,9295 | -0,0149 | 0,0560 | 0,7905 | 0,9823 | Other Clinical Pain | PTGS2 |
| rs2910576 | 5 | 58236921 | A | T | 0,7905 | -0,0094 | 0,0353 | 0,7906 | 0,9823 | Neuraxial pain | |
| rs17740111 | 16 | 84373822 | G | C | 0,1833 | 0,0099 | 0,0374 | 0,7911 | 0,9823 | Migraine | ATP2C2 |
| rs10795033 | 10 | 3404880 | C | T | 0,6062 | -0,0078 | 0,0297 | 0,7929 | 0,9823 | Migraine | LOC105376360 |
| rs6311 | 13 | 46897343 | C | T | 0,4555 | -0,0076 | 0,0293 | 0,7945 | 0,9823 | Other Clinical Pain | HTR2A |
| rs7223530 | 17 | 3565158 | G | C | 0,3126 | 0,0082 | 0,0315 | 0,7948 | 0,9823 | Migraine | TRPV1 |
| rs705162 | 10 | 123492159 | G | A | 0,2890 | 0,0083 | 0,0321 | 0,7955 | 0,9823 | Migraine | SUV39H2 |
| rs6296 | 6 | 77462543 | C | G | 0,2594 | -0,0085 | 0,0329 | 0,7957 | 0,9823 | Migraine | LOC105377864 |
| rs7718446 | 5 | 146369972 | A | G | 0,2773 | -0,0084 | 0,0326 | 0,7958 | 0,9823 | Migraine | SUV39H2 |
| rs2545457 | 8 | 139649042 | G | A | 0,6215 | -0,0077 | 0,0300 | 0,7976 | 0,9823 | Post-operative Pain | KCNK9 |
| rs2234693 | 6 | 151842200 | T | C | 0,4443 | 0,0076 | 0,0298 | 0,7990 | 0,9823 | Temporomandibular Disorder | ESR1 |
| rs11729628 | 4 | 120663127 | G | T | 0,2353 | 0,0089 | 0,0349 | 0,7991 | 0,9823 | Arthritis | RP11-501E14.1 |
| rs2856836 | 2 | 112774506 | A | G | 0,2897 | -0,0083 | 0,0327 | 0,8002 | 0,9823 | Neuraxial Pain | IL1A |
| rs1304037 | 2 | 112774659 | T | C | 0,2897 | -0,0083 | 0,0327 | 0,8002 | 0,9823 | Neuraxial Pain | IL1A |
| rs2071375 | 2 | 112777861 | C | T | 0,2897 | -0,0083 | 0,0327 | 0,8002 | 0,9823 | Neuraxial Pain | IL18RAP |
| rs17561 | 2 | 112779646 | C | A | 0,2897 | -0,0083 | 0,0327 | 0,8002 | 0,9823 | Neuraxial Pain | IL1A |
| rs1218551 | 1 | 154828697 | C | T | 0,6587 | 0,0078 | 0,0310 | 0,8016 | 0,9823 | Migraine | KCNN3 |
| rs197422 | 1 | 111774890 | C | A | 0,3790 | -0,0074 | 0,0295 | 0,8018 | 0,9823 | Other Clinical Pain | KCND3 |
| rs3761422 | 22 | 24430704 | T | C | 0,5719 | -0,0074 | 0,0295 | 0,8018 | 0,9823 | Migraine | ADORA2A-AS1 |

| | | | | | | | | | | | |
|---|---|---|---|---|---|---|---|---|---|---|---|
| rs6517442 | 21 | 37917643 | C | T | 0,6612 | 0,0077 | 0,0313 | 0,8047 | 0,9848 | Post-operative pain | |
| rs6693567 | 1 | 150538184 | C | T | 0,7343 | -0,0081 | 0,0332 | 0,8072 | 0,9853 | Migraine | |
| rs11636768 | 15 | 87152280 | G | A | 0,1658 | -0,0095 | 0,0390 | 0,8080 | 0,9853 | Migraine | LOC105370955 |
| rs4233367 | 1 | 161193247 | T | C | 0,6040 | -0,0071 | 0,0297 | 0,8099 | 0,9853 | Neuraxial Pain | ADAMTS4 |
| rs208294 | 12 | 121162450 | T | C | 0,5530 | -0,0071 | 0,0295 | 0,8100 | 0,9853 | Post-operative Pain | LOC105370032 |
| rs11624776 | 14 | 93129246 | A | C | 0,3352 | 0,0073 | 0,0308 | 0,8126 | 0,9853 | Migraine | |
| rs8192619 | 6 | 132645209 | G | A | 0,0493 | -0,0158 | 0,0668 | 0,8127 | 0,9853 | Fibromyalgia | TAAR1 |
| rs7427106 | 3 | 38637010 | C | G | 0,1517 | -0,0095 | 0,0401 | 0,8129 | 0,9853 | Migraine | SCN5A |
| rs2070037 | 13 | 46892935 | T | C | 0,2144 | 0,0086 | 0,0363 | 0,8135 | 0,9853 | Musculoskeletal Pain | HTR2A |
| rs71647933 | 1 | 33480000 | A | G | 0,1468 | -0,0096 | 0,0410 | 0,8146 | 0,9853 | Neuropathic Pain | ZSCAN20 |
| rs5993882 | 22 | 19950010 | T | G | 0,2351 | 0,0079 | 0,0342 | 0,8169 | 0,9853 | Temporomandibular Disorder, Cancer Pain | COMT |
| rs6961071 | 7 | 156182007 | A | G | 0,5357 | -0,0068 | 0,0293 | 0,8169 | 0,9853 | Analgesia | |
| rs1487275 | 12 | 72016512 | C | A | 0,7161 | 0,0076 | 0,0329 | 0,8172 | 0,9853 | Migraine | TPH2 |
| rs61883178 | 11 | 16296233 | C | A | 0,1903 | 0,0084 | 0,0366 | 0,8178 | 0,9853 | Other Clinical Pain | SOX6 |
| rs1145324 | 15 | 90462133 | A | G | 0,0440 | -0,0164 | 0,0719 | 0,8191 | 0,9853 | Post-operative pain | IQGAP1 |
| rs6928 | 22 | 21760715 | C | G | 0,5552 | -0,0066 | 0,0292 | 0,8206 | 0,9853 | Temporomandibular Disorder | MAPK1 |
| rs1800497 | 11 | 113400106 | G | A | 0,1716 | -0,0088 | 0,0387 | 0,8209 | 0,9853 | Migraine | ANKK1 |
| rs6741923 | 2 | 237890564 | C | G | 0,7039 | -0,0072 | 0,0317 | 0,8210 | 0,9853 | Migraine | RAMP1 |
| rs746530 | 14 | 94330956 | A | G | 0,6711 | -0,0069 | 0,0307 | 0,8214 | 0,9853 | Musculoskeletal Pain | |
| rs2336244 | 1 | 33477789 | G | C | 0,1373 | -0,0095 | 0,0421 | 0,8222 | 0,9853 | Neuropathic Pain | ZSCAN20 |
| rs10903399 | 10 | 1181928 | T | C | 0,3128 | -0,0070 | 0,0314 | 0,8234 | 0,9853 | Migraine | ADARB2 |
| rs1046914 | 10 | 1182266 | T | C | 0,3128 | -0,0070 | 0,0314 | 0,8234 | 0,9853 | Migraine | ADARB2 |
| rs1514185 | 1 | 60719084 | C | T | 0,6582 | -0,0068 | 0,0305 | 0,8236 | 0,9853 | Post-operative pain | LOC101926964 |
| rs1042717 | 5 | 148827083 | G | A | 0,2010 | -0,0080 | 0,0362 | 0,8258 | 0,9869 | Temporomandibular Disorder | ADRB2 |
| rs2032582 | 7 | 87531302 | A | C | 0,5508 | 0,0064 | 0,0295 | 0,8268 | 0,9871 | Analgesia | ABCB1 |
| rs11588154 | 1 | 54836263 | T | G | 0,8226 | -0,0084 | 0,0386 | 0,8278 | 0,9871 | Arthritis | C1orf177 |
| rs9381462 | 6 | 12873543 | A | G | 0,5017 | -0,0062 | 0,0290 | 0,8307 | 0,9871 | Migraine | PHACTR1 |
| rs2952768 | 2 | 207629510 | T | C | 0,3408 | 0,0065 | 0,0304 | 0,8317 | 0,9871 | Analgesia | |
| rs2956 | 11 | 14967575 | T | A | 0,3126 | 0,0066 | 0,0313 | 0,8319 | 0,9871 | Migraine | CALCA |
| rs8080108 | 17 | 49436349 | T | C | 0,2883 | 0,0067 | 0,0320 | 0,8335 | 0,9871 | Migraine | |
| rs4652898 | 1 | 33475090 | A | C | 0,1478 | -0,0086 | 0,0408 | 0,8338 | 0,9871 | Neuropathic Pain | ZSCAN20 |
| rs2287037 | 2 | 102362568 | C | T | 0,4071 | 0,0062 | 0,0296 | 0,8338 | 0,9871 | Neuraxial Pain | IL18RAP |
| rs1229984 | 4 | 99318162 | T | C | 0,9404 | 0,0124 | 0,0603 | 0,8365 | 0,9871 | Migraine | ADH1B |
| rs25531 | 17 | 30237328 | T | C | 0,0564 | 0,0129 | 0,0627 | 0,8371 | 0,9871 | Analgesia | LOC105371720 |
| rs2020917 | 22 | 19941361 | C | T | 0,3119 | 0,0065 | 0,0315 | 0,8373 | 0,9871 | Musculoskeletal Pain | COMT |
| rs1386486 | 12 | 72018440 | A | G | 0,6420 | 0,0063 | 0,0310 | 0,8379 | 0,9871 | Migraine | TPH2 |
| rs2835914 | 21 | 37726547 | G | C | 0,3109 | -0,0065 | 0,0320 | 0,8388 | 0,9871 | Cancer Pain | KCNJ6 |
| rs2605100 | 1 | 219470882 | A | G | 0,7052 | 0,0067 | 0,0328 | 0,8390 | 0,9871 | Post-operative pain | RP11-95P13.1 |
| rs62281806 | 3 | 172244356 | C | T | 0,1298 | -0,0088 | 0,0436 | 0,8393 | 0,9871 | Post-operative pain | FNDC3B |
| rs79220007 | 6 | 26098246 | T | C | 0,0384 | 0,0150 | 0,0760 | 0,8436 | 0,9871 | Arthritis | HFE |
| rs2069718 | 12 | 68156382 | A | G | 0,6113 | 0,0059 | 0,0302 | 0,8450 | 0,9871 | Neuraxial Pain | IFNG |
| rs6546952 | 2 | 75074636 | C | T | 0,5231 | -0,0058 | 0,0300 | 0,8460 | 0,9871 | Nociception | TACR1 |
| rs3922843 | 3 | 38582852 | A | G | 0,7569 | -0,0066 | 0,0343 | 0,8467 | 0,9871 | Migraine | SCN5A |
| rs35430524 | 15 | 88855322 | C | A | 0,1077 | -0,0092 | 0,0474 | 0,8469 | 0,9871 | Neuraxial Pain | ACAN |
| rs1865442 | 8 | 68661930 | C | T | 0,1796 | 0,0074 | 0,0383 | 0,8472 | 0,9871 | Neuraxial pain | C8orf34 |
| rs79895530 | 9 | 107654141 | C | T | 0,1376 | 0,0080 | 0,0418 | 0,8474 | 0,9871 | Arthritis | RNU6-996P |

| | | | | | | | | | | | |
|---|---|---|---|---|---|---|---|---|---|---|---|
| rs2183080 | 14 | 54902268 | G | C | 0,1045 | 0,0090 | 0,0470 | 0,8479 | 0,9871 | Neuraxial Pain | GCH1 |
| rs1875999 | 5 | 76969157 | T | C | 0,3666 | -0,0058 | 0,0303 | 0,8485 | 0,9871 | Musculoskeletal Pain | CRHBP |
| rs7967762 | 12 | 48026431 | C | T | 0,1616 | -0,0074 | 0,0388 | 0,8489 | 0,9871 | Arthritis | RP1-228P16.4 |
| rs10842226 | 12 | 23806655 | G | A | 0,4020 | 0,0057 | 0,0301 | 0,8490 | 0,9871 | Arthritis | SOX5 |
| rs4804217 | 19 | 7634461 | C | T | 0,3537 | -0,0057 | 0,0301 | 0,8501 | 0,9871 | Neuropathic pain | PCP2 |
| rs2069705 | 12 | 68161231 | G | A | 0,6998 | 0,0060 | 0,0320 | 0,8505 | 0,9871 | Neuraxial Pain | |
| rs2076054 | 22 | 32436887 | C | T | 0,7654 | -0,0065 | 0,0349 | 0,8518 | 0,9871 | Migraine | SUV39H2 |
| rs4252548 | 19 | 55368304 | C | T | 0,0255 | -0,0171 | 0,0931 | 0,8539 | 0,9871 | Arthritis | IL11 |
| rs10802789 | 1 | 239669380 | C | T | 0,4288 | 0,0054 | 0,0295 | 0,8547 | 0,9871 | Analgesia | CHRM3 |
| rs4742323 | 9 | 7286743 | C | G | 0,3731 | 0,0055 | 0,0307 | 0,8564 | 0,9871 | Migraine | |
| rs1676303 | 14 | 76525821 | C | T | 0,8838 | -0,0083 | 0,0459 | 0,8570 | 0,9871 | Temporomandibular Disorder | |
| rs10156191 | 7 | 150856517 | C | T | 0,2632 | -0,0060 | 0,0336 | 0,8573 | 0,9871 | Migraine | AOC1 |
| rs34003284 | 13 | 53328741 | C | A | 0,3068 | -0,0057 | 0,0320 | 0,8577 | 0,9871 | Other Clinical Pain | C6orf106 |
| rs10028494 | 4 | 69105219 | A | C | 0,2202 | 0,0064 | 0,0359 | 0,8585 | 0,9871 | Analgesia | UGT2B7 |
| rs7645358 | 3 | 38586334 | A | G | 0,1247 | -0,0080 | 0,0451 | 0,8590 | 0,9871 | Migraine | SCN5A |
| rs7766029 | 6 | 88137716 | T | C | 0,4964 | 0,0049 | 0,0288 | 0,8636 | 0,9871 | Migraine | CNR1 |
| rs3793243 | 7 | 73707017 | A | G | 0,6121 | -0,0051 | 0,0298 | 0,8641 | 0,9871 | Migraine | STX1A |
| rs740603 | 22 | 19957654 | A | G | 0,5472 | -0,0050 | 0,0294 | 0,8647 | 0,9871 | Analgesia, Post-operative pain | COMT |
| rs2271275 | 10 | 1185028 | C | T | 0,6847 | 0,0052 | 0,0314 | 0,8676 | 0,9871 | Migraine | ADARB2 |
| rs2995082 | 1 | 167437008 | T | C | 0,4886 | -0,0049 | 0,0294 | 0,8682 | 0,9871 | Cancer Pain | CD247 |
| rs9316233 | 13 | 46859220 | C | G | 0,1840 | 0,0063 | 0,0381 | 0,8695 | 0,9871 | Temporomandibular Disorder | HTR2A |
| rs558025 | 6 | 154120830 | A | G | 0,2365 | -0,0056 | 0,0341 | 0,8695 | 0,9871 | Analgesia | OPRM1 |
| rs4790522 | 17 | 3566559 | A | C | 0,5593 | -0,0048 | 0,0294 | 0,8702 | 0,9871 | Migraine | TRPV1 |
| rs737866 | 22 | 19942586 | T | C | 0,3136 | 0,0051 | 0,0315 | 0,8713 | 0,9871 | Analgesia | COMT |
| rs737865 | 22 | 19942598 | A | G | 0,3136 | 0,0051 | 0,0315 | 0,8713 | 0,9871 | Musculoskeletal Pain | COMT |
| rs2591168 | 2 | 154761421 | G | A | 0,7584 | 0,0057 | 0,0352 | 0,8720 | 0,9871 | Cancer Pain | KCNJ3 |
| rs6926377 | 6 | 144784218 | A | C | 0,3128 | 0,0049 | 0,0310 | 0,8748 | 0,9871 | Other Clinical Pain | UTRN |
| rs11714003 | 3 | 54200440 | A | G | 0,1556 | 0,0062 | 0,0397 | 0,8760 | 0,9871 | Migraine | CACNA2D3 |
| rs2424248 | 20 | 19669680 | G | A | 0,1463 | 0,0064 | 0,0413 | 0,8772 | 0,9871 | Other Clinical Pain | SLC24A3 |
| rs62242105 | 3 | 20588903 | G | A | 0,2992 | -0,0049 | 0,0318 | 0,8774 | 0,9871 | Arthritis | RNU6-815P |
| rs11172113 | 12 | 57133500 | T | C | 0,3780 | -0,0046 | 0,0300 | 0,8792 | 0,9871 | Migraine | LRP1 |
| rs1060826 | 17 | 27762841 | T | C | 0,6249 | 0,0046 | 0,0304 | 0,8794 | 0,9871 | Neuraxial Pain | NOS2 |
| rs7121 | 20 | 58903752 | C | T | 0,5304 | -0,0045 | 0,0295 | 0,8799 | 0,9871 | Migraine | GNAS |
| rs9981884 | 21 | 39213707 | G | A | 0,4713 | 0,0044 | 0,0290 | 0,8804 | 0,9871 | Post-operative pain | BRWD1 |
| rs4775319 | 15 | 60921365 | G | A | 0,6393 | -0,0045 | 0,0307 | 0,8827 | 0,9871 | Neuropathic pain | RORA |
| rs702757 | 4 | 147488120 | T | A | 0,3126 | 0,0046 | 0,0313 | 0,8836 | 0,9871 | Migraine | EDNRA |
| rs3111020 | 2 | 154710877 | T | C | 0,4439 | -0,0043 | 0,0294 | 0,8836 | 0,9871 | Post-operative Pain | KCNJ3 |
| rs2236857 | 1 | 28835097 | T | C | 0,2951 | -0,0046 | 0,0316 | 0,8842 | 0,9871 | Temporomandibular Disorder | OPRD1 |
| rs689466 | 1 | 186681619 | T | C | 0,1655 | 0,0057 | 0,0392 | 0,8853 | 0,9871 | Migraine | |
| rs606148 | 6 | 154114852 | A | C | 0,9098 | 0,0073 | 0,0508 | 0,8858 | 0,9871 | Post-operative Pain | OPRM1 |
| rs613341 | 6 | 154122144 | T | C | 0,9098 | 0,0073 | 0,0508 | 0,8858 | 0,9871 | Post-operative Pain | OPRM1 |
| rs7718461 | 5 | 76962223 | A | G | 0,4132 | 0,0042 | 0,0294 | 0,8865 | 0,9871 | Musculoskeletal Pain | CRHBP |
| rs11030096 | 11 | 27643996 | T | C | 0,4903 | 0,0042 | 0,0296 | 0,8867 | 0,9871 | Neuraxial pain | BDNF-AS |
| rs7147286 | 14 | 54891947 | G | A | 0,3230 | -0,0044 | 0,0311 | 0,8881 | 0,9871 | Neuraxial Pain | GCH1 |
| rs2878172 | 14 | 54906952 | A | G | 0,4081 | -0,0041 | 0,0293 | 0,8887 | 0,9871 | Neuraxial Pain | GCH1 |
| rs11959113 | 5 | 148848933 | G | A | 0,2472 | -0,0047 | 0,0337 | 0,8901 | 0,9871 | Analgesia | |

| | | | | | | | | | | | |
|---|---|---|---|---|---|---|---|---|---|---|---|
| rs6314 | 13 | 46834899 | G | A | 0,0921 | 0,0070 | 0,0512 | 0,8919 | 0,9871 | Fibromyalgia | LOC105371720 |
| rs2653349 | 6 | 55277539 | A | G | 0,8111 | -0,0050 | 0,0371 | 0,8924 | 0,9871 | Post-operative Pain | HCRTR2 |
| rs563649 | 6 | 154086832 | C | T | 0,0843 | 0,0071 | 0,0528 | 0,8927 | 0,9871 | Nociception | OPRM1 |
| rs11014504 | 10 | 18495059 | T | C | 0,4473 | -0,0039 | 0,0291 | 0,8938 | 0,9871 | Migraine | CACNB2 |
| rs6271 | 9 | 133657152 | C | T | 0,0566 | -0,0085 | 0,0638 | 0,8945 | 0,9871 | Migraine | DBH-AS1 |
| rs1814270 | 16 | 55683165 | T | C | 0,4310 | 0,0039 | 0,0298 | 0,8951 | 0,9871 | Cancer Pain | SLC6A2 |
| rs986222 | 10 | 90171130 | G | A | 0,4718 | -0,0038 | 0,0289 | 0,8951 | 0,9871 | Migraine | |
| rs11757063 | 6 | 96437010 | G | A | 0,2059 | 0,0046 | 0,0362 | 0,8979 | 0,9871 | Migraine | UFL1-AS1 |
| rs3024496 | 1 | 206768519 | A | G | 0,4419 | 0,0037 | 0,0289 | 0,8979 | 0,9871 | Temporomandibular Disorder | IL10 |
| rs3754701 | 2 | 237858561 | A | T | 0,3576 | 0,0039 | 0,0307 | 0,8984 | 0,9871 | Migraine | RAMP1 |
| rs2600685 | 2 | 174762320 | T | C | 0,3974 | 0,0038 | 0,0301 | 0,8991 | 0,9871 | Migraine | CHRNA1 |
| rs7897594 | 10 | 18129251 | A | G | 0,2705 | 0,0041 | 0,0326 | 0,9006 | 0,9871 | Migraine | |
| rs6703152 | 1 | 118187574 | C | A | 0,6429 | -0,0038 | 0,0304 | 0,9010 | 0,9871 | Post-operative pain | COL11A1 |
| rs3783641 | 14 | 54893421 | T | A | 0,1969 | -0,0045 | 0,0367 | 0,9019 | 0,9871 | Neuraxial Pain | GCH1 |
| rs7076100 | 10 | 18470608 | T | A | 0,4074 | -0,0036 | 0,0295 | 0,9020 | 0,9871 | Migraine | CACNB2 |
| rs5761159 | 22 | 25706341 | G | T | 0,3636 | 0,0038 | 0,0310 | 0,9021 | 0,9871 | Neuropathic pain | GRK3 |
| rs17576 | 20 | 46011586 | A | G | 0,3420 | 0,0038 | 0,0308 | 0,9025 | 0,9871 | Neuraxial Pain | MMP9 |
| rs7581446 | 2 | 33198734 | C | T | 0,4934 | -0,0035 | 0,0294 | 0,9043 | 0,9871 | Arthritis | LTBP1 |
| rs599945 | 6 | 154121435 | C | A | 0,9079 | -0,0060 | 0,0503 | 0,9052 | 0,9871 | Post-operative Pain | OPRM1 |
| rs616585 | 6 | 154122747 | A | G | 0,9079 | -0,0060 | 0,0503 | 0,9052 | 0,9871 | Post-operative Pain | OPRM1 |
| rs9340799 | 6 | 151842246 | A | G | 0,3554 | -0,0036 | 0,0308 | 0,9068 | 0,9871 | Temporomandibular Disorder | ESR1 |
| rs3024491 | 1 | 206771701 | C | A | 0,4407 | 0,0033 | 0,0289 | 0,9080 | 0,9871 | Post-operative Pain | IL19 |
| rs609148 | 6 | 154109880 | G | A | 0,2363 | -0,0039 | 0,0340 | 0,9091 | 0,9871 | Nociception | OPRM1 |
| rs17350991 | 1 | 174114330 | G | T | 0,2615 | 0,0037 | 0,0327 | 0,9098 | 0,9871 | Migraine | |
| rs3780039 | 8 | 139664421 | A | C | 0,2817 | -0,0037 | 0,0329 | 0,9103 | 0,9871 | Cancer Pain | KCNK9 |
| rs978851 | 10 | 98900544 | C | T | 0,6918 | 0,0035 | 0,0309 | 0,9103 | 0,9871 | Migraine | HPSE2 |
| rs2075572 | 6 | 154090869 | G | C | 0,5890 | -0,0033 | 0,0292 | 0,9114 | 0,9871 | Nociception | OPRM1 |
| rs2530552 | 7 | 34658764 | A | G | 0,3760 | -0,0034 | 0,0304 | 0,9114 | 0,9871 | Other Clinical Pain | NPSR1-AS1 |
| rs9479757 | 6 | 154090209 | G | A | 0,0887 | 0,0056 | 0,0511 | 0,9123 | 0,9871 | Nociception | OPRM1 |
| rs1923884 | 13 | 46847701 | C | T | 0,1369 | 0,0046 | 0,0422 | 0,9124 | 0,9871 | Cancer Pain | HTR2A |
| rs5742912 | 12 | 6349184 | A | G | 0,0267 | 0,0097 | 0,0894 | 0,9132 | 0,9871 | Migraine | SCNN1A |
| rs3212227 | 5 | 159315942 | T | G | 0,2307 | -0,0037 | 0,0346 | 0,9142 | 0,9871 | Neuraxial pain | IL12B |
| rs3025039 | 6 | 43784799 | C | T | 0,1424 | -0,0043 | 0,0414 | 0,9172 | 0,9871 | Neuraxial Pain | POLR1C |
| rs10491334 | 5 | 111436706 | C | T | 0,1877 | 0,0039 | 0,0378 | 0,9176 | 0,9871 | Temporomandibular Disorder | CAMK4 |
| rs3777580 | 6 | 45942727 | A | C | 0,3583 | -0,0031 | 0,0302 | 0,9181 | 0,9871 | Migraine | CLIC5 |
| rs12202891 | 6 | 12767986 | C | T | 0,1590 | 0,0041 | 0,0398 | 0,9182 | 0,9871 | Migraine | PHACTR1 |
| rs533586 | 6 | 154092539 | C | T | 0,6736 | -0,0031 | 0,0307 | 0,9187 | 0,9871 | Nociception | OPRM1 |
| rs7330636 | 13 | 46849457 | C | T | 0,3984 | -0,0030 | 0,0296 | 0,9193 | 0,9871 | Cancer Pain | HTR2A |
| rs1801708 | 4 | 147481217 | G | A | 0,3123 | 0,0030 | 0,0313 | 0,9226 | 0,9871 | Migraine | EDNRA |
| rs466448 | 21 | 26171790 | A | G | 0,4570 | 0,0028 | 0,0292 | 0,9232 | 0,9871 | Temporomandibular Disorder | |
| rs7787744 | 7 | 150824008 | A | G | 0,3508 | 0,0030 | 0,0309 | 0,9237 | 0,9871 | Post-operative pain | AOC1 |
| rs2049046 | 11 | 27702228 | T | A | 0,4835 | 0,0028 | 0,0297 | 0,9242 | 0,9871 | Migraine | BDNF |
| rs2038740 | 6 | 35146765 | C | T | 0,7227 | 0,0031 | 0,0332 | 0,9244 | 0,9871 | Post-operative pain | TCP11 |
| rs1053989 | 5 | 76969210 | C | A | 0,4076 | 0,0027 | 0,0294 | 0,9255 | 0,9871 | Musculoskeletal Pain | CRHBP |
| rs998259 | 14 | 54888313 | C | T | 0,2392 | -0,0032 | 0,0348 | 0,9260 | 0,9871 | Neuraxial Pain | GCH1 |
| rs7438135 | 4 | 69095621 | G | A | 0,4796 | 0,0027 | 0,0296 | 0,9265 | 0,9871 | Analgesia | UGT2B7 |

| | | | | | | | | | | | |
|---|---|---|---|---|---|---|---|---|---|---|---|
| rs7439366 | 4 | 69098620 | T | C | 0,4796 | 0,0027 | 0,0296 | 0,9265 | 0,9871 | Analgesia | UGT2B7 |
| rs4794106 | 17 | 50160933 | T | C | 0,5579 | -0,0027 | 0,0296 | 0,9269 | 0,9871 | Temporomandibular Disorder | LOC105371818 |
| rs11078454 | 17 | 3522260 | T | C | 0,4640 | -0,0027 | 0,0295 | 0,9283 | 0,9871 | Migraine | TRPV3 |
| rs2234677 | 2 | 113117932 | G | A | 0,2501 | -0,0030 | 0,0340 | 0,9286 | 0,9871 | Neuraxial Pain | IL1RN |
| rs726281 | 6 | 151981443 | G | A | 0,7212 | 0,0028 | 0,0322 | 0,9300 | 0,9871 | Migraine | ESR1 |
| rs998424 | 16 | 55698034 | G | A | 0,3281 | 0,0027 | 0,0307 | 0,9309 | 0,9871 | Neuropathic pain | SLC6A2 |
| rs1800896 | 1 | 206773552 | T | C | 0,4429 | 0,0025 | 0,0289 | 0,9323 | 0,9871 | Temporomandibular Disorder | IL19 |
| rs10992729 | 9 | 93418793 | C | T | 0,3308 | 0,0026 | 0,0308 | 0,9335 | 0,9871 | Other Clinical Pain | |
| rs2004295 | 6 | 39187090 | A | G | 0,2618 | -0,0027 | 0,0335 | 0,9347 | 0,9871 | Migraine | |
| rs1809889 | 12 | 124316680 | T | C | 0,7436 | 0,0027 | 0,0335 | 0,9351 | 0,9871 | Arthritis | FAM101A |
| rs1801394 | 5 | 7870860 | A | G | 0,5309 | 0,0023 | 0,0289 | 0,9362 | 0,9871 | Temporomandibular Disorder | MTRR |
| rs1133076 | 8 | 133113438 | G | A | 0,4813 | 0,0023 | 0,0290 | 0,9367 | 0,9871 | Neuropathic Pain | TG |
| rs7684253 | 4 | 56861145 | C | T | 0,5647 | 0,0023 | 0,0294 | 0,9369 | 0,9871 | Migraine | |
| rs5746849 | 22 | 19955474 | A | G | 0,5399 | -0,0023 | 0,0290 | 0,9373 | 0,9871 | Analgesia | COMT |
| rs4587017 | 4 | 69081680 | T | G | 0,5143 | -0,0023 | 0,0296 | 0,9373 | 0,9871 | Analgesia | UGT2B7 |
| rs10915437 | 1 | 4122946 | A | G | 0,3522 | -0,0024 | 0,0308 | 0,9376 | 0,9871 | Migraine | |
| rs146377178 | 8 | 25529457 | C | T | 0,0231 | -0,0076 | 0,0976 | 0,9377 | 0,9871 | Migraine | |
| rs1878672 | 1 | 206770368 | G | C | 0,4431 | 0,0022 | 0,0289 | 0,9380 | 0,9871 | Post-operative Pain | IL19 |
| rs28577186 | 16 | 4438190 | G | A | 0,6791 | -0,0024 | 0,0308 | 0,9389 | 0,9871 | Migraine | DNAJA3 |
| rs3808353 | 7 | 1093336 | G | A | 0,1684 | -0,0030 | 0,0393 | 0,9395 | 0,9871 | Migraine | C7orf50 |
| rs1277441 | 12 | 118168184 | G | A | 0,6565 | -0,0023 | 0,0309 | 0,9399 | 0,9871 | Analgesia | TAOK3 |
| rs4866176 | 5 | 20245445 | C | T | 0,0515 | -0,0049 | 0,0667 | 0,9410 | 0,9873 | Neuropathic Pain | CDH18 |
| rs728273 | 7 | 112428046 | G | C | 0,5792 | 0,0021 | 0,0295 | 0,9426 | 0,9873 | Temporomandibular Disorder | IFRD1 |
| rs11615115 | 12 | 100408674 | A | G | 0,0442 | -0,0050 | 0,0707 | 0,9432 | 0,9873 | Migraine | SLC17A8 |
| rs17120227 | 12 | 58895568 | C | T | 0,0581 | 0,0044 | 0,0614 | 0,9434 | 0,9873 | Post-operative pain | LRIG3 |
| rs2066713 | 17 | 30224647 | G | A | 0,3831 | -0,0021 | 0,0305 | 0,9453 | 0,9874 | Migraine | SLC6A4 |
| rs546240 | 11 | 30512075 | C | T | 0,6213 | 0,0021 | 0,0303 | 0,9458 | 0,9874 | Migraine | MPPED2 |
| rs8007267 | 14 | 54912273 | C | T | 0,1864 | 0,0025 | 0,0372 | 0,9460 | 0,9874 | Other Clinical Pain | |
| rs285026 | 16 | 77066192 | G | T | 0,5681 | 0,0019 | 0,0292 | 0,9485 | 0,9890 | Other Clinical Pain | |
| rs6515020 | 20 | 19524260 | C | T | 0,0958 | -0,0032 | 0,0501 | 0,9495 | 0,9891 | Migraine | SLC24A3 |
| rs733701 | 6 | 39204086 | C | T | 0,2538 | -0,0021 | 0,0334 | 0,9508 | 0,9891 | Migraine | KCNK5 |
| rs8181477 | 10 | 18493951 | A | C | 0,4468 | -0,0018 | 0,0293 | 0,9511 | 0,9891 | Migraine | CACNB2 |
| rs62098013 | 18 | 53337491 | G | A | 0,3738 | -0,0017 | 0,0299 | 0,9537 | 0,9909 | Other Clinical Pain | DCC |
| rs208296 | 12 | 121163150 | G | A | 0,3316 | -0,0017 | 0,0306 | 0,9560 | 0,9911 | Musculoskeletal Pain | P2RX7 |
| rs7290221 | 22 | 19955157 | C | G | 0,5396 | -0,0015 | 0,0290 | 0,9591 | 0,9911 | Analgesia | COMT |
| rs3020377 | 6 | 151951263 | G | A | 0,6697 | 0,0016 | 0,0315 | 0,9595 | 0,9911 | Musculoskeletal Pain | COMT |
| rs6985606 | 8 | 53248556 | T | C | 0,4934 | -0,0014 | 0,0289 | 0,9601 | 0,9911 | Post-operative Pain | OPRK1 |
| rs3024505 | 1 | 206766559 | G | A | 0,1502 | 0,0021 | 0,0411 | 0,9601 | 0,9911 | Post-operative Pain | IL19 |
| rs2716212 | 17 | 69507512 | A | G | 0,3923 | 0,0015 | 0,0300 | 0,9604 | 0,9911 | Post-operative pain | MAP2K6 |
| rs858003 | 21 | 37700681 | G | A | 0,2064 | 0,0018 | 0,0368 | 0,9610 | 0,9911 | Post-operative Pain | LOC107985507 |
| rs1530586 | 4 | 1759200 | C | T | 0,7893 | 0,0018 | 0,0365 | 0,9611 | 0,9911 | Post-operative pain | TACC3 |
| rs28428925 | 3 | 107575787 | G | A | 0,1369 | 0,0020 | 0,0426 | 0,9628 | 0,9911 | Other Clinical Pain | BBX |
| rs11895478 | 2 | 154714611 | C | T | 0,2983 | -0,0015 | 0,0327 | 0,9630 | 0,9911 | Post-operative Pain | KCNJ3 |
| rs12947578 | 17 | 80272935 | C | T | 0,3896 | -0,0014 | 0,0303 | 0,9632 | 0,9911 | Migraine | RNF213 |
| rs589046 | 6 | 154072003 | C | T | 0,2487 | -0,0015 | 0,0336 | 0,9647 | 0,9913 | Analgesia | OPRM1 |
| rs17486278 | 15 | 78575140 | A | C | 0,3792 | -0,0013 | 0,0305 | 0,9650 | 0,9913 | Neuraxial pain | CHRNA5 |

| | | | | | | | | | | | |
|---|---|---|---|---|---|---|---|---|---|---|---|
| rs4411121 | 1 | 118214411 | C | T | 0,3418 | -0,0013 | 0,0305 | 0,9664 | 0,9914 | Arthritis | SPAG17 |
| rs33389 | 5 | 143320934 | C | T | 0,1276 | 0,0018 | 0,0432 | 0,9669 | 0,9914 | Temporomandibular Disorder | NR3C1 |
| rs4707436 | 6 | 88142032 | G | A | 0,2501 | -0,0013 | 0,0330 | 0,9679 | 0,9916 | Migraine | CNR1 |
| rs2455858 | 17 | 3546111 | T | A | 0,3994 | -0,0012 | 0,0301 | 0,9688 | 0,9916 | Migraine | TRPV3 |
| rs3792603 | 4 | 55435891 | A | G | 0,2139 | -0,0013 | 0,0355 | 0,9698 | 0,9918 | Migraine | CLOCK |
| rs2228570 | 12 | 47879112 | A | G | 0,5897 | -0,0011 | 0,0296 | 0,9713 | 0,9923 | Migraine | VDR |
| rs548646 | 6 | 154097012 | T | C | 0,6726 | -0,0011 | 0,0306 | 0,9719 | 0,9923 | Post-operative Pain | OPRM1 |
| rs1570360 | 6 | 43770093 | A | G | 0,6957 | -0,0010 | 0,0313 | 0,9745 | 0,9941 | Migraine | POLR1C |
| rs900379 | 5 | 44369554 | C | T | 0,6514 | 0,0009 | 0,0307 | 0,9766 | 0,9953 | Temporomandibular disorders | FGF10 |
| rs795484 | 12 | 118152057 | T | C | 0,6565 | -0,0008 | 0,0309 | 0,9806 | 0,9959 | Analgesia | TAOK3 |
| rs35260355 | 1 | 33480230 | C | T | 0,1458 | -0,0010 | 0,0411 | 0,9813 | 0,9959 | Neuropathic Pain | ZSCAN20 |
| rs4815670 | 20 | 4236217 | A | G | 0,5493 | -0,0006 | 0,0291 | 0,9834 | 0,9959 | Cancer Pain | ADRA1D |
| rs2946505 | 8 | 12953643 | T | G | 0,8077 | 0,0008 | 0,0372 | 0,9837 | 0,9959 | Migraine | SUV39H2 |
| rs3093664 | 6 | 31576865 | A | G | 0,0306 | -0,0017 | 0,0847 | 0,9839 | 0,9959 | Migraine | TNF |
| rs495491 | 6 | 154061407 | A | G | 0,2491 | 0,0006 | 0,0336 | 0,9850 | 0,9959 | Nociception | OPRM1 |
| rs3811047 | 2 | 112913833 | A | G | 0,7015 | 0,0006 | 0,0323 | 0,9857 | 0,9959 | Musculoskeletal Pain | IL37 |
| rs1330349 | 9 | 115078463 | G | C | 0,5501 | -0,0005 | 0,0295 | 0,9859 | 0,9959 | Arthritis | TNC |
| rs11786084 | 8 | 141641609 | G | A | 0,3133 | 0,0005 | 0,0315 | 0,9862 | 0,9959 | Other Clinical Pain | |
| rs73271865 | 7 | 21359709 | C | T | 0,0280 | 0,0015 | 0,0872 | 0,9862 | 0,9959 | Temporomandibular Disorder | |
| rs12596162 | 16 | 87117889 | C | T | 0,3145 | 0,0005 | 0,0309 | 0,9867 | 0,9959 | Neuropathic Pain | LOC105371394 |
| rs1332847 | 6 | 12892522 | C | T | 0,3036 | -0,0005 | 0,0311 | 0,9874 | 0,9959 | Migraine | PHACTR1 |
| rs2296972 | 13 | 46854336 | A | C | 0,7078 | 0,0005 | 0,0318 | 0,9884 | 0,9959 | Neuropathic pain | HTR2A |
| rs8040868 | 15 | 78618839 | T | C | 0,4302 | -0,0004 | 0,0295 | 0,9891 | 0,9959 | Neuraxial pain | CHRNA3 |
| rs1426371 | 12 | 108236003 | G | A | 0,2530 | -0,0003 | 0,0333 | 0,9927 | 0,9970 | Arthritis | WSCD2 |
| rs4659479 | 1 | 236872754 | G | A | 0,5984 | 0,0002 | 0,0296 | 0,9939 | 0,9970 | Migraine | MTR |
| rs17034687 | 3 | 3638168 | C | G | 0,0788 | 0,0004 | 0,0529 | 0,9942 | 0,9970 | Neuraxial Pain | |
| rs6724624 | 2 | 233911933 | C | G | 0,1911 | -0,0003 | 0,0381 | 0,9947 | 0,9970 | Analgesia | |
| rs10166942 | 2 | 233916448 | T | C | 0,1911 | -0,0003 | 0,0381 | 0,9947 | 0,9970 | Migraine | |
| rs2805050 | 1 | 162867060 | A | C | 0,9502 | -0,0004 | 0,0677 | 0,9953 | 0,9970 | Fibromyalgia | CCDC190 |
| rs2010963 | 6 | 43770613 | C | G | 0,6526 | 0,0000 | 0,0306 | 0,9995 | 0,9997 | Migraine | POLR1C |
| rs540825 | 6 | 154093311 | A | T | 0,7630 | 0,0000 | 0,0340 | 0,9997 | 0,9997 | Analgesia | OPRM1 |

* According to GRCh38 release; ^ in Human Pain Gene database

rsID, variant ID in dbSNP; SE, standard error; FDR, false discovery rate

**Supplementary Table S10.** Summary statistics from our GWAS of variants reported by *Galvan A. et al .* and by *Nishizawa D. et al.* as significantly associated with pain relief and opioid requirements, respectively.

| rsID | Chromosome | Position (bp)* | Allele 0 | Allele 1 | Allele 1 frequency | BETA | SE | *P* -value | FDR |
|---|---|---|---|---|---|---|---|---|---|
| *Galvan A. et al.* | | | | | | | | | |
| rs12948783 | 17 | 76.503.318 | G | A | 0,17 | 0,066 | 0,039 | 0,091 | 0,58 |
| rs13421094 | 2 | 157.185.290 | A | G | 0,16 | -0,057 | 0,039 | 0,145 | 0,58 |
| rs12211463 | 6 | 92.757.440 | T | G | 0,22 | -0,043 | 0,036 | 0,224 | 0,60 |
| rs7104613 | 11 | 14.058.384 | C | T | 0,07 | 0,056 | 0,058 | 0,332 | 0,63 |
| rs2473967 | 6 | 113.158.133 | G | T | 0,94 | -0,054 | 0,063 | 0,392 | 0,63 |
| rs10413396 | 19 | 44.309.549 | G | T | 0,05 | 0,042 | 0,069 | 0,539 | 0,63 |
| rs7757130 | 6 | 112.996.060 | C | A | 0,07 | 0,035 | 0,059 | 0,549 | 0,63 |
| rs2884129 | 10 | 17.543.150 | T | G | 0,21 | 0,016 | 0,036 | 0,664 | 0,66 |
| *Nishizawa D. et al.* | | | | | | | | | |
| rs1283671 | 8 | 107.421.459 | C | T | 0,11 | 0,031 | 0,047 | 0,509 | 0,81 |
| rs1283720 | 8 | 107.460.100 | G | A | 0,14 | 0,019 | 0,042 | 0,652 | 0,81 |
| rs72752701 | 9 | 125.992.274 | A | C | 0,06 | 0,015 | 0,060 | 0,809 | 0,81 |

* According to GRCh38 release

rsID, variant ID in dbSNP; SE, standard error; FDR, false discovery rate

**Supplementary Table S11.** Summary statistics from our GWAS of variants reported by *Mocci e. et al .* , sorted on the basis of their *P* -value of association with pain intensity in our study.

| rsID | Chromosome | Position (bp) * | Allele 0 | Allele 1 | Allele 1 frequency | BETA | SE | *P* -value | FDR |
|---|---|---|---|---|---|---|---|---|---|
| rs143384 | 20 | 35437976 | G | A | 0,43 | -0,084 | 0,029 | **0,0039** | 0,38 |
| rs11764590 | 7 | 1993168 | C | T | 0,23 | 0,087 | 0,035 | **0,013** | 0,65 |
| rs583104 | 1 | 109278685 | G | T | 0,79 | -0,079 | 0,035 | **0,027** | 0,82 |
| rs1537375 | 9 | 22116072 | T | C | 0,53 | 0,058 | 0,029 | **0,046** | 0,82 |
| rs3904683 | 1 | 243253223 | T | C | 0,40 | -0,059 | 0,030 | **0,048** | 0,82 |
| rs938724 | 8 | 140647034 | G | A | 0,63 | 0,058 | 0,030 | 0,051 | 0,82 |
| rs6478241 | 9 | 116490350 | A | G | 0,63 | -0,056 | 0,030 | 0,066 | 0,90 |
| rs1325266 | 1 | 66694919 | A | G | 0,42 | -0,053 | 0,030 | 0,077 | 0,90 |
| rs4420638 | 19 | 44919689 | A | G | 0,16 | 0,065 | 0,040 | 0,105 | 0,90 |
| rs2111592 | 2 | 207184857 | G | A | 0,34 | -0,050 | 0,032 | 0,116 | 0,90 |
| rs12445022 | 16 | 87541726 | G | A | 0,36 | -0,046 | 0,031 | 0,129 | 0,90 |
| rs11145043 | 9 | 69073560 | T | G | 0,44 | -0,043 | 0,030 | 0,151 | 0,90 |
| rs7335163 | 13 | 53415840 | T | G | 0,44 | 0,042 | 0,029 | 0,153 | 0,90 |
| rs10063803 | 5 | 177240326 | C | A | 0,84 | 0,057 | 0,040 | 0,160 | 0,90 |
| rs1050316 | 1 | 156464911 | G | T | 0,69 | -0,043 | 0,031 | 0,164 | 0,90 |
| rs967823 | 17 | 52239916 | A | G | 0,38 | -0,042 | 0,030 | 0,170 | 0,90 |
| rs9426902 | 1 | 153746270 | G | A | 0,40 | 0,040 | 0,030 | 0,182 | 0,90 |
| rs2395607 | 6 | 34805950 | C | T | 0,16 | -0,052 | 0,040 | 0,185 | 0,90 |
| rs2160875 | 12 | 4418156 | C | T | 0,56 | 0,037 | 0,029 | 0,204 | 0,90 |
| rs3914722 | 2 | 50763901 | G | A | 0,12 | 0,058 | 0,046 | 0,211 | 0,90 |
| rs11751469 | 6 | 33836770 | C | T | 0,35 | -0,038 | 0,030 | 0,213 | 0,90 |
| rs1413573 | 13 | 66377697 | G | A | 0,49 | -0,036 | 0,029 | 0,215 | 0,90 |
| rs4895846 | 6 | 129063222 | T | C | 0,58 | 0,037 | 0,030 | 0,220 | 0,90 |
| rs13207082 | 6 | 27283600 | A | G | 0,05 | -0,085 | 0,070 | 0,222 | 0,90 |
| rs301805 | 1 | 8420956 | T | G | 0,51 | 0,032 | 0,028 | 0,261 | 0,97 |
| rs1350166 | 12 | 69242534 | G | T | 0,41 | -0,033 | 0,030 | 0,263 | 0,97 |
| rs17343925 | 2 | 103809919 | G | T | 0,47 | -0,032 | 0,029 | 0,283 | 0,97 |
| rs775760 | 3 | 77537446 | A | C | 0,73 | -0,035 | 0,033 | 0,289 | 0,97 |

| | | | | | | | | | |
|---|---|---|---|---|---|---|---|---|---|
| rs583514 | 3 | 173396377 | T | C | 0,51 | -0,031 | 0,030 | 0,289 | 0,97 |
| rs9804988 | 12 | 23829625 | C | T | 0,10 | -0,049 | 0,049 | 0,318 | 0,98 |
| rs8046109 | 16 | 75326198 | A | G | 0,58 | 0,029 | 0,029 | 0,330 | 0,98 |
| rs2421015 | 10 | 122423575 | A | G | 0,05 | 0,057 | 0,065 | 0,384 | 0,98 |
| rs7924025 | 10 | 98998562 | T | C | 0,11 | 0,039 | 0,046 | 0,393 | 0,98 |
| rs3802847 | 11 | 113041581 | T | C | 0,39 | -0,025 | 0,030 | 0,400 | 0,98 |
| rs6658904 | 1 | 50641303 | G | T | 0,38 | -0,025 | 0,030 | 0,409 | 0,98 |
| rs7959516 | 12 | 110184419 | T | G | 0,09 | -0,040 | 0,051 | 0,438 | 0,98 |
| rs16988333 | 22 | 30156824 | A | G | 0,07 | -0,043 | 0,058 | 0,456 | 0,98 |
| rs2282888 | 7 | 21436514 | G | A | 0,64 | -0,023 | 0,031 | 0,461 | 0,98 |
| rs615030 | 18 | 57482122 | C | T | 0,29 | -0,023 | 0,032 | 0,475 | 0,98 |
| rs7716347 | 5 | 120796579 | C | T | 0,30 | -0,022 | 0,032 | 0,484 | 0,98 |
| rs11599236 | 10 | 104694914 | T | C | 0,47 | -0,020 | 0,029 | 0,494 | 0,98 |
| rs10948201 | 6 | 45125757 | C | A | 0,30 | 0,022 | 0,032 | 0,498 | 0,98 |
| rs1198583 | 1 | 98063822 | A | G | 0,83 | 0,026 | 0,040 | 0,511 | 0,98 |
| rs12612492 | 2 | 23870886 | C | T | 0,13 | 0,028 | 0,044 | 0,530 | 0,98 |
| rs11665070 | 18 | 37572600 | G | A | 0,66 | -0,019 | 0,031 | 0,531 | 0,98 |
| rs10782959 | 1 | 93346012 | A | G | 0,73 | -0,021 | 0,033 | 0,532 | 0,98 |
| rs773108 | 12 | 55976127 | A | G | 0,30 | -0,018 | 0,032 | 0,559 | 0,98 |
| rs2721348 | 7 | 120896344 | G | T | 0,18 | 0,020 | 0,037 | 0,584 | 0,98 |
| rs1245576 | 10 | 72050912 | T | C | 0,59 | 0,017 | 0,030 | 0,586 | 0,98 |
| rs2856238 | 3 | 50120758 | T | C | 0,57 | 0,016 | 0,030 | 0,592 | 0,98 |
| rs1951537 | 14 | 29091615 | A | G | 0,85 | 0,021 | 0,041 | 0,603 | 0,98 |
| rs17822981 | 2 | 210490771 | A | G | 0,27 | 0,017 | 0,032 | 0,606 | 0,98 |
| rs1934534 | 6 | 149711896 | T | C | 0,36 | -0,015 | 0,030 | 0,606 | 0,98 |
| rs12134493 | 1 | 115135325 | C | A | 0,10 | -0,024 | 0,048 | 0,618 | 0,98 |
| rs12532479 | 7 | 40388035 | T | C | 0,10 | -0,024 | 0,050 | 0,628 | 0,98 |
| rs2627316 | 15 | 80750475 | A | G | 0,50 | -0,013 | 0,029 | 0,642 | 0,98 |
| rs10774625 | 12 | 111472415 | A | G | 0,51 | 0,013 | 0,029 | 0,644 | 0,98 |
| rs12070469 | 1 | 15210626 | C | T | 0,37 | -0,014 | 0,030 | 0,646 | 0,98 |
| rs4909945 | 11 | 10652192 | T | C | 0,67 | 0,014 | 0,031 | 0,653 | 0,98 |

| | | | | | | | | | |
|---|---|---|---|---|---|---|---|---|---|
| rs1552284 | 8 | 22105096 | A | G | 0,44 | -0,013 | 0,029 | 0,654 | 0,98 |
| rs8057124 | 16 | 71938506 | T | C | 0,74 | 0,014 | 0,033 | 0,664 | 0,98 |
| rs1852470 | 7 | 114387214 | T | G | 0,57 | -0,013 | 0,029 | 0,667 | 0,98 |
| rs9349379 | 6 | 12903725 | A | G | 0,39 | -0,012 | 0,029 | 0,679 | 0,98 |
| rs8018823 | 14 | 37248972 | G | A | 0,29 | -0,013 | 0,032 | 0,691 | 0,98 |
| rs6790925 | 3 | 30438593 | C | T | 0,37 | -0,012 | 0,030 | 0,692 | 0,98 |
| rs3918286 | 6 | 160447636 | A | G | 0,33 | -0,011 | 0,030 | 0,714 | 0,98 |
| rs3863241 | 8 | 72978100 | C | T | 0,57 | 0,010 | 0,029 | 0,726 | 0,98 |
| rs618869 | 18 | 55580920 | T | C | 0,87 | -0,015 | 0,042 | 0,727 | 0,98 |
| rs12568655 | 1 | 174465194 | G | A | 0,40 | 0,009 | 0,030 | 0,760 | 0,98 |
| rs13114738 | 4 | 102363708 | C | T | 0,08 | -0,016 | 0,056 | 0,772 | 0,98 |
| rs9653003 | 18 | 22616147 | T | C | 0,48 | 0,008 | 0,029 | 0,774 | 0,98 |
| rs11729080 | 4 | 111582716 | G | A | 0,13 | -0,012 | 0,043 | 0,783 | 0,98 |
| rs16931821 | 12 | 83824 | T | C | 0,60 | 0,008 | 0,030 | 0,788 | 0,98 |
| rs9320821 | 6 | 121526572 | C | A | 0,16 | -0,011 | 0,040 | 0,790 | 0,98 |
| rs6119879 | 20 | 32517586 | C | T | 0,20 | -0,009 | 0,036 | 0,792 | 0,98 |
| rs554843 | 5 | 114318900 | C | A | 0,44 | -0,007 | 0,029 | 0,802 | 0,98 |
| rs11624776 | 14 | 93129246 | A | C | 0,34 | 0,007 | 0,031 | 0,813 | 0,98 |
| rs4244883 | 15 | 91003267 | T | G | 0,40 | 0,007 | 0,030 | 0,815 | 0,98 |
| rs17689882 | 17 | 45829462 | G | A | 0,22 | -0,008 | 0,036 | 0,817 | 0,98 |
| rs8614 | 17 | 29261788 | C | A | 0,19 | -0,008 | 0,037 | 0,821 | 0,98 |
| rs3021146 | 4 | 2956459 | A | G | 0,32 | -0,006 | 0,031 | 0,853 | 0,98 |
| rs11153082 | 6 | 96611790 | A | G | 0,36 | 0,006 | 0,031 | 0,853 | 0,98 |
| rs1570620 | 13 | 46627739 | C | T | 0,76 | 0,006 | 0,034 | 0,871 | 0,98 |
| rs2424245 | 20 | 19669072 | C | T | 0,15 | 0,006 | 0,041 | 0,877 | 0,98 |
| rs11172113 | 12 | 57133500 | T | C | 0,38 | -0,005 | 0,030 | 0,879 | 0,98 |
| rs1895910 | 12 | 108180501 | T | G | 0,22 | 0,005 | 0,035 | 0,882 | 0,98 |
| rs1876767 | 2 | 22378060 | G | T | 0,36 | -0,004 | 0,031 | 0,887 | 0,98 |
| rs4502841 | 5 | 30862908 | G | A | 0,52 | -0,004 | 0,029 | 0,897 | 0,98 |
| rs698915 | 1 | 150415842 | A | G | 0,74 | 0,003 | 0,034 | 0,925 | 0,98 |
| rs164741 | 16 | 89625890 | A | G | 0,71 | 0,003 | 0,033 | 0,926 | 0,98 |

| | | | | | | | | | |
|---|---|---|---|---|---|---|---|---|---|
| rs4860809 | 4 | 67004677 | T | C | 0,54 | -0,003 | 0,030 | 0,931 | 0,98 |
| rs12379660 | 9 | 93420205 | G | A | 0,33 | 0,003 | 0,031 | 0,933 | 0,98 |
| rs7684253 | 4 | 56861145 | C | T | 0,56 | 0,002 | 0,029 | 0,937 | 0,98 |
| rs16826012 | 1 | 39253847 | T | C | 0,17 | 0,002 | 0,039 | 0,964 | 0,99 |
| rs1431196 | 18 | 53305732 | A | G | 0,44 | 0,001 | 0,029 | 0,973 | 0,99 |
| rs7222591 | 17 | 49429657 | G | T | 0,41 | 0,000 | 0,029 | 0,989 | 0,99 |
| rs10166942 | 2 | 233916448 | T | C | 0,19 | 0,000 | 0,038 | 0,995 | 0,99 |

* According to GRCh38 release

rsID, variant ID in dbSNP; SE, standard error; FDR, false discovery rate

**Supplementary Table S12**. Summary statistics from our GWAS of variants reported by *Zorina-Lichtenwalter. et al* . , sorted on the basis of their *P* -value of association with pain intensity in our study.

| rsID | Chromosome | Position (bp)* | Allele 0 | Allele 1 | Allele 1 frequency | BETA | SE | *P* -value | FDR |
|---|---|---|---|---|---|---|---|---|---|
| rs11751591 | 6 | 33826438 | G | A | 0,14 | -0,114 | 0,042 | **0,006** | 0,15 |
| rs7190 | 18 | 5889766 | A | G | 0,64 | 0,079 | 0,030 | **0,009** | 0,15 |
| rs6506342 | 18 | 5871149 | A | G | 0,50 | 0,055 | 0,029 | 0,058 | 0,48 |
| rs3936100 | 18 | 5872443 | G | T | 0,38 | 0,053 | 0,030 | 0,077 | 0,48 |
| rs2263329 | 6 | 34627766 | T | C | 0,36 | -0,052 | 0,031 | 0,089 | 0,48 |
| rs12937096 | 17 | 52221081 | C | A | 0,33 | -0,051 | 0,031 | 0,099 | 0,48 |
| rs174811 | 3 | 76739411 | G | A | 0,83 | 0,064 | 0,039 | 0,102 | 0,48 |
| rs767896 | 6 | 33823738 | C | T | 0,33 | -0,045 | 0,031 | 0,139 | 0,57 |
| rs6446187 | 3 | 49869678 | C | A | 0,48 | -0,038 | 0,029 | 0,194 | 0,70 |
| rs11751469 | 6 | 33836770 | C | T | 0,35 | -0,038 | 0,030 | 0,213 | 0,70 |
| rs1859100 | 7 | 114554560 | T | G | 0,55 | 0,032 | 0,029 | 0,266 | 0,80 |
| rs11505922 | 7 | 114370596 | T | C | 0,43 | 0,027 | 0,029 | 0,355 | 0,90 |
| rs769668 | 4 | 139937563 | T | C | 0,34 | -0,028 | 0,031 | 0,367 | 0,90 |
| rs60658082 | 18 | 53380711 | C | T | 0,53 | 0,023 | 0,029 | 0,425 | 0,90 |
| rs3818528 | 6 | 33693314 | G | A | 0,66 | -0,024 | 0,031 | 0,428 | 0,90 |
| rs8097318 | 18 | 53023439 | T | C | 0,54 | 0,022 | 0,029 | 0,440 | 0,90 |
| rs7303854 | 12 | 15206307 | T | A | 0,34 | 0,021 | 0,031 | 0,491 | 0,90 |
| rs10250103 | 7 | 114654887 | C | T | 0,40 | -0,018 | 0,030 | 0,547 | 0,90 |
| rs10953758 | 7 | 114389808 | A | G | 0,56 | -0,017 | 0,029 | 0,559 | 0,90 |
| rs11877758 | 18 | 37558147 | T | G | 0,32 | 0,018 | 0,031 | 0,561 | 0,90 |
| rs12055409 | 6 | 33833733 | A | G | 0,65 | -0,016 | 0,030 | 0,590 | 0,90 |
| rs10269986 | 7 | 114571392 | A | G | 0,49 | 0,015 | 0,029 | 0,598 | 0,90 |
| rs55697235 | 16 | 71459311 | G | A | 0,04 | 0,031 | 0,073 | 0,668 | 0,91 |
| rs1547668 | 6 | 33807669 | A | G | 0,80 | 0,016 | 0,036 | 0,669 | 0,91 |
| rs34486623 | 18 | 52838138 | C | T | 0,42 | -0,012 | 0,030 | 0,687 | 0,91 |
| rs2219428 | 2 | 210382843 | C | G | 0,56 | 0,010 | 0,029 | 0,731 | 0,92 |
| rs17410557 | 18 | 53250021 | T | C | 0,40 | 0,006 | 0,030 | 0,832 | 0,92 |
| rs6961970 | 7 | 114261077 | C | A | 0,18 | -0,008 | 0,037 | 0,835 | 0,92 |
| rs10228350 | 7 | 114420608 | A | T | 0,35 | -0,006 | 0,030 | 0,837 | 0,92 |

| | | | | | | | | | |
|---|---|---|---|---|---|---|---|---|---|
| rs482786 | 6 | 33739822 | T | C | 0,26 | -0,006 | 0,033 | 0,850 | 0,92 |
| rs2587363 | 13 | 53341798 | G | A | 0,59 | 0,004 | 0,030 | 0,896 | 0,92 |
| rs4502841 | 5 | 30862908 | G | A | 0,52 | -0,004 | 0,029 | 0,897 | 0,92 |
| rs28453001 | 8 | 112288701 | G | A | 0,49 | -0,003 | 0,029 | 0,918 | 0,92 |

* According to GRCh38 release

rsID, variant ID in dbSNP; SE, standard error; FDR, false discovery rate

**Supplementary Table S13.** Summary statistics from our GWAS of variants reported by *Toikumo S. et al .* , sorted on the basis of their *P* -value of association with pain intensity in our study.

| rsID | Chromosome | Position (bp) * | Allele 0 | Allele 1 | Allele 1 frequency | BETA | SE | *P*- value | FDR |
|---|---|---|---|---|---|---|---|---|---|
| rs757081 | 11 | 17330136 | C | G | 0,32 | 0,088 | 0,031 | **0,0047** | 0,64 |
| rs28715885 | 22 | 42045087 | T | G | 0,17 | -0,095 | 0,038 | **0,012** | 0,66 |
| rs34731055 | 7 | 2067293 | C | T | 0,23 | 0,086 | 0,035 | **0,015** | 0,66 |
| rs2034244 | 5 | 56946947 | T | C | 0,25 | -0,071 | 0,033 | **0,033** | 0,70 |
| rs17621391 | 7 | 140476796 | T | C | 0,27 | -0,071 | 0,033 | **0,035** | 0,70 |
| rs78116502 | 13 | 74125684 | A | G | 0,16 | 0,081 | 0,039 | **0,040** | 0,70 |
| rs61867344 | 10 | 104923885 | T | A | 0,22 | -0,070 | 0,035 | **0,044** | 0,70 |
| rs1002772 | 12 | 19156787 | G | A | 0,71 | 0,064 | 0,032 | **0,044** | 0,70 |
| rs187698281 | 18 | 55220120 | A | T | 0,05 | -0,141 | 0,071 | **0,046** | 0,70 |
| rs2247036 | 3 | 49844916 | C | T | 0,46 | -0,057 | 0,030 | 0,056 | 0,74 |
| rs12193842 | 6 | 83612439 | A | C | 0,31 | -0,058 | 0,031 | 0,062 | 0,74 |
| rs2294220 | 1 | 166914892 | A | C | 0,38 | -0,055 | 0,031 | 0,072 | 0,74 |
| rs10932180 | 2 | 207162189 | T | C | 0,37 | -0,054 | 0,031 | 0,077 | 0,74 |
| rs34811474 | 4 | 25407216 | G | A | 0,21 | -0,064 | 0,036 | 0,080 | 0,74 |
| rs9836291 | 3 | 49660026 | G | A | 0,26 | 0,058 | 0,033 | 0,082 | 0,74 |
| rs2072560 | 11 | 116791110 | T | C | 0,94 | -0,103 | 0,061 | 0,092 | 0,79 |
| rs6797509 | 3 | 136865930 | T | C | 0,69 | 0,052 | 0,032 | 0,101 | 0,79 |
| rs729826 | 4 | 3015063 | A | C | 0,40 | 0,046 | 0,030 | 0,131 | 0,79 |
| rs7631379 | 3 | 181691269 | T | C | 0,18 | 0,055 | 0,038 | 0,143 | 0,79 |
| rs115506546 | 3 | 49770574 | A | G | 0,03 | -0,137 | 0,095 | 0,146 | 0,79 |
| rs429358 | 19 | 44908684 | T | C | 0,12 | 0,065 | 0,045 | 0,150 | 0,79 |
| rs1261094 | 18 | 55200861 | A | G | 0,04 | -0,102 | 0,072 | 0,155 | 0,79 |
| rs10078184 | 5 | 118483610 | C | G | 0,27 | -0,046 | 0,033 | 0,162 | 0,79 |
| rs7187662 | 16 | 49580127 | T | C | 0,19 | 0,051 | 0,037 | 0,162 | 0,79 |
| rs1246731 | 1 | 191373432 | C | T | 0,49 | 0,041 | 0,030 | 0,165 | 0,79 |
| rs9462029 | 6 | 34847426 | A | G | 0,16 | -0,055 | 0,040 | 0,166 | 0,79 |
| rs11973114 | 7 | 1873634 | G | A | 0,20 | 0,051 | 0,037 | 0,168 | 0,79 |

| | | | | | | | | | |
|---|---|---|---|---|---|---|---|---|---|
| rs622726 | 1 | 241628245 | T | C | 0,66 | -0,041 | 0,031 | 0,175 | 0,79 |
| rs59918340 | 8 | 141222157 | A | G | 0,45 | 0,037 | 0,029 | 0,204 | 0,90 |
| rs72807818 | 2 | 51591881 | G | A | 0,14 | 0,051 | 0,042 | 0,229 | 0,93 |
| rs138736131 | 3 | 49957009 | G | T | 0,08 | 0,064 | 0,055 | 0,247 | 0,93 |
| rs4757141 | 11 | 13285548 | A | G | 0,26 | -0,037 | 0,033 | 0,269 | 0,93 |
| rs467523 | 2 | 32076562 | G | A | 0,54 | -0,031 | 0,029 | 0,289 | 0,93 |
| rs1333907 | 9 | 119911110 | A | T | 0,64 | 0,033 | 0,031 | 0,290 | 0,93 |
| rs6942045 | 6 | 33383919 | C | T | 0,30 | 0,033 | 0,032 | 0,299 | 0,93 |
| rs56016894 | 6 | 68901006 | A | T | 0,09 | -0,051 | 0,051 | 0,314 | 0,93 |
| rs78286408 | 4 | 97663403 | C | T | 0,04 | -0,072 | 0,072 | 0,319 | 0,93 |
| rs4902704 | 14 | 69236871 | G | C | 0,59 | -0,029 | 0,029 | 0,322 | 0,93 |
| rs72805578 | 16 | 89616083 | C | A | 0,20 | -0,035 | 0,037 | 0,346 | 0,93 |
| rs79842130 | 15 | 73621748 | C | T | 0,04 | 0,066 | 0,072 | 0,363 | 0,93 |
| rs10764437 | 10 | 18359576 | A | G | 0,53 | 0,026 | 0,029 | 0,372 | 0,93 |
| rs12672629 | 7 | 21492213 | A | G | 0,70 | -0,027 | 0,032 | 0,390 | 0,93 |
| rs9601084 | 13 | 78586744 | C | A | 0,22 | 0,030 | 0,035 | 0,396 | 0,93 |
| rs11012732 | 10 | 21541175 | A | G | 0,36 | 0,026 | 0,031 | 0,401 | 0,93 |
| rs11664298 | 18 | 79818986 | G | A | 0,17 | 0,032 | 0,039 | 0,407 | 0,93 |
| rs13107325 | 4 | 102267552 | C | T | 0,07 | -0,048 | 0,059 | 0,411 | 0,93 |
| rs359250 | 2 | 60253838 | G | T | 0,62 | 0,025 | 0,030 | 0,412 | 0,93 |
| rs2657294 | 10 | 75193267 | G | C | 0,41 | -0,024 | 0,030 | 0,418 | 0,93 |
| rs9375696 | 6 | 130038566 | C | T | 0,60 | 0,024 | 0,030 | 0,419 | 0,93 |
| rs7318716 | 13 | 56210960 | A | T | 0,68 | -0,025 | 0,031 | 0,427 | 0,93 |
| rs76376207 | 2 | 50866560 | C | T | 0,06 | 0,048 | 0,061 | 0,432 | 0,93 |
| rs2963999 | 5 | 153796513 | G | T | 0,53 | 0,023 | 0,029 | 0,434 | 0,93 |
| rs10104041 | 8 | 94559374 | G | A | 0,32 | -0,024 | 0,031 | 0,439 | 0,93 |
| rs10053440 | 5 | 167269956 | C | G | 0,93 | -0,042 | 0,057 | 0,453 | 0,93 |
| rs10764281 | 10 | 20760364 | A | G | 0,39 | -0,021 | 0,030 | 0,478 | 0,93 |
| rs203462 | 17 | 19909228 | T | C | 0,37 | -0,021 | 0,029 | 0,479 | 0,93 |
| rs12532894 | 7 | 127969463 | C | T | 0,26 | -0,023 | 0,033 | 0,483 | 0,93 |
| rs13023972 | 2 | 207642950 | T | C | 0,47 | -0,020 | 0,029 | 0,495 | 0,93 |

| | | | | | | | | | |
|---|---|---|---|---|---|---|---|---|---|
| rs887970 | 2 | 39624074 | C | T | 0,33 | 0,021 | 0,031 | 0,497 | 0,93 |
| rs62032342 | 16 | 25326830 | A | G | 0,16 | 0,026 | 0,040 | 0,510 | 0,93 |
| rs1966265 | 5 | 177089630 | G | A | 0,21 | 0,023 | 0,036 | 0,519 | 0,93 |
| rs12994080 | 2 | 170742572 | A | G | 0,64 | 0,019 | 0,030 | 0,521 | 0,93 |
| rs12916494 | 15 | 66525707 | G | T | 0,09 | 0,033 | 0,051 | 0,523 | 0,93 |
| rs59165315 | 1 | 37829653 | C | T | 0,31 | 0,020 | 0,031 | 0,526 | 0,93 |
| rs34898535 | 16 | 31014320 | C | T | 0,42 | 0,019 | 0,030 | 0,532 | 0,93 |
| rs1151623 | 20 | 63737253 | T | C | 0,79 | 0,022 | 0,036 | 0,535 | 0,93 |
| rs12616436 | 2 | 103731567 | T | C | 0,44 | 0,019 | 0,030 | 0,536 | 0,93 |
| rs4548017 | 6 | 97951645 | A | G | 0,61 | -0,018 | 0,030 | 0,541 | 0,93 |
| rs13291079 | 9 | 93598368 | T | C | 0,42 | 0,017 | 0,029 | 0,560 | 0,93 |
| rs1915159 | 15 | 46114524 | A | G | 0,53 | 0,017 | 0,030 | 0,575 | 0,93 |
| rs9989163 | 14 | 102768675 | G | A | 0,46 | 0,016 | 0,029 | 0,575 | 0,93 |
| rs7980687 | 12 | 123338164 | G | A | 0,21 | -0,020 | 0,037 | 0,591 | 0,93 |
| rs2582974 | 2 | 103962465 | T | C | 0,59 | -0,016 | 0,030 | 0,593 | 0,93 |
| rs67883051 | 20 | 21539505 | G | A | 0,21 | 0,019 | 0,035 | 0,594 | 0,93 |
| rs3752823 | 12 | 19375704 | G | A | 0,10 | 0,025 | 0,048 | 0,600 | 0,93 |
| rs11171733 | 12 | 56062482 | G | A | 0,44 | 0,015 | 0,030 | 0,619 | 0,93 |
| rs67468823 | 3 | 77225381 | A | G | 0,26 | -0,016 | 0,033 | 0,624 | 0,93 |
| rs6466488 | 7 | 114505470 | G | A | 0,53 | 0,014 | 0,029 | 0,624 | 0,93 |
| rs8134789 | 21 | 45199643 | G | A | 0,64 | -0,014 | 0,030 | 0,638 | 0,93 |
| rs62379821 | 5 | 120755395 | T | A | 0,28 | -0,015 | 0,032 | 0,638 | 0,93 |
| rs7018617 | 9 | 125724803 | G | T | 0,62 | 0,014 | 0,030 | 0,654 | 0,94 |
| rs3820500 | 1 | 117470700 | G | A | 0,66 | -0,013 | 0,031 | 0,669 | 0,94 |
| rs1483078 | 7 | 49919302 | C | T | 0,70 | -0,014 | 0,032 | 0,673 | 0,94 |
| rs3739749 | 9 | 95062284 | C | T | 0,07 | 0,022 | 0,057 | 0,694 | 0,94 |
| rs10181521 | 2 | 143686312 | A | G | 0,36 | 0,011 | 0,031 | 0,719 | 0,94 |
| rs1599859 | 17 | 67841077 | C | G | 0,21 | -0,013 | 0,036 | 0,721 | 0,94 |
| rs618869 | 18 | 55580920 | T | C | 0,87 | -0,015 | 0,042 | 0,727 | 0,94 |
| rs293531 | 6 | 82957217 | T | C | 0,72 | 0,011 | 0,033 | 0,736 | 0,94 |
| rs34201437 | 3 | 67891777 | A | C | 0,90 | 0,016 | 0,048 | 0,742 | 0,94 |

| | | | | | | | | | |
|---|---|---|---|---|---|---|---|---|---|
| rs1427675804 | 2 | 52865308 | GTATGTTTAGA | G | 0,45 | -0,009 | 0,030 | 0,749 | 0,94 |
| rs4456576 | 18 | 53236485 | C | G | 0,43 | 0,009 | 0,029 | 0,763 | 0,94 |
| rs2297600 | 1 | 31741980 | T | G | 0,16 | 0,010 | 0,039 | 0,790 | 0,96 |
| rs9354627 | 6 | 67751094 | G | A | 0,53 | 0,008 | 0,030 | 0,795 | 0,96 |
| rs6927072 | 6 | 151936552 | T | G | 0,66 | 0,007 | 0,031 | 0,809 | 0,96 |
| rs9355403 | 6 | 162791546 | G | A | 0,20 | -0,009 | 0,037 | 0,816 | 0,96 |
| rs12032174 | 1 | 237692868 | C | T | 0,62 | 0,006 | 0,030 | 0,835 | 0,96 |
| rs1163089 | 10 | 103284207 | G | A | 0,49 | 0,006 | 0,030 | 0,851 | 0,96 |
| rs2784738 | 1 | 8406157 | G | A | 0,28 | -0,006 | 0,032 | 0,856 | 0,96 |
| rs6742231 | 2 | 219490035 | G | C | 0,34 | 0,006 | 0,031 | 0,857 | 0,96 |
| rs7739264 | 6 | 19785357 | C | T | 0,53 | 0,005 | 0,030 | 0,859 | 0,96 |
| rs4334682 | 3 | 74900305 | T | C | 0,83 | 0,007 | 0,039 | 0,862 | 0,96 |
| rs17681972 | 14 | 46773906 | G | A | 0,50 | -0,004 | 0,029 | 0,883 | 0,98 |
| rs35274404 | 14 | 37338411 | C | T | 0,28 | 0,004 | 0,032 | 0,896 | 0,98 |
| rs4559047 | 5 | 134512969 | C | T | 0,60 | 0,003 | 0,030 | 0,910 | 0,98 |
| rs12591658 | 15 | 73847612 | C | G | 0,83 | 0,003 | 0,039 | 0,946 | 0,99 |
| rs3764002 | 12 | 108224853 | C | T | 0,26 | -0,002 | 0,033 | 0,961 | 0,99 |
| rs11925666 | 3 | 195791789 | A | G | 0,21 | -0,002 | 0,037 | 0,966 | 0,99 |
| rs11620149 | 13 | 89163828 | T | C | 0,15 | -0,001 | 0,040 | 0,971 | 0,99 |
| rs6705514 | 2 | 26991069 | T | C | 0,58 | -0,001 | 0,030 | 0,972 | 0,99 |

* According to GRCh38 release

rsID, variant ID in dbSNP; SE, standard error; FDR, false discovery rate